STUDY ON TREATMENT TECHNOLOGIES FOR PERFLUOROCHEMICALS IN WASTEWATER(Dissertation_全文)

AUTHOR(S):

Qiu, Yong

STUDY ON TREATMENT TECHNOLOGIES FOR PERFLUOROCHEMICALS IN WASTEWATER

QIU YONG

2007

ABSTRACT

Perfluorochemicals (PFCs) were produced by industries and consumed "safely" as surfactants, repellents, additives, fire-fighting foams, polymer emulsifiers and insecticides for almost fifty years. However they are now considered as persistent, bioaccumulated and toxic (PBT) chemicals, and ubiquitously distributed in waster, air, human body and biota. Although some efforts were contributed to reduce PFCs in environment, such as development of alternatives and recycling processes, huge amount of persisted PFCs have already been discharged in environment and accumulated in biota including humans. In some industrialized areas, such as Yodo river basin in Japan, water environment and human blood were polluted by some PFCs, and thus reduction and control of PFCs were urgently required for the purpose of environmental safety and human health in these areas. Unfortunately, some studies implied that current water and wastewater treatment processes seemed ineffective to remove PFCs in trace levels. Therefore, this study will try to develop some proper technologies to treat trace level of PFCs in wastewater. In order to achieve this main objective, several works have been accomplished as follows.

Current available literature has been reviewed to obtain a solid background for this study. Basic information of PFCs was summarized in physiochemical properties, PBT properties, productions and applications, regulations and *etc*.. Analytical methods for PFCs, especially of LC-ESI-MS/MS, were reviewed including pretreatment processes in diverse matrices, which derived objectives of chapter III. Distributions and behavior of PFCs were briefly discussed in water environments, biota sphere and human bloods. Available control strategies were shown in detail about alternatives, industrial recycling processes, and newly developed treatment processes. Current wastewater treatment processes showed inefficient removal for some PFCs, deriving objectives of chapter IV on the PFC behavior in treatment process. Newly developed treatment technologies seemed able to decompose PFCs completely but unsuitable for application in WWTP. Therefore, granular activated carbon (GAC) adsorption and ultra violet (UV) photolysis were developed in chapter V and VI as removal and degradation processes respectively.

Fifteen kinds of PFCs were included in this study, consisting of twelve kinds of perfluorocarboxylic acids (PFCAs) with 4~18 carbons and three kinds of perfluoroalkyl sulfonates (PFASs) with 4~8 carbons. An integral procedure was developed in chapter III to pretreat wastewater samples. LC-ESI-MS/MS was applied to quantify all PFCs in trace level. Pretreatment methods were optimized between C_{18} and WAX-SPE processes for aqueous samples, and between IPE, AD-WAX and ASE-WAX processes for particulate samples. Standard spiking experiments were regularly conducted for each wastewater sample to calculate recovery rate and control analytical quality. As the result, WAX-SPE showed better performance on samples with very high organics concentrations, and C_{18}-SPE performed better for long-chained PFCs. ASE-WAX was proposed as the optimum method to pretreat particulate samples because of the simple and time saving operations. 9H-PFNA was used as internal standard to estimate matrix effect in wastewater.

Behavior of PFCs in a municipal WWTP has been studied in chapter IV by periodical surveys for six times in half a year. All PFCs used in this study were detected in WWTP influent and effluent. According to their carbon chain lengths, all PFCs can be classified into "*Medium*", "*Long*" and "*Short*" patterns to simplify behavior analysis. PFCs in same pattern showed similar properties and behavior in

wastewater treatment facilities. Very high concentrations of PFCs existed in WWTP influent, indicating some point sources of industrial discharge in this area. "*Medium*" PFCs, such as PFOA(8), PFNA(9) and PFOS(8), were primary contaminants in the WWTP and poorly removed by overall process. Performances of individual facilities were estimated for removal of each PFC. Primary clarification and secondary clarification were helpful to remove all PFCs in both aqueous phase and particulate phase. "*Medium*" PFCs in aqueous phase were increased after activated sludge process, but other PFCs can be effectively removed. Ozone seemed ineffective to decompose PFCs because of the strong stability of PFC molecules. Sand filtration and biological activated carbon (BAC) filtration in this WWTP can not remove PFCs effectively too, which required further studies. Performances of combined processes were estimated by integrating individual facilities along the wastewater flow. Activated sludge process coupled with clarifiers showed satisfied removal of most PFCs in the investigated WWTP except "*Medium*" PFCs.

Adsorption characteristics of PFCs onto GAC have been studied by batch experiments in chapter V. Freundlich equation and homogenous surface diffusion model (HSDM) were applied to interpret experimental data. Isothermal and kinetics experiments implied that PFC adsorption on GAC was directly related with their carbon chain lengths. By ascendant carbon chain length, adsorption capacity for specific PFC was increased, and diffusion coefficient (D_s) was decreased. D_s of GAC adsorption was also decreased gradually in smaller GAC diameters. Coexisted natural organic matters (NOMs) reduced adsorption capacities by mechanism of competition and carbon fouling. Carbon fouling was found reducing adsorption capacity much more intensively than competition by organics. Acidic bulk solution was slightly helpful for adsorption of PFCs. However adsorption velocity or kinetics was not affected by NOM and pH significantly. GAC from Wako Company showed the best performance among four kinds of GACs, and Filtra 400 from Calgon Company was considered more suitable to removal all PFCs among the commercial GACs. Preliminary RSSCT and SBA results implied that background organics broke through fixed GAC bed much earlier than trace level of PFCs. Medium-chained PFCs can be effectively removed by fixed bed filtration without concerning biological processes.

Direct photolysis process has been developed in chapter VI to decompose PFCAs in river water. Irradiation at UV_{254} nm and $UV_{254+185}$ nm can both degrade PFCAs. Stepwise decomposition mechanism of PFCAs was confirmed by mass spectra analysis, and *consecutive* kinetics was proposed to simulate experimental data. PFASs can also be degraded by $UV_{254+185}$ photolysis, although the products have not been identified yet. Coexisted NOMs reduced performance of UV photolysis for PFCAs by competition for UV photons. Sample volume or irradiation intensity showed significant influence on degradation of PFCAs. Local river water polluted by PFOA can be cleaned up by $UV_{254+185}$ photolysis effectively. Ozone-related processes were also studied but ineffective to degrade PFC molecules. However, PFCs could be removed in aeration flow by another mechanism.

KEYWORDS

Perfluorochemicals (PFCs), wastewater treatment plant (WWTP), LC-MS/MS, behavior patterns, GAC adsorption, UV photolysis

ACKNOWLEDGEMENT

This dissertation was accomplished in Research Center for Environmental Quality Management, Kyoto University (RCEQM) in four years. I would like to express my grateful thanks to Prof. Shigeo FUJII, my supervisor, who offered me the opportunity to join this study. Without his professional suggestions and financial support, this work was impossible to be finished.

Thanks are given to Prof. Hiroaki TANAKA and Prof. Sadahiko ITOH in Kyoto University for their valuable comments on this dissertation and helpful advices on further studies. Acknowledgement is also given to Japanese Monbugakusho Scholarship for the financial support in three years.

I would like to thank PFOS research group members for their cooperative and excellent works. Thanks are also given to staffs and students in RCEQM for their kindness and helps in my life.

At last but not least, I would like to thank my family for their vital support and consistent encouragement. Their expectation is always the power source for me to struggle all difficulties in my life.

To my beloved parents

TABLE OF CONTENTS

LIST OF FIGURES

LIST OF TABLES

ABBREVIATIONS

AC	activated carbon
AD	alkaline digestion
AFFF	aqueous fire fighting foam
AOPs	advanced oxidation processes
ASP	activated sludge process
ASE	accelerated solvent extraction
ASH	Air-Sparged Hydrocyclone
ATR	attenuated total reflectance
BAC	biological activated carbon filtration
B-P	bottle-Point experiment
DCBR	differential column batch reactor
DOC	dissolved organics carbon
DW	Mitsubishi diasorb W1030
EBCT	empty bed contact time
ECF	electro-chemical fluorination
EP	electronic precipitation
ESI	electrospray ionization
F400	Calgon filtrasorb 400
FTIR	Fourier transform infrared spectroscopy
GAC	granular activated carbon
GC	gas chromatography
HDPE	high density polyethylene
HSDM	homogeneous surface diffusion model
IPE	ion-pair extraction
IPE	ion-pair extraction
IS	internal standard
ISR	ionization suppression rate
LC	liquid chromatograph
LOD	limits of detection
LOQ	limits of quantification
MS/MS	tandem mass spectrometer
O3	ozone contactor
PBT	Persistence, bioaccumulation and toxicity
PC	primary clarifier
PDM	pore diffusion model
PFAS	perfluoroalkyl sulfonates
PFBA	perfluorobutyric acid
PFBuS	perfluorobutane sulfonate
PFCA	perfluorocarboxylates
PFCs	perfluorochemicals
PFDA	perfluorodecanoic acid
PFDoA	perfluorododecanoic acid
PFHpA	perfluoroheptanoic acid
PFHxA	perfluorohexanoic acid
PFHxDA	perfluorohexadecanoic acid
PFHxS	perfluorohexane sulfonate
PFNA	perfluorononanoic acid
PFOA	perfluorooctanoate
PFOA	perfluorooctane acid
PFOcDA	perfluorooctadecanoic acid
PFOS	perfluorooctane sulfonate
PFOSA	perfluorooctane sulfonamide
PFPeA	perfluoropentanoic acid
PFTeDA	perfluorotetradecanoic acid
PFUnA	perfluoroundecanoic acid
$\sum$PFC	total PFC
PK	GAC Norit PK1~3
PLE	pessurized liquid extraction
POPs	persisted organic pollutants
PP	polypropylene
PR	process recovery
PSDM	pore-surface diffusion model
RE	removal efficiency
RO	reverse osmosis
RSD	relative standard deviations
RSSCT	rapid small-scale column tester
SBA	short bed adsorber
SC	second clarifier
SF	sand filtration
SPE	solid phase extraction
TFA	trifuoroacetate
UV	ultra violet
UV_{254}	UV irradiation at 254nm
$UV_{254+185}$	UV irradiation at 254nm and 185nm
WAX	weak anion-exchange
WHA	humic acid from Wako Company
WW	wastewater effluent from WWTP
WWTP	wastewater treatment plant

CHAPTER I INTRODUCTION

1.1 Research Background

Persisted organic pollutants (POPs) have been concerned for decades and recently perfluorochemicals (PFCs) appeared in the list of POPs. Because of their extraordinary thermal and chemical stability, PFCs have been manufactured for various applications and consumed as surfactants, repellents, additives, fire-fighting foams, polymer emulsifiers and insecticides for about fifty years. However, they are now considered as persistent, bioaccumulated and toxic (PBT) chemicals and found ubiquitously distributed in the environment and biota. Unlike other organohalogen chemicals, PFCs have unique structures and properties and their behavior in the environment is still unclear due to limited studies. PFCs and related chemicals are of greatly increasing scientific interests, which is shown by publication numbers in **Fig. 1.1**.

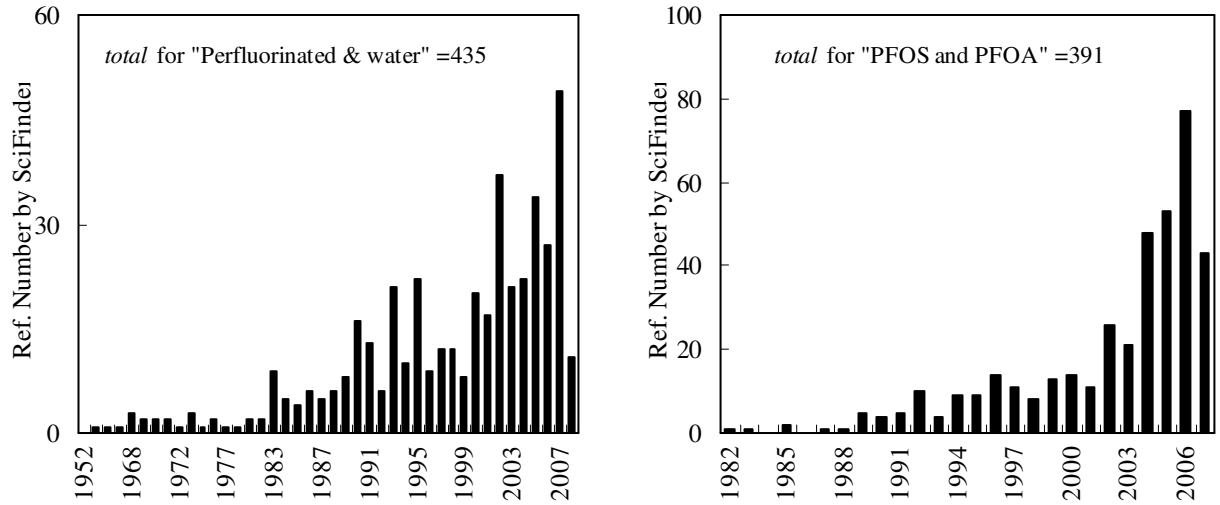

Figure 1.1 Annual publications of PFCs searched by SciFinder

Current studies roughly revealed global distributions and the environmental behavior of PFCs and related chemicals. Perfluorooctanoate (PFOA) and perfluorooctane sulfonate (PFOS), dominant PFCs in environment, have been detected everywhere including surface water, groundwater, drinking water, air, rainfalls, soil, animals, wildlife and human blood, and so on. Developed countries and industrializing areas were highly polluted by PFCs, such as America, Japan, Europe and coastal China. Major source of PFCs in the environment was supposed to be direct discharge from global fluoropolymer manufacturers (Armitage, *et al.*, 2006). Although alternatives and recycling processes were developed to reduce industrial discharge, huge amount of PFCs had been already discharged to the environment and accumulated in biota sphere. Environmental monitoring results have identified that surface water, drinking water, aerosol dust and human serum in Kinki area of Japan were contaminated by PFOA, indicating very high exposure and risk to local residents. Unfortunately, current water and wastewater treatment processes seemed not effective to remove PFCs in trace levels. Therefore, regulatory actions, scientific studies and engineering solutions are of urgent necessities to control PFCs in this area. This study will try to contribute to this theme by developing some treatment technologies to deal with 15 kinds of PFCs in wastewater. The PFCs in this study are shown in **Table 1.1**.

Analysis of trace level PFCs in wastewater is fundamental to study their behavior in wastewater

treatment processes. Liquid chromatograph coupled with tandem mass spectrometer (LC-MS/MS) is considered as a standard method to determine trace level PFCs, although some other instrumental methods are also available such as GC-MS, NMR and FTIR. Analysis by LC-MS/MS often suffers from interferences in wastewater matrix, which can be estimated by volumetric internal standard (IS). Pretreatment methods can be optimized to reduce matrix effect in wastewater samples.

Table 1.1 Basic information of 15 kind PFCs used in this study

Abbr. name	Full name	Molecular Structure	M. W.	CAS No.
PFBA	Perfluorobutyric Acid	$CF_3(CF_2)_2COOH$	214.0	375-22-4
PFPeA	Perfluoropentanoic Acid	$CF_3(CF_2)_3COOH$	264.1	2706-90-3
PFHxA	Perfluorohexanoic Acid	$CF_3(CF_2)_4COOH$	314.1	307-24-4
PFHpA	Perfluoroheptanoic Acid	$CF_3(CF_2)_5COOH$	364.1	375-85-9
PFOA	Perfluorooctane Acid	$CF_3(CF_2)_6COOH$	414.1	335-67-1
PFNA	Perfluorononanoic Acid	$CF_3(CF_2)_7COOH$	464.1	375-95-1
PFDA	Perfluorodecanoic Acid	$CF_3(CF_2)_8COOH$	514.1	335-76-2
PFUnA	Perfluoroundecanoic Acid	$CF_3(CF_2)_9COOH$	564.1	2058-94-8
PFDoA	Perfluorododecanoic Acid	$CF_3(CF_2)_{10}COOH$	614.1	307-55-1
PFTeDA	Perfluorotetradecanoic Acid	$CF_3(CF_2)_{12}COOH$	714.1	376-06-7
PFHxDA	Perfluorohexadecanoic Acid	$CF_3(CF_2)_{14}COOH$	814.1	67905-19-5
PFOcDA	Perfluorooctadecanoic Acid	$CF_3(CF_2)_{16}COOH$	914.1	16517-11-6
PFBuS	Perfluorobutane Sulfonate	$CF_3(CF_2)_3SO_3K$	338.2	29420-49-3
PFHxS	Perfluorohexane Sulfonate	$CF_3(CF_2)_5SO_3K$	438.2	3871-99-6
PFOS	Perfluorooctane Sulfonate	$CF_3(CF_2)_7SO_3K$	538.2	2795-39-3

Effluents of municipal WWTPs were suspected as one important source of PFCs in water environment. Study on behavior of PFCs in WWTPs was very limited, and stayed on the surface by analyzing PFCs only in influent, effluent and activated sludge. Performances of facilities in typical WWTP have not been estimated yet, which might be useful to understand the differences between treatment processes on PFCs removal. Furthermore, periodical surveys should be conducted to improve data qualities.

Granular activated carbon (GAC) filtration is an appreciated process to remove odors from drinking water as well as trace organics. However, GAC filtration has shown diverse or even opposite performances on PFCs removal in different studies. Results of environmental monitoring indicated ineffective removal of PFCs in drinking water by waterworks equipped by GAC filters, but reports from laboratory experiments and industrial projects ensured satisfied performance to remove some PFCs. GAC adsorption for PFCs might be strongly affected by coexisted NOMs in mechanism of competition and carbon fouling. Improper operations will make GAC filter both ineffective and expensive. Therefore, study on GAC adsorption process is not only interesting to understand their debating but also helpful to improve practical operations in water treatment processes.

Degradation of PFCs in normal conditions seems very difficult because advanced oxidation processes (AOPs) were unable to decompose PFC molecules. Some processes in critical conditions have been developed to decompose PFCs completely, such as subcritical water oxidation, ultra violet (UV) photolytic catalysis, and sonochemical irradiation. However, they focused on removal of PFCs in concentrations of mg/L, and might not be applicable in WWTP. Therefore, degradation process in normal conditions should be developed to reduce PFCs in wastewater. Direct UV photolysis was simple for operation and

easy for construction in WWTP, and thus proposed to degrade some PFCs in wastewater.

In a brief summary, this study will try to reveal behavior of PFCs in a WWTP, develop GAC adsorption to remove PFCs from wastewater, and apply direct UV photolysis to degrade PFCs in wastewater.

1.2 Research Objectives

Essential goal of this study is to develop proper technologies to remove trace level of PFCs in wastewater. In order to achieve this goal, following steps are necessary.

(1) To develop an integral analytical procedure to determine PFCs in wastewater samples including aqueous phase and particulate phase.

(2) To investigate a WWTP periodically to understand behavior of PFCs in treatment facilities and estimate their performances on PFCs removal.

(3) To develop suitable techniques to remove PFCs in wastewater. In this study, GAC adsorption is proposed for this purpose.

(4) To develop suitable processes to degrade PFCs in wastewater and river water. In this study, direct UV photolysis is proposed for this purpose.

1.3 Structure of Dissertation

This dissertation consists of seven chapters. Overall contents are introduced by chapters as follows.

Chapter 1 gave a brief introduction of this research, including research background, objectives and dissertation structures.

Chapter 2 reviewed current available literature on PFCs, including their basic properties, analytical methods, environmental behavior, control strategies and engineering solutions.

Chapter 3 developed an integral analytical procedure to analyze PFCs in wastewater. Pretreatment methods have been optimized for aqueous samples and particulate samples respectively.

Chapter 4 revealed behavior of PFCs in a municipal WWTP. Performances of individual facilities and combined processes on PFC removal were estimated.

Chapter 5 showed characteristics of GAC adsorption for PFCs in wastewater. Batch experiments were conducted to obtain isotherms and kinetics of adsorption. Influence factors on adsorption were studied such as background organics, solution pH, GAC diameters and materials. Freundlich equation and homogeneous surface diffusion model (HSDM) were successfully applied to explain experimental data.

Chapter 6 applied direct UV photolysis to decompose PFCs in river water. Stepwise degradation mechanism was proved by mass spectra analysis. Forward kinetics was proposed and validated by experimental results. Background organics, irradiation intensity and UV wave length showed influences on removal of PFOA. River water contained high concentration of PFOA can be effectively cleaned by $UV_{185+254\,nm}$ irradiation.

Chapter 7 gave conclusions of this study and recommendations for further research.

CHAPTER II REVIEWS ON PERFLUOROCHEMICALS

The PFOS story is likely to emerge as one of the apocryphal examples of 20th century experimentation with widespread chemical exposures: prolific use and almost no testing for safety, until unexpectedly and almost serendipitously, it is discovered as a contaminant virtually everywhere.

—"Scotchgard strikes back", Our Stolen Future

2.1 Introduction of PFCs

Science of fluorochemistry begins with fluorine, which is most abundant in halogen family and most reactive to all elements. Because of the highest electro negativity of fluorine in all halogens and even all elements in periodic table, carbon-fluorine bond (C-F) shows stronger polarity and highest strength in nature. This stability confers a variety of unique properties to fluorochemicals (3M Company, 1999). This section will give an introduction to properties of PFCs.

2.1.1 Basic properties of PFCs

2.1.1.1 Physiochemical properties

As shown in **Table 1.1**, fifteen kinds of PFCs in two major groups were selected for this study, including twelve kinds of perfluorocarboxylates (PFCA) and three kinds of perfluoroalkyl sulfonates (PFAS). Perfluorooctanoate (PFOA) and perfluorooctane sulfonate (PFOS) are the typical chemicals for these two groups, which have eight carbons and the common name as "C8". Their chemical structures are shown in **Table 2.1**.

Table 2.1 Structures of PFCA and PFAS

Perfluorocarboxylate (PFCA)	Perfluoroalkyl sulfonate (PFAS)
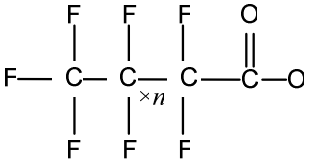	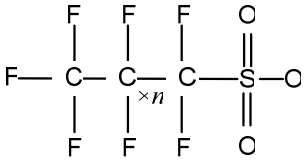
$CF_3(CF_2)_nCOO^-$	$CF_3(CF_2)_nSO_3^-$
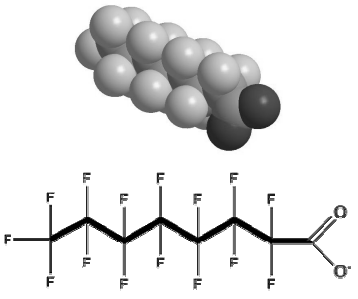	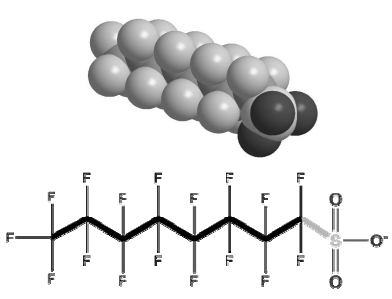
PFOA (8)	PFOS (8)

PFCA and PFAS molecules consist of one perfluorinated carbon chain and one special functional group. The functional group, such as carboxylic or sulfonic group, can affiliate with water and make PFCs hydrophilic. Different hydrophilic moiety showed diverse behavior in aqueous environment. The perfluorinated tail is covered by strongest C-F bonds, and surrounded by fluorine atoms which have similar size with carbon atom. This kind of structure protects PFC molecules from breaking down by oxidants

such as OH radicals. The longer is carbon chain length, the more strongly hydrophobic is PFC molecule. Combination of hydrophobic and hydrophilic moieties, and high stability under extremely thermal and oxidative conditions, make PFCs perfect surfactants which can be applied in extremely critical conditions.

Table 2.2 Basic physiochemical properties of PFCs

PFCs	pKa[a]	M. Point[b] ℃	B. Point[c] ℃(Hg)	Specific Gravity	Standard Reagents		
					Supplier	Appearance	Purity, %
PFBA (4)			120.8-121	1.65	TCI	yellow liquid	95
PFPeA (5)			70 (40mm)	1.71	TCI	yellow liquid	>98
PFHxA (6)			159-160	1.76	TCI	Clear liquid	>98
PFHpA (7)			175 (742mm)	1.79	TCI	Crystalline	>96
PFOA (8)	2.5[a]	55-56, 37-50	189 (736mm)	1.70	Wako	white powder	>95
PFNA (9)		63-66, 65	122 (30mm)		TCI	white powder	>95
PFDA (10)		83-85, 88	218 (740mm)		TCI	white powder	>97
PFUnA (11)		96-101	160 (60mm)		Wako	white powder	>96
PFDoA (12)		107-109	245 (740mm)		Wako	white powder	96
PFTeDA(14)		130-135	270 (740mm)		Wako	white powder	>96
PFHxDA(16)		154-155	211 (100mm)		Wako	white powder	95
PFOcDA(18)		162-164	235 (100mm)		Wako	white powder	>97
PFBuS (4)		>300			TCI	white powder	95
PFHxS (6)					Fluka	white powder	>98
PFOS (8)	-3.27[a]	>400, 277		2.05	Wako	white powder	98

Note: ***a*** = PFOA (OECD, 2002), PFOS (US EPA, 2002); ***b*** = melting point, data from material safety data sheet (MSDS) of Wako Company and ExFluor Company; ***c*** = boiling point, from ExFluor MSDS.

Table 2.2 shows physiochemical properties of PFCs used in this study. Number following abbreviation in brackets referred to the carbon chain length. By ascendant carbon chain length, melting points and specific gravities of PFCAs were increased gradually, and their physical appearances were changed from liquid to solid, which implied correlations between carbon chain length and physiochemical properties in homologous series. Boiling points were estimated in different pressures and therefore no obvious tendency appeared. PFCs are not volatile, and their global distributions are considered mainly attributed to PFC-related precursors and telomers which are volatile and might generate PFCs by degradation after transport to remote areas, *e.g.*, Arctic area.

2.1.1.2 Persistence, bioaccumulation and toxicity (PBT)

Although PFCs have been produced and consumed "safely" for about fifty years, they were considered as persistent, bioaccumulated and toxic (PBT) chemicals in scientific studies and government reports recently (Renner, 2001; OECD, 2002; US EPA, 2002).

Persistence

3M Company published its reports on hydrolysis (Hatfield, 2001a) and aqueous photolytic degradation (Hatfield, 2001b) of PFOA(8), which showed rather long half-life times in natural environment. PFOS(8) also showed its resistance to advanced oxidation processes including ozone, ozone/UV, ozone/H_2O_2 and Fenton reagent (Schröder and Meesters, 2005). In this study, COD of each PFC was analyzed and all PFCs had no response to oxidation by chromium potassium oxide ($Cr_2O_7^{2-}$) or potassium permanganate acid (MnO_4^-), which confirmed their stabilities in critic environment.

Bioaccumulation

K_{ow}, known as partition coefficient between octane and water phases, is useful to estimated bioaccumulation potentials. However, it is not available for most of PFCs because PFCs are surfactants and third layer is formed during measurement (OECD, 2002; US EPA, 2002). Bioaccumulation factors (BAFs) or bioconcentration factors (BCFs) are calculated by dividing the average concentrations in organism by the concentrations in water environment. BAFs represent accumulation potentials of organics from environment to organisms.

Preliminary study showed dietary BAFs of PFOS(8) were 2,796 in bluegill sunfish and 720 in carp (OECD, 2002) respectively. BAFs of PFOA(8) were about 2 in fathead minnow and 3~8 in carp (US EPA, 2002), which are quite lower than PFOS(8). First survey of PFOS(8) in Japan showed quite high BAFs of PFOS to fishes in Tokyo Bay, which were as high as 1,260~19,950 (Taniyasu, *et al.*, 2002). Survey in Great Lakes also shows that BAFs of PFOS is about 1,000 for benthic invertebrates (Kannan, *et al.*, 2005). Another research in Ai river of Japan showed rather high BAF of PFOS in wild turtles as 10,964 and very low BAF of PFOA equal to 3.2 (Morikawa, *et al.*, 2006). Similar situation occurred for rainbow trout under synthetic PFC spiking waters. Dietary BAFs of PFCAs were ranged from 0.038 to 1.0, while BAFs of PFASs were ranged from 4 to 23,000, both increased with length of carbon chain (Martin, *et al.*, 2003b; 2003a). Recent research on lake trout in Great Lakes in North America also showed similar trend of increasing BAFs by carbon chain length. BAFs of PFCA(8~10) showed linear increase from 3.2 to 3.9, while BAFs of PFAS(6,8) changed from 500 to 12,600 (Furdui, *et al.*, 2007). Increase of BAFs by ascendant PFCs carbon chain length indicated that long-chained PFCs or more hydrophobic PFCs had stronger bioaccumulative potentials and bioconcentration levels. Furthermore, BAFs of PFASs were greater than PFCAs in equivalent carbon chain length, which indicated that acid function groups also played important role to determine accumulation potentials.

Biomagnification factors (BMFs) are calculated by dividing the average concentrations in predators to those in preys. BMFs can be applied to estimate accumulation potentials of organics in food chains. One study in Great Lakes reported BMF of PFOS(8) to be 10~20 for mink or bald eagles to their prey items (Kannan, *et al.*, 2005). Another survey of US coastal marine food chain showed that BMFs of bottlenose dolphin are 0.1~13 for PFCA(8~12) and 0.8~14 for PFAS(6,8), which were also increased by ascendant carbon chain length (Houde, *et al.*, 2006a). It can be concluded that BMFs of PFCs(8) were around 10 in aquatic ecosystems.

Toxicity

Because PFCs are different to normal lipophile toxic substances, their toxicology is still unknown in mechanism and need more studies to elucidate the profile. Although a lot of researches have been conducted for the toxicity of PFCs, the results were in diverse qualities and difficult to summarize in systematically. Generally, medium- and long-chained PFCs may be more toxic than short-chained ones by their longer half life times in rodents. Review on PFOS(8) toxicity showed that subchronic exposure led to significant weight loss accompanied by hepatotoxicity, and reductions of serum cholesterol and thyroid hormones (OECD, 2002). Reviews also revealed the influence of PFOS(8) on generations for rodent animals in laboratory (Lau, *et al.*, 2003; Thibodeaux, *et al.*, 2003) and on human birth in Japan (Inoue, *et al.*, 2004a).

US EPA reviewed studies on toxicity of PFOA(8), which showed diverse behavior between gender and generations of laboratory animals. Average half life of PFOA in human body was estimated to be 4.37

years (US EPA, 2003). PFOA(8) behaved in different ways between species and sexes due to renal clearance, and undergoes enterohepatic circulation. However, it was also reported that PFOA(8) can be eliminated and detoxified in the human body (Kudo and Kawashima, 2003). Pharmacokinetic profiles of PFOA(8) in the adults may be different from those in sexually immature rats (Lau, *et al.*, 2004).

Studies on toxicity of PFCs other than C8 were still very few. PFBuS(4) has much shorter half-life time than PFOS(8), therefore seems less toxic. PFHxS(6) was detected in human serum in similar level of PFOA(8) and 10 times less than PFOS(8). Both PFNA(9) and PFDA(10) were peroxisome proliferators, and PFDA(10) has longer half-life time in rats and shows quite high toxic potency (Lange, *et al.*, 2006). Pharmacokinetic and structure-activity studies on the relationship between toxicity and carbon chain length would arouse interests of toxicologists in future.

2.1.2 Production and applications

2.1.2.1 Production of PFCs

PFCs used in industries were mainly derived from two major classes named perfluoroalkyl sulfonates (PFASs) and perlfuorocarboxylate acid (PFCAs), which were produced in processes of electro-chemical fluorination (ECF) and telomerization respectively, as shown in **Fig.2**.

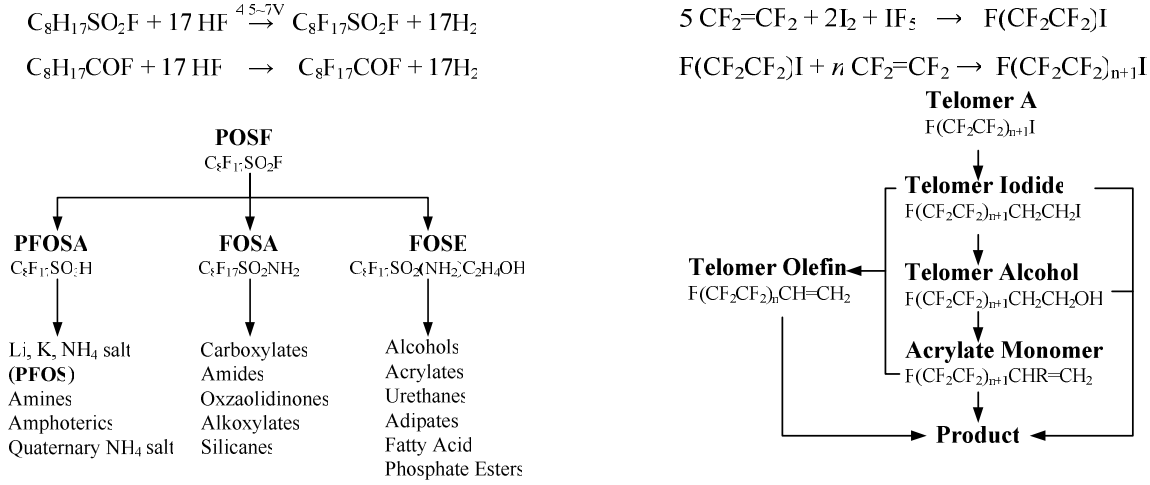

(*a*) ECF process and derivatives (*b*)Telomerization process and derivatives

Figure 2.1 Manufacture processes for PFCs (*a*) ECF and (*b*) Telomerization

Electro-chemical fluorination (ECF) was developed in 1945 by Dr. Simons in Penn State University, and adopted by 3M Company to produce organofluorine chemicals. In this process, electric current was passed through dispersed solution of alkyl organics and HF, causing hydrogen atoms to be replaced by fluorine atoms (3M Company, 1999). The process and derivatives are briefly shown in **Fig. 2.1*a*** (OECD, 2002). In ECF process, impurities were existed in output and finally introduced to industrial products. Predominant products were straight chain homologs, which occupied 70% of total amount. Cleaved, branched and cyclic structures were also formed during synthesis to be 20~25% of output. Others were byproducts of high molecular weight fluorochemicals (3M Company, 1999). ECF process was ceased after 3M Company phased out its product of PFOS.

Telomerization process was developed by DuPont, and related products based on telomerization are manufactured by a number of companies, including DuPont, Asahi Glass, Atofina, Clariant, and Daikin (Lange, *et al.*, 2006). The process and derivatives are shown in **Fig. 2.1*b*.** Telomer was generated by reaction of perfluoroethylene (CF_2=CF_2) and perfluoroalkyl iodides (CF_3CF_2I). Telomerization process

exclusively generated linear products with even number of carbon atoms. Telemerization process is still applied in industries to produce PFCs now.

2.1.2.2 Application of PFCs

As a big family, industrial applications of PFCs involve lots of derivatives whose physiochemical properties and toxicity are still unknown. **Table 2.3** shows number of PFOS-related chemicals which were proposed by different organizations. More than one hundred chemicals are original from PFCs, making study of PFCs behavior quite difficult as well as control of PFCs in environment.

Table 2.3 PFOS-related chemicals

Organization	Time	Numbers[a]
RPA&BRE	2004	96
US EPA	2002	88[b]
US EPA	2006	183[b]
OECD	2002	172[b]
OSPAR	2002	48
Canada EPA	2006	57

Note: ***a***=PFOS-related; ***b***=include different carbon chain length

Some attempts were conducted to estimate environmental loadings of PFCAs and PFASs. Global historical production of PFCAs in 1951~2004 were estimated to be 4,400~8,000 tons and the total emissions to environment were 3,200~7,300 tons (Prevedouros, *et al.*, 2006). Emissions of PFAS-related chemicals were estimated to be 4,650 tons per year in 1990~2000 (Footitt, *et al.*, 2004). Majority of industrial emissions were considered to be fluoropolymer manufacturing and aqueous fire-fighting foam production (Armitage, *et al.*, 2006). More information about PFC-related chemicals and their applications was available in literature (OECD, 2002; US EPA, 2002; 2003; Brooke, *et al.*, 2004; Canada, 2004; Footitt, *et al.*, 2004; 2005; Poulsen, *et al.*, 2005; Lange, *et al.*, 2006; UNEP, 2006).

2.1.3 Regulations related with PFCs

2.1.3.1 Timeline of regulations for PFCs

Table 2.4 shows timeline of important events related with PFCs invention, development, applications, scientific activities and governmental policies. Invention of PFCs can be dated back to seventy years ago. Although PFCs were detected in human blood in 1968 and in drinking water in 1984, concerns of these chemicals were aroused in recent five years. Because production of PFOA is expected to last over 2015, control of PFOA will become more important in the future after the phase out of PFOS production.

2.1.3.2 Discharge criteria of PFCs

Exposure criteria of PFCs for human health were still in debating and there was no agreement yet. One reason referred to the unreliable original data for assessment, and the other reason was related with the negotiation between government and industries.

Rather high screening levels of PFOA(8) was established by West Virginia of USA (WV DEP, 2002), which were 150 μg/L for water environment and 1360 μg/L for aquatic life. The criteria was soon applied to assess PFOA(8) in air and water around DuPont telomer manufacturing sites, which came to a conclusion that telomer manufacture was not significant source of PFOA to environment (CRG of DuPont and URS Diamond, 2003). However, the independence of WV DEP was strongly questioned and doubted by scientists, and the criteria were argued to be quite overestimated.

Minnesota Department of Health recommended 7 μg/L in drinking water as the safe level of PFOA(8) for human health in 2002, and then revised it to be 0.5 μg/L in 2007. Other PFCs were also included in the criteria as 0.3 μg/L for PFOS(8), 1 μg/L for PFCA(4~6), and 0.6 μg/L for PFAS(4,6), because all of them have been detected in local surface waster and drinking water (MDH, 2007). North California

Division of Water Quality proposed 2 μg/L of PFOA(8) to be interim maximum allowable concentration, which was calculated by reference dose of 0.3 μg/kg-day (NC DWQ, 2006).

Table 2.4 Timeline of important event related with PFCs

Time	Orgz.	Actions or event
1938		Dr. RJ Plunkett discover Teflon by accident as a failed experiment
1949	*DuPont*	Introduce and produce Teflon
1953	*3M*	Discover Scotchgrad by accidental spilling on tennis shoes
1956	*3M*	Start to sell Scotchgard Protector
1968		Dr. DR Taves firstly publish two forms of fluoride in human serun
1978	*3M*	Detect PFOS/PFOA in blood of workers
1981	*3M*	First publish that telomer is transform to PFOA in rat
1984	*DuPont*	Find tap water near DuPont Works contains 0.8~1.5 μg/L PFOA
1986	*DuPont*	Begin selling Teflon-based Stainmaster to protect carpets
1988	*3M*	Reports wide existence of fluorochemicals in blood-bank samples
1999	*DuPont*	Dump 55000 pounds of PFOA into Ohio River
2000	*DuPont*	Release 31,250 pounds of PFOA into air
2000	*3M*	Announce phasing out production of PFOS and related chemicals
2002	*US EPA*	Review of data that links C8 to health problems
2002	*OECD*	Issue hazard assessment of PFOS and its salts
2003	*JP EPA*	Start 1st survey on surface water, aquatic life and sediment
2003	*3M*	Replaces C8 in Scotchgard with a C4 chemical
2003	*JP*	Detect high PFOA in Kinki area including Yodo River Basin
2004	*US EPA*	Start own scientific studies on C8 chemical
2004	*CA*	Issue exposure to PFOS and related precursors by Health Canada
2005	*OECD*	Product survey of PFCs and related chemicals
2005	*US EPA*	Issue risk assessment of PFOA-related chemicals on human health
2005	*DE*	Issure review on alternatives to PFCs in Denmark
2006	*NE*	Issure review of PFCs in drinking water in Netherland
2006	*SW*	Propose PFOS as POPs candidate to Stockholm Convention
2006	*US EPA*	Initiate 2010/15 PFOA stewardship program

Source: Adapted from Fluoride Action Network Pesticide Project, 2005

2.2 Analytical Methods for PFCs

Analysis is fundamental on trace organics researches including PFCs, which should be considered firstly and seriously. Furthermore, it was considered that veil of PFCs problem were uncovered by the development of instrumental analysis, especially by application of LC-MS/MS. In this section, instrumental analysis for PFCs was summarized in its history and pretreatment methods, which was important for PFCs analysis in wastewater.

2.2.1 History of PFCs analysis

2.2.1.1 Non-specific quantified methods

The first attempt to analyze organofluorine can be traced back as early as 1968, when organic fluorinated chemicals were firstly detected in human serum (Martin, *et al.*, 2004a). Forty years ago, only

combustion method was available to analyze organofluroines, which was named as Wickbold oxy-hydrogen flame method. Organic fluorine was combusted to inorganic form and absorbed by sodium hydroxide solution, which will be further titrated by thorium nitrate for quantification. Combustion method can only analyze total amount of fluorine content, and adsorbents like activated carbon is necessary to extract organofluorine from water. This method was applied for the first time to analyze organofluorine in water sample, by coupling with fluorine-selective electrode for quantification (Fritsche and Hüttenhain, 1994).

Organofluorine can also be detected by neutron activation and X-ray fluorescence, which are also non-specific methods. Anion PFASs were successfully measured by these methods (Levine, *et al.*, 1997). NMR method, which can determine CF_2 and CF_3 group simultaneously, is also non-specific. Although by coupling with LC-MS/MS, ^{19}F NMR was successfully applied to quantify PFCAs (Moody, *et al.*, 2001; Ellis, *et al.*, 2004a) and further identify branched PFCs (Martin, *et al.*, 2004a), this method was criticized to possibly yield erroneous results (de Voogt and Saez, 2006).

2.2.1.2 Specific quantified methods

Fourier transform infrared spectroscopy (FTIR) was used to determine atmospheric telomer alcohols successfully (Ellis, *et al.*, 2003). By applying smog chamber, FTIR can be used to quantify telomer alcohols and olefins in atmosphere to study their atmospheric behavior and degradation mechanisms (Andersen, *et al.*, 2003; 2004; Hurley, *et al.*, 2004b; 2005). By coupling attenuated total reflectance (ATR), ATR-FTIR can quantify aqueous PFOS as low as 25 μg/L (Strauss, *et al.*, 2002; Hebert, *et al.*, 2004). Detection limits of FTIR for PFCs in water sample were several times higher than GC-MS or LC-MS and thus hindered its application in PFCs analysis.

Gas chromatography (GC) can directly determine neutral and volatile PFASs with high vapor pressures, such as sulfonamides, telomer alcohols, and olefins (Jahnke, *et al.*, 2006; Shoeib, *et al.*, 2006). Available derivatives consisted of benzyl ester or methyl iodide for PFASs, and butyl ester or diazomethane with PFOA (de Voogt and Saez, 2006). Although GC-chemical ionization MS (GC-CI-MS) can successfully determine airborne fluorinated sulfonamides and telomer alcohols (Martin, *et al.*, 2002), analysis of PFCAs was not satisfied because the necessary derivazation for amenable analysis was not reproducible on reaction yields (de Voogt and Saez, 2006). PFASs also had rather low vapor pressures and unstable derivatives (Hekster, *et al.*, 2002).

Liquid chromatography (LC) is more flexible for environmental sample analysis, especially for non-volatile trace organics. Conductimeter (Hori, *et al.*, 2004c) or fluorescence detector (Ohya, *et al.*, 1998) was reported to be able to quantify PFCs successfully. LC-electrospray ionization (ESI) -MS/MS is considered to be current standard method for analysis of trace level organics for its stability and reliable performance. Because most of researches applied LC-ESI-MS/MS for PFCs analysis, this topic will be specially discussed later (see 2.2.2).

2.2.1.3 Biological analysis for PFCs

Biological analysis is helpful to estimate toxicity of PFCs. The first bioassay of PFCs was report in 1977 for two kinds of air force fire-fighting foams (Wang, 1977). Some studies showed that zooplankton can be used as index to estimate PFOS toxicity (Boudreau, *et al.*, 2003; Sanderson, *et al.*, 2003; 2004). Microorganism like *Myriophyllum sibiricum* and *M. spicatum* as aquatic macrophytes can be applied to evaluate toxicity of PFOS (Hanson, *et al.*, 2005a) and PFOA (Hanson, *et al.*, 2005b) respectively. Eggs of sea birds were also possible to estimate temporal trends of PFOS in biota (Holmström, *et al.*, 2005).

2.2.2 LC-ESI-MS/MS analysis for PFCs

2.2.2.1 Introduction of LC-MS/MS analysis for PFCs

The separation limit of LC and detection limit of MS are similar and as low as pg level, which allows LC and MS integral system to determine trace level of organics. ESI was found the best interface for all LC-MS systems (Kuehl and Rozynov, 2003; Martin, *et al.*, 2004a). Ion-trap MS, triple quadrupole MS and high-solution TOF-MS were compared by their different performances on PFCs analysis. Triple quadrupole MS was most often applied in PFCs analysis. Ion-trap MS seemed more suitable for qualitative analysis and isomers identification. High-solution TOF-MS was considered optimum method for PFASs analysis, which offered both high selectivity and high sensitivity (Berger, *et al.*, 2004).

Although LC-MS showed satisfied performances on PFC analysis, strong interferences might occur in analysis as matrix effect. Therefore, if possible, tandem MS/MS was required to quantify environmental samples for its higher selectivity (Field, *et al.*, 2005). If only single quadrupole MS was available, more thorough clean up steps should be conducted to remove the interferences (de Voogt and Saez, 2006).

2.2.2.2 Development of LC-MS/MS analysis for PFCs

Table 2.5 has summarized LC-MS/MS analysis for PFCs in various matrices, which was arranged in as human blood, marine mammals, aquatic life, water environment and aerosol dust. Ion-pair method was the most popular pretreatment process for blood and biota samples, and solid phase extraction (SPE) was more important or necessary for water samples pretreatment. Reverse-phase C_{18} column was most popular for LC separation. Compatible guard column can effectively extend life of LC column, and was usually applied to protect LC column. Optimum LC mobile phase for polar PFCs was water and methanol, with pH buffer of ammonium acetate in different concentrations. Acetonitrile was also applied in some studies. Because methanol can enhance ionization (Maestri, *et al.*, 2006), application of water/methanol as mobile phase was helpful to alleviate strong ionization suppression which often happened in environmental sample analysis.

Analytical quality was controlled by spiking experiments. Limits of detection (LOD) and limits of quantification (LOQ) were quite different in these reports, which might be caused by qualities of instruments and different calculation methods. It seemed most methods can achieve satisfied limits and generate 70~130% in recovery rates, which is acceptable for trace level organics analysis. Internal standard was necessarily applied in PFCs analysis to compensate matrix effect from environmental samples. Isotopically labeled PFCs standards are currently available and applied in many studies. PFCAs in different carbon chain length, such as PFHpA and PFDoA, can also be internal standards, which are named as structurally similar internal standards. Problems of this kind of internal standards refer to their possible existence in environmental samples.

Table 2.5 Review of LC-MS/MS analysis for PFCs in environmental matrices

Ref.N.	Analyte	Matrix	Pretreatment	Stationary phase	[NH4Ac][a] /CH_3OH	IS	MS	LOD	LOQ	Recovery	No.	Location	Conc.	Unit
Calafat, et al., 2006	PFAS(6,8),PFCA(6,8~12),Et-FOSA,Me-FOSA	human serum	Online solid-phase extraction by Oasis-HLB column	Betasil C8 column (50×3 mm)	20 mM	^{18}O-PFOSA, ^{18}O-PFOS, ^{13}C-PFOA	TIS-MS/MS	0.05~0.2			54	US	PFOS=10.4~40 PFOA=2~7	ng/mL
Hansen, et al., 2001	PFOA, PFAS(6,8), PFOSA	human serum	TBAS-MTBE ion pair	Betasil C-18 50×2.1 mm	2mM	THPFOS	Q-ToF-MS/MS	1~2	~5		65		PFOS=28.4,PFOA=6.4,PFHxS=6.6	ng/mL
Harada, et al., 2004	PFOS,PFOA	human serum	TBA-MTBE ion pair, Filtration	Zorbax XDB-C18 (150×2.1 mm)	10mM /CH3CN		ESI-MS	0.04~0.06	0.1		225	Japan	PFOS=3.5~28 PFOA=2.8~12	ng/mL
Kannan, et al., 2004	PFAS(6,8),PFOA,PFOSA	blood,serum, plasma	TBAS-MTBE ion pair, 0.2µm nylon filter	Keystone Betasil C-18, 50×2 mm	2mM	PFBS	ESI-MS/MS		1~20	72~117%	473	10 countries	PFOS max. US/Poland >30, India <2	ng/mL
Kärrman, et al., 2005	PFAS(4,6,8,10), PFCA(6,8~12,14), PFOSA	human serum	Adjusted by formic acid, SPE by octadecyl column(C18)	Discovery HS C18 (50×2.1mm,4µm)	2mM	PFHpA	ESI-MS	0.1~0.5		64~112%	20	Swedish	0.3~194	ng/mL
Kärrman, et al., 2006	PFAS(4,6,8,10),PFCA(6~12,14),PFOSA	human serum	50% Formic acid extraction, centrifuge 10000rpm 30min, SPE by Bond Elut C18	Discovery HS C18 (50×2.1 mm, 3µm) with C18 guard column	2mM	7H-PFHpA, PFHpA, THPFOS	ESI-MS/MS	0.1~0.5	0.3~1.5	100~154%	3802	Australia	PFOS=20.8, PFOA=7.6, PFHxS=6.2	ng/mL
Kuklenyik, et al., 2004	PFCA(5~12),PFAS(6,8), PFOSA,Me-PFOSA, Et-PFOSA	human serum and milk	Formic acid adjust, automatic SPE by Oasis-HLB cartridge	Betasil C8 column (3×50 mm)	20mM	^{13}C-PFOA, THPFOS	TIS-MS/MS		0.1~1		20	US	PFOS=3.6~164,PFOA=0.2~10.4,PFHxS=0.4~11.2	ng/mL
Maestri, et al., 2006	PFOS,PFOA	human tissue	Acetonitrile extract, SPE by tC18, again by strong anion-exchange(SAX)	Waters XTerra,containing silica and organosiloxane		PFNA	ESI-MS	0.1		80~102%	7	Italy	PFOS=1~13.6,PFOA=0.3~1.8	ng/g
Olsen, et al., 2003	PFAS(6,8), PFOA, PFOSA, PFOSAA, M570, M560	human serum	Add NH4Ac, Votex agitation, MTBE	Genesis Lighting C18 (50×2mm , 4µm)	20mM	THPFOS	ESI-MS/MS				645	US	PFOS=4~1656	ng/mL
So, et al., 2006b	PFAS(4,6,8),PFCA(6~11),FTCA8:2,FTUCA8:2	human milk	Formic extraction, SPEby Oasis WAX, 0.2µm nylon filter	Keystone Betasil C-18, 50×2.1 mm	2mM	^{13}C-PFOA	ESI-MS/MS		1~10	78~105%	19	China	PFOS=45~360,PFOA=47~210, PFHxS=100, PFNA=62	ng/L
Yeung, et al., 2006	PFAS(4,6,8),PFCA(6,8~12),PFOSA	human serum	TBAS-MTBE ion pair, 0.1µm nylon filter	Keystone Betasil C-18 (50×2.1 mm) Zorbax XDB-C8 guard column (12.5×2.1 mm)	2mM	^{13}C-PFOA	ESI-MS/MS		0.2	55~96%	85	China	PFOS=3.7~79.2	ng/mL
Bossi, et al., 2005	PFAS(6,8),PFCA(8~11), PFOSA	seal liver	TBAS-MTBE ion pair	Betasil C-18 50×2.1 mm	2mM	PFHpA	ESI-MS/MS	o.2~1.2		80~110%	75	Greenland	PFOS=12.5~95.6, PFNA=1.8~4.9,PFDA=1.3~3.5,PFUnA=1.4~9	ng/g
Butt, et al., 2007	PFAS(6,8), PFCA(7~15), FTUCA(8,10):2	seal liver	TBAS-MTBE ion pair, Add HFP(hexafluoropropanol)	ACE C18 (50×2.1mm,3µm) C18 guard column (4×2 mm)	10mM	^{13}C-FTUCA(8,10):2 ^{13}C-PFCA(8~10) ^{13}C-PFOS	ESI-MS/MS				58	Arctic	PFOS=20~80, PFNA=1~5,PFDA=1~5,PDUnA=5~15	ng/g

Ref.N.	Analyte	Matrix	Pretreatment	Stationary phase	[NH4Ac][a] /CH_3OH	IS	MS	LOD	LOQ	Recovery	No.	Location	Conc.	Unit
Furdui, et al., 2007	PFAS(6,8,10),PFCA(7~15),PFOSA,FTUCA(8,10):2	trout body	TBAS+MTBE extraction, HFP centrifuge, 0.2μm PP filter	Genesis C18 (50×2.1mm,4μm)C18 guard column	0	^{13}C-PFCA (8~10), ^{13}C-PFOS, ^{13}C-FTUCA(6,8,10):2	ESI-MS/MS	1~16pg/g		>65%	46	US	PFCA=6.9~19, PFSA=5.8~130	
Gulkowska, et al., 2006	PFAS(4,6,8),PFCA(6~11)	sea food	TBAS-MTBE ion pair, 0.1μm nylon filter	Keystone Betasil C-18 (50×2.1 mm) with Zorbax XDB-C8 guard (12.5×2.1mm)		^{13}C-PFOA	ESI-MS/MS		0.25~1.7	67~102%	27	China	PFOS=0.6~13.9	ng/g
Hoff, et al., 2005	PFOS	carp etc.,liver	TBAS-MTBE ion pair	Keystone Betasil C-18 (50×1 mm) Optiguard C18 pre-column	2mM	THPFOS	ESI-MS/MS		10		81	Belgium	(Canal)=250~9031,(pond)=633~1822,(basin)=11~162	ng/g
Holmstrom, et al., 2005	PFOS,PFOA	guillemot eggs	TBAS-MTBE ion pair	Thermo Hypersil-Keystone C18(50×2.1 mm) with C18-precolumn(10×2 mm)	10mM		ESI-MS/MS	3			146	Sweden	PFOS=25->614, PFOA=ND	ng/g
Houde, et al., 2005	PFCA(7~15), FTUCA(8,10), PFAS(6,8), PFOSA	plasma of bottlenose dolphins	TBAS-MTBE ion pair	Luna 3μm C8 column (50×2 mm)	10mM	^{13}C-PFOA	API-MS/MS		0.3~0.8	71~155%	13	Atlantic	PFOS=49~1171	ng/g
Kannan, et al., 2002	PFAS(6,8), PFOA, PFOSA	liver and blood	TBAS-MTBE ion pair, 0.1μm nylon filter	Keystone Betasil C18 column,50×2mm	2mM		ESI-MS/MS		1~72	66~144%	175	Italy	PFOS=61(max.878 in Dolphin)	ng/g
Martin, et al., 2004c	PFOS,PFCA(8~15),PFOSA	trout liver	TBAS-MTBE ion pair	Genesis C8 (50×2.1mm)	10mM	PFHpA	ESI-MS/MS	2		~68%			PFCA=ND~90,t-PFOS=50~600	ng/g
Sinclair, et al., 2006	PFAS(4,6,8), PFOA, PFOSA	water, fish, and birds	Water-SPE by Oasis HLB, tissue-Ion pair TBA-MTBE	Keystone Betasil C-18 50×2 mm	2mM	PFBuS, 13C-PFOA	ESI-MS/MS		1.5~7.5	100±30%	204	US	PFOS(bird)=11~882,(fish)=9~315	ng/g
So, et al., 2006a	PFAS(4,6,8), PFCA(6~12),PFOSA	mussel and oyster	Alkaline digestoin, SPE by Oasis HLB	Keystone Betasil C-18 50×2.1 mm	2mM		ESI-MS/MS		2.6~63 pg	76~93%		China,Japan	PFOS=0.1~0.59,PFHxS=0.06~0.5,PFBuS=0.009~0.03,PFOSA=0.04~2.96	ng/g
Tao, et al., 2006	PFAS(6,8,10),PFCA(7~11),PFOSA	liver,blood, egg	TBAS-MTBE ion pair	Keystone Betasil C-18 100×2.1 mm	2mM	PFBS,^{13}C-PFOS,^{13}C-PFOA	ESI-MS/MS		0.05~2.5		181	Southern Ocean	PFOS(liv)=2.2~5.1,(egg)=2.1~3.1,(bld)=0.2~1.4	ng/mL, ng/g
Tseng, et al., 2006	PFCA(8,10), PFOS	tissue	TBAS-MTBE ion-pair	Betasil C-18 50×2.1 mm	1mM	PFDoA	ESI-MS	2.5~25 dry	5~50 dry		9	Taiwan	t-PFC=ND~1100	ng/g
van de Vijver, et al., 2003	PFOS, PFCA(8~10)	maine mammal tissue	TBAS-MTBE ion pair	Betasil C-18 50×1 mm	2mM/CH_3CN	THPFOS	ESI-MS/MS		10~110	61~110%		North sea	PFOS=470~178550;PFNA=90~270;PFDA=50~120;PFUnA=30~150	ng/g
Verreault, et al., 2005	PFAS(6,8), PFCA(8~15)	gulls plasma, liver, brain	tissue - TBA-MTBE ion-pair	Luna 3μm C8 column (50×2mm)	10mM/10mM	^{13}C-PFOA	ESI-MS/MS			60~141%	33	Arctic	tPFOS=48~349,PFCA=42~262	ng/g
			2 mM NH4OAc/methanol, agitation, directly injection	ACE C18 column 150×2.1 mm	2mM/2mM	7HPFHpA, 3,5-BTPA	ToF-HRMS/MS							

Ref.N.	Analyte	Matrix	Pretreatment	Stationary phase	[NH4Ac]^{a} /CH_3OH	IS	MS	LOD	LOQ	Recovery	No.	Location	Conc.	Unit
Boulanger, et al., 2004	PFOS,PFOSi,PFOA,PFOSAA,FOSA,EtFOSAA,EtFOSE,EtFOSA	lake water	Filtration, SPE by Alltech C18 Extract-Clean High Capacity Cartridge	Zorbax Extend C18 column (150×2.1mm) Narrow Bore C18 Guard(12.5×2.1mm)	2mM		MS, (IT)-MS/MS	2~6	0.6~13	56~176%	16	Great Lakes	PFOS=21~70,PFOA=27~50,EtFOSAA=4~11	ng/L
Hansen, et al., 2002	PFOS,PFOA	tap&surface water	Centrifuge, SPE	Keystone Betasil C-18, 50×2.1 mm	2mM		ESI-MS/MS	5~25	10~50	83~112%	40	US	PFOS=27~144,PFOA=25~598	ng/L
Harada, et al., 2003	PFOS	tap&surface water	Filtration, SPE by Prep-C Agri C18	Zorbax XAD C18 column (150×2.1mm)	10mM/CH_3CN		ESI-MS				23	Japan	(Up)=0.7~8,(WWTP)=300~440,(Down)=36~157,(Drink)=0.1~4(max.51)	ng/L
Loewen, et al., 2005	FTCA(6,8,10):2, FTUCA(6,8,10):2, PFOS,PFCA(8~12)	rain water	extract by 5g C18 silica gel, elute by CH3OH, evaporate	DiscoveryC18 analytical column 50×2.1mm	0	^{13}C-FTCA 10:2, ^{13}C-FTUCA10:2, PFMe2OA	ESI-MS/MS	0.08~1.1					PFOS=0.59,PFCAs=ND	ng/L
Moody, et al., 2002	PFAS(4,6,8),PFCA(5~12,14)	surface water, fish liver	TBAS+MTBE extraction, 0.2μm nylon filter	Genesis C18 (50×2.1mm,4μm),C18 guard column	10mM	PFDoA	ESI-MS/MS	0.01~0.03		68~93%	55	Canada	PFAS(fish)=2~73,(river)=ND~2260;PFCA(fish)=0.07~1,(river)=ND~113	μg/L
Saito, et al., 2003	PFOS	surface water	Filtration, SPE by Prep-C Agri C18	Zorbax XDB-C18 guard column 150×2.1 mm	10mM/CH_3CN		ESI-MS	0.1		75~105%	142	Japan	(river)=0.3~157,(coast)=0.2~25.2,(Ara,Tama,Yodo)=0.7~157	ng/L
Saito, et al., 2004	PFOS,PFOA	surface water	Filtration, SPE by Prep-C Agri C18	Zorbax XDB-C18 guard column 150×2.1 mm	10mM/CH_3CN		ESI-MS	0.04~0.06		92~106%		Japan	PFOS=0.2~67000,PFOA=0.6~526	ng/L
Schultz, et al., 2004	PFAS(4,6,8), FTS(6,8,10):2	Groundwater by AFFF	Direct injection	Betasil C-18 150×2 mm	0	Hexafluoroglutaric acid	FAB-MS/MS		0.3~0.6	89~120%	182	US	t-PFC=182~14600	μg/L
Skutlarek, et al., 2006	PFAS(4,6,8), PFCA(4~12)	river,drinking water	SPE by Strata-x column (200mg)	Nucleodur Sphinx-RP (150×2mm, 3μm)	10mM/CH_3CN-CH_3OH	^{13}C-PFOS, ^{13}C-PFOA	ESI-MS/MS	2		62~117%	38	Germany	(river)av.PFC=~94, tPFC=446~4385,(Drk)tPFC=598,PFOS=519	ng/L
Takino, et al., 2003	PFOS	river water	online extraction by TFC	Zorbax Eclipse XDB C18 (150×4.6mm)	10mM		APPI-MS	5.4	18					ng/L
Tseng, et al., 2006	PFCA(8,10), PFOS	wastewater	SPE by RP-C18 (Supelclean ENVI-18 SPE)	Betasil C-18 50×2.1 mm	1mM	PFDoA	ESI-MS	0.2~2	0.5~6		9	Taiwan	t-PFC=ND~400	ng/L
Weremiuk, et al., 2006	PFOS,PFOA	river water	centrifuge 12000rpm, Filtration, SPE by Oasis HLB	ACE-EPS C18 (150×2mm)	10mM		ESI-MS/MS	0.05		69~83%		Germany	PFOS(Up)=3.4,(Do)=14.5,PFOA(Up)=2.4,(Do)=12	ng/L
Yamashita, et al., 2004	PFAS(4,6,8),PFCA(8,9), PFOSA	ocean water	Sep-pak tC18, Oasis HLB for SPE	Betasil C-18 50×2.1 mm (XDB-C8guard column)	2 mM	THPFOS	ESI-MS/MS	0.4~5.2pg		16~124% 82~137%	20	Pacific & Altantic	PFOS=12.7~25;PFHxS=3.3~5.6;PFOA=154~172	ng/L
Yamashita, et al., 2005	PFAS(4,6,8),PFCA(8~9),PFOSA	ocean water	HLB-SPE, wash by 40% CH3OH, elute by CH3OH, 0.2μm nylon filter		2 mM	THPFOS	ESI-MS/MS				87	Global ocean	PFOS=0.3~57;PFOA=2~192;PFNA=0.2~71. (highest in Tokyo bay)	ng/L

Ref.N.	Analyte	Matrix	Pretreatment	Stationary phase	[NH4Ac]^{a} /CH_3OH	IS	MS	LOD	LOQ	Recovery	No.	Location	Conc.	Unit
Boulanger, et al., 2005	PFOS,PFOA,PFOSA,PFOSAA,EtFOSA,PFOSi	WWTP inf.,eff.,river	SPE by Oasis HLB	Zorbax SB C8 column, 150×3 mm	0.15%HAc/CH_3OH-CH_3CN		ESI-MS/MS	2~6		72~92%		US	PFOS(eff)=26,(river)=23, PFOA(eff)=22,(river)=8.7	ng/L
Higgins, et al., 2005	PFAS(6,8,10),PFCA(8~12,14),FOSAA,MeFOSAA,EtFOSAA	sludge, sediment	cycling extraction by 1% HAc in 90% CH3OH, in ultrasonic cleaner	Targa Sprite C18 column (40×2.1 mm),C18 guard column	2mM		ESI-MS/MS	0.7~2.2 (sldg) 0.04~0.25(sedi)		65~97%		US	PFCA=5~152, PFAS=55~3370	ng/g dry
Schröder, 2003	PFOS, PFOA, anionic and nonionic surfactant	sewage sludge	Soxhlet extraction, hot steam extraction and pressurised liquid extraction (PLE)	Multospher 100 RP 5-5 C8(250×4.6 mm) PF-C8 column (150×4.6 mm)	0		ESI-MS		10~20	105~120%		Germany		µg/g
Schultz, et al., 2006	PFAS(4,6,8,10), PFCA(6~10), 6:2FTS, FOSA	Inf. and Eff. of WWTP	Direct injection, 500µL	Betasil C-18 (150×2 mm),C-18 guard cartridge (4×3mm)	2mM	^{13}C-PFOA	ESI-MS/MS		0.5 ng/L	82~100%	20	US	PFOS(inf)=1.7~89,(eff)=2.5~97;PFOS(inf)=1.4~40,(eff)=1.1~13	ng/L
Zhao, et al., 2007	PFOS, PFCA(4,6~10)	wastewater, riverwater, tapwater	SPE:CTAB-coated silica or SDS-coated alumina.Nylon membrane filtration	Acclaim 120 C18,(150×4.6mm)	100 mM		ESI-MS/MS	0.05~0.28		57~112%		China	river=0.7~7.9;wastewater=0.3~5.5	ng/L
Powley, et al., 2005a	PFCA(6~12,14)	soil,sediment and sludge	CH3CN + NaOH digestion, agitation, Envi-Carb graphitized carbon adsorb matrix	Zorbax Rx-C8, 15cm×2.1mm	0.15% HAc/CH_3CN	13C-PFOA	ESI-MS/MS		1	70~120%				µg/L
Powley, et al., 2005b	PFOA	pans,cookwares	100℃ extraction by water, C18-SPE/ASE by ethanol/water	2.1mm×50mm, 4µm Genesis C8	2 mM	13C-PFOA	ESI-MS/MS		100					pg/cm2
Sasaki, et al., 2003	PFOS	air dust	vaccum 1400m3 air, ASE-200 extraction, SPE by C18	Zorbax XBD C18, 150×2.1 mm	10mM		ESI-MS		0.1µg/L		12	Japan	PFOS=38~427	ng/g
Moriwaki, et al., 2003	PFOS,PFOA	vaccum dust	CH_3OH + Ultrasonic extract, centrifuge, filtreation 0.2µm	TOSOH TSK-GEL ODS-80TsQA (150×2 mm)	1mM	SDS-d25	ESI-MS/MS	0.1~0.5	10~50	73~89%	16	Japan	PFOS=11~2500,PFOA=69~3700	ng/g
Young, et al., 2007	PFOS,PFCA(8~12)	ice	SPE by C18 cartridge	Genesis C18 (50×2.1mm,4µm) with C18 guard column	0	^{13}C-PFCA (8~11), ^{13}C-PFOS	ESI-MS/MS					Arctic	PFOA=114~587,PFOS=18~48,PFNA=73~860	kg/y

Note: ***a*** = 2mM means 2mM NH4Ac in water / pure methanol

Strong efforts have been contributed to improve analytical qualities (Risha, *et al.*, 2005; van Leeuwen, *et al.*, 2006). One research involved 38 participating laboratories from 13 countries to estimate analysis diversity of PFAS(4,6,8), PFCA(4,6~12) and perfluorooctane sulfonamide (PFOSA) in five kinds of matrices. Agreements of analysis between different laboratories were decreased in sequence of human blood> human plasma> fish liver> water> fish muscle. The poor results for fish tissues and water samples indicated that improvement was required to extract and cleanup these kind samples (van Leeuwen, *et al.*, 2006). Improvement of matrix effect control could be achieved by applying new extraction materials (Zhao, *et al.*, 2007), by refined cleanup process (Schröder, 2003; Powley, *et al.*, 2005a), or by directly elimination of pretreatment steps in large-volume-injection method (Schultz, *et al.*, 2006a). More information about PFCs analytical quality control was available in some critic reviews (Martin, *et al.*, 2004a; de Voogt and Saez, 2006; Marta, *et al.*, 2006; van Leeuwen and de Boer, 2007).

2.2.3 Pretreatment methods for PFCs analysis

Because sensitivity and selectivity of instruments are usually fixed and difficult to improve, optimization of pretreatment methods are important or even the only choice to improve analysis qualities. There were many possible pretreatment methods to extract analytes from matrix and clean up interferences as shown in **Table 2.5**, which were summarized in **Figure 2.2** by different matrices.

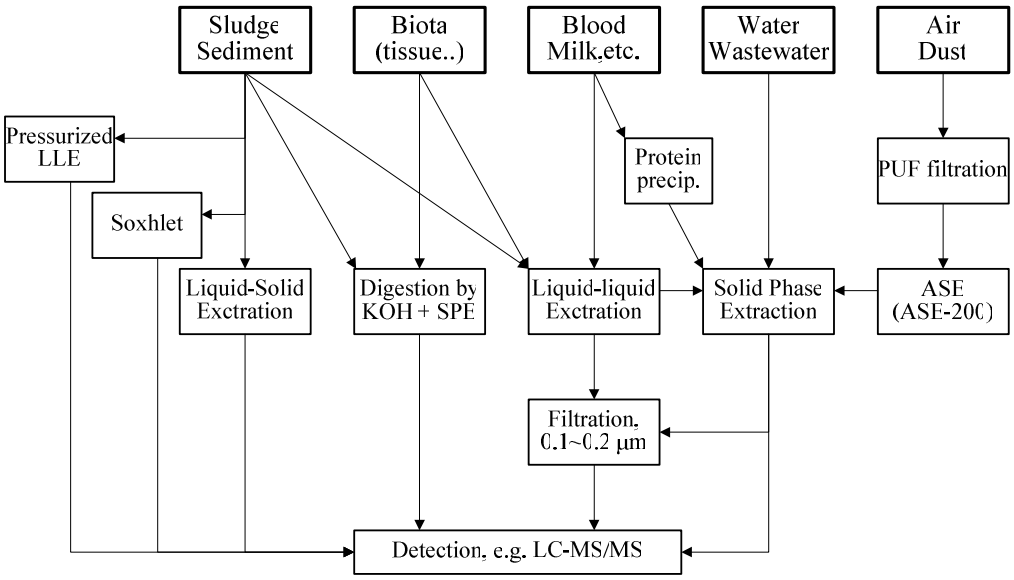

Figure 2.2 Sample pretreatment methods for PFCs analysis

Ion-pair extraction (IPE) was firstly developed for PFCs analysis in biomatrix (Hansen, *et al.*, 2001), and soon expanded to analyze blood, sludge and sediments (Schultz, *et al.*, 2006b). IPE process is very simple and easy for operation, but sometimes it suffers from low extraction efficiency. Solid phase extraction (SPE) by C_8/C_{18} cartridge or silica gel showed reliable performance to concentration trace level of PFCs and clean up strong matrices, which were popularly applied for PFCs analysis in blood, water and air samples. A new cartridge, oasis weak anion-exchange (WAX), was developed by Waters Company for PFCs analysis and successfully applied in biota samples (Taniyasu, *et al.*, 2005).

Extraction of PFCs from sludge and sediments are difficult because of the complexity of solid surfaces. Although pressurized liquid extraction (PLE), soxhlet extraction and liquid-solid extraction (LSE) showed good performances on PFCs extraction (Schröder, 2003), complicated operations usually limited their

applications in PFCs analysis. Many studies applied simple and easy IPE to extract PFCs in solid. Alkaline digestion and formic acidification can both neutralize and precipitate proteins and lipids by adjusting pH, and therefore to clean up sample matrix. In strong basic solution, proteins were negative charged and binding PFCs would be released into aqueous phase. This method was optimized to analyze PFCAs and PFASs in biota and sludge samples (Taniyasu, *et al.*, 2005).

2.3 Environmental behavior of PFCs

2.3.1 Source, sink and fate of PFCs

Estimation of PFCs source, sink and fate in environment is necessary and useful to understand behavior of PFCs in the environment. Some reports and reviews on this topic were available in literature (Hekster, *et al.*, 2002; OECD, 2002; US EPA, 2002; 2003; Brooke, *et al.*, 2004; Footitt, *et al.*, 2004; 2005; Lange, *et al.*, 2006; Prevedouros, *et al.*, 2006; UNEP, 2006). Sources of PFCs were considered mainly from industrial discharge, as well as degradation of PFC derivatives. Major industrial emissions were suspected from fluoropolymer manufacturing and aqueous fire-fighting foam production. Global emission of total PFCAs was estimated to be 3,200~7,300 tons to environment (Prevedouros, *et al.*, 2006) and those of PFASs was 4,650 tons per year in last decade (Footitt, *et al.*, 2004). Sink of PFCs was expected to be deep ocean transfer for PFCAs (Yamashita, *et al.*, 2005) and biota accumulation and sorption for PFASs, as well as combustion and thermolysis degradation.

Degradation of volatile PFC derivatives was suspected to be another source of PFCs in the environment. PFC derivatives can transport in atmosphere and precipitate in remote areas to result global distribution. This hypothesis was supported by the detection of PFAS-related precursors in precipitation in Canada (Loewen, *et al.*, 2005). PFC-related precursors can generate PFCs during degradation by biological or other processes, *e.g.* from PFOSA to PFOS and from 8:2FTOH to PFOA. Degradation of PFAS precursors was proposed to explain the increase of PFOS concentration after overall processes in WWTP (Higgins, *et al.*, 2005; Schultz, *et al.*, 2006b). Volatile PFCA derivatives were also hypothesized to transport by atmosphere to arrive remote areas (Ellis, *et al.*, 2004b; Hurley, *et al.*, 2004a; 2004c; Armitage, *et al.*, 2006; Martin, *et al.*, 2006). Behavior of PFCAs in atmosphere was complicated. A three-dimensional global atmospheric chemistry model (IMPACT) indicated that 8:2FTOH can be degraded in atmosphere to form PFOA and other PFCAs (Wallington, *et al.*, 2006), which supports fluorotelomer alcohols to be a significant global source of PFCAs pollution (Renner, 2006a). Telomer alcohol as 8:2 FTOH was found to degrade into telomer acids and PFOA(8) in aqueous phase as well as in atmospheric environment. In anaerobic aqueous environment, telomer alcohol was oxidized to telomer acid via β-oxidation and further transformed to unsaturated acid and ultimately produced PFOA(8) (Dinglasan, *et al.*, 2004). Direct evidence for degradation of telomer alcohol to PFCAs in aqueous environment was obtained in laboratory activated sludge systems (Wang, *et al.*, 2005a; 2005b). In order to elucidate behavior of PFCs in environment, more data and studies are required.

2.3.2 PFCs contaminations in water environment

Surface water in developed countries and industrialized areas were usually highly polluted by PFCs, such as US (Hansen, *et al.*, 2002; Takino, *et al.*, 2003), Japan (Saito, *et al.*, 2003; 2004), Germany (Skutlarek, *et al.*, 2006) and coastal China (So, *et al.*, 2004). Direct discharge from industries and consumption of aqueous fire fighting foam (AFFF) were considered as main sources of PFCs in surface water (Moody, *et al.*, 2002; Saito, *et al.*, 2004). Drinking water in these areas was also polluted by PFCs.

Occurrence of high concentrations of PFCs in tap water indicated poor performances of current water treatment processes to remove PFCs from surface water (Saito, *et al.*, 2003; 2004; Skutlarek, *et al.*, 2006). Investigation of surface water in East Asia demonstrated very high pollution of PFOA in Japan (Yamashita, *et al.*, 2004) and PFOS in Korea and China (So, *et al.*, 2004). These contaminants caused further pollution in biota, such as marine mammal (So, *et al.*, 2006a; Tseng, *et al.*, 2006) and sea food (Gulkowska, *et al.*, 2006). Similar situation was found in New York area of US (Sinclair, *et al.*, 2006).

Groundwater was very easy to be polluted by PFCs because most PFCs could strongly adsorb to particles. Very high concentrations of PFCs were often detected around spots where AFFF was consumed (Saito, *et al.*, 2004; Schultz, *et al.*, 2004). AFFF often coexisted with priority pollutants like jet fuels and chlorinated solvents, which made study on their environmental fates quite complicated (Moody and Field, 2000). Water in lakes has rather long retention time and also very easy to be contaminated by PFCs. Current study on Great Lakes in North America revealed ubiquitous distributions of PFCs in water (Boulanger, *et al.*, 2004) and aquatic life (Furdui, *et al.*, 2007). The distribution patterns and original sources were also identified by isotopic analysis which had been successfully applied in ocean water (Van de Vijver, *et al.*, 2003).

2.3.3 PFCs contaminations in biota sphere

Globally distribution of PFCs was firstly reported in wildlife (Giesy and Kannan, 2001). Later studies showed more evidences on their global distribution in biota (Berger and Haukas, 2005), including PFCs distribution in Arctic animals (Martin, *et al.*, 2004b). Higher contaminations of PFCs in serum of pandas from zoos were detected than in serum of pandas from rural zones, indicating higher exposure at industrial areas (Dai, *et al.*, 2006). Contaminations of PFCs in wildlife were in different patterns and caused by multiple sources (Hoff, *et al.*, 2005; Houde, *et al.*, 2006b).

PFCs were detected in marine mammals everywhere (Kannan, *et al.*, 2002; Bossi, *et al.*, 2005; Houde, *et al.*, 2005; Butt, *et al.*, 2007), including South Pacific Ocean (Tao, *et al.*, 2006) and polar bear in Arctic Ocean (Smithwick, *et al.*, 2005). PFASs, mainly PFOS, were found dominant in most species because of its rather high BAFs (Kannan, *et al.*, 2002). However, long-chained PFCAs (9~15) entered scientific visions because of their similar BAFs with PFOS (Bossi, *et al.*, 2005; Verreault, *et al.*, 2005). Studies on temporal trends of PFCs in human, fish, bird, and marine mammal samples indicated that exposure of PFCs increased significantly over the past 15~25 years. For example, PFOS in Swedish guillemot eggs increased 7~11% per year during 1968~2003 (Holmström, *et al.*, 2005).

2.3.4 PFCs contaminations in humans

PFCs were often detected in human blood, serum and plasma (Hansen, *et al.*, 2001), as well as in tissues (Maestri, *et al.*, 2006). PFCs in human serum seemed directly correlated with contaminations in surface water or drinking water, which were highly suspected to be caused by local industrial emissions. People in US (Olsen, *et al.*, 2003; Calafat, *et al.*, 2006) and Korea were estimated to have highest concentration of PFOS in blood (>30 ng/mL) among eleven countries, while Indian people had the lowest concentration as 3 ng/mL (Kannan, *et al.*, 2004). Contamination of PFOA was identified in human serum of residents in Osaka and Kyoto of Japan (Harada, *et al.*, 2004), and very high concentrations of PFOS were detected in blood of people living in coastal cities of China. Despite of these locations with point source, however, PFCs were also detected in countries which only consume PFC products, such as Australia (Kärrman, *et al.*, 2006) and Sweden (Kärrman, *et al.*, 2005).

PFCs were detected in human milk in Australia (Kuklenyik, *et al.*, 2004) and China (So, *et al.*, 2006b), indicating very high exposure to infants. PFCs distributions in air dust (Moriwaki, *et al.*, 2003; Sasaki, *et al.*, 2003), WWTP (Boulanger, *et al.*, 2005; Weremiuk, *et al.*, 2006), snow (Young, *et al.*, 2007) and cookware (Powley, *et al.*, 2005b) were also determined which might be exposed to human directly or indirectly. Control and reduction of PFCs in industries and environment are in great need for purpose of human health and environmental safety.

2.4 Solutions for PFCs contamination

2.4.1 Alternatives of PFCs

2.4.1.1 Shorter chain PFCs

Scientists tried to develop replacements of long-chained PFCs by shorter-chained PFCs because latter compounds have less toxicity and bioaccumulation. PFBuS(4) derivatives have been identified as alternatives for PFOS(8) for repellent, cleaning agents, waxes, floor polishes and *etc.*. By addition of extra hydrocarbon group, PFBuS(4) moiety can stand on surface and perform as well as PFOS(8) moiety. 3M Company was the first to adopt shorter-chained PFCs to produce PFCs. After its phase-out of PFOS product, 3M Company issued a non-perfluorochemical product to replace Scotchgard which can only works on water. Since June in 2003, 3M Company has applied PFBuS(4) for its polymer production for new Scotchgard (Renner, 2006c). Carbon chain length of PFC moiety can be further reduced in industrial products. PolyFox fluorosurfactant, an environmental friendly chemical made by OMNOVA Solution Inc., attached as many as 20 of CF3- or CF3CF2- groups at the end of each polyether backbones to perform as well as former chemicals, and was considered as currently best alternative to C8 surfactants (Renner, 2006c). Fluoropolymers were also used as alternatives for monomers, because degradation and PFCs releasing of polymer can be considered negligible. For example, fluorotelomers were used in impregnation for textile, carpet, paper coating and floor polisher (Poulsen, et al., 2005).

2.4.1.2 Non-fluorine alternatives

Non-fluorine surfactants and polymers can also be applied to alternate long-chained PFCs. In case of repellents, propylated aromatics made by Rütgers Kureha Solvents, such as naphthalenes and biphenyls, were available to take place of PFC polymers. Silicone surfactants or surfactants based on aliphatic alcohols were proposed to replace fluorosurfactants in some cases. For example, silicone polymers made by Worlée-Chemie as wetting agents can alternate PFOS(8), as well as sulfosuccinates in paint and varnish fields (Poulsen, *et al.*, 2005). Despite of alternatives, new manufacturing process was developed in semiconductor industries to completely avoid usage of PFOS (Poulsen, *et al.*, 2005).

In case of aqueous fire-fighting foams (AFFF), silicone and hydrocarbon based surfactants were available as alternatives. However, they usually cannot acquire the necessary performances without addition of fluorosurfactants (Poulsen, *et al.*, 2005). Therefore, PFHxS(6) based surfactants might be the only practical alternatives for AFFF. Another proposal was protein-based foams which was a previous technology and abandoned before (Moody and Field, 2000).

In summary, nowadays most popular alternatives are C_4 and C_6 perfluorinated derivatives, which have less toxicity and bioaccumulation in environment. Silicon and hydrocarbon based surfactants and polymers are also available to substitute PFCs in some applications, but they encounter problems like low efficiencies or unsatisfied performances.

2.4.2 Wastewater treatment processes

PFCs in environment were suspected mainly from industrial production (Armitage, *et al.*, 2006), and rather high PFC concentrations have been detected in locations around industrial point source, such as 3M in Minnesota (3M Chemolite, 2005; Oliaei, *et al.*, 2006), DuPont in New Jersey and West Virginia of USA (Corporate Remediation Group of DuPont and URS Diamond, 2003; Welcker, 2006), and some industries in Yodo River basin of Japan (Lien, *et al.*, 2006). In these areas, reduction of PFC emissions from industries and improvement of WWTP performance are important to control PFCs contaminations.

2.4.2.1 Industrial recycling processes

Since 1970s (Seki and Sato, 1975; Rudolph and Massonne, 1977), several techniques have been developed or applied to recover and recycle industrial materials containing PFCs in polymerization process (Sulzbach, *et al.*, 1999; Jones and Fu, 2004; Ferrero and Deregibus, 2006). Most of them showed satisfied recoveries to extract PFCs from waste stream or exhaust gas, as described in **Table 2.6**. These processes mainly consisted of four major steps, including *pretreatment*, *concentration*, *extraction* and *elution*. By these four steps, hundreds mg/L of PFC surfactants could be recycled by recovery rates over 95%. However, the discharge of wastewater from PFCs recycling processes still contained several mg/L (about 2~10 mg/L) PFCs, which should be further removed before discharging to the environment.

In *pretreatment* step, solids in waste stream of polymerization process were properly removed by washing process, filtration, acidification or non-ionic surfactant stabilization. Fluorine ions in aqueous phase were also precipitated by aluminum to reduce their adverse effects on quality of recycling reagents (Schultz, 2001). In case of exhaust gas, washing procedure was necessary to trap PFCs into water stream.

In *concentration* step, PFCs in aqueous phase were accumulated to rather high concentrations for further extraction process. This step was very useful and important for PFC dilute solutions. Recycled washing of exhaust gas by scrubbing solution can concentrate PFCs from aerosol phase into aqueous phase as high as 20 wt%. Reverse osmosis (RO) was a promising and reliable method to accumulate PFCs in aqueous phase to more than 30 wt% (Jones and Fu, 2004). Oxidation of telomers or related intermediates under higher temperature can generate 99 wt% of PFOA solution for successive extraction step (Rudolph and Massonne, 1977)

In *extraction* step, PFCs were transported between different phases, usually from aqueous phase to adsorbent. Weak basic anion-exchange resin was optimized to extract PFCs from aqueous phase and to elute them for reuse (Seki and Sato, 1975; Felix, *et al.*, 2003; Burkard, *et al.*, 2004; Hintzer, *et al.*, 2006). Activated carbon and silica gel can also extract PFCs from concentrated solutions, which were alternatives for anion-exchange resins (Rudolph and Massonne, 1977; Bec, 2006). Other methods referred to construct organics layer or metal hydroxide precipitation in aqueous phase to extract PFCs. Organics layer can be formed in diluted solutions by distillation at 60℃, which was a little bit higher than melting points of PFCs (Schultz, 2001). PFCAs were firstly esterified with excessive alcohols like methanol, and the ester was separated successively in organic layer formed by distillation (Obermeier and Stefaniak, 1995). By addition of base and hydrogen donors, PFCs can be accumulated and extracted into additive layer during thermolysis procedure at about 200℃ (Shtarov, *et al.*, 2006). By addition of divalent or trivalent salts, layered double hydroxides were formed to accumulate PFCs and then precipitated from aqueous solutions (Sulzbach, *et al.*, 1999; Fuda, *et al.*, 2004). These processes were more promising than resins because of simple equipment and no requirement of column regeneration.

Table 2.6 Summary of PFC recycling processes in the industries [a]

Citation [b]	*Target*	*Reactor*	*Process Description*	*Demerit*	*Removal*
Seki, 1975	Emusifier	Resin column	Wash polymer (NaCl solution) → Acidify (pH4) → Resin adsorption (weak basic anion-exchange) → Acid wash → Elute by NH_4OH	Incomplete recovery	89~95%
Rudolph, 1977	Telomer, PFCIs	Distiller + Column	Oxidation (Oleum/Cl_2 +ZnS+elevated T) → Liquid (99% PFCA) → Adsorpton (Silica gel) → Elution (weak/strong solvent) → Regenrate	Heat	>99.5%
Obermeier, 1995	Emusifier	Distiller + Sep. vessel	Release PFOA (60% H_2SO_4) → Esterlfication (CH_3OH and PFOA) → Distillation (70℃) → Separation → Hydrolysis (NH_4OH)	Addition of PFOA	<10 mgF/L
Schultz, 2001	Dilute soluton	Distiller + Sep. vessel	Remove F^- (AlF_3) → Acidify (pH4) → Distillation (60℃, organic / water layer) → Wash organic layer (Acid) → Elute by NH_4OH	Large NH_4OH, operation	<7 mgF/L
Felix, 2003	Emusifier +solids	Resin column	Stablization in solid (non-ionic surfactant) → Resin adsorptoin (Strong base anion-exchange resin) → Elution (87%CH_3OH, 7% H_2SO_4)	Incomplete recovery	>95%
Fuda, 2004	Dilute soluton	Sep. vessel	Additives (pH8,metal salt) → Coagulation (Layered double hydroxide) → Seperation (Precipitation) → Dissolve (pH<1, reuse)	Waste of metals	>98%
Bec, 2006	Dilute soluton	Filter +RO +GAC bed	Remove solid (Filtration,coagulation) → Concentration (series of RO unit) → Adsorption (PAC/GAC-bed) → Elution (CH_3OH+H_2SO_4)	Complicated equipments	>98%
Shtarov, 2006	PFCA, FTOH	Oven + Vaccum	Additives (Bronsted base, H-donor) → Thermolysis (~195℃) → Seperation (Additives layer) → Vaccum Drying (Recover PFCs)	High temperature	>98%
Sulzbach, 1999	Exhaust gas	Scrubber + Sep. vessel	Wash exhaust gas (high density alkaline) → Precipitation (Add metal salt) → Further clean-up and recycling	Waste of metals	<1mg/m3
Jones, 2004	Exhaust gas	Scrubber + RO+Al-bed	Wash exhaust gas (pure water) → Concentration (Seires of RO units) → Adsorption (Alumina) → Elution (Reuse)	Complicated equipments	<2 mgF/L

Note: ***a*** = summary from US Patents; ***b*** = only first author is shown in the column.

In *elution* step, PFCs were washed out from adsorbents for recycling, and the adsorbents are regenerated simultaneously. For weak basic anion-exchanger, aqueous ammonia performed the best to elute strong PFCAs and regenerate resins (Seki and Sato, 1975; Kuhls, 1981; Obermeier and Stefaniak, 1995; Schultz, 2001). In case of activated carbon and silica gel, multi-solution like methanol and sulfuric acid was necessary to elute PFCs and regenerate adsorption capacities.

2.4.2.2 Industrial wastewater treatment processes

Despite of these recycling processes for industrial production, some removal techniques were also available to treat high concentration PFCs in industrial wastewater. GAC filtration was proved effective to control industrial discharge by 3M Company, who constructed a treatment plant with 18 large GAC vessels to remove PFOA(8) from WWTP effluent. The removal efficiency of GAC column was more than 99% of 2 mg/L PFOA (3M Chemolite, 2005). Another effective filtration method was RO membrane filtration, which can treat 0.5~1500mg/L PFOS in semiconductor wastewater by efficiencies over 99% (Tang, *et al.*, 2006; 2007).

Precipitation was helpful to remove PFCs from wastewater, *e.g.* electronic precipitation (EP) which was often applied to remove heavy metal or recover phosphorous. In preliminary experiments in this study, EP was found to be able to remove several tens μg/L of PFOA and PFOS effectively from pure water and wastewater. Similar with recycling process in high concentration, layered double hydroxides precipitation can also effectively remove low concentration of PFOA in wastewater (Yang, *et al.*, 2006).

PFC molecules tend to be accumulated on interface of phases and thus aeration is possible to physically

remove PFCs from water by adsorptive fine bubbles (Zhang, *et al.*, 2005a). One commercial unit was Air-Sparged Hydrocyclone (ASH), which was developed by this mechanism to recover AFFFs in US airforce of navy. ASH can remove 70~90% of PFC surfactants by centrifugation after introduction of flocculent and high-pressure air bubbles (Schultz, *et al.*, 2003).

Although some techniques are available for industrial wastewater, they were not popularly applied and the discharge also contains high level of PFCs, which requested reliable performance of wastewater treatment plant (WWTP) for further removal. Therefore, municipal wastewater treatment process should be seriously considered for this critic situation.

2.4.2.3 Municipal wastewater treatment processes

Behavior of trace level PFCs in WWTPs was expected quite different to industrial wastewater. PFCs analysis in wastewater and sludge was difficult because of strong matrix and low efficiency of extraction in pretreatment. Current studies are still not enough to draw general and reliable conclusions on PFC behavior in WWTP. Few articles have been published on PFC behavior in WWTP, as shown in **Table 4.1**. In most studies, only the influent and effluent were analyzed to estimate performance of overall process. There was only one study which estimated performances of individual facilities in activated sludge process to reveal the first and interesting vision of PFC behavior inside WWTP (Schultz, *et al.*, 2006b).

A survey in ten US WWTPs showed no obvious removal of PFOS(8) in ten plants except one WWTP with influent as high as 400 μg/L. PFOA(8) in effluent of seven WWTPs was increased by 10~100% of influent which contained 16~49 μg/L PFOS (Schultz, *et al.*, 2006a). Surveys of WWTPs in Iowa of US also showed no removal of PFOS(8) and PFOA(8), as well as other PFCs (Boulanger, *et al.*, 2005; Sinclair and Kannan, 2006). Studies in WWTP of Japan obtained similar results of poor or even negative removal of PFOA and PFOS by activated sludge process (Nozoe, *et al.*, 2006). These results implied that activated sludge process might be ineffective to remove PFOS(8) or PFOA(8), and certain amount of PFCs was discharged from WWTPs to environment. PFCs precursors like telomer alcohols, sulfonamides or esters were suspected to degrade to PFASs and PFCAs during activated sludge process. In one study, Trickling filter was considered as one source of PFOS(8) by degradation of precursors (Schultz, *et al.*, 2006b), which implied that filtration might be also ineffective to remove PFCs.

Physical adsorption processes

Anion-exchange resin was popular adopted in industrial recycling process and also possible to apply in municipal WWTP. Ion-exchange resin column could concentrate PFOS and PFOA from wastewater by factor of 181, which was much higher than GAC adsorption (Lampert, *et al.*, 2007). Calcium fluoride (CaF_2) was found to be capable of adsorbing PFOS(8) and PFOA(8) from aqueous phase, which can be applied to HF wastewater by addition of $Ca(OH)_2$ to remove PFCs and HF simultaneously. However, rather slow adsorption velocity limited its application (Lampert, *et al.*, 2007).

Granular activated carbon (GAC) filters are often applied to ensure the removal of odor and color from drinking water, as well as trace organics. Laboratory studies showed effective removal of PFOA(8) by carbon adsorption (Schaefer, 2006). Industrial application of GAC column by 3M Company also confirmed the efficiency of adsorption. However, GAC filtration was greatly affected by operation parameters and improper operations would make GAC bed both expensive and ineffective (Ho, 2004). Results of environmental monitoring revealed strong correlations between PFC concentrations in surface and in drinking water, indicating ineffective removal by current waster treatment process including GAC filters (Skutlarek, *et al.*, 2006)

Electro sorption process applied direct electric current in PFCs polluted drinking waters and was proved effective to reduce PFOA in aqueous phase. This process can concentrate PFOA from aqueous solution to both electrodes by three ways: attraction and ion-exchange in electric double layer, surfactant accumulation to electrode-solution interface, and micellar formation which further concentrate PFOA after accumulation. Despite of these assumption, electro sorption in voltage of 6V resulted in 14~64% reduction of PFOA with initial concentrations from 0.05~25mg/L in drinking water (Welcker, 2006).

Biodegradation processes

PFASs and PFCAs were considered stable and persist in environment without natural degradations (OECD, 2002; US EPA, 2002). PFOS(8) was found not degradable by activated sludge (Schröder, 2003). Behavior of PFC-related precursors in activated sludge was studied to reveal degradation pathways to PFCs. Perfluorinated carbon bonds of 8:2 FTOH were found to be defluorinated and mineralized by microorganisms under conditions similar to wastewater treatment plant. The biodegradation process was considered to be charged by mechanism of both β–oxidation and enzyme-catalyzed reaction, which generated short-chained fluorinated carbon metabolites (Wang, *et al.*, 2005a; 2005b).

Catabolite software engine (CATABOL) was applied to simulate PFCs biodegradation products. Although 60% of 171 kinds of PFCs can be degraded, persistent metabolites were formed in significant quantities. Furthermore, PFCs seemed to be transformed to more bioaccumulative and toxic products, such as PFOS(8) and PFOA(8), which occupied 27% and 17% of final products respectively (Dimitrov, *et al.*, 2004).

2.4.3 Degradation processes for PFCs

2.4.3.1 Advanced oxidation processes (AOPs)

Advanced oxidation processes (AOPs) involve the generation of hydroxyl radicals in sufficient quantity to effect water purification. These common processes include O_3/H_2O_2, O_3/UV and UV/H_2O_2. UV/TiO_2 process and Fenton reagent are also effective to specific wastewater (Gottschalk, *et al.*, 2000). AOPs such as O_3, O_3/UV, O_3/H_2O_2 and Fenton reagents were identified unable to decompose PFOS in normal state, but able to degrade PFOS precursors and partially fluorinated polymers effectively (Schröder and Meesters, 2005).

Some oxidation processes can decompose PFCs completely in critical conditions or coupled with catalysts. PFOS can be completely oxidized by subcritical water oxidation, with catalyst of zerovalent metals like iron. PFOS molecules were observed to be strongly adsorbed on Fe_3O_4 sediments and further decomposed to carbon dioxide and fluorine ions due to oxidation by molecular oxygen in subcritic water (Hori, *et al.*, 2006).

2.4.3.2 Photolysis and photo-catalysis processes

Ultraviolet (UV) is usually applied in water treatment process for disinfection. PFCAs were proposed to decompose by UV photolysis in stepwise degradation mechanism. Direct photolysis (220~240nm) was able to completely degrade 560 mg/L PFCAs (Hori, *et al.*, 2004a), although one early research claimed that no removal of PFOA(8) was observed under either direct or indirect photolysis (Hatfield, 2001b). Synthetic catalyst, such as heteropolyacid photocatalyst ($H_3PW_{12}O_{40}$), was able to accelerate degradation of PFOA greatly (Hori, *et al.*, 2003; 2004b). UV irradiation in shorter wave length can generate higher energy photons and result in higher removal efficiency. Direct UV irradiation at 185 nm mercury lamp or 172 nm xenon quasi molecular laser light was found able to degrade some PFCs completely in satisfied

speed (Zhang, *et al.*, 2005b).

Another photolytic method involved persulfate ions coupled with UV irradiation. Sulfate radicals were generated from persulfate ions by UV irradiation to react with PFCA molecules and form positively charged PFCA radicals, which were eventually decomposed to CO_2 and HF in water (Hori, *et al.*, 2005a). In case of long-chained PFCAs like PFUnA(11), which was colloidal particles in water because of high concentration (~770 mg/L) and low solubility, aqueous/liquid CO_2 biphasic system was applied to disperse long-chained PFCAs into aqueous solution under high pressure (Hori, *et al.*, 2005b).

Although UV/TiO_2 was found ineffective to decompose PFOS, it was effective to decompose PFCAs. By introduction of 310~400 nm UV irradiation, 45% of about 300 mg/L PFOA dissolved in perchloric acid can be completely degraded in 24 hours by molecular oxygen with catalyst of TiO_2 (Dillert, *et al.*, 2007). A new process of photo-electro-catalysis, which applied immobilized TiO_2/Ni–Cu photocatalyst with negative bias potential (-0.1V) under UV 254 nm irradiation, was more effective (2~3 times faster) than photocatalysis by TiO_2 to decompose PFOA(8) completely with initial concentration of 25 mg/L. Photogenerated electrons were supposed to initiate reduction of PFC molecules on surface of catalyst, and bias potential can accelerate decomposition process (Chen, *et al.*, 2006).

2.4.3.3 Incineration and sonochemical processes

During combustion or incineration, PFCs may completely defluorinated into CO_2 and HF, or into stable state of CaF_2 which is possibly reused as industrial materials. The products of PFCs by incineration were determined by temperature. When papers containing PFOA-related precursors and polymers were incinerated at 600~1000℃, no emission of PFOA occurred during 2 seconds of incineration time (Yamada, *et al.*, 2005). Under lower temperature at 550℃, thermolysis of fluoropolymers such as polytetrafuoroethylene (PTFE, Teflon) mainly generated trifuoroacetate (TFA). Long-chained PFCA(3~14) were also detected in thermolysis products, which implied floropolymers as one source of PFCs in environment (Ellis, *et al.*, 2001). Thermolysis products of PFOA at 307℃ were perfluoroheptene ($C_5F_{11}CF_2{=}CF_2$), 1H-perfluoroheptane ($C_5F_{11}CF_2{=}CF_2H$) and SiF_4 (Krusic, *et al.*, 2005). While fluorotelomer coated paper was heated in microwave oven at around 200℃, PFOA will be generated and migrated to popcorn oil and finally uptake by human (Renner, 2006b).

In summary, if incineration temperature was higher than 600℃, PFCs will be completely decomposed by combustion. This conclusion was supported by TOC analysis of PFCs standard solutions, in which carbon element in PFCs was completely changed to CO_2 in combustion chamber at 690℃. If incineration temperature was low than 600℃, incomplete combustion occurred and harmful PFCs might be generated and discharged into environment, *e.g.*, persistent (Martin, *et al.*, 2000; Cahill, *et al.*, 2001) and toxic (Berends, *et al.*, 1999) TFA from fluoropolymers at 550℃ .

Another kind of pyrolyzation refers to sonochemical process, which involved ultrasonic irradiation to clarify pollutants. Under ultrasonic irradiation (20℃, 3 W/cm^2), both PFOS and PFOA were pyrolyzed on the surface of cavitation bubbles formed by the irradiation. PFOS molecules were firstly changed to become PFOA by releasing the sulfonate group, and the product of PFOA was consequently degraded to short-chained PFCAs (Moriwaki, *et al.*, 2005).

2.5 Summary

This chapter reviewed available literature about PFCs in respects of basic properties, analytical

methods, environmental behavior and engineering solutions. LC-MS/MS was proved to be robust and reliable for PFCs analysis, and more concerns should be given to pretreatment process to reduce matrix effect. Therefore, detailed discussion about optimum pretreatment methods was given in chapter III.

Surface water, groundwater and drinking water were polluted by PFCs in developed countries and industrialized areas, which showed positive correlation with PFC contaminations in biota and human blood. For example, Yodo River basin was identified highly polluted by PFOA and local residents had rather high concentrations of PFOA in their blood. Unfortunately current water treatment processes were suspected ineffective to remove PFCs from surface water and wastewater. Therefore periodical surveys were conducted in a municipal WWTP to estimate performances of individual facilities and combined processes, which were discussed in chapter IV.

Efforts to control PFCs in environment, such as alternatives for PFCs, recycling and reuse procedures, industrial wastewater treatment processes, and municipal WWTP processes were summarized in detail to show a complete figure on current available methods and strategies. GAC adsorption and UV photolysis were expected effective to remove trace level of PFCs in wastewater, and therefore they were developed in chapter V and VI respectively.

CHAPTER III DEVELOPMENT OF ANALYTICAL METHODS FOR PERFLUOROCHEMICALS

3.1 Introduction

Instrumental analysis of fluorinated organics can be traced back to early 1960s when Wickbold Combustion Method was applied to determine total organofluorine in human serum. Later other methods including NMR, X-ray and FTIR were developed to qualify PFCs. GC coupled with ECD/FID/MS can quantify some PFC derivatives successfully. Development of LC coupled tandem MS greatly enhanced analytical chemistry and techniques for PFCs. Given advantage of stability to wide range of sample sources, electro-spray ionization (ESI) was considered the best interface for various kinds of LC-MS/MS. LC-ESI-MS/MS was considered standard method for PFCs analysis and applied in majority of academic studies (de Voogt and Saez, 2006). Therefore, LC-ESI-MS/MS method will be applied in this study to analyze 15 kinds of PFCs in synthetic water and wastewater samples.

Two major difficulties hindered analysis of PFCs in environmental samples, which were trace level of analytes and strong matrix effect in samples. Solid phase extraction (SPE) can overcome these two difficulties simultaneously by concentrating analytes and removing matrix and inorganic compounds. Analysis of PFCs by SPE-LC-MS/MS was firstly reported about six years ago (Hansen, *et al.*, 2001), and then widely adopted to determine PFCs in various matrices like blood, tissue, surface water, wastewater and sludge. Instead of SPE by C_{18} cartridge which contains strong hydrophobic sorbent to trap very slightly hydrophobic molecules, a newly developed cartridge named Oasis® WAX (Weak Anion-eXchange) was effective to clean up matrix effect by orthogonal interactions of hydrophobic adsorption and ion-exchange mechanism (Waters, 2006; Young and Tran, 2006). WAX cartridge were successfully applied to analyze various PFCs in wastewater and sludge samples (Taniyasu, *et al.*, 2005). Therefore, analysis methods will be optimized between SPE processes by C_{18} and WAX cartridges in this chapter.

Analysis of particulate PFCs is rather difficult because of low efficiency to extract PFCs from solids. Simple ion-pair extraction (IPE) was firstly applied to extract PFCs in wildlife tissues (Hansen, *et al.*, 2001), and later modified to analyze PFCs in sludge samples from WWTP (Higgins, *et al.*, 2005; Schultz, *et al.*, 2006c). Alkaline digestion (AD) was helpful to remove lipids and proteins by precipitation and improve extraction efficiencies because PFC molecules were possibly bound to proteins (Taniyasu, *et al.*, 2005). Therefore, AD coupled SPE pretreatment can effectively improve qualities for PFCs analysis in biota and sludge (Powley, *et al.*, 2005a). Accelerated solvent extraction (ASE) applied high pressure and temperature to accelerate extraction process, which was also practical and promising to extract PFOS and PFOA from suspended solids. These three methods, such as IPE, AD and ASE, will be studied in this chapter to improve PFCs analysis in particulate phase. By optimization for aqueous and particulate samples, an integral procedure could be proposed for PFCs analysis in wastewater samples.

Erroneous results may occur throughout pretreatment and instrumental analysis. In order to control the analysis quality, spiking experiments were conducted on each environmental sample to estimate the average process recoveries. Furthermore, 9H-PFNA was applied to estimate matrix effects of ionization suppression.

3.2 Aims

Major aim in this chapter is to establish an integral procedure to analyze PFCs in wastewater samples, including aqueous phase and particulate phase. LC-MS/MS was applied to analyze PFCs in trace levels. Pretreatment methods for aqueous and particulate samples were optimized to reduce matrix effect from wastewater. Objectives of this chapter are shown as follows:

(1) To identify qualities of LC-MS/MS for each PFC, including RSD, LOD and LOQ.

(2) To optimize C_{18} and WAX cartridge for aqueous sample pretreatment.

(3) To optimize ion-pair, alkaline digestion, and accelerated solvent extraction for particulate sample.

(4) To integrate analysis of aqueous and particulate phase into a complete procedure and validate it by PFC distribution properties.

3.3 Experimental Methods

3.3.1 Analysis of PFCs by LC-MS/MS

3.3.1.1 PFC standards

In this paper, 12 kinds of PFCAs and 3 kinds of PFASs were selected as target chemicals. Their basic information is included in **Table 1.1** and **Table 2.2**. Standard reagents were obtained from local companies, such as Wako Pure Chemical (Wako) and Tokyo Chemical Inc. (TCI), with purities in range of 95~98%. Single PFC stock solution was prepared by dissolving 0.1~1 g PFCs into 0.1 L pure methanol and stored in polypropylene (PP) bottle at 4℃. PFCs standard solutions were prepared by diluting different volumes of single stock solutions together into 50% methanol solvent. These multi component standard contained same concentration of each PFC.

PFCs standards are usually predominant by linear molecules. Branched isomers are possibly eluted right earlier than linear PFCs, which forms "shoulder" before the main peak. Distribution of isomers could be successfully quantified by high resolution MS/MS (Berger, *et al.*, 2004; Ingrid Langlois, 2006) and further applied to identify the contaminant sources (de Silva and Mabury, 2004; 2006). However, because of the limitations of instruments, PFCs isomer distributions were not identified in this study.

PFCs in different carbon chain lengths were reported as impurities in PFC standards (Martin, *et al.*, 2004a). PFC standards used in this study also contained these kinds of impurities, although these impurities were not quantified. Existence of impurities as other PFCs will reduce the response of LC-MS to specific analyte. However, in multi component standard solutions, the loss of mass by impurities might be compensated by the excessive mass as impurities in other PFCs. Involving with this compensative mechanism, the influences of impurities on analysis were difficult to be identified. Variances caused by impurities were expected very small and could be ignored by considering the very high relative standard deviations (RSD) of LC-MS/MS. PFC concentrations in this study were calculated by gross mass of salt or acid over solution volume without modification by purities.

3.3.1.2 LC-MS/MS conditions for PFCs

PFCs were determined by the system of liquid chromatograph coupled with tandem mass spectrometer (LC-ESI-MS/MS). Optimized conditions of LC and MS system are shown in **Table 3.1**.

In LC system, reverse phase C_{18} column was applied as stationary phase, and pure water with 10 mM CH_3COONH_4 as pH buffer (solvent A) and pure acetonitrile (solvent B) were used as mobile phase

Gradient flow was applied to accelerate PFCs elution and clean up the column, which played an important role for LC separation. Solvent A:B in mobile phase was kept constant at 50:50 for one minute at the beginning time, then changed to 0:100 gradually in six minutes and kept constant for more three minutes. After that, solvent A:B was changed back from 0:100 to 50:50 in one minute and kept in constant until next injection. Because re-equilibrated time for LC column in cycling injection was about 15 minutes, the time interval for sample analysis was set to be 20 minutes.

Table 3.1 Optimized conditions for LC-MS/MS operation

	LC system		***MS/MS system***
Instrument	Ultra Microprotein Analyzer	*Instrument*	Finnigan Mat TSQ 7000
Column	Agilent Zorbax XDB C-18 (2.1×150 mm, 5 μm)	*Scan mode*	Selected ion mode (MS : *m/z* of parent ion)
Guard column	XDB C-8 (2.1×10 mm, 5 μm)		(MS^2: *m/z* of daughter ion)
Autosampler	GL-7420	*Interface*	Electrospray ionization
Injected volume	10 μL	*Spray voltage*	4200 V
Temperature	40 ℃	*Electron multiplier*	1500 V
Flow rate	0.1 mL/min	*Capillary temperature*	175 ℃
Mobile phase	A: 10 mM CH_3COONH_4/H_2O	*Sheath gas*	N_2 (70 psi)
	B: CH3CN	*Auxiliary gas*	N_2 (15 mL/min)
Gradient table	1→7 min, A:B=50:50→0:100	*Collision gas*	Ar (1.3 mTorr)

In MS/MS system, sheath gas pressure was determined by LC flow rate. Spray voltage, capillary temperature, auxiliary gas flow rate, and collision gas pressure were optimized by loop injection to maximize response for PFOA. Electron multiplier voltage was optimized by suitable peak height for PFCs standard solutions. Information of LC-MS/MS analysis for PFCs was summarized in **Table 3.2**.

Table 3.2 Analytical parameters of PFCs by LC-MS/MS

Analyte	Mol.Formula	Mol. Weight	Parent ion[a]		Daughter ion[b]		Collision	R. Time[c]
				m/z		*m/z*	(eV)	(min)
PFBA	$CF_3(CF_2)_2COOH$	214.04	$[M-H]^-$	213	$[M-COOH]^-$	169	-15	2.8
PFPeA	$CF_3(CF_2)_3COOH$	264.05	$[M-H]^-$	263	$[M-COOH]^-$	219	-15	2.9
PFHxA	$CF_3(CF_2)_4COOH$	314.05	$[M-H]^-$	313	$[M-COOH]^-$	269	-15	3.2
PFHpA	$CF_3(CF_2)_5COOH$	364.06	$[M-H]^-$	363	$[M-COOH]^-$	319	-15	3.4
PFOA	$CF_3(CF_2)_6COOH$	414.07	$[M-H]^-$	413	$[M-COOH]^-$	369	-15	3.6
PFNA	$CF_3(CF_2)_7COOH$	464.08	$[M-H]^-$	463	$[M-COOH]^-$	419	-15	4.1
PFDA	$CF_3(CF_2)_8COOH$	514.08	$[M-H]^-$	513	$[M-COOH]^-$	469	-15	4.8
PFUnA	$CF_3(CF_2)_9COOH$	564.09	$[M-H]^-$	563	$[M-COOH]^-$	519	-15	6.1
PFDoA	$CF_3(CF_2)_{10}COOH$	614.10	$[M-H]^-$	613	$[M-COOH]^-$	569	-15	7.1
PFTeDA	$CF_3(CF_2)_{12}COOH$	714.11	$[M-H]^-$	713	$[M-COOH]^-$	669	-15	8.7
PFHxDA	$CF_3(CF_2)_{14}COOH$	814.14	$[M-H]^-$	813	$[M-COOH]^-$	769	-15	10.5
PFOcDA	$CF_3(CF_2)_{16}COOH$	914.14	$[M-H]^-$	913	$[M-COOH]^-$	869	-15	11.8
9H-PFNA	$H(CF_2)_8COOH$	446.09	$[M-H]^-$	445	$[M-COOH-HF]^-$	381	-15	3.5
PFBuS	$CF_3(CF_2)_3SO_3K$	338.19	$[M-K]^-$	299	SO_3^-	80	-90	3.4
PFHxS	$CF_3(CF_2)_5SO_3K$	438.20	$[M-K]^-$	399	SO_3^-	80	-90	4.3
PFOS	$CF_3(CF_2)_7SO_3K$	538.23	$[M-K]^-$	499	SO_3^-	80	-90	6.4

Note: (***a***) [M-H]- or [M-K]- presents residual negative ion by releasing one proton (H) or potassium atom (K) from PFC molecule (M); (***b***) HF is further released from 9H-PFNA despite of carboxylic group (COOH) as other PFCAs; (***c***) average of Retention Time which varies ±5% in different matrices.

After general conditions were optimized and fixed, MS/MS system was tuned for each PFC. Prior to analysis, single PFC standard solution was introduced to MS/MS system by loop injection to optimize capillary voltage, tube lens voltage, lens 1-1 voltage and collision energy for each PFC. Sensitivity of MS/MS system might be changed along analysis so that this stepwise tune should be conducted periodically, *e.g.* once a month.

3.3.1.3 Analytical quality of LC-MS/MS

PFCs standard solution of 100μg/L was injected into LC-MS/MS for more than six times to estimate the relative standard deviation (RSD) of LC-MS and LC-MS/MS analysis. Limit of detection (LOD) for LC-MS/MS is defined as concentration with signal-noise ratio (S/N) equal to three (Hansen, *et al.*, 2001; Saito, *et al.*, 2003). Direct determination of LOD for each PFC was difficult so that minimum concentration quantified by software was considered as LOD.

Eleven PFCs standard solutions in range of 1~500 μg/L were prepared and analyzed by LC-MS/MS to determine range of linearity between peak areas and PFC concentrations. After that, seven of PFCs standard solutions in the linearity range were analyzed to determine their standard deviation from the calibration curve Three times of the standard deviation was considered as LOQ (EPA, 2000). RSD, LOD and LOQ were not specified for wastewater samples.

Spiking experiments were conducted to calculate process recovery (PR) for each PFC. Before SPE process, some multi component PFCs standards (C_{std}) were added inside samples. After LC-MS/MS analysis, PFC concentration in spiked sample was calibrated as $C_{std+smpl}$, and PFC in original sample was C_{smpl}. PR for the PFC was calculated as follows,

$$PR_i = \frac{C_{std+smpl} - C_{smpl}}{C_{std}} \tag{3.1}$$

where PR_i was the process recovery for i PFC. PR was dependant on the relationship between spiking and original concentrations in samples as C_{smpl}/C_{std}. Usually spiking concentration should be close with original values. In this study, the spiked concentrations of all PFC were made uniform (20 ng/L) to simplify operations.

Organics loading on solid phase extraction (SPE) cartridge should not exceed adsorption capacity of cartridge. In this study, the loading limit of organics for Presep C-Agri (C_{18}, 220 mg) and Oasis WAX (60 mg) cartridge was 15 mgC and 6 mgC respectively. Then the volume of wastewater sample for SPE pretreatment can be calculated by loading limits of cartridge and DOC concentration of each sample.

3.3.1.4 Estimation of matrix effect

In wastewater samples, ionization of PFCs were often suppressed because of the strong background organics (de Voogt and Saez, 2006; Sinclair and Kannan, 2006). A simple method to estimate ionization suppression was to compare different responses of the internal standard (Matuszewski, *et al.*, 1998). Furthermore, a method based on the responses to spiked external standards in different matrix was developed to estimate SPE efficiency and matrix effect simultaneously (Matuszewski, *et al.*, 2003; Claude R. Mallet, 2004). This method involved four kinds of samples: standard solution, sample by SPE, sample spiked before SPE, and sample by SPE spiked before LC injection. Although it can estimate matrix effect on each analyte, much systematic variance would be introduced by considering the high RSD value for LC-MS/MS analysis (13±6%). Therefore, method based on internal standard was adapted to estimate ionization suppression by matrix effect from wastewater samples.

Sodium dodecyl sulfonate (SDS) and 9H-perfluorononanoic acid (9H-PFNA) were selected as internal standard candidates to estimated matrix effect. Their structures are shown in **Table 3.3**. SDS was reported as internal standard to analyze PFOS in dust successfully (Moriwaki, *et al.*, 2003), but unfortunately it was detected in PFCs standard solutions in this study, and not qualified to be internal standard. Hydrogen substituted PFCA were applied as internal standard for PFCs analysis, including 9H-PFNA (Risha, *et al.*, 2005), 7H-PFHpA and TH-PFOS (Hansen, *et al.*, 2001; Kärrman, *et al.*, 2004; Harada, *et al.*, 2005).

Table 3.3 Molecular structure of internal candidates

SDS	9H-PFNA
sodium dodecyl sulfate	*9H-perfluorononanoic acid*
$C_{12}H_{25}SO_4Na$	$C_9H_2F_{16}O_2$
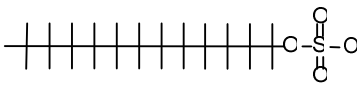	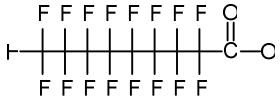

After SPE process, internal standard was spiked into the elution before LC-MS/MS analysis. Ionization suppression rate (ISR) can be calculated based on the peak areas of 9H-PFNA as follows,

$$ISR = \frac{P_{IS,M}}{P_{IS,0}} \tag{3.2}$$

where $P_{IS,M}$ was the peak area of internal standard in matrix, and $P_{IS,0}$ was the peak area of internal standard in LC mobile phase without matrix. If ionization suppression occurred, ISR value would be in range of 0~1. The lower is the ISR value, the stronger suppression occurs for ionization. Criteria of ISR < (1-RSD) was proposed to confirm ionization suppression, which ensured that difference of responses to internal standard was not caused by instrumental system variances.

3.3.2 Pretreatment for aqueous sample

Wastewater sample contains aqueous phase and particulate phase. In aqueous phase, PFCs are homogenously distributed as anions because of their lower p*Ka* values (Swedish Chemicals Inspectorate (KemI) and Swedish EPA, 2004). The main purpose of aqueous sample pretreatment was to improve extraction efficiency and to reduce interferences in matrix. C_{18} and WAX cartridge were applied in SPE process in this study to optimize pretreatment procedure for aqueous wastewater samples.

3.3.2.1 Description of C_{18}-SPE process

Presep C-Agri cartridge (220mg, 6mL) was obtained from Waters Company, which was designed to extract slightly hydrophobic organics by abundant C_{18} alkane on silica base. This kind of cartridges were widely applied to extract PFCs from serum and tissues (Harada, *et al.*, 2004; Holm, *et al.*, 2004; Inoue, *et al.*, 2004b; Kannan, *et al.*, 2004; Calafat, *et al.*, 2006; Kärrman, *et al.*, 2006), surface water (Hansen, *et al.*, 2002; Moody, *et al.*, 2002; 2003; Saito, *et al.*, 2004) and wastewater (Schröder, 2003; Boulanger, *et al.*, 2005; Schultz, *et al.*, 2006c). The process of C_{18}-SPE is summarized in **Fig. 3.1*a***.

Firstly, water samples were prepared in 750mL stainless steel bottles in specific volume by calculation of loading limit and DOC concentrations. PFCs standard solution was added before SPE process to calculate process recovery. Presep C-Agri (C_{18}) cartridge was firstly conditioned by passing 10mL of

pure methanol and successively rinsed by 20mL of pure water. After that, the cartridge was placed on Electric Concentrator (Waters Company) to automatically load water samples in flow rate of 10mL/min or less. At the end of loading, the stainless steel bottle and tubes were rinsed by 20mL or two times of 10mL pure water. The rinsed water was also passed through cartridge. After passing all of the samples through cartridge, additional 10mL pure water is added to clean syringe in concentrator. After one extraction was finished, 10mL methanol and 20mL pure water were passed through concentrator in sequence to rinse the syringe and tubes. After loading the samples, C_{18} cartridges were connected to dehydrate manifold to remove moisture under vacuum state at about 10 MPa for more than one hour. Then C_{18} cartridge was eluted in gravity by 3mL of pure methanol into 10 mL PP tube. At the end of elution, the cartridge was vacuumed again for 2 minutes to draw out residual methanol in the cartridge. The elution in PP tube was dried by gentle nitrogen gas flow, normally at 20~30mL/(min.tube). Finally, 0.5mL of 50% acetonitrile/water solution was added inside the PP tube to reconstruct the sample for LC-MS/MS analysis.

LC vials in small volume (0.2mL) were reported to possibly adsorb PFCs, and the decreased responses for same sample were also observed in this study. Therefore LC-MS/MS analysis should be finished in 24 hours and the samples can not be stored in LC vials for long time.

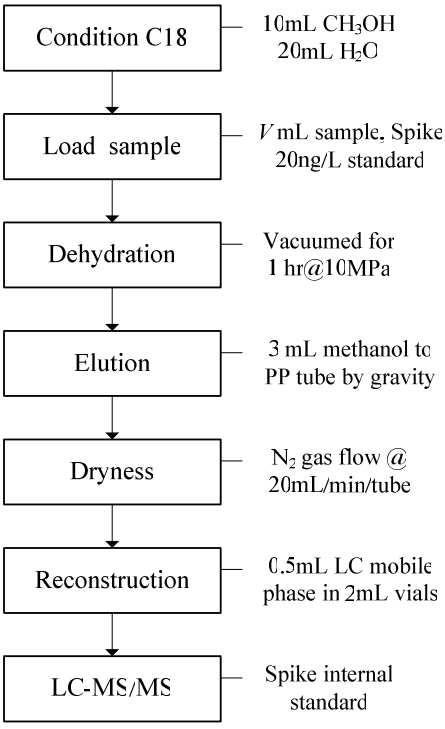

(*a*) C18-SPE process

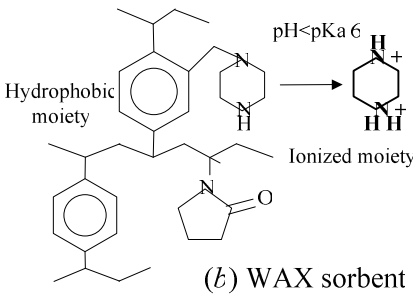

(*b*) WAX sorbent

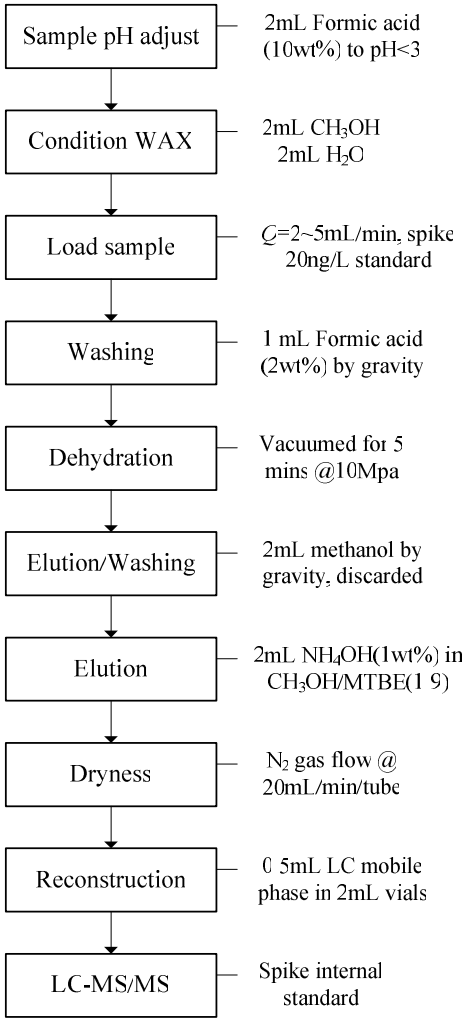

(*c*) WAX-SPE process

Figure 3.1 Scheme of SPE process by C_{18} and WAX cartridge

3.3.2.2 Description of WAX SPE process

Matrix in environmental sample hindered analytical quality of LC-MS/MS and was impossible to eliminate completely from the sample. Carefully designed SPE process, *e.g.* orthogonal of two dimensional method, might significantly reduce the interferences in final elution and alleviate matrix effect on ionization (Waters, 2006). Oasis WAX (mixed mode Weak Anion-eXchange) cartridge was specially designed by Waters Company to selectively extract strong hydrophobic acid from various matrices. WAX sorbent contains hydrophobic structure like C_{18} sorbent and weak ionized part like anion-exchanged resin, as shown in **Fig. 3.1*b***. WAX sorbent performs adsorption and ion exchange in parallel, which combines merits of both C_{18} cartridge and ion exchange cartridge. Given the application of orthogonal extraction in reverse phase adsorption and ion exchange mechanisms, WAX cartridge can clean up the matrix (Young and Tran, 2006) and satisfy the analysis of strong matrix samples such as wastewater and activated sludge (Taniyasu, *et al.*, 2005). The WAX-SPE process was modified from Waters Company guidance and shown in **Fig. 3.1*c***.

Formic acid, methyl t-butyl ester (MTBE) and 2M ammonium in methanol were ordered from Wako Company to prepare 2 wt% and 10 wt% formic acid solutions, and 1 wt% ammonium in methanol/MTBE (1:9) solution. DOC loading on WAX cartridge (60mg, 3mL) was controlled to be less than 6 mgC per cartridge. In case of WWTP influent and primary effluent with very high DOC concentrations (30~60 mg/L), 100 mL sample was introduced to WAX cartridge. In case of wastewater in lower DOC concentrations, 250 mL sample was loaded. Before SPE process, pH of sample was adjusted to be less than 3 by 1~2 mL of 10% formic acid, in order to ionize WAX sorbent to be positive charged completely during SPE process.

WAX cartridge was firstly conditioned by 2mL methanol and later rinsed by 2mL pure water. After that, the cartridge was connected with Electronic Concentrator. Then pH adjusted sample was loaded on the cartridge at flow rate of 2~3 mL/min. During this step, both hydrophobic organics and negative charged ions were adsorbed or bonded to the cartridge. At the end of loading, 10 mL or twice of 5mL pure water was added into stainless steel bottle and pass through the cartridge to rinse syringe and tubes.

After extraction, WAX cartridge was washed in gravity by 1 mL of 2 wt% formic acid to ensure combination of PFCs with anion-exchange part of WAX sorbent. Then bulk water in cartridge was removed in vacuum for short time (2~5 minutes). Loaded WAX cartridge was firstly eluted by 2 mL of pure methanol to wash out hydrophobic but non-ionic organics, while PFCs were still retained by ion-exchanged part of WAX sorbent. Finally PFCs in the cartridge were eluted by 1% ammonium in methanol/MTBE (1:9) solution, which combined the elution ability to release PFC molecules interacted with ion-exchanged part and hydrophobic part. Some strong hydrophobic humic acid with higher pK_a value might not be washed out and remained in the cartridge after final elution. The elution in ammonium solvent was evaporated by gentle nitrogen gas and then reconstructed by 0.5 mL of LC mobile phase. Process recoveries were calculated from results of spiking experiments.

3.3.3 Pretreatment for Particulate Sample

PFCs in particulate phase have different behavior to aqueous phase. As surfactants, PFCs have very small surface energy and tend to accumulate on interface of liquid and solid phases. As strong acid with low pK_a values, PFCs exist in anion state in the environment and are potential to interact with functional

groups on solid surface by electro-static forces and chemical bond. Furthermore, combination of PFCs with proteins was reported in blood and serum (Han, *et al.*, 2003; Jones, *et al.*, 2003), which supported the hypothesis that PFCs could be absorbed inside organisms. Up to date, most studies applied ion pair extraction (IPE) process to extract PFCs from solid, which was simple and easy on operation (Hansen, *et al.*, 2001). Alkaline digestion (AD) process seemed helpful to release protein-combined PFCs in biomatrix samples (Taniyasu, *et al.*, 2005). Accelerated solvent extraction (ASE) process applied strong organic solvent in high pressure and temperature to extract analytes in very short time. The three methods will be evaluated by analyzing same sludge samples.

3.3.3.1 Description of Ion-pair process

Ion-pair extraction (IPE) method, the simplest and easiest among the three methods, was popularly applied in environmental analysis. Scheme of IPE process for PFCs analysis is shown in **Fig. 3.2*a***. *t*-butyl ammonium hydrogen sulfate (TBAS, CAS:32503-27-8) was ordered from Wako Company and prepared into 0.5 M to be ion pair reagent. 0.1 M NaOH and 0.25 M Na_2CO_3 were also prepared for extraction. Before digestion, TBAS solution was adjusted to pH 10 by NaOH. At first, about 1g of condensed sludge was weighed in 15mL PP centrifuge tube. Then, 1 mL of TBAS (pH 10) and 2 mL of 0.25 M Na_2CO_3 solution were added inside and homogenized with sludge by Vortex agitator to start alkaline digestion. Standard solution was spiked at this step to calculate process recovery for each PFC. After that, 5 mL of pure MTBE was added into the mixed liquor, which was further moved to a shaker with 150 rpm agitation for 24 hours. In order to extract PFCs completely, reaction time in this study was much longer than 20 minutes applied in the literature (Hansen, *et al.*, 2001),.

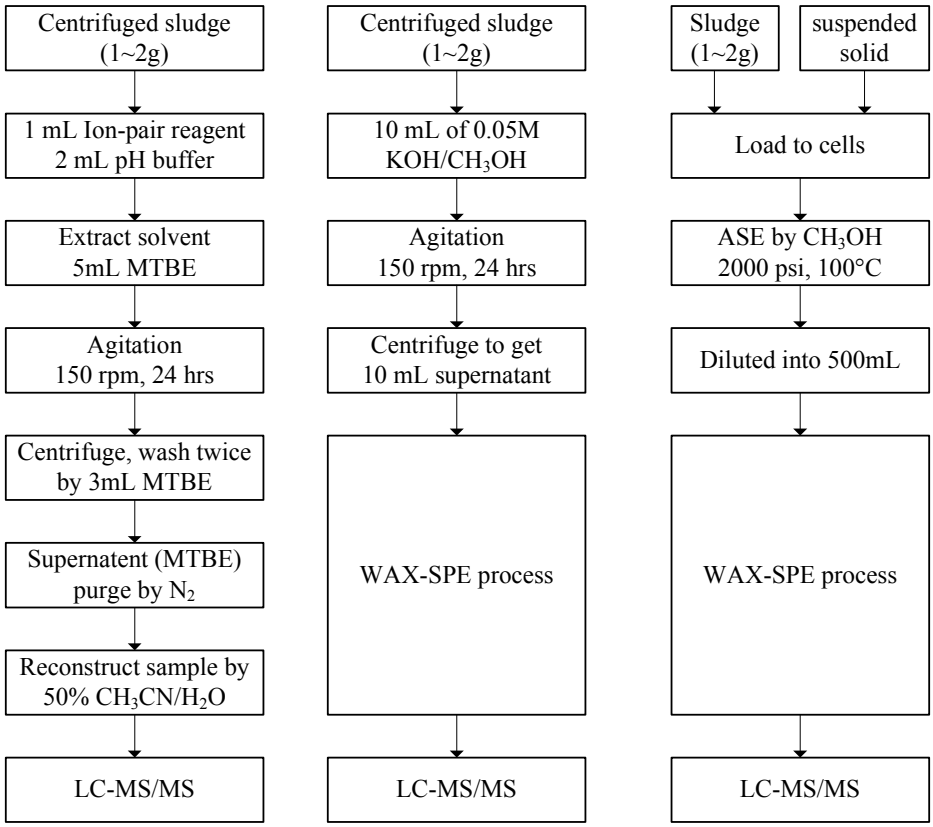

(*a*) IPE process (*b*) AD-WAX process (*c*) ASE-WAX process

Figure 3.2 Scheme of IPE, AD-WAX and ASE-WAX process

After extraction, the mixed liquor was separated into three phases by centrifugation at 3000 rpm for half an hour, such as MTBE, sludge and water phase. The MTBE phase in supernatant was pored out into a new centrifuge tube. Then, 3mL of MTBE was added to wash remains in the centrifuge tube and then centrifuged in same conditions. After supernatant of washing MTBE was collected, the washing step was repeated again. Finally about 11mL of MTBE phase was obtained, and adjusted to 12mL by addition of pure MTBE. The MTBE phase was centrifuged once more to clarify sludge fragments which might be introduced in transfer of supernatant. After that, 3 mL of MTBE phase in supernatant was taken out by pipette precisely and moved into new 10 mL PP tubes. Later processes of nitrogen gas purge and reconstruction were as same as operation in C_{18}-SPE process.

3.3.3.2 Description of AD-WAX process

In alkaline digestion coupled WAX-SPE (AD-WAX) process, solid sample was firstly digested by strong alkaline solution, and the digested mixed liquor was further cleaned by WAX SPE process (Taniyasu, *et al.*, 2005). If C_{18} cartridge was applied for further clean up, washing steps should be considered seriously, *e.g.* washing loaded HLB cartridge by 40% methanol (So, *et al.*, 2006a). Alkaline digestion was also applied in a new SPE method named dispersive solid-phase extraction. In this method, sediments and sludge were firstly soaked into acetonitrile and then extracted by addition of 0.2M NaOH. The crude extract was mixed with glacial acetic acid and cleaned up by Envi-Carb graphitized carbon adsorbent. After separation of carbon adsorbent, PFCAs remained in solution for direct LC-MS/MS analysis (Powley, *et al.*, 2005a).

AS-WAX process was adapted in this study, which is briefly shown in **Fig. 3.2*b***. Particle NaOH was firstly dissolved into pure methanol to prepare 0.05M NaOH/methanol solution as alkaline digestion reagent. After 1g of condensed sludge was prepared in 15 mL centrifuge tube, 10 mL of alkaline digestion reagent was added inside. The centrifuge tube was then capped and homogenized by Vortex agitator. At this time, standard solution was spiked inside the sample to calculate process recovery. After that, the centrifuge tube was placed in a shaker and agitated in same conditions with IPE process. After shaking for 24 hours, the homogeneous liquor was centrifuged at 3000 rpm for 30 minutes to clarify solid from supernatant. The supernatant was carefully pored out and diluted into 100 mL by pure water. The diluted sample was pretreated by WAX-SPE process which was described before.

3.3.3.3 Description of ASE-WAX process

Extraction process can be accelerated in one hour by ASE methods which applied high pressure and temperature. Accelerated solvent extractor (ASE-200) was supplied by Dionex Company, which can successfully extract hydrocarbon contaminates from petrol contaminated soil in less than 10 minutes (Dionex, 2004). Similar process called pessurized liquid extraction (PLE) was also applied to analyze PFCs on sludge samples (Schröder, 2003). ASE process was validated by previous works to be feasible to extract PFOS and PFOA by pure methanol from activated sludge (Nozoe, 2006). In this study, more kinds of PFCs were examined and WAX-SPE process was applied to clean up matrix instead of C_{18}-SPE process. Scheme of ASE-WAX process is briefly described in **Fig. 3.2*c*** and the operation conditions of ASE are shown in **Table 3.4**.

Table 3.4 Conditions of ASE to extract PFCs from sludge

DIONEX Accelerated Solvent Extractor (ASE-200)					
System pressures			*Operation parameters*		
Nitrogen gas	0.9	kgf	Cycling times	3	
Solvent pressure	5	kgf	Static time	15	mins
System air	50	kgf	Purge time	60	sec
Compression oven	120	kgf	Cell volume	33	mL
Vacuum state	5	MPa	Flush volume	60	%
Cell extraction	2000	psi	Oven temperature	100	℃

About 1g of condensed sludge, as same as IPE and AD-WAX processes, was weighed on filtration paper and moved into ASE cell for extraction. Glass fiber filtration paper was placed on the bottom of stainless steel cylinder cell, and covered by 1 mm glass beads in depth of 2 cm. After the sludge sample was transferred inside, the cylinder cell was filled by glass beads and sealed. As shown in **Table 3.4**, ASE process was performed under 2000 psi and 100℃, and finished in 45 minutes. ASE cells should be carefully sealed to ensure no leakage during extraction. The extracted sample from ASE was firstly diluted about ten times to be 500mL, of which 250mL was taken out and processed by WAX-SPE process for LC-MS/MS analysis. WAX-SPE sample with 20% methanol has very high DOC concentration, but no significant effects were observed on SPE efficiency.

Moisture in sludge sample may affect extraction efficiency by ASE. Previous work concluded that sludge in air-dried state showed higher extraction efficiency for PFOS and PFOA than sludge in oven-dried state (105℃). This study repeated the experiments but analyzed more kinds of PFCs.

3.4 Results and Discussion

3.4.1 Quality of LC-MS/MS analysis

LC-MS and LC-MS/MS analysis of PFC external standard solution shows linearity range of 1~150 μg/L by injection volume of 10μL. Response of higher concentrations was suppressed by instrumental sensitivity which was depended on electron multiplier voltage numbers. Average standard deviations of PFCs analysis by LC-MS and LC-MS/MS were 10% and 13% respectively, as shown in **Table 3.5**.

LOD for LC-MS and LC-MS/MS were estimated to be 1 and 3 μg/L respectively. LOQ were calculated by the analysis of seven standard solutions in the range of 1~150 μg/L. LOQ of LC-MS and LC-MS/MS was calculated to be 8 and 16μg/L for respectively. LOD and LOQ for analysis in wastewater and sludge samples can be calculated by extraction times.

3.4.2 Analysis for aqueous sample

3.4.2.1 Influence by C_{18} and WAX cartridge

Process recoveries (PR) for C_{18}-SPE and WAX-SPE processes

Table 3.5 Quality control results of PFCs analysis by SPE-LC-MS/MS method

Method	Item	Condition	PFCAs												PFASs			IS	PFCs
			C4	C5	C6	C7	C8	C9	C10	C11	C12	C14	C16	C18	C4	C6	C8	9HC9	Aver.[c]
SD, %	LC-MS	(n=3)	14	6	9	5	4	3	18	22	1	18	7	18	11	11	8		10±6
	LC-MS/MS	(n=7)	11	7	29	10	8	8	10	8	12	13	16	23	9	9	11	17	13±6
LOD, μ g/L	LC-MS	S/N=3	3	1	1	0.5	0.5	0.5	0.5	0.5	0.5	0.5	3	3	-	1	1		1±0.9
	LC-MS/MS	S/N=3	3	3	3	1	1	1	1	1	1	3	5	3	5	5	5	1	3 ± 2
LOQ, μ g/L	LC-MS	(n=6)	6	18	5	7	4	7	5	10	7	7	8	-	-	16	10	-	8 ± 3
	LC-MS/MS	(n=7)	15	14	17	11	20	15	8	10	14	10	18	-	19	16	23	26	16 ± 5
PR in wastewater DOC=2~60ppm	C-18 [a]	(n=22~50)	**0.09** (0.3)	**0.26** (0.5)	**0.31** (0.4)	**0.65** (0.6)	**0.86** (1.3)	**0.87** (1.1)	**0.89** (0.9)	**0.51** (0.4)	**0.33** (0.5)	**0.65** (1.0)	**0.16** (0.4)	**0.27** (0.4)	**0.55** (0.6)	**0.82** (0.4)	**0.82** (0.8)	**0.61** (0.4)	0.6±0.2
	WAX [a]	(n=22~40)	**0.21** (0.2)	**0.32** (0.3)	**0.42** (0.3)	**0.61** (0.5)	**0.97** (0.9)	**1.03** (1.2)	**0.42** (0.5)	**0.28** (0.3)	**0.50** (1.0)	**0.63** (1.4)	**0.22** (0.3)	**0.06** (0.1)	**0.81** (0.8)	**1.2** (1.0)	**0.61** (0.7)	**0.63** (0.3)	0.6±0.3
PR in wastewater DOC=26~60ppm	C-18 [b]	(n=4)	**0.03** (0.05)	**0.04** (0.09)	**0.03** (0.03)	**0.23** (0.2)	**1.3** (1.6)	**0.22** (0.2)	**0.53** (0.7)	**0.09** (0.03)	**0.02** (0.06)	**0.09** (0.23)	**0.02** (0.02)	-	**0.76** (0.7)	**0.51** (0.5)	**1.29** (2.0)		0.35± 0.4
	WAX [b]	(n=4)	**0.22** (0.2)	**0.43** (0.4)	**0.40** (0.3)	**0.43** (0.4)	**0.68** (1.0)	**0.23** (0.3)	**0.56** (1.0)	**0.11** (0.1)	**0.09** (0.1)	**0.72** (1.2)	**0.10** (0.22)	-	**0.38** (0.5)	**0.93** (1.2)	**0.18** (0.1)		0.39± 0.5
PR in WWTP activated sludge	Ion Pair	(n=2)	-	-	-	1.5	0.64	1.1	1.1	0.64	0.53	1.8	3.3			3.0	1.8	-	1.5±1.0
	AD-WAX	(n=2)	-	-	-	0.16	0.31	0.65	0.60	0.19	0.42	0.33	0.29			0.41	0.83	-	0.4±0.2
	ASE-WAX	(n=11)	**0.24** (0.4)	**0.28** (0.4)	**0.45** (0.3)	**0.87** (0.8)	**1.2** (1.3)	**1.3** (1.1)	**1.1** (1.0)	**0.84** (0.7)	**0.83** (0.9)	**0.62** (1.1)	**0.32** (0.5)	**0.25** (0.4)	**0.35** (0.3)	**0.80** (0.7)	**1.3** (1.5)	-	0.7±0.4

Note: ***a*** = all sample from WWTP; ***b*** = WWTP influent and primary effluent; ***c*** = average on each row.

are shown in **Table 3.5** as average values of all samples for each PFC. PR of C_{18}-SPE process varied in 0.1~0.9 and PR of WAX-SPE process were in range of 0.2 ~ 1.2. Average values of PR for each PFC in the two SPE processes were both equal to 0.6. **Figure 3.3** showed correlations of PR of PFCs to their carbon chain lengths. WAX cartridge showed better performances for short-chained PFCs like PFCA(4~9) and PFAS(4,6), and C_{18} cartridge performed better for long-chained PFCs. One possible explanation was that long-chained PFCs had higher pK*a* values and might not be completely dissociated under pH3 in WAX-SPE process.

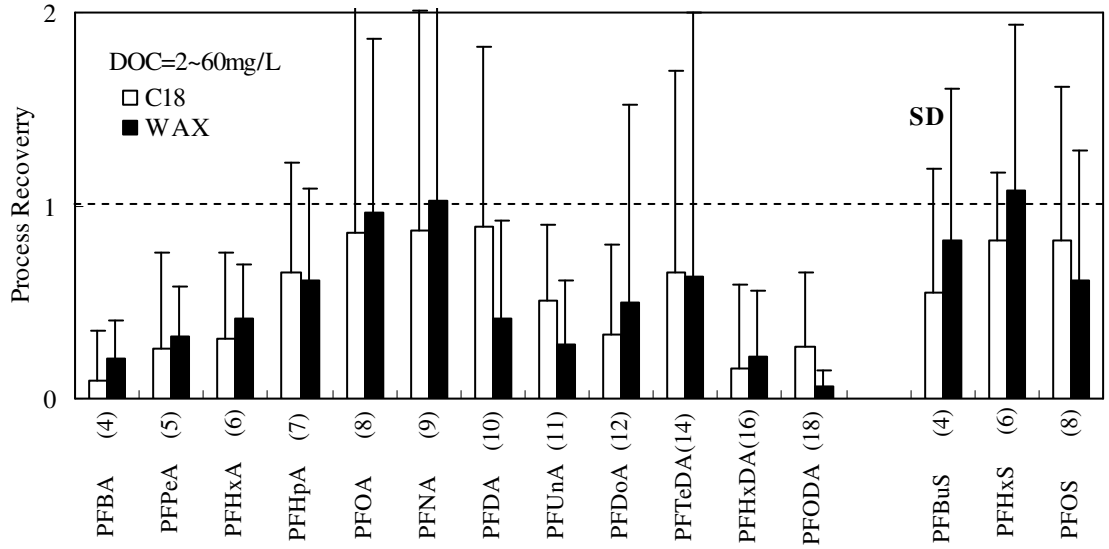

Figure 3.3 Process recoveries of C_{18} and WAX-SPE for wastewater samples (*n*=40)

Both C_{18} and WAX cartridges showed unsatisfied recoveries for short-chained PFC(4~6) and long-chained PFCA(12~18). Furthermore, PR for PFCA(4~9) were gradually increased and then decreased by ascendant carbon chain lengths. This tendency was similar with other studies (Skutlarek, *et al.*, 2006). One possible reason was attributed to their ascendant hydrophobic properties. SPE process combined adsorption effect in sample loading step and desorption effect in elution step. Short-chained PFCs were strongly hydrophilic and difficult to be trapped by hydrophobic sorbent completely. However, long-chained PFCs were totally opposite, which were strongly hydrophobic and uneasy to be eluted from cartridge. Another possible explanation referred to the stronger interferences by "ghost peak" at early retention time, which might suppress short-chained PFC peaks more seriously. Although WAX-SPE can clean up strong organic matrix, interference can not be eliminated completely, so that analysis of short-chained PFCs by WAX-SPE process was still suffered from the early elution. Long-chained PFCs were reported to be easily adsorbed onto surface of containers in PP or PE materials(van Leeuwen and de Boer, 2007), which might resulted in poor recoveries of long-chained PFCs by both SPE methods.

As a brief summary, C_{18} and SPE cartridge showed satisfied quality to analyze some PFCs like PFCA(7~11) and all PFAS. C_{18} cartridge had advantages to concentrate long-chained PFCs, and WAX cartridge performed better in short-chained PFCs.

3.4.2.2 Ionization suppression by dissolved organics

Figure 3.4 shows the relationship between ionization suppression rate (ISR) and DOC loading per 100mg cartridge for wastewater samples. Assuming that DOC concentration represented matrix strength of wastewater, the relationship between ISR and DOC loading showed valuable information about matrix

effect on PFCs analysis.

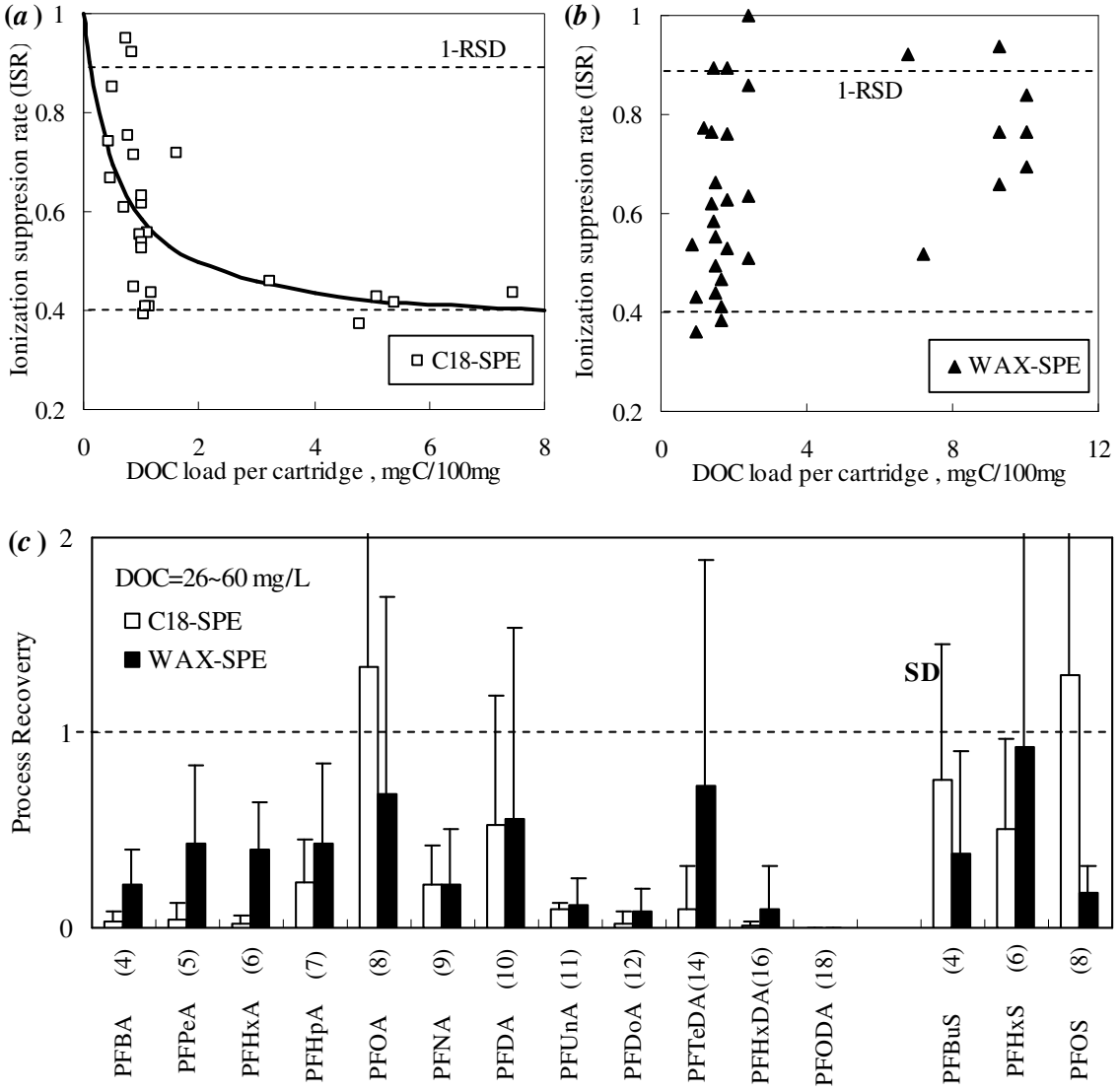

Figure 3.4 Matrix effect on ionization by C_{18} and WAX-SPE process

ISR values by C_{18}-SPE process were located in 0.4~0.9, as shown in **Fig. 3.4*a***. According to the criteria of ISR < (1-RSD), the ionization was suppressed by matrix. ISR curve had a plateau so that the data can be fitted by Monod type function, which was represented by continuous line in the figure. The maximum ISR was 0.36 and the half saturated constant was about 0.5 mgC/100mg. Influent and primary effluent samples from WWTP had very high DOC loadings (3~7 mg/100mg), and their ISR were located in the plateau, which implied that matrix effect from influent and primary effluent samples were very strong. **Figure 3.4*b*** shows ISR values of wastewater samples by WAX-SPE process. ISR values of WWTP influent and primary effluent were increased from 0.4 by C_{18}-SPE to 0.7 by WAX-SPE. This result implied that ionization suppressions can be controlled by proper pretreatment methods. ISR values of wastewater sample with lower DOC loadings (< 2 mgC/100mg) were not improved by WAX-SPE process.

During WAX-SPE process, neutral and weak ionized hydrophobic organics were removed from cartridge by methanol washing prior to final elution. After elution by ammonium, some humic substances still remained in the cartridge and not enter the final elution. While in C_{18}-SPE process, all hydrophobic organics were extracted in the cartridge and washed out completely by pure methanol to final elution. In

case of strong matrix as in influent samples (~40 mgDOC/L), the advantages of WAX over C_{18} were obvious and significant, as shown by the PR in **Fig. 3.4*c***. However, in weak matrix as in sand filtration effluent samples (<5 mgDOC/L), the advantages of WAX-SPE process were not significant and therefore very differences existed between ISR of these samples by WAX and C_{18}-SPE processes.

3.4.2.3 Influence by DOC concentrations

Figure 3.5 shows PR of each PFC in wastewater samples with different DOC concentrations. The samples shown in the figure were pretreated by C_{18}-SPE process. Wastewater samples can be classified into three catalogues according to their DOC concentrations. Influent and primary effluent samples, represented by DOC-H in range of 26~60 mg/L, had highest DOC concentrations in all aqueous samples from WWTPs. Samples from activated sludge process, as shown by DOC-M in range of 4~6 mg/L, were typical effluents of WWTPs. DOC-L in range of 2~4 mg/L included samples of effluent from advanced treatment facilities like ozonation and biological activated carbon filtration.

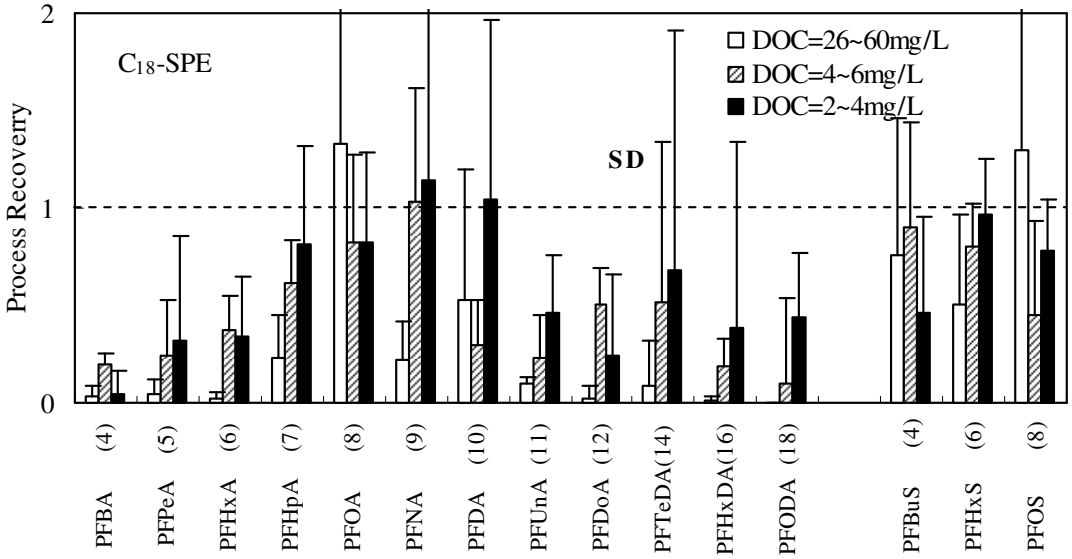

Figure 3.5 Influence of DOC on process recoveries for PFCs analysis (n=5)

Process recoveries of DOC-H samples varied from 0.2 to 0.8, with the highest value for PFOA. For each PFC, PR of DOC-H was smaller than those of either DOC-M or DOC-L. Average value of PR for each PFC in DOC-H samples was calculated to be 0.38±0.2, which implied unsatisfied performance of current analysis. PR of DOC-M samples varied in range of 0.3~1.7 and the average value of PR was 0.81±0.5. PR of DOC-L samples varied in range of 0.2~1.8 and the average value of PR was 0.94±0.7. With the decreasing of DOC concentration, analytical quality was increased based on the average values of PR in wastewater samples.

3.4.2.4 Description of optimized procedure

As a brief summary, an optimized procedure was proposed as follows for PFCs analysis in wastewater samples.

(1) C_{18} or WAX cartridge should be selected for SPE process according to the target PFCs and the DOC concentrations. For samples with strong matrix such as WWTP influent, WAX cartridge should be applied to control the ionization suppression.

(2) Sample volume for SPE should be controlled by DOC loadings on the cartridge, which were 14

mgC for Presep C-Agri (C_{18}) cartridge and 6 mgC for WAX cartridge.

(3) Spiking experiment before SPE for each sample should be conducted to calculate average process recovery. Ultra pure water should be extracted by SPE to control the blank values.

(4) Final PFCs concentrations should be modified by specific process recoveries which were calculated from spiking experiments.

3.4.3 Analysis for particulate sample

3.4.3.1 IPE, AD-WAX and ASE-WAX process

PR of same sludge sample by IPE, AD-WAX and ASE-WAX processes were shown in **Table 3.5**. Average values of PR for each PFC followed the sequence of ASE-WAX > IPE > AD-WAX. PFCs were reported to be less soluble in lipid but easily combined with proteins (de Voogt and Saez, 2006). Different with the homogeneous distribution in water sample, PFCs in sludge were distributed by adsorption on the surface of cells, absorption inside of cells and binding with proteins. In spiking experiments, standard solution was spiked right before the extraction process, and the contact time with sludge was expected too short for PFCs to be assimilated into cells and combined with proteins. Therefore, process recovery of sludge samples might not represent the extraction efficiency directly.

In fact, SPE process can be coupled with ion-pair extraction to improve the analytical quality, which was already applied to measure PFCs in sludge samples (Schultz, *et al.*, 2006c). AD might extract more compounds from sludge because the relatively lower PR implied stronger matrix in the extracts. Compared with AD-WAX for 24 hours by intensive agitation, methanol extraction by ASE-WAX for half an hour seemed not enough to extract PFCs completely. However, ASE was automatic and very easy for operation, therefore it was recommended as optimum to extract PFCs on solid phase. Furthermore, AD solvent could be applied in ASE instead of pure methanol to improve the extraction efficiency.

3.4.3.2 Influent of sludge state on ASE-WAX process

Previous work reported state of sludge will influence analysis results by ASE-C_{18} process (Nozoe, 2006). **Figure 3.6** shows the ratios of PFCs concentration analyzed in condensed sludge and oven-dried sludge. For most of PFCs, results of condensed sludge were much higher than oven-dried sludge, especially for long-chained PFCA(12~18). For shorter chain PFCA(4~6), results of oven-dried sludge were slightly higher than condensed sludge.

After dehydration under 105℃, the sludge was crusted into solid state and became very difficult for solvent to penetrate the mass. On the contrary, wet sludge contained 95% of water and extraction solvent can easily distribute inside the mass and penetrate the cell. Long-chained PFCs might be distributed mainly inside the cell so that ASE can not extract them from oven-dried sludge in short time. On the other hand, more hydrophilic short-chained PFCA(4~6) should be easier for extraction. Ion suppression on short chain PFCA(4~6) was another explanation for the poor results for short-chained PFC analysis in wet state sludge because stronger matrix were existed in the elution. In summary, condensed sludge in wet state was recommended for ASE-WAX process.

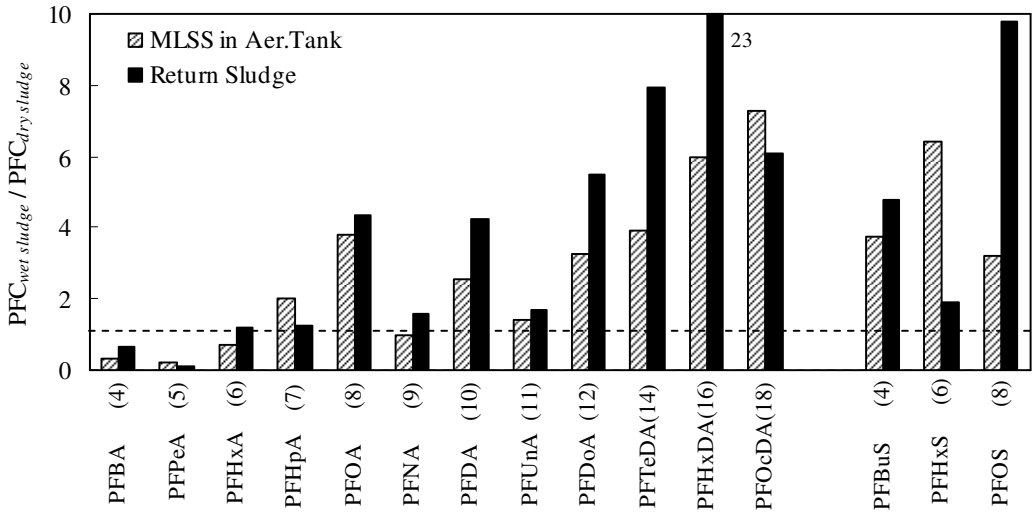

Figure 3.6 Influence of sludge state (dry/wet) on ASE-WAX process

3.4.3.3 Description of optimized procedure

As a brief summary, ASE-WAX process was adopted to extract and analyze PFCs in solid phase. The whole procedure was described as follows.

(1) Firstly, wastewater was filtrated to obtain suspended solids, and the mixed liquor was centrifuged to get condensed sludge. The solids were moved into refrigerator to keep in wet state.

(2) SS concentrations were measured by duplicate filtration for wastewater, and moistures of condensed sludge are determined by filtration and oven-dried SS concentrations

(3) ASE process was applied to extract PFCs in solid samples.

(4) PFCs concentrations in solid phase could be normalized with concentrations in aqueous phase, which should be agreed with their distributions between two phases.

3.4.4 Integral procedure for wastewater sample

3.4.4.1 Integration of aqueous and particulate phases

Usually PFCs concentrations in wastewater samples are required to be expressed by the sum of aqueous and particulate phase. Concentrations in particulate phase can be uniformed to aqueous phase by the concentration of suspended solid (SS). PFC concentration (C_w) in wastewater can be calculated by following equation.

$$C_W = \frac{C_A \cdot V_A + C_P \cdot V_P}{V_A + V_P} = C_A \cdot \frac{V_A}{V_W} + C_{P,s} \cdot S_s \tag{3.3}$$

where V_W and C_W are volume of wastewater and inside PFC concentration respectively, V_A and C_A are volume of filtrate for SPE and PFC concentration in the filtrate, V_P and C_P are volume of sludge and PFC concentration on solid in unit of ng/(L solid), $C_{P,s}$ is PFC concentration in unit of ng/(g dry solid), and S_s is suspended solid concentration in unit of g/L.

Because volumes of particulate phase after filtration or centrifugation were very difficult to determine, calculation by SS was easier and practical. For wastewater samples, SS was very small and C_P can be ignored, so that volume of wastewater was not changed during filtration or centrifugation, which meant $V_A \approx V_W$ and $C_W \approx C_A + C_{P,s}S_s$. For sludge sample, V_P can not be ignored after centrifugation, so that V_A

should be identified to calculated concentration in sum. An alternative method for direct measurement of V_A is to calculate from moisture of condensed sludge (M_P), as shown in **Eq. (3.4)**.

$$\frac{V_A}{V_W} = 1 - \frac{S_s}{1000 \cdot (1 - M_P)} \tag{3.4}$$

where S_s is suspended solid in wastewater with unit of g/L. In this study, M_P was typically 95%, which implied that centrifugation had condensed sludge by ten times. Therefore, V_A / V_W could be used as 0.9 for calculation without introduction of much variance. After that, total concentration of each PFC in wastewater can be calculated from previous results in aqueous and particulate phase.

A complete procedure was proposed to analyze PFCs in wastewater sample including optimized pretreatment procedure for aqueous and particulate phase samples, as shown in **Fig. 3.7**.

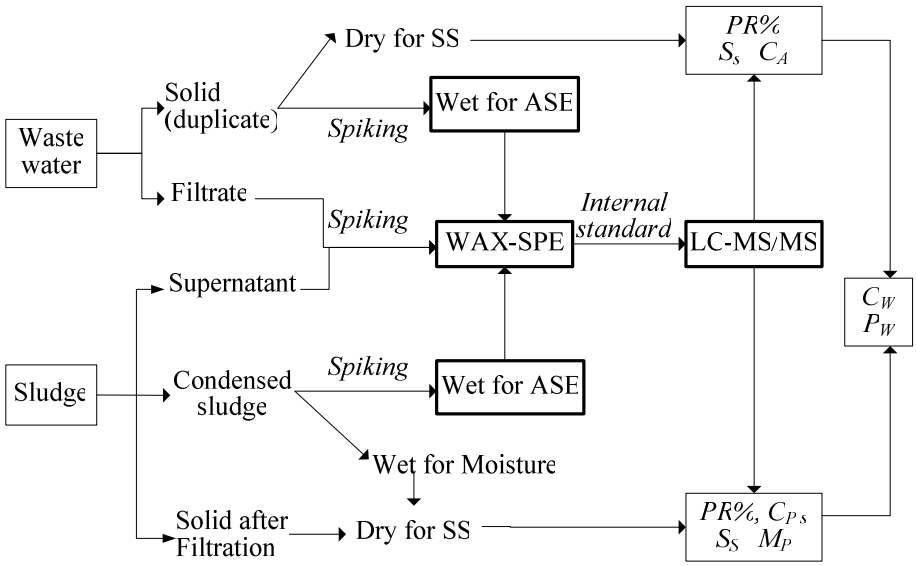

Figure 3.7 The integral procedure for PFCs analysis in wastewater

3.4.4.2 Validation of process by distribution coefficient

PFCs in aqueous and particulate phase can be integrated not only by sum as total concentration, but also by quotient as parturition between two phases. Distribution coefficients of PFCs in sludge samples are calculated by following equation.

$$D_W = \frac{C_P \cdot V_P}{C_A \cdot V_A} = \frac{(C_{P,s} S_s) \cdot V_W}{C_A \cdot V_A} = \frac{C_{P,s} S_s}{0.9 \cdot C_A} \tag{3.5}$$

where D_W is distribution coefficient between aqueous and particulate phase, C_A, $C_{P,s}$, V_A, V_P, V_W and S_s are the same with **Eq. (3.3)**. Centrifugation effect was ten times in average and value of V_A / V_W is simplified to be constant as 0.9.

Distributions of PFCs in activated sludge and return sludge were expected close to each other because of their similar properties. This hypothesis could be applied to evaluate the analytical quality by the integral process to measure PFCs in wastewater samples. **Figure 3.8** summarizes average distributions of each PFC in activated sludge and return sludge, which is sampled for three times monthly.

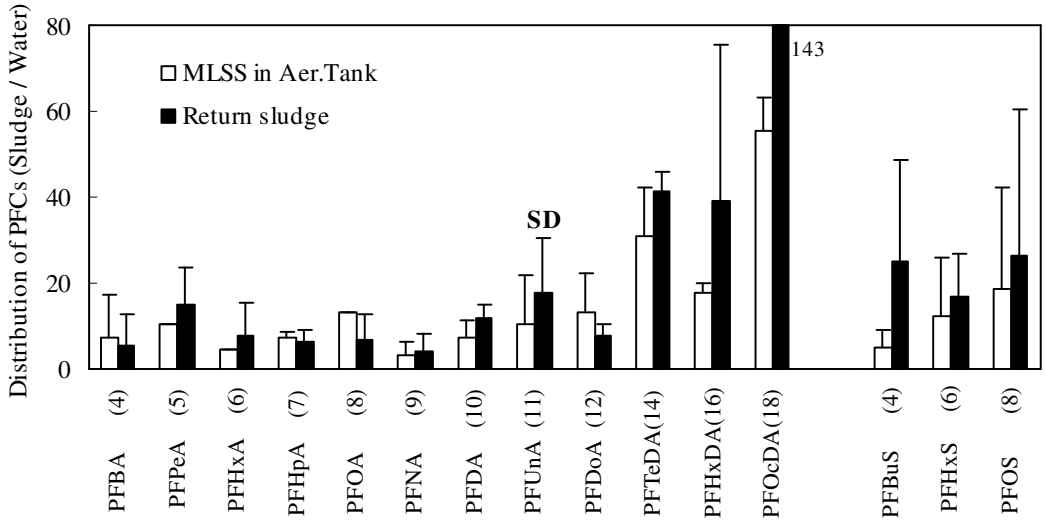

Figure 3.8 Distribution coefficients of PFCs between particulate and aqueous phase (n=2)

Two conclusions can be drawn from **Fig 3.8** in view of different sludge and different PFCs. For most PFCs, distribution coefficients in activated and return sludge were close to each other (0.5~2 times) except PFBuS(4), which implied PFBuS(4) was not properly analyzed by current methods. Distribution for PFCA(4~12) varied in 5~15, but gradually increased by ascendant carbon-chain lengths, which was caused by their increasing hydrophobicity or water insolubility. The longer was the carbon chain, the stronger did PFC molecules distribute in particulate phase. Similar results were concluded from other researchers by comparing PFOA to PFDA and PFUnA in WWTP (Sinclair and Kannan, 2006).

Therefore, the complete procedure was validated by the distribution results, which were close between activated and return sludge, and increased by PFC carbon chain length. These two criteria should be applied to estimate the data quality acquired from integral procedure.

3.5 Summary

A complete procedure for PFCs analysis in wastewater was developed in this chapter. LC-MS/MS was applied to quantify PFCs. Pretreatment for aqueous sample was optimized between C_{18} and WAX SPE process, and pretreatment for particulate sample was optimized among IPE, AD-WAX and ASE-WAX processes. 9H-PFNA was applied as internal standard to estimate matrix effect. An integral procedure for PFCs analysis was proposed and validated for PFC analysis in wastewater. The achievement was concluded as follows.

(1) Quality of LC-MS/MS analysis was represented by RSD as 13%, LOD and LOQ as 3 and 16μg/L, which were about two times higher than LC-MS analysis. Process recoveries in wastewater varied in a wide range but averaged in recovery of 0.6~0.7 based on all available data.

(2) For aqueous samples, both C_{18} and WAX cartridge can be used for pretreatment with average recovery of 0.6. WAX-SPE performed well for short-chained PFCs, and C_{18}-SPE was better for long-chained PFCs. WAX-SPE process can control matrix effect, and was recommended to apply for strong matrix samples. Ionization suppression was increased with DOC concentration and saturated at 60%.

(3) For pretreatment of particulate samples, ASE-WAX process was recommended for its time saving and automatic operations. Condensed sludge in wet state seemed more suitable for extraction

than in oven-dried state by ASE.

(4) For wastewater samples, a complete procedure was integrated from aqueous and particulate phases. PFCs distribution between two phases in sludge sample were calculated and applied as criteria to evaluate the quality of analytical data.

CHAPTER IV BEHAVIOR OF PERFLUOROCHEMICALS IN A WASTEWATER TREATMENT PLANT

4.1 Introduction

Wastewater treatment plant was considered as one possible source for environmental PFCs, because occurrence of PFCs have been already reported in wastewater effluent in cities of US (Boulanger, *et al.*, 2005; Schultz, *et al.*, 2006a; 2006c; Sinclair and Kannan, 2006), European countries (Alzaga and Bayona, 2004) and Japan (Nozoe, *et al.*, 2006), as well as in the sludge samples from sewage treatment plant (Schröder, 2003; Higgins, *et al.*, 2005; Houde, *et al.*, 2006a).

The research of PFCs in wastewater and sludge was very limited, which obstructed understanding of PFC behavior in WWTP process. **Table 4.1** shows concentrations of PFCAs and PFASs in wastewater treatment systems which were summarized from literature. In same WWTP, concentrations and removal of PFCs were quite different to each other, *e.g.*, PFOA(8) and PFOS(8) were usually higher than other PFCs. Although similar activated sludge processes were applied in these investigated WWTPs, specific PFC had different concentrations and removal rates in different WWTPs,

Table 4.1 PFC concentrations in wastewater (ng/L) and sludge (ng/g)

			PFCA (6~14)						PFAS (4~10)		
No. of WWTPs			C6		C8	C9	C10		C10	C6	C8
USA [a]	1	Inf.	19		15	~0	5.6		4	7.7	15
		Eff.	6.4		11	3.4	2.3		8.2	1.2	24
					C8				C10		
USA, Iowa [b]	1	Inf.(Eff.)			>4 (22)				>400 (26)		
					C8	C9	C10	C12		C6	C8
USA, Iowa [c]	6	Eff.			67~697	6~107	2~34	3~8		2~13	4~31
			C6	C7	C8	C9	C10		C4	C6	C8
USA [d]	10	Inf.	0~31	0~25	4.9~89	0~7.3	0~1.7		0~27	2.3~11	1.4~400
		Eff.	8.3~18	0~23	2.5~97	0~6.1	0~3.3		0~20	0~7.1	1.1~130
USA, San [e]			C11	C14	C8	C9	C10	C12		C6	C8
Francisco	13	Sldg.	0~8	0~7	5~30	0~10	1~73	0~33		~0	14~2610

Note: ***a***=(Schultz, *et al.*, 2006c), ***b***=(Boulanger, *et al.*, 2005), ***c***=(Sinclair and Kannan, 2006), ***d***=(Schultz, *et al.*, 2006a), ***e***=(Higgins, *et al.*, 2005).

Current researches mainly considered influent and effluent of WWTP to estimate overall performance. To understand the performance of specific process was not only helpful to reveal PFC behavior, but also valuable for process operations in WWTP. Furthermore, wastewater and sludge was not analyzed in integral method, which was different from the actual state in WWTP. Therefore, studies were necessary for performance by individual process and distribution characteristics of PFCs in sludge.

As a developed country, Japan has advanced service and large capacity in wastewater treatment plants. According to information from Japanese government, about 95% of municipal areas in Japan and 72% of population have been served by sewage system and treatment plants till summary of 2003. Some processes were developed and applied in WWTP, among which conventional activated sludge process (ASP) was the oldest but predominant one. In order to control eutrophication in environment, ASP was modified to remove nitrogen and phosphorous by alteration of the environment of activated sludge.

Figure 4.1 shows the capacity for 13 kinds of major processes applied in Japan in 2004, which was concluded from public information from Japan Society of Sewage Engineering.

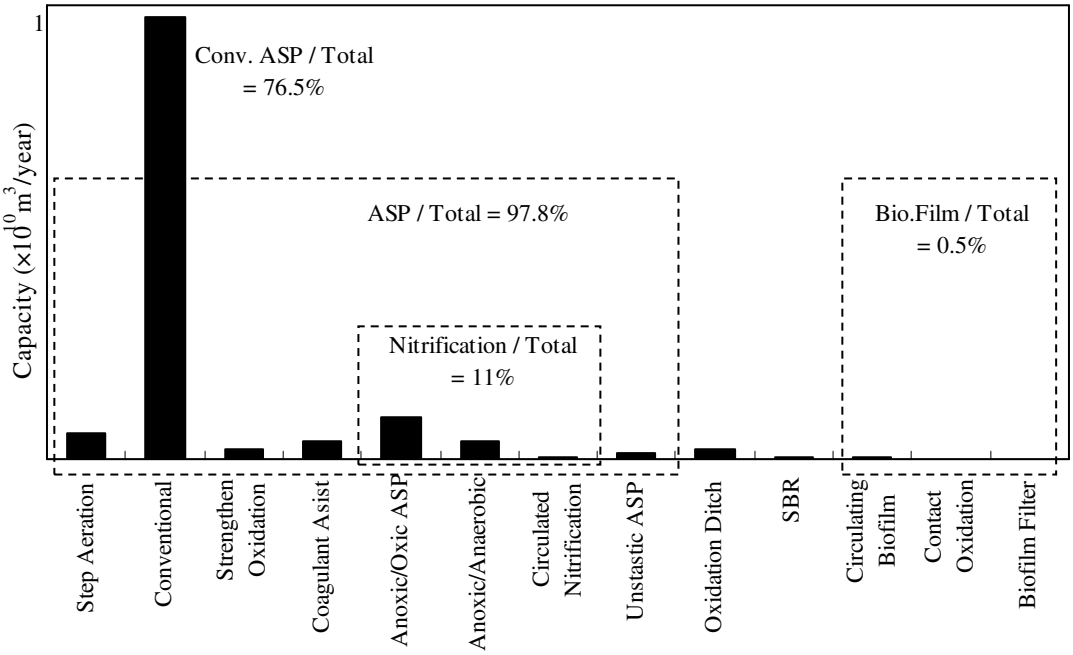

Figure 4.1 Capacities of treatment processes in WWTP all over Japan (2004)

According to the **Fig. 4.1**, conventional ASP was predominant (>75%) over all other treatment processes, which was mainly consisted of primary clarifier, aeration tank and second clarifier. Modified ASP to remove nitrogen, including anoxic/oxic (A/O), anoxic/anaerobic (A/A), and circulated nitrification process, occupied 11% of total treatment capacity. ASP related process, including eight among thirteen processes, occupied around 98% of total treatment capacity. Therefore, study on PFC behavior in ASP is rather helpful to obtain whole vision of current PFCs treatment in Japan.

4.2 Aims

Major aim of this chapter is to understand behavior of PFCs in one municipal WWTP in Japan. Six regular surveys were conducted monthly in half a year. Based on the PFCs distributions along treatment process, their behavior can be classified and analyzed by different patterns. Performance of WWTP can be evaluated for individual facilities and combined processes. Specific objectives of this chapter are shown as follows.

(1) To conduct periodical surveys in half a year and analyze PFCs in aqueous and particulate phases by integral procedure proposed in Chapter III.

(2) To calculate mass flux of each PFC along the process, and to classify them into different patterns. To estimate their behavior in activated sludge process and advanced treatment facilities.

(3) To estimate PFCs distributions between aqueous and particulate phases along the process to understand their distribution properties.

(4) To evaluate performance of individual facilities and combined processes to remove each PFC and total PFC (∑PFC).

4.3 Sampling Site Information

4.3.1 Information of investigated WWTP

Konanchubu wastewater treatment plant (K-WWTP) near Lake Biwa was selected for investigation, because of its sophisticated processes which represent both ASP relation process and advanced treatment process, as shown in **Fig. 4.2**.

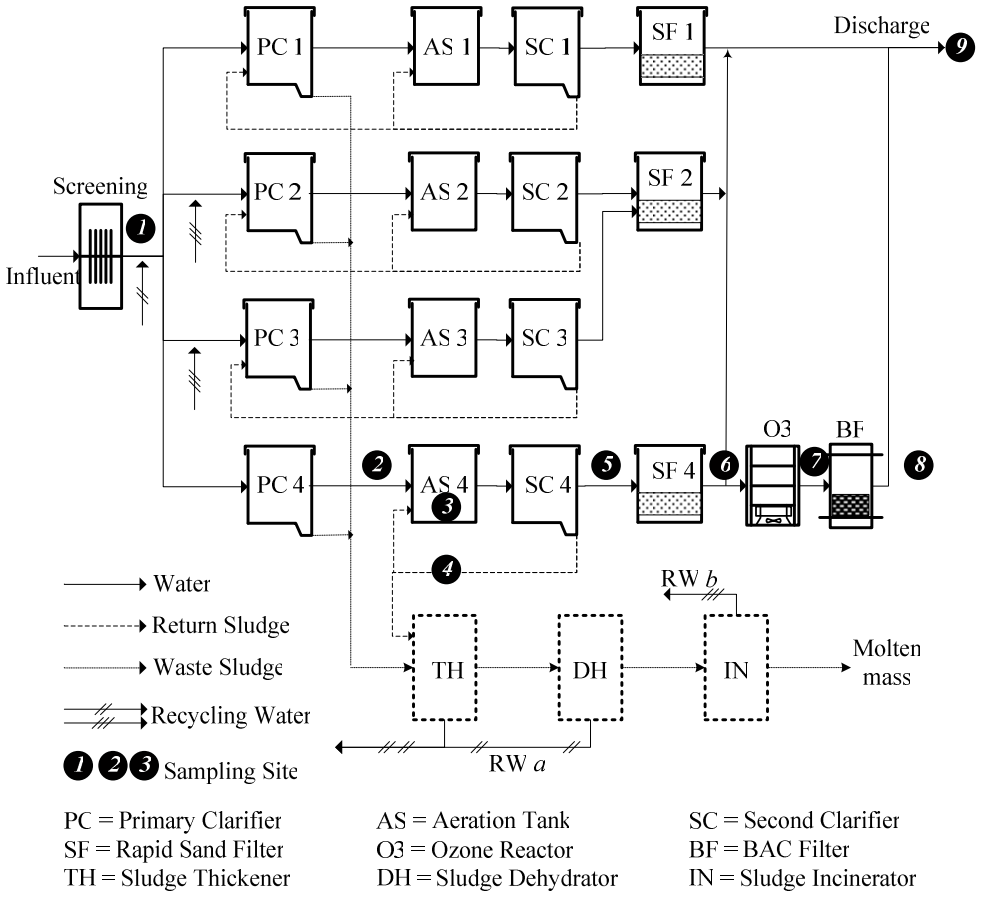

Figure 4.2 Scheme of process in K-WWTP and locations of sampling sites

K-WWTP is located in Kisatsu city of Shiga prefecture, with treatment capacity of approximate 0.8 million tons per day, and serves about 0.8 million people in 30,000 hectare. All effluent of the WWTP is directly discharged into Lake Biwa, the drinking water source for over 14 million people in Kansai district. Complicated processes including A/O and step A/O were adopted to meet increasing strict criteria on COD, SS and nutrients. Further facilities of advanced treatment process including ozonation (O_3) and biological activated carbon filtration (BF) were experimentally built in 2004 to refine treatment of partial stream wastewater. After all of these processes, COD and TN in discharged water is less than 3.0 mg/L and TP is less than 0.02 mg/L.

4.3.2 Information of sampling sites

As shown in **Fig. 4.2**, the 4th series was selected for investigation, which combined processes of primary clarifier (PC), step A/O tank (AS), second clarifier (SC), sand filtration (SF), ozone contactor (O3), and biological activated carbon filtration (BAC). Samples were taken from nine sites as shown in **Fig. 4.2** from Oct. 17 to Dec. 7 2006. Detail information about these sampling sites is given in **Table 4.2**.

Table 4.2 Information of sampling sites in K-WWTP

Process	Label	Symbol	Sampling points	Volume L	Composite (24hr)	Flow rate m^3/d
Step A/O ASP	1	Inf	Influent of primary sedimentation tank	2	Yes	196553
	2	PC	Effluent of primary clarifier	2	Yes	27274
	3	AS	Mixed liquor in 2nd oxic tank	2		40226
	4	RS	Mixed liquor in returen sludge	2		13589
	5	SC	Effluent of secondary sedimentation tank	2	Yes	26351
AOP	6	SF	Inf.of ozonation (Eff. From sand filter)	4		19859
	7	O3	Effluent of ozone contact tank	4		6500
	8	BAC	Effluent of activated carbon bed	4		6500
	9	Eff	Discharged water	2	Yes	225631
		ES	Excessive activated sludge			286

All the samples were collected and stored into 2-liter PET bottles which were consider to be safe for PFCs by less adsorption and releasing of analytes (Saito, *et al.*, 2003; 2004). The composite samples were collected one an hour by auto sampler everyday. Other samples were taken by spot from 9:00 a.m. to 10:00 a.m. in each sampling date.

4.4 Materials and Methods

4.4.1 Sampling methods

2L of PET bottles were obtained in super market as containers for commercial drinking water. The bottles were firstly unsealed and washed by pure methanol. Then, they were rinsed and fulfilled by pure water to keep inner wall surface in wet state. After that, they were stored in room temperature till the sampling date.

Sampling related apparatus, such as steel funnel and sample bottles, was transported to WWTP in the early morning at sampling date. At sampling site, the bottle was firstly rinsed by sample for three times, and then filled with sample rapidly. After that, the bottle was moved into thermo-stat box with frozen materials or ice water to keep temperature lower than 4℃. After sampling, the thermo-stat box was immediately transported to laboratory for pretreatment and measurement.

4.4.2 Analytical methods

The wastewater samples from K-WWTP were pretreated by the integral procedure developed in Chapter III for analysis of PFCs (**Fig. 3.7**). Pretreatment was immediately started after samples from K-WWTP were brought to laboratory and should be finished within the same day.

Different methods were applied to wastewater and sludge. The wastewater samples were firstly filtrated by 1 μm GF/B glass fiber filtration paper in duplicates. Büchner funnel made by PP material was used to reduce the time for filtration and possible adsorption of PFCs on glassware. The filtrates were collected and introduced to C_{18}-SPE and WAX-SPE process following by LC-MS/MS for PFCs analysis. One of the filtrated papers was dried at 105℃ for more than 2 hours to determine the suspended solid in the sample, while another filtrated paper with solid was introduced to ASE-WAX-LC-MS/MS to determine PFCs in particulate phase. Suspended solid was effectively removed before rapid sand filtration so that analysis for PFCs in particulate phase at sites 5~9 was not performed.

Sludge samples from aeration tank (site 3) and return sludge (site 4) were firstly homogenized by intensive shaking and then 100 mL sample was filtrated by 1 μm GF/B glass fiber filtration paper. Büchner funnel was preferable to save the time for filtration. Remained sludge sample was centrifuged at 3000 rpm for half an hour to condense sludge for about ten times. The supernatant was collected and filtrated by same method with wastewater sample. The condensed sludge was moved into beaker and stored in refrigerator. Duplicate samples of condensed sludge were dried in oven at 105℃ to calculate moisture, by which dry weight of condensed sludge can be calculated from wet weight directly. After that, condensed sludge was applied ASE-WAX-LC-MS/MS to analyzed particulate PFCs. Quality control on PFCs analysis in wastewater sample was explained in Chapter III.

About 12 mL of filtrate for each sample was prepared in disposable 15mL PP centrifuge tube for TOC and UV_{254} measurement (TOC-5000A and UV-2500PC, Shimadzu Company, Osaka, Japan). Dissolved organic carbon (DOC) was expressed in term of TOC in filtrate. Absorbance at 254nm (UV_{254}) of samples was also recoded to calculate specific UV absorbance (SUVA) by dividing UV_{254} on DOC.

4.5 Results and Discussion

4.5.1 Removal of DOC and SS

DOC concentrations along the treatment processes are shown in **Fig. 4.3** by average values of six surveys. DOC concentration of influent in K-WWTP was 37mgDOC/L in average with standard deviation of 30%, which implied that water quality was fluctuated in influent. DOC of effluent from primary clarifier was increased by 11% of WWTP influent, indicating detached organics from surface of particles to aqueous phase. Activated sludge played an important role to remove DOC from wastewater, for the sharp decrease of concentration from primary clarifier effluent to aeration tank sample, as shown in **Fig. 4.3*a***. After aeration tank, DOC was further removed by successive processes, as shown in **Fig. 4.3*b***. DOC concentrations were decreased from SC effluent to BAC effluent continuously in constant difference of 0.5 mg/L. This result implied that the combined processes can refine effluent step by step.

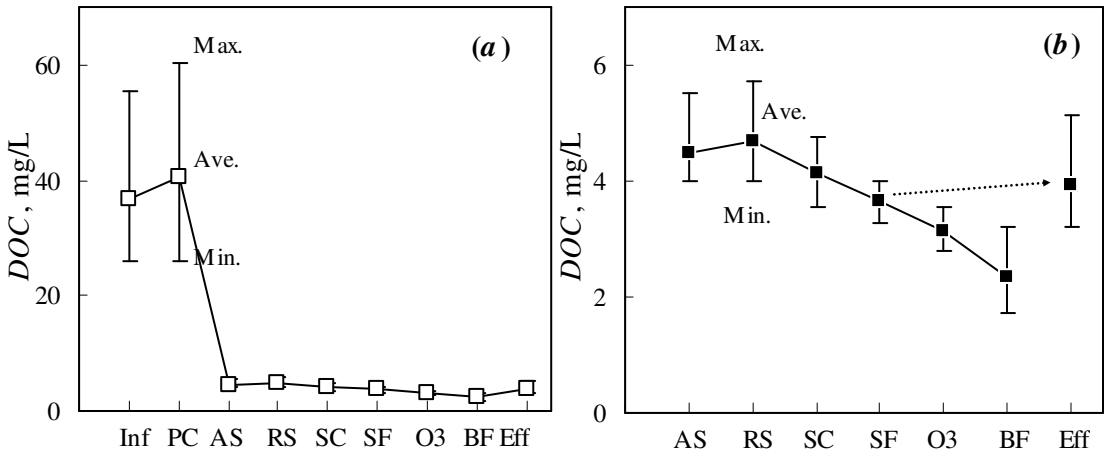

Figure 4.3 DOC concentration along the process (n=6)

Figure 4.4 shows concentrations of suspended solid (SS) along the treatment processes, in average values of three times of measurements. SS in WWTP influent after screening was about 160mg/L, 62% of which was removed by primary clarifier, as shown in **Fig. 4.4*a***. Activated sludge further removes SS effectively, and effluent from second clarifier was about 1.5 mg/L, as 1% of influent value. Mixed liquor

of suspended solid (MLSS) of activated sludge and return sludge are also shown in the figure, whose average values were 4.9 and 7.1 g/L respectively.

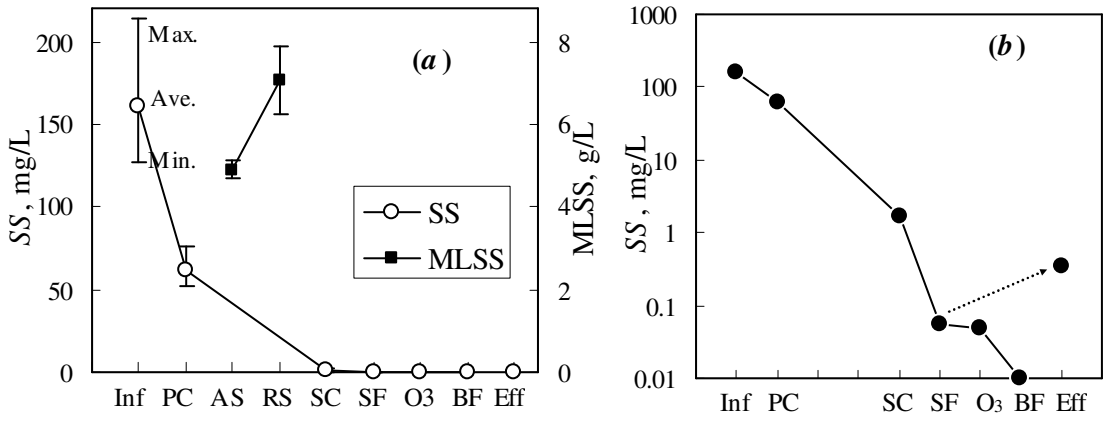

Figure 4.4 SS concentration along the process (n=3)

Suspended solid was sufficiently removed before second clarifier and usually can not be detected in latter processes. In order to estimate their performances on SS removal, filtration volume was increased to 4L and the results were shown in **Fig. 4.4*b*** by logarithm scale. SF and BAC showed further ability to remove SS from 1 mg/L to 0.1 and 0.01 mg/L step by step. However, O3 had no effect on the SS removal. WWTP effluent was mixture of three streams of sand filtration effluents. WWTP effluent was different from sand filtration in 4th series for both COD and SS concentration, which was plotted by dash arrow.

As a brief summary, majority of DOC and SS was removed by activated sludge processes primary clarifier. Latter processes can further removed DOC and SS in series, except for ozonation process on SS removal. Arrangement of processes in reasonable sequence gave the combined processes reliability to meet discharge criteria for DOC and SS.

4.5.2 Analysis of PFCs mass flows in K-WWTP

4.5.2.1 PFCs concentrations along treatment processes

Averages of PFC concentrations in aqueous phase at each sampling site are shown in **Table 4.3**. All PFCs investigated in this study were detected in aqueous phase samples. Some PFCs were lower than LOQ of LC-MS/MS analysis but still calculated by the detected peaks for the purpose of integral analysis. In order to reflect average performance of treatment processes, the maximum value of six concentrations for each aqueous PFC was excluded from average to reduce effects of shock loading.

Aqueous PFCs concentrations in WWTP influent were varied in range of 18~125 ng/L, with PFNA(9) and PFBuS(4) as the maximum. Discussion in chapter III showed that PFBuS(4) can not be assessed properly according to the distribution criteria, so that PFNA(9) was considered as the most dominant PFC in influent. Other dominant PFCs included PFOA(8), PFTeDA(14) and PFHpA(7) with concentrations of 80~95 ng/L in aqueous phase. In individual facilities of WWTP, PFOA(8) and PFNA(9) were dominant which varied in range of 50~120 ng/L and often exceeded 100 ng/L, PFHpA(7) and PFOS(8) were about 30ng/L, and the other PFCs were less than 20ng/L. In WWTP effluent, PFNA(9) and PFOA(8) were still dominant by concentrations of 84 and 64 ng/L respectively. PFOS(8) and PFHpA(7) were 29 and 23 ng/L in effluent, and concentrations of other PFCs were around 10 ng/L.

Results of particulate PFCs are shown in **Table 4.4**. In particulate phase of WWTP influent, PFC

concentrations were increased by carbon-chain length, which can be explained by the increasing hydropobicity and stronger ability of PFC molecules to attach on solid. PFOA(8) in particulate phase was exceptional from the sequence, which was 240 ng/g and higher than both PFNA(9) and PFDA(10). In activated sludge process, PFTeDA(14) and PFOS(8) showed the highest concentrations over than 100 ng/g, indicating their rather strong interactions with sludge. PFOA(8) was also concentrated in sludge with concentration of about 90 ng/g. Other PFCs varied in 10~60 ng/g in sludge. Because SS was sufficiently removed by activated sludge process, solid was not detected (NS) from SC to final effluent, and PFCs in particulate phase of these samples were considered negligible.

PFC concentrations in aqueous phase and particulate phase can be uniformed in same unit as μg/L by **Eq. (3.3)** and **Eq. (3.4)**. Distribution coefficient of each PFC to activated and return sludge is shown in **Fig. 4.5**, which was similar with discussion before (**Fig. 3.8**).

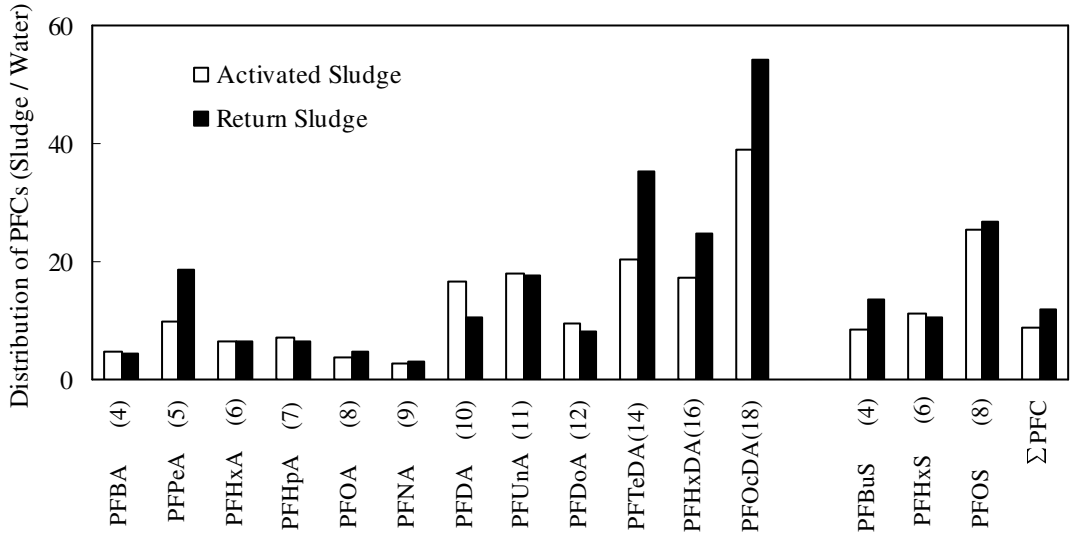

Figure 4.5 PFC distributions in activated and return sludge in K-WWTP

4.5.2.2 Mass flows of PFCs in K-WWTP

Mass flow of each PFC can be calculated by product of concentration and flow rate. Mass flow of ∑PFC, as sum of concentrations for all 15 PFCs, is shown in **Fig. 4.6** to demonstrate general behavior of PFCs in K-WWTP. The PFC amounts in aqueous and particulate phase along process were uniformed into g/day and drawn by width-scaled arrows to explicit their relationships. Loadings of PFCs in aeration tank were expressed by numbers instead of width-scaled arrows, because their values were rather higher than in other processes. PFC loadings in advanced treatment processes, including ozonation and BAC filter, were rather lower than others, so that their PFC loadings were drawn in larger scales than other aqueous phase. PFCs in WWTP influent and effluent, which represented sum of four different series, were also shown in the figure by dash arrows and italic numbers. Mass flows for each PFC in K-WWTP were shown in figures of **Appendix A.**

Table 4.3 PFC concentrations in aqueous phase (ng/L, *n*=5)

Site (Q,m^3/d)	Influent (196,553)	PC eff. (27,274)	AS inside (40,226)	R. Sludge (13,589)	SC eff. (26,351)	SF eff. (26,359)	Ozone eff. (6,500)	BAC eff. (6,500)	Effluent (225,631)
PFBA (4)	**24** (10~57)	**36** (7~50)	**8** (6~24)	**8** (4~18)	**4** (3~44)	**4** (ND~16)	**5** (4~13)	**5** (ND~13)	**7** (ND~10)
PFPeA (5)	**55** (11~83)	**54** (35~74)	**23** (9~33)	**23** (7~39)	**20** (17~35)	**22** (7~47)	**13** (8~25)	**10** (6~22)	**19** (5~63)
PFHxA (6)	**31** (ND~93)	**29** (ND~75)	**17** (13~23)	**17** (9~25)	**13** (8~29)	**16** (7~74)	**12** (6~36)	**14** (10~36)	**12** (ND~27)
PFHpA (7)	**79** (30~116)	**45** (8~115)	**30** (10~177)	**31** (13~80)	**13** (4~39)	**30** (10~80)	**22** (6~132)	**26** (9~114)	**23** (5~82)
PFOA (8)	**95** (24~237)	**56** (12~111)	**117** (47~286)	**70** (41~111)	**50** (29~88)	**88** (65~136)	**84** (48~131)	**98** (45~159)	**64** (32~109)
PFNA (9)	**125** (15~340)	**61** (9~135)	**74** (36~248)	**71** (41~253)	**67** (56~97)	**112** (70~254)	**109** (66~289)	**104** (50~364)	**84** (44~386)
PFDA (10)	**15** (ND~51)	**9** (ND~22)	**10** (6~19)	**12** (8~28)	**8** (6~99)	**18** (9~74)	**12** (9~16)	**12** (6~50)	**16** (7~40)
PFUnA (11)	**23** (ND~39)	**17** (ND~50)	**12** (5~32)	**12** (4~23)	**9** (4~14)	**12** (5~21)	**13** (4~32)	**14** (9~19)	**13** (8~18)
PFDoA (12)	**22** (ND~186)	**19** (5~55)	**18** (2~69)	**17** (2~63)	**12** (7~23)	**11** (5~61)	**29** (4~60)	**21** (9~67)	**12** (8~49)
PFTeDA(14)	**92** (5~161)	**77** (27~172)	**19** (3~110)	**20** (ND~99)	**15** (ND~28)	**16** (4~117)	**27** (ND~79)	**15** (ND~101)	**11** (ND~29)
PFHxDA(16)	**22** (5~128)	**56** (18~211)	**9** (5~65)	**12** (4~203)	**7** (4~208)	**22** (4~61)	**11** (4~55)	**7** (ND~68)	**10** (3~162)
PFOcDA(18)	**47** (16~91)	**35** (12~58)	**8** (3~13)	**6** (4~18)	**9** (4~55)	**9** (5~33)	**6** (5~30)	**8** (ND~63)	**10** (6~57)
PFBuS (4)	**125** (40~262)	**40** (13~169)	**36** (14~105)	**24** (8~108)	**34** (15~71)	**29** (17~49)	**18** (8~81)	**26** (7~49)	**31** (8~88)
PFHxS (6)	**18** (ND~36)	**15** (4~20)	**8** (4~23)	**9** (6~21)	**7** (4~11)	**8** (6~23)	**9** (7~32)	**10** (7~29)	**12** (7~61)
PFOS (8)	**19** (4~212)	**11** (7~17)	**21** (5~79)	**25** (17~84)	**19** (17~32)	**26** (23~29)	**29** (23~37)	**31** (18~53)	**29** (22~110)

Table 4.4 PFC concentrations in particulate phase (ng/g dry, *n*=3)

Site (Q,m^3/d)	**Influent (196,553)**	**PC eff. (27,274)**	**AS inside (40,226)**	**R. Sludge (13,589)**	**SC eff. (26,351)**	**SF eff. (26,359)**	**Ozone eff. (6,500)**	**BAC eff. (6,500)**	**Effluent (225,631)**
PFBA (4)	**41**	**110**	**8** (ND~23)	**5** (ND~15)	NS	NS	NS	NS	NS
PFPeA (5)	**31**	**65**	**46** (ND~115)	**61** (14~122)	NS	NS	NS	NS	NS
PFHxA (6)	**68**	**122**	**22** (8~48)	**15** (4~23)	NS	NS	NS	NS	NS
PFHpA (7)	**77**	**110**	**44** (21~72)	**28** (12~54)	NS	NS	NS	NS	NS
PFOA (8)	**238**	**727**	**87** (28~190)	**49** (18~96)	NS	NS	NS	NS	NS
PFNA (9)	**122**	**92**	**40** (19~55)	**30** (14~55)	NS	NS	NS	NS	NS
PFDA (10)	**169**	**65**	**35** (12~67)	**18** (14~24)	NS	NS	NS	NS	NS
PFUnA (11)	**625**	**200**	**44** (2~84)	**30** (5~79)	NS	NS	NS	NS	NS
PFDoA (12)	**1392**	**464**	**35** (8~58)	**20** (10~34)	NS	NS	NS	NS	NS
PFTeDA(14)	**2087**	**1456**	**80** (28~140)	**101** (36~195)	NS	NS	NS	NS	NS
PFHxDA(16)	**480**	**457**	**33** (19~47)	**44** (32~59)	NS	NS	NS	NS	NS
PFOcDA(18)	**354**	**350**	**65** (32~143)	**46** (28~67)	NS	NS	NS	NS	NS
PFBuS (4)	**379**	**396**	**62** (20~119)	**46** (39~55)	NS	NS	NS	NS	NS
PFHxS (6)	**118**	**234**	**19** (4~45)	**14** (8~18)	NS	NS	NS	NS	NS
PFOS (8)	**508**	**687**	**110** (8~194)	**96** (9~212)	NS	NS	NS	NS	NS

About 360 g PFCs were daily introduced to K-WWTP, two thirds of which were attached on particles. After treatment by WWTP, about 80% of ∑PFC was removed from influent and 70 g residual PFCs were discharged into Lake Biwa. This result indicated moderate performance of K-WWTP to remove ∑PFC. However, by considering aqueous phase, only 60% of the influent ∑PFC was removed.

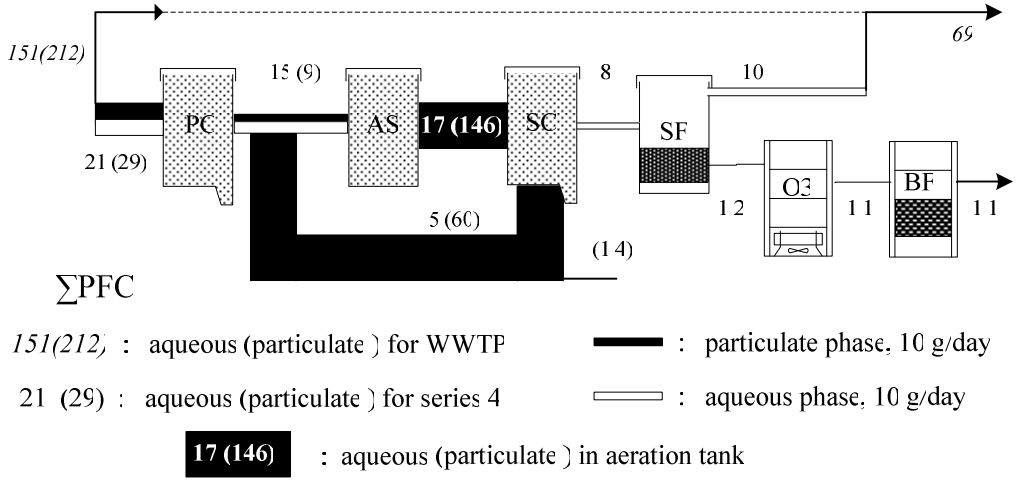

Figure 4.6 Mass flow of ∑PFC in K-WWTP

PFCs were expected to have similar behavior in four series. About 50 g/day was introduced to 4th series with 60% on particles. Around 80% of ∑PFC in influent was removed by PC, ASP, and SF combined processes. ∑PFC mass flow was rather high in activated sludge and return sludge, with distribution coefficients of 9~12, which supported the hypothesis of PFCs accumulation in aeration tank and their circulation by return sludge. This fact was similar to other study in literature (Schultz, *et al.*, 2006c). SF, O3 and BAC seemed unable to reduce ∑PFC effectively.

4.5.3 PFC behavior patterns in K-WWTP

Mass flow of individual PFCs can be analyzed as same as ∑PFC, however, pattern analysis was helpful to understand PFCs behavior more easily. **Table 4.5** shows PFCs behavior in WWTP such as loading strength of influent, removal rates of PC and activated sludge process (AS+RS+SC), which were correlated with their carbon chain lengths. Therefore, these 15 kinds of PFCs were coarsely classified into three patterns as "*medium*", "*long*" and "*short*" to understand their common characteristics better. This classification was specified in K-WWTP and proposed as the first time in this field.

4.5.3.1 "Medium" pattern PFCs

"*Medium*" pattern PFCs include PFOA(8), PFNA(9) and PFOS(8), with carbon-chain length of 8~9. Typical characteristics of PFCs in this pattern are their negative removals by ASP, and poor or even negative treatment efficiency in aqueous phase. "*Medium*" PFCs in process effluent was close to their amounts in influent aqueous phase, so that these PFCs seemed to penetrate WWTP process directly. Considering the performance of whole plant, only 2% of aqueous "*Medium*" PFCs were removed.

Figure 4.7 shows the aqueous concentrations of "*Medium*" pattern PFCs, which implies the similarity among the three chemicals. Aqueous concentrations in influent of PFOA(8) and PFNA(9) were four times higher than PFOS(8). However, if considered particulate phase, PFOS(8) had similar concentration with PFOA(8) and PFNA(9) because of its higher distribution to particulate phase. PC showed moderate removal for these PFCs both in aqueous and particulate phase.

Table 4.5 Description of PFC behavior patterns in K-WWTP

	Medium PFCs	***Long PFCs***	***Short PFCs***
PFCs included	PFOA, PFNA, PFDA, PFOS *PFCA(8-9),PFAS(8)*	PFUnA,PFDoA,PFTeDA, PFHxDA,PFOcDA *PFCA(10-12,14,16,18)*	Other PFCs *PFCA(4-7),PFAS(4-6)*
Description	PFCs break through WWTP processes with poor treatment	High loading on particles in influent. Removal by PC-AS-SC	Less toxic and bioaccumulated Reduced by PC-AS-SC
Influent concentrations	**Moderate** 100~150 ng/L 10~80% on SS	**High** 100~420 ng/L >80% on SS	**Weak** 30~50 ng/L 10~50% on SS
Removal by PC	**Moderate** 39 ~ 52%	**Strong** 45 ~ 81%	**Weak** 3 ~ 62%
Removal by ASP	**Negative** -110 ~ -13%	**Effective** 31 ~ 83%	**Postive** 10 ~ 77%
Overall removal in aqueous	**Poor / negative** -51 ~ 33%	**Postive** 37 ~ 78%	**Effective** 61 ~ 71%
Overall removal in aqu. & part.	**Poor** 42 ~ 71%	**High** 90 ~ 97%	**Moderate** 68 ~ 82%

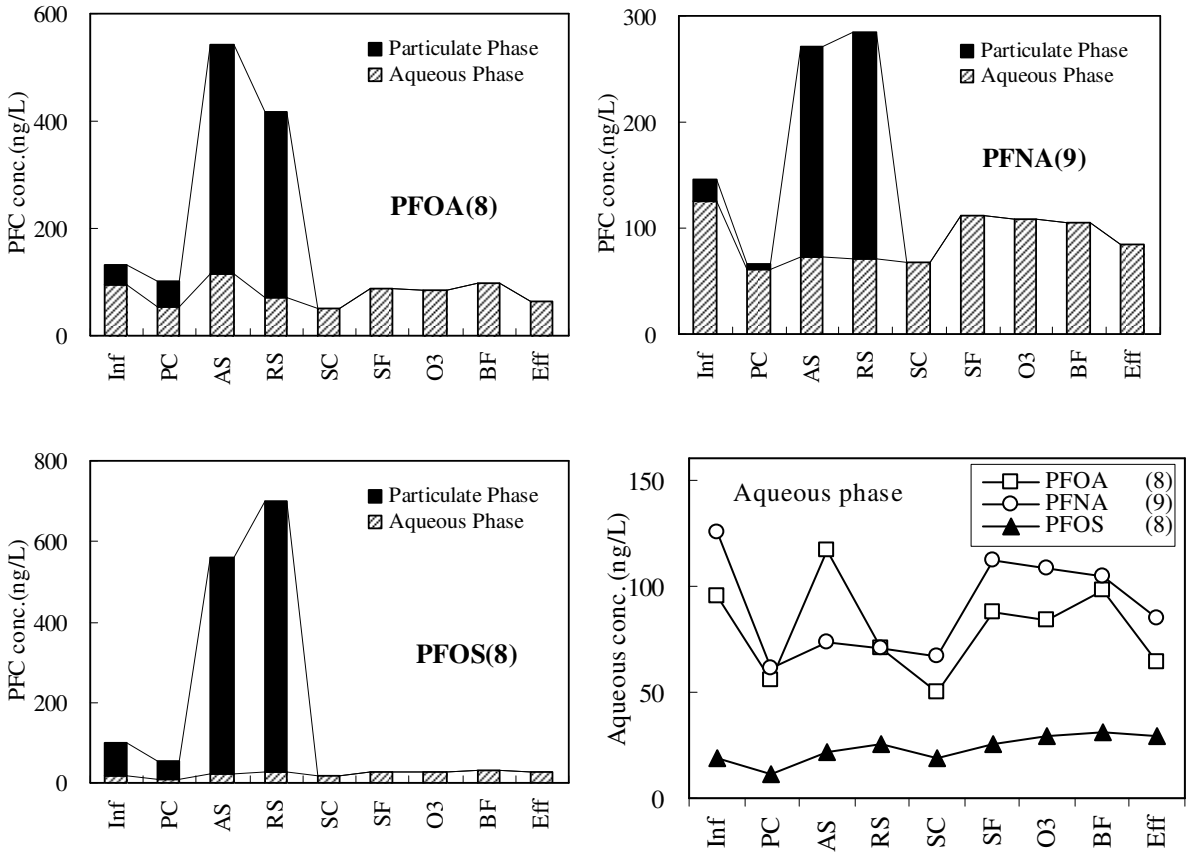

Figure 4.7 Concentrations of "*Medium*" PFCs along treatment processes

Aqueous concentrations of PFOS(8) and PFOA(8) were almost doubled in aeration tank (AS). One possible reason referred to desorption of PFCs from return sludge. Another explanation was the

generation of PFCs by possible biodegradation of precursors, which was also proposed in literature to explain the increase of PFOS (Schultz, *et al.*, 2006c). However, the intermediate products of degradation were difficult to be identified and analyzed, so that they were not measured in this study.

SC effluent contained less PFCs in aqueous phase than AS and RS, which might be explained by the sorption of PFCs to the new increment of activated sludge and the Poly-PAC added in the forth anoxic chamber to enhance coagulation. SF, O3 and BAC showed ineffective removal on "*Medium*" PFCs. Reason of increasing concentration in aqueous phase by SF was not clear yet. PFC molecules were considered strong enough to resist oxidation of ozone-related processes and therefore O3 seemed unable to remove PFCs. Ineffective removal of BAC filter might be caused by break through of GAC fixed bed.

PFOA(8) and PFNA(9) should be seriously concerned in this pattern, because they occupied in very higher concentrations and penetrate treatment processes from influent to effluent directly, which might be harmful to human health by considering their carcinogenetic toxicities. PFOS(8) should also be cared because it was strongly combined with particles and accumulated in sludge in very high extent among all 15 kinds of PFCs in this study.

4.5.3.2 "Long" pattern PFCs

"*Long*" pattern PFCs include PFCA(10~18), with carbon length longer than 10. Typical properties of "*Long*"PFCs are their heavy loadings in influent, and highly distributions to suspended solids. "*Long*" PFCs can be strongly removed by sedimentation in primary clarifier. **Figure 4.8** shows the aqueous and particulate concentrations of four typical "*Long*" PFCs, such as PFUnA(11), PFDoA(12), PFTeDA(14) and PFOcDA(18). All of them had very high concentrations in influent, which were higher than most of other PFCs except PFOA(8) and PFNA(9). Because of their strong hydrophobicity, PFCs in this pattern were attached to particles strongly both in influent and in sludge. "*Long*" pattern PFCs were removed by primary clarifier effectively, as 76%, 81%, 61% and 75% for PFCA(11,12,14,18) respectively. Concentrations of "*Long*" PFCs in aqueous phase are also shown in **Fig. 4.8**, which were also decreased by sedimentation.

PFCA(11~14) were reported to exist in primary sludge (Schultz, *et al.*, 2006c), which supported the capacity of primary clarifier to remove "*Long*" PFCs. After removal by sedimentation, "*Long*" PFCs were further reduced by ASP, which mechanism was still unknown yet because PFCs were expected not degradable in biological treatment. By primary clarification and activated sludge process, PFCA(10~18) were reduced from concentrations as high as 120~400 ng/L to 15ng/L, and not changed much in the following processes.

As general properties of "*Long*" pattern, PFCs had heavy loaded in influent and effectively removal by primary sedimentation. Concentrations of these PFCs were decreased after activated sludge process, which need further study on the mechanism. These PFCs were accumulated in activated sludge in similar extent to PFOA(8) but lower than PFOS(8). "*Long*" PFCs occupied 49% of ∑PFC in influent and contributed only 13% to effluent. PFDoA(12) and PFTeDA(14) should be concerned in this pattern because of the highest influent loading among all the 15 PFCs.

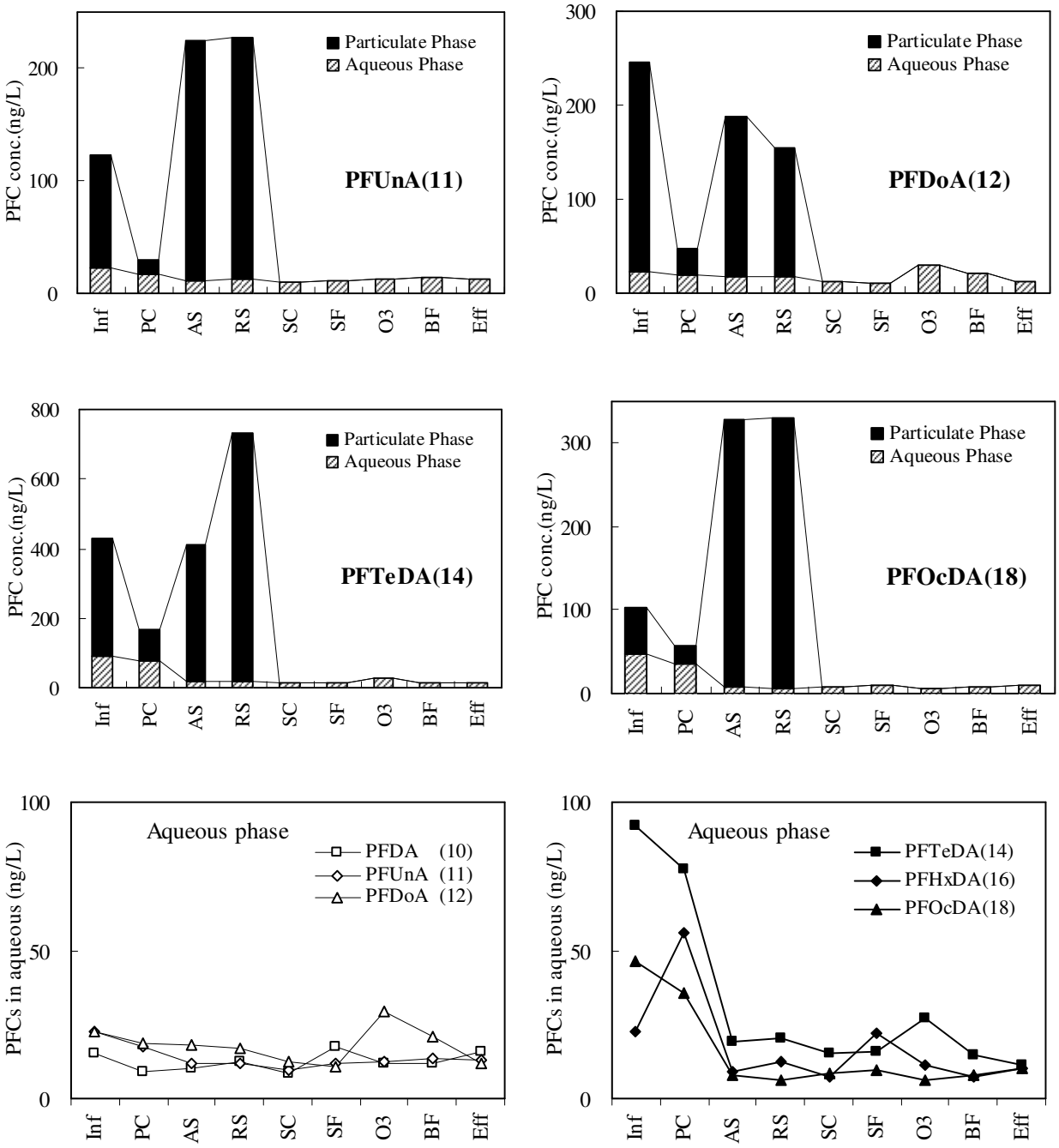

Figure 4.8 Concentrations of "*Long*" PFCs along treatment processes

4.5.3.3 "Short" pattern PFCs

Other six kinds of PFCs in this study were allocated to "*Short*" pattern, which contained shorter-chained PFCA(4~7) and PFAS(4~6). Concentrations of PFCs in this pattern were decreased gradually by activated sludge and further processes. Figure **4.9** shows the sum concentrations for three typical and aqueous phase concentrations for all "*Short*" PFCs. Influent concentrations of PFCs in "*Short*" pattern were varied in range of 30~90 ng/L, lower than "*Medium*" and "*Long*" PFCs. Primary clarification can remove "*Short*" PFCs by some extents, except for PFBA(4), which was increased abnormally. Concentrations of "*Short*" PFCs were all decreased by ASP and not changed much after ASP. According to their low aqueous concentrations and low distributions to sludge, "*Short*" pattern PFCs were not

strongly accumulated in activated sludge.

As general properties for "*Short*" pattern, PFCs had lower concentrations in influent and can be reliably removed by activated sludge process. "*Short*" pattern PFCs occupied 40% of aqueous ∑PFC of influent and contributed 29% of effluent. "*Short*" pattern PFCs are less toxic than other PFCs with longer chains like PFOA(8), and seemed reliably removed by current process, therefore all of them did not require urgent concerns.

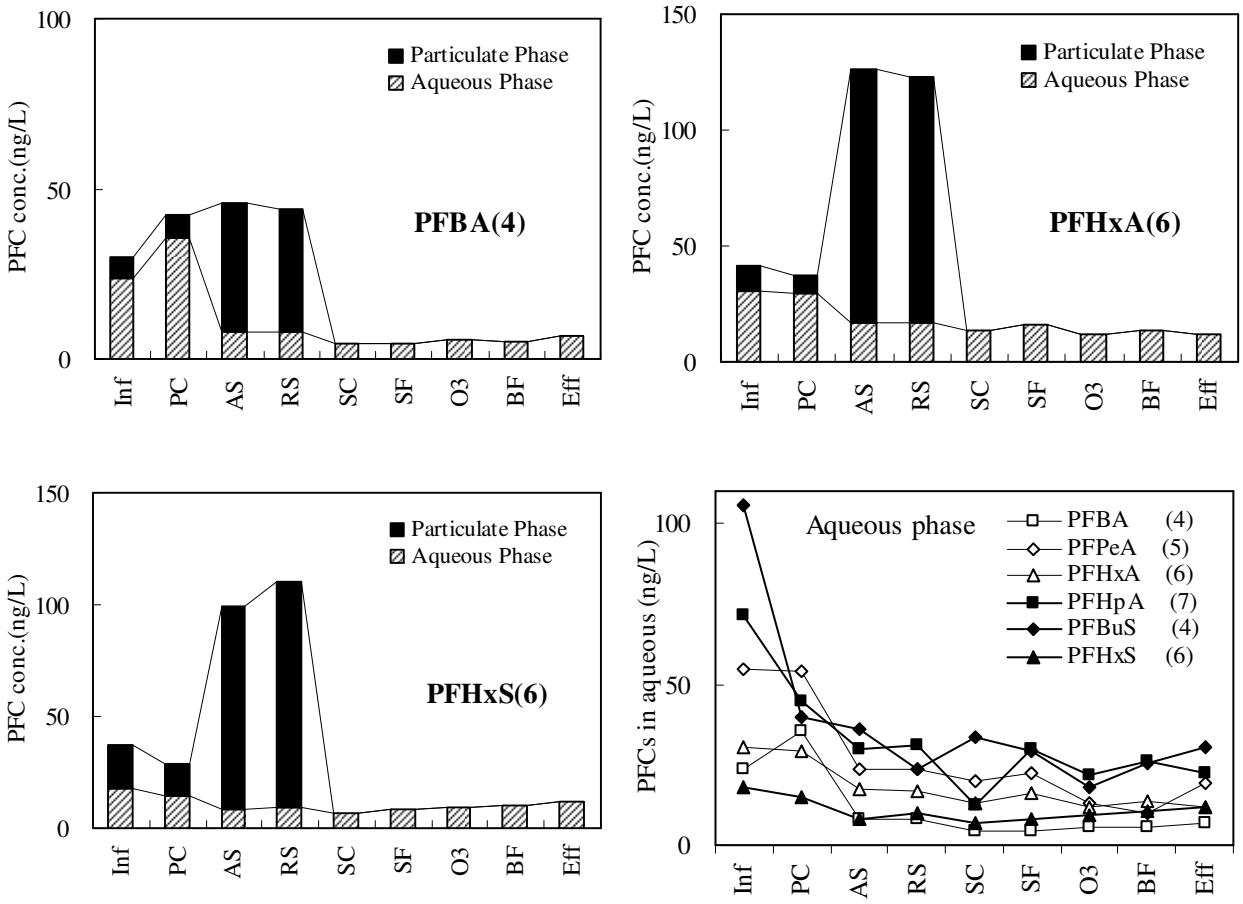

Figure 4.9 Concentrations of "*Short*" pattern PFCs along process.

4.5.3.4 Analysis on sources and sinks of PFCs

As best known in the literature, long-chained PFCs were very rarely detected in aqueous phase of WWTP influent, with only one example of PFUnA from industrial wastewater(Sinclair and Kannan, 2006). Considering the rather high concentration of "*Long*" PFCs in K-WWTP influent, there PFCs were supposed to come from industrial wastewater streams. "*Long*" PFCs showed strong affiliation to particles, and were accumulated in activated sludge. These PFCs could be removed effectively by primary clarification and transported into primary and excessive sludge, which were incinerated as final disposal. Because PFCs were known to be completely decomposed in municipal incinerators, their final sinks were expected to be CO_2 and HF.

Except of industrial discharge, sources of "*Medium*" PFCs could also be contributed by commercial products. PFOA concentrations in aqueous phase of WWTP influent were reported to be 15~20 ng/L in domestic wastewater (Boulanger, *et al.*, 2005; Schultz, *et al.*, 2006c), and 140~400 ng/L for industrial contained wastewater (Sinclair and Kannan, 2006). In K-WWTP, PFOA and PFNA in aqueous influent

were 80~125ng/L, which source could be mainly signed to industrial discharge. However source from domestic wastewater can not be excluded because PFOA in WWTP influent was once reported in a domestic WWTP as high as 89 ng/L (Schultz, *et al.*, 2006a). The increase of "*Medium*" PFCs by activated sludge process might be caused by biodegradation of related precursors. "*Medium*" PFCs can not be effectively removed by K-WWTP and contributed 55% of final discharge of ∑PFC. Then, the sink of "*Medium*" PFCs was allocated to environmental wasters as Lake Biwa. Primary and secondary clarifiers can remove "*Medium*" PFCs for some extent, which were finally decomposed to be CO_2 and HF by incineration of sludge.

"*Short*" PFCs were less toxic than medium-chained and longer-chained PFCs and effectively removed by K-WWTP. Furthermore, they were considered as environmental friendly materials and applied to alternate medium-chained PFCs for industry application, like PFBA(4) to take place of PFOA(8) (Poulsen, *et al.*, 2005). Therefore these PFCs did not require urgent concerns on their sources and sink.

Because of properties as surfactants, PFCs might also be removed by floating with fine bubbles, especially for more hydrophobic molecules. All tanks in K-WWTP were covered and exhaust gas was collected and treated by activated carbon adsorption before discharge in to air. Therefore, adsorption on activated carbon for odor control might be another sink for all PFCs in this study.

4.5.3.5 Brief Summary

As a brief summary, 15 kinds of analyzed PFCs were classified into three patterns according to their carbon chain lengths and behavior in K-WWTP. PFCs in "*Medium*" pattern, including PFCA(8~10) and PFOS(8), broke through WWTP processes without effective removal. PFCA(8~9) should be serious concerned in K-WWTP because of the very high concentration in influent and effluent. PFOS(8) should also be concerned by its very strong affiliation to activated sludge. PFCs in "*Long*" pattern, including PFCA(10~12,14,16,18), were strongly attached on SS and effectively removed by primary clarification. PFDoA(12) and PFTeDA(14) should be concerned because of their relatively high influent loadings. "*Short*" pattern, which mainly contained shorter-chained PFCs as PFCA(4~7) and PFAS(4,6), were not harmful and effectively removed by K-WWTP, and thus less concerned.

Sources and sinks of PFCs were briefly analyzed for the three patterns. Industrial discharge was highly suspected as the source of PFCs in K-WWTP. Medium and long chained PFCs were strongly accumulated in activated sludge. Incineration of primary and excessive sludge was considered as sink of removed PFCs. "*Medium*" pattern PFCs can not be removed effectively, and transported to the water environment.

4.5.4 Process Estimation for PFC Removal in K-WWTP

4.5.4.1 Removal efficiency of individual facility

Removal efficiency (RE) of individual facility on each PFC and ∑PFC can be calculated by comparing the PFC concentrations in influent and effluent of the specific facility, as shown in following equations.

$$sRE_{i,j} = \frac{C_{ij,in} - C_{ij,out}}{C_{ij,in}} \tag{4.1}$$

$$sRE_i = \left(\sum_j C_{ij,in} - \sum_j C_{ij,out} \right) \Big/ \sum_j C_{ij,in} \tag{4.2}$$

where $sRE_{i,j}$ is removal efficiency in *i* unit for *j* PFC, sRE_i is removal efficiency of ∑PFC by *i* unit. $C_{ij,in}$ is

concentration of *j* PFC in influent to *i* unit and $C_{ij,out}$ represents the concentration in effluent. **Table 4.6** shows results of s$RE_{i,j}$ and sRE_i calculated for primary clarifier(PC), aeration tank(AS), second clarifier(SC), rapid sand filtration(SF), ozonation(O3) and BAC filter(BAC). s$RE_{i,j}$ for "*Medium*" PFCs was calculated in both aqueous phase and uniformed phases. s*RE* for whole process was calculated based on uniformed phases. The negative values were shown in bold font.

PC played positive role on removal of all kinds of PFCs, with highest s*RE* for PFDoA(12) as 81%. PC contributed main removal of PFCs because RE by PC was similar to that by *whole* WWTP. Aeration tank positively removed "*Long*" PFCs, but unable to remove "*Medium*" PFCs. The increase of concentrations might be caused by degradation of related precursors. Second clarifier was helpful to remove PFCs by s*RE* about 25%, as same roles with primary clarifier. Sand filtration increased concentrations of both "*Medium*" and "*Long*" pattern PFCs. Releasing of PFOS(8) by trickling filter was reported and proposed to be cause by biodegradation of related precursors (Schultz, *et al.*, 2006c). However, more studies are needed to draw reliable conclusions. Ozonation and BAC filter seemed also ineffective to remove PFCs, especially for "*Medium*" PFCs.

Table 4.6 Removal efficiency of individual unit for each PFC in K-WWTP

s$RE_{i,j}$	Removal efficiency of single unit						*whole* WWTP
	PC	AS	SC	SF	O_3	BF	Inf→Eff
PFOA (8)[a]	0.41	**-1.10**	0.30	**-0.77**	0.04	**-0.16**	0.33
PFNA (9)[a]	0.52	**-0.21**	0.05	**-0.67**	0.03	0.04	0.33
PFOS (8)[a]	0.43	**-0.95**	0.24	**-0.34**	**-0.14**	**-0.07**	-0.51
PFOA (8)[b]	0.24	-0.16					0.52
PFNA (9)[b]	0.54	-0.11					0.42
PFOS (8)[b]	0.47	0.60					0.69
PFDA (10)[b]	0.39	**-0.13**	0.32	**-1.12**	0.34	**-0.01**	-0.05
PFUnA (11)[b]	0.76	0.60	0.23	**-0.25**	**-0.07**	**-0.10**	0.90
PFDoA (12)[b]	0.81	0.62	0.27	0.14	**-1.77**	0.28	0.95
PFTeDA(14)[b]	0.61	0.89	0.24	**-0.02**	**-0.72**	0.45	0.97
PFHxDA(16)[b]	0.16	0.89	0.41	**-2.03**	0.49	0.35	0.90
PFOcDA(18)[b]	0.45	0.86	**-0.43**	**-0.09**	0.36	**-0.34**	0.90
∑PFC	0.51	0.54	0.20	**-0.47**	0.06	**-0.01**	0.81

Note: ***a*** = aqueous phase, ***b*** = sum of aqueous and particulate phases.

4.5.4.2 Removal efficiencies of combined processes

Removal efficiency by combined process was also calculated by considering the s*RE* for single unit in sequence to estimate the integral performance.

$$cRE_{i,j} = \frac{C_{0j} - C_{ij,out}}{C_{oj}} = 1 - \prod_i \left(1 - sRE_{i,j}\right) \tag{4.3}$$

where c$RE_{i,j}$ is removal efficiency for *j* PFC by combined process from influent to *i* unit, s$RE_{i,j}$ is removal efficiency by single *i* unit, C_{oj} is concentration in WWTP influent, and $C_{ij,out}$ is concentration of *j* PFC in the flow out of *i* unit. cRE_j for ∑PFC was calculated from sRE_i in similar method by eliminating

subscript *j* in **Eq. (4.3)**. **Table 4.7** shows results of c$RE_{i,j}$ and cRE_i calculated for primary clarifier (PC), second clarifier (PC→SC), rapid sand filtration (PC→SF), ozonation (PC→O_3) and BAC filter (PC→BF). Only primary concerned PFCs were listed in the table and the maximum values were shown in bold font.

PFCs were removed by activated sludge process in acceptable extents, with removal rates of 50~80% for "*Medium*" pattern PFCs and >92% for "*Long*" pattern PFCs. Activate sludge process was reported to remove 30%, 36% and 60% of PFCA(6,8,10) by 5~20ng/L in influent (Schultz, *et al.*, 2006c), which was comparable to 71%, 52% and 63% in this study respectively. One domestic plant with 7% industrial wastewater was reported to remove PFOS(8) from 400 ng/L to 130 ng/L by primary sediment and activated sludge process (Schultz, *et al.*, 2006a), which was also close to average removal rate for "*Medium*" PFCs as 66% in K-WWTP.

Table 4.7 Removal efficiency of combined process for each PFC in K-WWTP

c$RE_{i,j}$	Removal efficiency by combined process					*whole* WWTP
	PC	PC→SC	PC→SF	PC→O_3	PC→BF	Inf→Eff
PFOA (8)[a]	0.24	**0.63**	0.34	0.37	0.27	0.52
PFNA (9)[a]	**0.54**	0.54	0.22	0.25	0.28	0.42
PFOS (8)[a]	0.47	**0.81**	0.75	0.71	0.69	0.71
PFUnA (11)[b]	0.76	**0.92**	0.91	0.90	0.89	0.90
PFDoA (12)[b]	0.81	**0.95**	0.96	0.88	0.91	0.95
PFTeDA(14)[b]	0.61	**0.96**	0.96	0.94	0.97	0.97
total-PFC [c]	0.51	**0.84**	0.77	0.78	0.78	0.81

Note: ***a***="*Medium*" pattern; ***b***="*Long*" pattern, ***c***=cRE_i for ∑PFC. All data are calculated by aqueous and particulate phase together.

4.5.4.3 Brief Summary

Clarifier was the most important facility in WWTP to remove PFCs. Both primary and secondary clarifiers showed effective removal on aqueous PFCs. Activated sludge process showed opposite performances for "*Medium*" and "*Long*" PFCs. All of PFCs were accumulated in activated sludge for different extents and circulated with return sludge. Sand filtration, ozonation, BAC filter seemed unable to remove "*Medium*" and "*Long*" PFCs effectively. As result for combined process estimation, activated sludge process couple with clarifier can remove 40~70% of "*Medium*" PFCs, 95% of "*Long*" PFCs and 80% of "*Short*" PFCs. However, PFOA(8) and PFNA(9) in aqueous phase were only removed for about 30% and PFOS(8) was even increased for 50%.

4.6 Summary

By periodical surveys in K-WWTP, behavior of PFCs in WWTP process was classified into "*Medium*", "*Long*" and "*Short*" patterns according to their carbon chain lengths. PFCs showed similar behavior in same pattern, and different properties to other patterns. "*Medium*" PFC, such as PFCA(8,9) and PFOS(8), were considered primary contaminants in K-WWTP and poorly removed by overall processes. Individual facilities and combined processes were estimated by their remove performances of PFCs. Clarification showed effective removal on all PFCs. Activated sludge process showed opposite performances for "*Medium*" and "*Long*" PFCs. Sand filtration, ozonation, BAC filter seemed unable to remove PFCs

effectively. Results of this chapter were shown as follows.

(1) K-WWTP influent contained 36 mgDOC/L and 160mgSS/L in average, which were mainly removed in primary clarifier and aeration tank. Further processes including sand filtration, ozonation and BAC filtration can continuously remove DOC and SS to be lower than 2.3 mg/L and 0.01 mg/L respectively.

(2) All PFCs were detected at each sampling site. About 50% of ∑PFC in aqueous phase was removed by overall processes. By considering particulate phase concentration, around 80% of ∑PFC in sum of two phases was removed from WWTP influent. PFCA(8,9,14) had highest aqueous concentrations in influent as 95, 125 and 92 ng/L respectively. PFCA(8,9) and PFOS(8) occupied 50% of discharged ∑PFC, which should be seriously concerned.

(3) Behavior of PFCs in K-WWTP was classified into "*Medium*", "*Long*" and "*Short*" patterns according to their carbon chain lengths. "*Medium*" pattern consisted of PFCA(8~9) and PFOS(8). "*Long*" pattern included longer-chained PFCs as PFCA(10~12,14,16,18). "*Short*" pattern contained PFCA(4~7) and PFAS(4,6).

(4) "*Medium*" PFCs were poorly removed by current process. The average removal rate in aqueous phase was only 2% by overall processes. "*Long*" PFCs were attached on particles strongly and effectively removed by clarification. They occupied 49% in influent and but contributed only 13% to effluent. "*Short*" PFCs were less toxic and effectively removed by current processes.

(5) Performances of individual facilities and combined processes were estimated for PFCs in different patterns. Clarifier was very important for removal of all PFCs in K-WWTP. Activated sludge process showed removal of "*Long*" PFCs but increase of "*Medium*" PFCs. Sand filtration, ozonation, BAC filter seemed unable to remove "*Medium*" and "*Long*" PFCs effectively.

(6) All of PFCs were accumulated in activated sludge for different extents and circulated with return sludge. Activated sludge process couple with clarifier can remove 40~70% of "*Medium*" PFCs, 95% of "*Long*" PFCs and 80% of "*Short*" PFCs.

CHAPTER V REMOVAL OF PERFLUOROCHEMICALS BY ADSORPTION PROCESS

The adsorption of organic substances from aqueous solutions increases strongly and regularly as we ascend the homologous series. —*Traube's rule*

5.1 Introduction

Application of carbon can be dated back to 1550BC for medicinal purpose in Egypt. Study and utilization of carbon was started from late of 18th century. Sheele (1773) and Fontana (1777) recognized abundant adsorptive power of activated carbon for gases, and Lowitz (1785) recorded decolourization of water by activated carbon. Later, Napoleon used carbon to refine sugars, which was the first industrial application of carbon in aqueous phase. In beginning of 20th century, carbon was activated and activated carbon (AC) was firstly produced in Europe. The application of AC for water treatment was encouraged by its first appearance in 1927 to perfectly restore phenol polluted drinking water in Chicago (JACM, 1984). Nowadays AC adsorption is considered as a reliable and promising process in water treatment process to remove organics which involves of color, taste and odor.

A variety of natural and synthetic materials can be used for the production of AC, including coal, wood, lignite, sawdust, pulp, peat, oil shale, coconut shells, lignin, and sugar (Ho, 2004). By increasing temperature to as high as 600℃, volatile fractions are drawn off from raw materials and carbonization is accomplished in the absence of air. The carbonaceous materials are further activated under thermal conditions in 600~900℃ or chemical conditions like $ZnCl_2$ to increase surface area dramatically (JACM, 1984; Cooney, 1998). After activation, abundant pores are generated inside carbon materials, which are classified into four types by their diameters as primary micropores (<0.8 nm), secondary micropores (0.8~2.0 nm), mesopores (2~50 nm) and macropores (>50 nm) (IUPAC, 1972).

Nature of AC adsorption includes two different essential types, physical adsorption by van der Waals forces and chemisorption by chemical bond forces. Physically adsorbed molecules are attached on surface at a rapid rate and therefore are thermodynamically reversible because of relatively lower adsorptive heat as about 1 kcal/mol. Chemisorption heat is much higher to be 50~100 kcal/mol, which results in much stronger interactions and irreversible affinities between adsorbate and carbon surface (Kumar, *et al.*, 2004).

Isotherm data are helpful to estimate capacity of AC adsorption. Many models have been developed to interpret experimental isotherms. **Table 5.1** lists some generalized equations which can derivate popular models. Isothermal models based on assumption of local site adsorption in single layer, can be uniformed into Generalized Langmuir equation, which derives four popular models including famous Langmuir equation. If adsorbate amount is close to saturated concentration, multilayer adsorption will be dominant which can be described by BET equation. Based on Eucken-Polany potential theory, in which adsorption is determined by potential curve as $A=RT\ln(C_s/C)$, Dubinin and Raduskevich developed micropore volume filling theory, which can derive Freundlich equation, Dubinin-Raduskevich equation, Dubinin-Astakhov equation and Exponential Jaroniec equation. Dubinin-Astakhov equation is suitable for adsorptions in low concentration and especially for temperature varied systems. Among empirical models, Freundlich equation is most popular and satisfied for AC adsorption in large range of

concentrations (Nicholas and Paul, 1993; Cooney, 1998).

Table 5.1 Summary of isothermal models for GAC adsorption

Assumption	Name	Equations	Conditions	Comments
Single layer local site	*Generalized Langmuir*	$\frac{q}{q_m}=\left[\frac{(Kc)^n}{1+(Kc)^n}\right]^{m/n}$	n=m=1	Langmuir
			0<n=m<1	Langmuir-Freundlich
			n=1,0<m<1	General. Freundlich
			m=1,0<n<1	Tóth
Multilayer adsorption	*B.E.T.*	$\frac{q}{q_m}=\frac{1}{1-x}\cdot\frac{Kx/(1-x)}{1+Kx/(1-x)}, x=\frac{c}{c_s}$		Hüttig
				Sircar
				Lopez-Gonzalez&Dietz
Micropore filling	*Dubinin- Astakhov*	$\frac{q}{q_m}=\exp\left[-B(RT)^n\ln^n\frac{C_s}{C}\right]$	n=1	Freundlich
			n=2	Dubinin-Raduskevich
			n=i, $\sum$	Exponential Jaroniec
Empirical	*Freundlich*	$q=Kc^n$	Narrow c range, but large range for GAC	
	Radke-Prasunitz	$q=\frac{AKc}{1+(Kc)^n}$	Combine Henry (q=Kc) and Freundlich (q=Kc^m), better performance than either	
	Jossens	$Kc=q\cdot\exp(B\cdot q^m)$	Exponentially depend on isosteric heat	
	Tiemkin	$q=A+B\log c$	Suitable for gas catalyst	

Note: q is adsorbent loading rate, q_m is maximum loading rate, c is bulk concentration, c_s is saturated bulk concentration, K, A and B are adsorptive coefficients, n, m and R are constants, T is temperature.

Kinetic experimental data reveal adsorption velocity and thus are important for design and operation of processes. It is widely accepted that adsorption process contains four steps from liquid phase to sites on porous surface as (1) diffusion in liquid phase, (2) external mass transfer to particle surface, (3) internal diffusion inside of adsorbent including porous diffusion (*a*) and surface diffusion (*b*) and (4) attachment onto the sites (Weber and Smith, 1987). These four steps are shown in **Fig. 5.1** schematically.

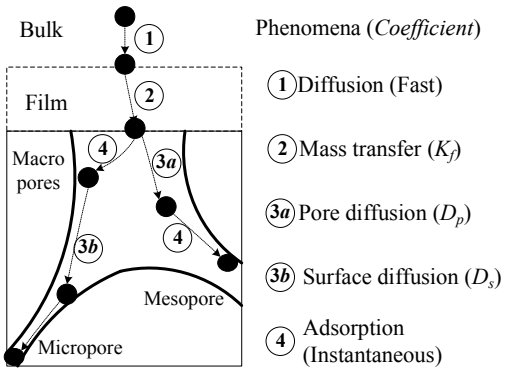

Figure 5.1 Adsorption steps to GAC

The first step is charged by overall mass balance and hydraulics behavior, which appears much faster than step 2 and 3. External mass transfer step is described by linear driving force model involving coefficient K_f, which is a function of hydraulics, physical properties of solvent, GAC size. K_f is independent on GAC nature, such as porosity or surface area. Intraparticle diffusion contains pore diffusion in aqueous phase and surface diffusion between adjacent sites, which is charged by surface properties, pore structure and adsorbate properties. Coefficients for pore diffusion (D_p), surface diffusion (D_s) or effective diffusion (D_{eff}) can describe intraparticle distributions inside pores. The last step, attachment on surface sites, is considered instantaneous and reversible, which is not rate limited step as same as step 1. Therefore, in order to simplify simulation, adsorption kinetics is usually assumed to be governed only by external mass transfer

and intraparticle diffusions (Baup, *et al.*, 2000). Dynamic models which combine film and intraparticle diffusion, can describe adsorption process successfully for both target chemicals and background organics. Simplest formation of these models is given by linear driving force theory approximation as $dq/dt = k(q_s-q)$, where q_s is equilibrium adsorbate loading to bulk concentration at time t (Weber and Smith, 1987).

Some complicated descriptions have been proposed in last 40 years for intraparticle diffusion step, as shown in **Table 5.2**. These models assume that pores and surfaces of GAC are homogenous and diffusivity follows Fick's Second Law. Pore diffusion model (PDM) was firstly developed but soon found to overestimate diffusivity, which implies that pore diffusion might not be dominant during adsorption. Therefore interests came to surface diffusion. Study proved that surface diffusivity was 20 times or more than porous diffusivity in adsorption of benzaldehyde to polystyrene Amberlite particles (Komiyama and Smith, 1974). Therefore, homogenous surface diffusion model (HSDM) seemed more applicable than PDM. HSDM has been successfully applied to explain breakthrough data of pilot scale GAC filter, of which most famous one was Michigan Adsorption Design and Applications Model. However, diffusivity estimated by HSDM is found dependent on initial concentrations. Then "lumped" model or pore-surface diffusion model (PSDM) to combine pore transport and surface diffusion simultaneously and describe intraparticle diffusion by effective diffusion coefficient D_{eff}, which includes pore diffusion D_p and initial concentration depended surface diffusion D_s. All of these models contain partially differential equations and numeric calculation is inevitable to solve these models.

Table 5.2 Summary of kinetic models for GAC adsorption

General model	Assumption	Solutions in aqueous phase	Application model
Fick's Second Law, D $\frac{\partial q}{\partial t} = D\frac{\partial C}{\partial r}$	Pore Diffusion[a]	$\varepsilon\frac{\partial C}{\partial t} + (1-\varepsilon)\rho_s\frac{\partial q}{\partial t} = \frac{\varepsilon}{r^2}\frac{\partial}{\partial t}\left(r^2 D_p\frac{\partial C}{\partial r}\right)$	Pore diffusion model (PDM, D_p)
	Surface Diffusion[a]	$-\nu\frac{\partial C}{\partial z} = \frac{\partial C}{\partial t} D_h\frac{\partial^2 C}{\partial z^2} + \rho_s\frac{1-\varepsilon}{\varepsilon}\frac{\partial q}{\partial t}$ $\frac{\partial q}{\partial t} = \frac{D_s}{r^2}\partial\left(r^2\frac{\partial q}{\partial r}\right)$	Homogenous surface diffusion model (HSDM, D_s)
	Lumped Diffusion[b]	$\frac{\partial q}{\partial t} = \left(D_p + \rho_s D_s\frac{\partial q}{\partial C}\right)\frac{\partial C}{\partial r}$	Pore-surface diffusion model (PSDM, D_{eff})
Linear Driving Force (LDF)[c]	$\frac{D_s}{K_f} = \frac{r}{5}$	$\frac{dq}{dt} = \frac{15 D_s}{r^2}(q^* - q)$	Simplified HDSM, D_s
	Infinite bath[d]	$\frac{\bar{q}}{q_\infty} = k\frac{(D_s t)^{1.2}}{r}$	Crank's solution
Fractal Theory[e] $\frac{dC}{dt^\alpha} = -k_{\alpha,n}C^n$	α=1, n=1[f]	$C/C_0 = \exp(-k_1 t)$	First order
	$\alpha\neq1$, n=1	$C/C_0 = \exp(-k_\alpha t^\alpha)$	Pseudo-first order
	α=1, n=2	$1/C - 1/C_0 = k_2 t$	Second order
	$\alpha\neq1$, n=2	$C/C_0 = \left[1+\exp(-k_\alpha t^\alpha)\right]^{-1}$	Pseudo-second order
	q, t	$q/q_e = 1-\left[1+(n-1)(t/\tau)^\alpha\right]^{-1/(n-1)}$	BSW(n, α)
	$\alpha\neq1$, $n\rightarrow1$	$q/q_e = 1-\exp(-t/\tau)^\alpha$	BSW(1, α), biological

Note: ***a***=(Weber and Smith, 1987); ***b***=(Hui, *et al.*, 2003); ***c***=(Carta and Lewus, 2000); ***d***=(Cooney, 1998); ***e***= (Gaspard, *et al.*, 2006); ***f***=α is fractal time index, n is fractional reaction order, τ is characteristic time. q and C are surface and aqueous concentrations at time t. q^* and q_e are equilibrium surface

loadings for C and C_0. ρ_s, r, ε and z are apparent density, radius, void fraction and depth of particles. D, D_s, D_p and D_{eff} are general, surface, pore and effective diffusion coefficients. v is flow rate, K_f is mass transfer coefficient.

First and second order models or their pseudo forms have been successfully applied to describe AC adsorption kinetics, such as pyridine (Mohan, *et al.*, 2004), antibiotics (Dutta, *et al.*, 1999) and phenol (Mohanty, *et al.*, 2006). These models are usually considered as empirical but recently uniformed into a new kinetics model based on fractal theory, as shown in **Table 5.2**. Fractal kinetics was proposed by dozen of years ago and later intensively applied in biophysics studies to simulate "*complex system*". The fractal kinetics gave up the homogenous assumption in diffusion kinetics, and developed fractal geometric description for complex network on heterogeneous surface. In case of GAC, fractal geometric description is based on pore size and distribution. A new model named as BSW(n,α) was proposed from fractal kinetics, and parameters of n and α were successfully determined for phenol, tannic acid and melanoidin adsorption on GAC (Gaspard, *et al.*, 2006).

Operation of AC adsorption was very important because improper operation could make AC filter ineffective and expensive. Performance of the adsorption process was influenced by characteristics of adsorbent and adsorbate, properties of flow and retention time (Nicholas and Paul, 1993; Ho, 2004). Among those influence factors, size relationship between adsorbate molecules and pore size distribution of AC was most important, because organics were more likely to adsorb into pores with approximately similar size (Newcombe, *et al.*, 1997; Bjelopavlic, *et al.*, 1999; Gauden, *et al.*, 2007). PFCs have rather small molecular weights and size, which is about 1~2 nm in length (approximately calculated by C-C bond length for straight carbon chain), therefore adsorption may mainly occur in micropores. Molecular structure of adsorbate can also affect adsorption. Hydroxyl groups in PFCAs and sulfonic group in PFASs will reduce adsorption, and adsorption of straight carbon chain was expected less than branched ones (Cooney, 1998).

Another important factor was related with surface function of activated carbon, which might be modified to specifically adsorb interested compounds (Newcombe, *et al.*, 1993; Vidic, *et al.*, 1997). Surface functional groups of activated carbon can be determined by X-ray photoelectron spectrum (Burke, *et al.*, 1992) or simply classified by titration (Menendez, *et al.*, 1995; Boehm, 2002; Barkauskas and Cannon, 2003). Activation methods can significantly influence carbon surface properties. AC activated by normal conditions (>750℃) is usually hydrophobic, called *H-type* carbons, which will be positive charged by adsorbing H^+ ions from water. Activation under lower temperature (200~400℃) will produce *L-type* carbons, which is hydrophilic and negative charged in water (Cooney, 1998). Obviously *H-type* carbon is helpful to adsorb PFCs from water. Except of modification by activation procedure, surface properties of activated carbon can be modified by control of solution pH (László, *et al.*, 2003), acid or base washing (Moreno-Castilla, *et al.*, 1995; Chen, *et al.*, 2003), oxidation like ozonation (Valdes, *et al.*, 2002; Valdes, *et al.*, 2003) and thermal treatment (Budarin, *et al.*, 2004).

The presence of natural organic matter (NOM) or wastewater organics may reduce adsorption capacities by competition for surface sites and carbon fouling (Li, *et al.*, 2003). Carbon fouling, which is also named as pore blockage, can reduce GAC capacity for trace organics greatly by blocking micropores after adsorption of large molecules like NOMs. Carbon fouling was usually happened in GAC filters because background organics break through the bed much earlier than trace organics and then fresh GAC will contact with NOMs before trace organics (Hand, *et al.*, 1997; Jarvie, *et al.*, 2005).

5.2 Aims

Major aim of this chapter is to study characteristics of GAC adsorption for PFCs removal and predict performance of fixed GAC bed to remove PFCs from wastewater. Isothermal and kinetic parameters, which are important for evaluation of GAC adsorption behavior, are estimated from batch mode experiments. Influences from coexisted organics, GAC diameters, pH *etc*. are also investigated and represented by variance of model parameters. Rapid small-scale column tester (RSSCT) and short bed adsorber (SBA) can be applied to predict the performance of fixed GAC bed. Objectives in detail are listed as below.

(1) To conduct "bottle-point" experiments to identify isotherms and kinetics of GAC adsorption for PFCs removal. Apply Freundlich equation and homogenous surface diffusion model (HSDM) to interpret experimental data of isotherms and kinetics.

(2) To study influences from coexisted organics, including competition and carbon fouling, from GAC type and diameter on adsorption isotherms and kinetics.

(3) To conduct preliminary continuous experiments such as RSSCT and SBA to get breakthrough curves of PFCs in GAC fixed bed.

5.3 Experimental Description

5.3.1 Materials

Four kinds of GACs were examined in the study as shown in **Table 5.3**, which were filtrasorb 400 (F400) from Calgon Company, diasorb W1030 (DW) from Mitsubishi Company, PK1~3 (PK) from Norit Company and GAC from Wako Company (Wako). GAC F400 was applied regularly for all experiments because it was widely applied in water treatment engineering, including the BAC filter in K-WWTP.

Table 5.3 Properties of GAC in this study

Company	Calgon Com.	Mitsubishi Corp.	Norit Corp.	Wako Com.
Name	Filtra 400	Diasorb W10-30	PK1~3	Wako GAC
Abbr.	F400	DW	PK	Wako
Material	Bituminous Coal	Coconut Shell	Peat Coal	Char Coal
Size(mm)	0.4~1.7	0.4~1.7	1~3	>3
S_{BET}(m^2/g)	~950	~1000	~875	-

As a standard preparation procedure, all GACs were firstly boiled in pure water for one hour to remove fine particles and preloaded organics. Floating impurities and grease were readily removed from water surface during boiling. Right after boiling, GAC is flushed by abundant pure water to cool and clean carbons. After intensive washing, carbons were submerged by pure water and stored in room temperature overnight to equilibrate surface properties. The water was discarded and GAC is moved into oven and dried up at 105℃ for around two days to remove moisture inside pores completely. Dried GAC was stocked in PP or stainless steel bottles with airtight covers to prevent exposure to atmosphere and possible adsorption of moisture and organics from air. By this clean process, adsorption capacity of GAC could be improved for about 10%, *e.g.* S_{BET} for F400 is increased from 950 m^2/g, which was claimed by company, to 1122 m^2/g by local laboratory analysis (Kimura, 2007).

Benefited from former clean process, GAC can be precisely weighed before experiments. After

weighing, dried GAC was moved into PP sampling bottles and soaked in small amount of pure water to pre-wet inner pores. This step is important and necessary because air inside pores might adversely reduce adsorption capacity and velocity. Vacuum state was applied for 0.5~2 hours to eliminate small bubbles inside GACs, which can accelerate pre-wet process that might lasts for 24 hours (Nicholas and Paul, 1993). After pre-wetted, excessive water was discarded by pipette and diluted PFCs solution will be added inside to contact with GAC and start adsorption experiments.

In order to obtain GAC in different diameters, dried GAC was firstly pulverized in a mortar by a pestle. Then the crushed GAC was separated by sieving in a series of standard sieves to different ranges of diameters. There were fine particles or powders attached on the surface of crushed GAC during pulverization, which should be removed before experiments. Therefore, sieved GAC was washed again by pure water, and used water with fine particles is poured out carefully. This wash step was repeated for several times until the water over GAC granules was clean and clear. The washed GAC was again dried in oven at 105℃ for around two days and stored in airtight bottles. Before experiment, these kinds of GAC were weight precisely and pre-wetted following method described before.

Dilute PFC solutions were prepared from stock solutions by diluting them together into pure water or wastewater matrix. Phosphorous buffer in 0.01N was prepared to control pH value close to 7, which contained 0.0039N K_2HPO_4 and 0.0061N KH_2PO_4. Lower strength of pH buffer was selected to reduce adverse harms of phosphorous ions on LC-MS system. GAC particles were pre-wetted by vacuum for two hours in small amount of pure water in 60 or 125mL PP sampling bottles. After that, water was discarded by pipette from the bottle.

Two kinds of background organics were examined in this study, including humic acid from Wako Company (WHA) and wastewater effluent from K-WWTP (WW). WHA is difficult to dissolve into pure water, and thus boiling was applied as first step to increase its solubility. After boiling in pure water for half an hour and cooling to room temperature, the mixed liquor was filtrated in Büchner funnel by 1 μm glass fiber filtration paper and insoluble solid was discarded. The filtrate was collected and stored in refrigerator at 4℃ for further dilution. After this process, DOC of WHA stock solution can be as high as 80 mg/L. Wastewaters of ASP effluent and BAC filtration effluent from K-WWTP (see **Fig. 4.2**) were sampled and filtrated by 1μm filtration paper, and they were stored in refrigerator for further experiments.

5.3.2 Experimental methods

5.3.2.1 Experimental apparatus

Major type of batch experiments for GAC adsorption was “Bottle-Point” (BP) experiments, in which each bottle represented one point in isotherms or kinetic curves. In this research, “Bottle-Point” experiment was adopted for isotherms and part of kinetics study. As shown in **Fig 5.2*a***, bottle-point experiments were conducted in a thermo-stat shaker (Eyela NTS-1300s, Rikakikai Company, Tokyo) with shaking speed of 120 rpm at 25℃. GAC was firstly weight and transferred into one PP bottle of volume as 60 or 125 mL, then processed pre-wet operations described before. After that, PFCs dilute solution was added to react with GAC, and the sampling bottle was capped immediately and placed into shaker. At sampling time, about 0.5 mL sample was moved from PP bottle to PP sampling vials by pipette and introduced for LC-MS analysis. In case of trace level concentration (<1 μg/L), the sampling bottle was taken out of the shaker and inner liquid is filtrated by 1 μm glass fiber filtration paper and applied SPE process for LC-MS analysis.

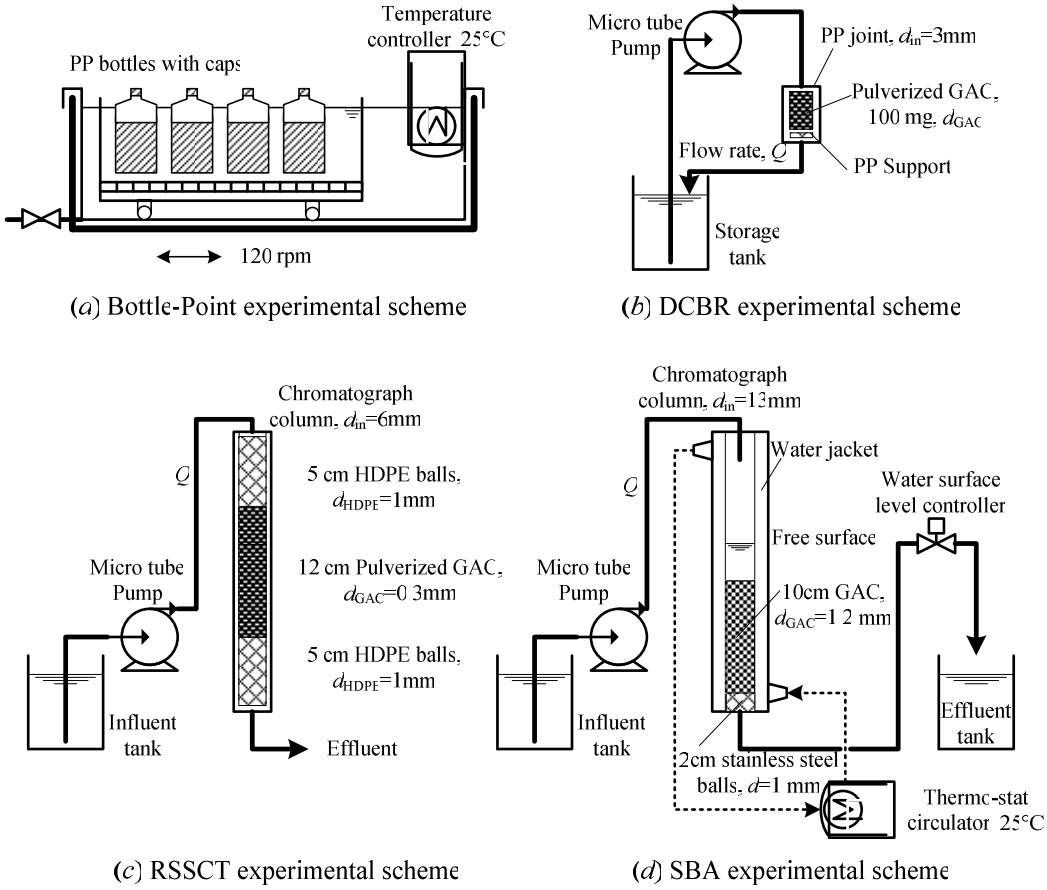

(*a*) Bottle-Point experimental scheme (*b*) DCBR experimental scheme

(*c*) RSSCT experimental scheme (*d*) SBA experimental scheme

Figure 5.2 Scheme of experimental apparatus for GAC adsorption (*a*)Bottle-Point, (*b*)DCBR, (*c*)RSSCT and (*d*)SBA

Differential column batch reactor (DCBR) was applied to estimated diffusion coefficient (D_s) for different GAC diameters. This method was successfully applied in estimation D_s of GAC adsorption for pesticides (Baup, *et al.*, 2000). The scheme of DCBR is shown in **Fig. 5.2*b***. About 100 mg of GAC in specific range of diameters was weight and pre-wetted by procedures described before. Then the wet GAC was packed into a small PP tube jointer with inner diameter of 3 mm. PE tube was cut into small pieces and squeezed to support GAC packing. PFCs dilute solution was circulated in constant flow rate by peristaltic pump and passed through GAC packing continuously. Magnetic stirring was necessary to mix inside liquid completely, however in case of small volume of storage (<0.1 L) and large flow rate (>10 mL/min), inside liquid was completely mixed by diffusion and hydraulic turbulence.

Rapid small scale column tester (RSSCT) was shown in **Fig. 5.2*c***. GAC was firstly pulverized into smaller diameters, which was usually less than 250 μm for RSSCT scaling, and pretreated in procedure described as before. After that, 2 g of pre-wetted GAC was packed into a chromatograph column, with 5 cm depth of high density polyethylene (HDPE) balls in diameter of 1 mm on the two ends of column. HDPE balls were helpful to homogenize hydraulic flows and reduce turbulence effects from influent and effluent position, and thus satisfied prerequisite of plug flow for fixed bed simulation. PFCs dilute solution was passed through the column continuously by peristaltic pump, with flow rate about 10 mL/min. Temperature of systerm was constant at 25℃ by thermo-stat circulator. The effluent from column was during interval of sampling and collected for LC-MS analysis.

Short bed adsorber (SBA) is effective to simulate preloaded or fouled GAC instead of RSSCT, because

surface area or adsorption capacity of preloaded GAC will increase by exposing blocked pores to outside during pulverization for RSSCT (Ho, 2004). Another benefit of SBA refers to the estimation of fixed bed GAC without scaling equations, because GAC in same diameters of actual process is used in SBA experiments. The scheme of SBA experiment is shown in **Fig. 5.2*d***. Chromatograph column with water jacket was packed by around 10cm depth of GAC in original size, with 2cm of stainless steel balls beneath as support. A three-way connector was placed in the effluent line and fixed at specific height to control water level inside the column by law of connected vessels. Thermo-stat circulator supplies water in 25℃ to circulate in water jackets of column sequentially. PFCs dilute solution was introduced to column in a constant flow rate by peristaltic pump. Empty bed contact time (EBCT) was designed to be close with BAC filter in K-WWTP which was 8 minutes. Therefore, flow rate was controlled to be 1~2 mL/min to keep EBCT as 5~10 minutes. The effluent from column was composite during interval of sampling and collected for LC-MS analysis.

5.3.2.2 Batch experimental conditions

Experimental conditions of PFCs adsorption experiment are briefly shown in **Table 5.4**. Equilibrium experiments in BP mode were abbreviated as "I" series in the table. Kinetics experiments contain BP and DCBR modes, which were abbreviated as "K" and "D" respectively. All experiments in the table were conducted in batch mode.

Runs I3~5 and D1,3 in **Table 5.4** were designed to determine influence of NOMs on adsorption process. In Runs I4 and D3, PFC stock solution was spiked into wastewater, and introduced to contact with GAC pre-wetted in reactors. Bulk solution pH was not controlled in NOM competition experiments. In Runs I5, GAC was firstly contacted with 30 mgC/L WHA solution for one week. Then preloaded GAC was filtrated and dried in oven at 105℃. Further operation was similar with Run I3.

Table 5.4 Experiments conditions of PFCs adsorption

		GAC			Adsorbate		Solution		Sampling	
	Runs	Name	Size *mm*	Conc. *g/L*	Name	Conc. *mg/L*	Vol. *mL*	pH	*time* *d*	*N*
Equil.	I-1	F400	original[c]	0.1, 0.3, 1, 2.6	Single PFOS,PFOA	1	50	6.8	7	4
	I-2	F400	original	0.5	Mixed PFOS+PFOA	0.5~5μg/L	50	6.8	21	5
	I-3	F400	0.1	0.2, 0.5, 1, 2	Multi PFCs(10)[e]	2~5	50	6.4	5	6
	I-4	F400	0.1	0.2, 0.5, 1, 2	PFCs(10) in WW[f]	2~5(2.3, 4.5)[g]	50	7.2	5	6
	I-5	F400[a]	0.1	0.2, 0.5, 1, 2	PFCs(10) in WW	2~5	50	6.4	5	6
	I-6	F400,DW, PK,Wako	0.1	0.2, 0.5, 1, 2	Multi PFCs(10)	2~5	50	6.8	5	4
Kinetic	K-1	F400	original	0.2, 1, 1, 1, 5	Single PFOS,PFOA	0.2, 1, 2, 5	50	6.8	0~7	10
	K-2	F400[b]	original	1	Multi PFCs(10)	~0.1	60	6.8	0~1	4
	D-1	F400	0.1~1.1[d]	1	Multi PFCs(10)	~0.1	100	6.4	0~4hr	5
	D-2	F400	0.2	1	Multi PFCs(10)	~0.1	100	3, 11	0~4hr	4
	D-3	F400	0.2	1	PFCs(10) in WW	~0.1(2.3,4.5)[g]	100	7.2	0~4hr	4

Note: I, K and D refer to isotherm, kinetic and DCBR. ***a***=preloaded in 30mg/L WHA for 5days; ***b***=pre-washed in 0.1N HCl and NaOH for 7dyas; ***c***=diameter in 0.43~1.7mm; ***d***=average diameter in seven degrades as 0.1, 0.2, 0.4, 0.6, 0.8, 0.9, 1.1mm; ***e***=PFCA(4~10), PFAS(4,6,8); ***f***=ASP and BAC effluent with 2.3 and 4.5mg/L DOC; ***g***=background DOC concentration (2.3, 4.5)mg/L

In Run D2, bulk pH was adjusted by 0.05 N HCl and 0.05 N NaOH to pH 3 and pH 12 before contact with GAC. During experiment, bottle caps were tighten and sealed to prevent access to atmospheric carbon dioxide which might change bulk pH. In Run K2, GAC was firstly soaked into 0.1 N HCl or 0.1 N NaOH for one week to saturate surface modification, and then contacted with PFC dilute solutions. GAC was washed by pure water before contact with PFC solution, which can alleviate shock of strong acid or base to LC column. In Run I-6, isotherms of GACs in different materials were examined, with same procedure to Run I-3.

5.3.2.3 Continuous experimental conditions

Experimental conditions of RSSCT and SBA are shown in **Table 5.5**. In RSSCT, PFC stock solutions were spiked into pure water and mixed wastewater effluent from K-WWTP. In SBA experiment, PFC stock solutions were spiked into tap water to get 50~500 μg/L in influent. WHA stock solutions were also added inside to obtain about 10 mg/L DOC. Because of methanol introduced from PFC solutions, TOC analysis failed to determine organics in influent and effluent. Therefore, UV_{254} nm and UV_{220} nm absorbance is used to roughly estimated breakthrough of humic acid and wastewater organics respectively.

Table 5.5 Experimental conditions for RSSCT and SBA runs

	GAC				Adsorbate			Column			
Runs	Name	d	m	ρ_p [b]	PFCs	NOM	Conc.	d_{in}	H	Vol.	Flux
		mm	g	g/mL		mg/L	mg/L	cm	cm	mL	L/d
RSSCT-1	F400	0.3	2	0.56	PFCs(10)	0	~0.1	0.6	12	3.5	6.1±1.0
RSSCT-2	F400	0.3	2	0.56	PFCs(10)	3.5[c]	~0.1	0.6	12	3.5	6.7±0.9
SBA	F400	orgl.[a]	5	0.47	PFCs(8)	10	0.5~5[d]	1.2	10	11	1.3±0.05

Note: ***a***=diameter in 0.43~1.7mm; ***b***=apparent density or package density; ***c***=matrices of RSSCT 1 and 2 are exchanged for short time; ***d***=initial concentration is increased form 0.5 to 5mg/L in middle of experiments.

5.3.2.4 Analytical methods

PFCs in GAC adsorption experiments were analyzed by LC-ESI-MS. If concentrations were expected to be lower than LOD (~0.5μg/L), C_{18}-SPE process was applied to concentrate trace level of PFCs in 50~100mL solution for 100~200 times by the method described in Chapter III. Loading capacity of Prep-C Agri (C_{18}) cartridge was not exceeded because of the small volume of loading samples.

WHA and WW were determined in terms of dissolved organic carbons (DOC) by TOC analyzer (TOC-5000A, Shimadzu Company, Kyoto). Absorbance at UV_{254} was also obtained by UV spectrometer (UV-2500PC, Shimadzu Company, Kyoto) for NOMs as redundancy.

5.3.3 Modeling and simulation

5.3.3.1 Isotherms models

Models based on different concepts were developed to interpret isothermal data, as shown in **Table 5.1**. Langmuir equation (LE) and Freundlich equation (FE), which contain two parameters, were applied to interpret isotherms. At the end of equilibrium experiments, equilibrium bulk concentrations are analyzed as C_{eq}, and adsorbate loading can be calculated as shown in **Eq. (5.1)**.

$$q = \frac{(C_0 - C_{eq})V_{bulk}}{m_{GAC}} = \frac{C_0 - C_{eq}}{S_{GAC}} \qquad \text{Eq. (5.1)}$$

where q is the adsorbed loading rate in μg/g, C_{eq} is equilibrium bulk concentration in μg/L, C_0 is initial bulk concentration in μg/L, V_{bulk} is volume of mixture in unit L, m_{GAC} is mass of GAC in the bottle in unit of g, and S_{GAC} is apparent concentration of GAC based on bulk volume in unit of g/L.

Parameters of k, q_{m} in LE and K, n in FE were determined by least square fitting of experiment data on q and C_{eq}, as shown in **Eq. (5.2)** and **(5.3)**.

$$\frac{C_{eq}}{q} = \frac{C_{eq}}{q_m} + \frac{1}{q_m k} \qquad (5.2)$$

$$\log q = n \log C_{eq} + \log K \qquad (5.3)$$

5.3.3.2 Kinetics models

HSDM and its simplified form (s-HSDM) were applied in this study to interpret kinetic data. As shown in **Table 5.2**, S-HSDM contained only normal differential equation and can be solved easily by numerical calculation, which was coupled with Freundlich equation and shown as follows.

$$\frac{dC}{dt} = -\frac{s \cdot dq}{dt} = \frac{15 D_s}{r^2}\left(C_0 - C - skC^n\right) \qquad (5.4)$$

where C and q are bulk and surface concentration at time t, C_0 is initial concentration, r is equivalent radius of GAC, s is concentration of GAC based bulk volume, k and n are parameters in Freundlich equation.

Solution of HSDM was complicated because of some partial differential equations. Orthogonal collocation technique was applied to approximate solute these equations, in which three points solution was considered enough for adsorption process in waters (Roy, *et al.*, 1993). One benefit of this method referred to the distribution profiles along radius inside GAC sphere, which offered insight vision of GAC during adsorption process. Detailed description of HSDM, including its concept and numeric solution techniques, and one example are shown in **Appendix B**.

After k and n were determined by isotherm experiment and data set of C~t were obtained from kinetic experiment, K_f and D_s values can be estimated by least square fitting method. Two equations were proposed as objective functions to search Ds, which emphasize on different time range.

$$Z1(K_f, D_s) = \sqrt{\frac{\sum [C_{sim}(K_f, D_s) - C_{\exp}]^2}{n}} \qquad (5.5)$$

$$Z2(K_f, D_s) = \sqrt{\sum \left[\frac{C_{sim}(K_f, D_s) - C_{\exp}}{C_{sim}(K_f, D_s) + C_{\exp}}\right]^2 \Big/ n} \qquad (5.6)$$

Data in early period had large values and contributed much to $Z1(K_f, D_s)$, while data in end period had very low concentrations and contributed much to $Z2(K_f, D_s)$. In case of s-HSDM, K_f was eliminated from the equations. Estimation by different function should come to similar D_s value if the model properly described the process.

5.4 Results and Discussion

5.4.1 Equilibrium time and simulation models

5.4.1.1 Time for equilibrium of adsorption

Figure 5.3 shows results of equilibrium time for PFOS(8) and PFOA(8) adsorptions by 1 g/L of GAC F400. When coexisted with organics, it takes a long time to reach equilibrium state on GAC, and bulk concentration seems reduced even after 21 days, as shown in **Fig. 5.3*a*** and **5.3*b***. This phenomenon was related with abundant micropores inside of GAC, in which molecules spent long time to enter the pores and react with surface. Report showed net adsorption on GAC may occur even after one month (Nicholas and Paul, 1993). The long equilibrium time on GAC can also be judged by simulation results, as shown in the table of **Appendix B**.

Adsorptions of PFCs in pure water are shown in **Fig. 5.3*c*** and **5.3*d***. Adsorption in pure water reached approximate equilibrium state earlier as one week. Crushed and sieved GAC-F400 in smaller size showed faster decrease and reached equilibrium earlier. Usually, powder activated carbon (<75 μm) was used to estimated isotherms in 2~3 days (Ho, 2004), which had close surface area with granular activated carbon but faster adsorption rate (Cooney, 1998). According to the figure, F400 with diameter 0.2 mm showed fastest adsorption rate and reach similar level of equilibrium concentration by GAC in original size. The difference of surface area between powder F400 and original size was less then 5% (Kimura, 2007). Therefore, GAC in smallest diameter 0.1 mm after sieving was applied for isotherm experiments in this study, and the experimental time was assumed to be 5 days.

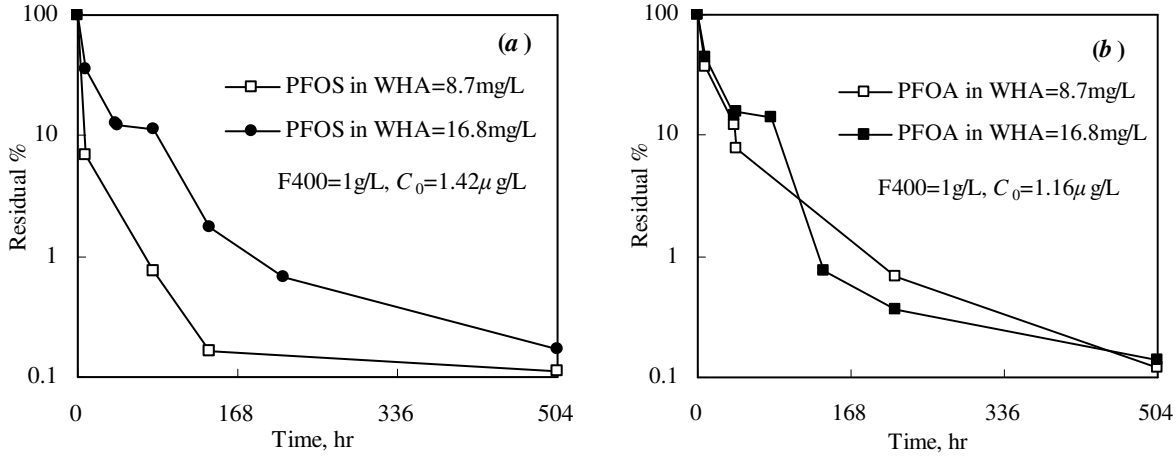

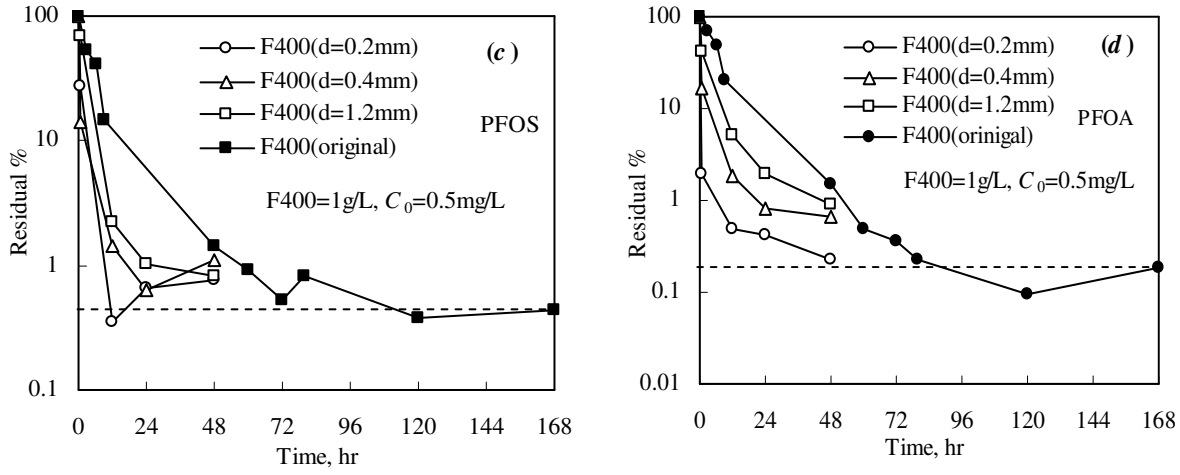

Figure 5.3 Equilibrium time for adsorption process of PFOS (*a*,*c*) and PFOA (*b*,*d*) in pure water and background organics

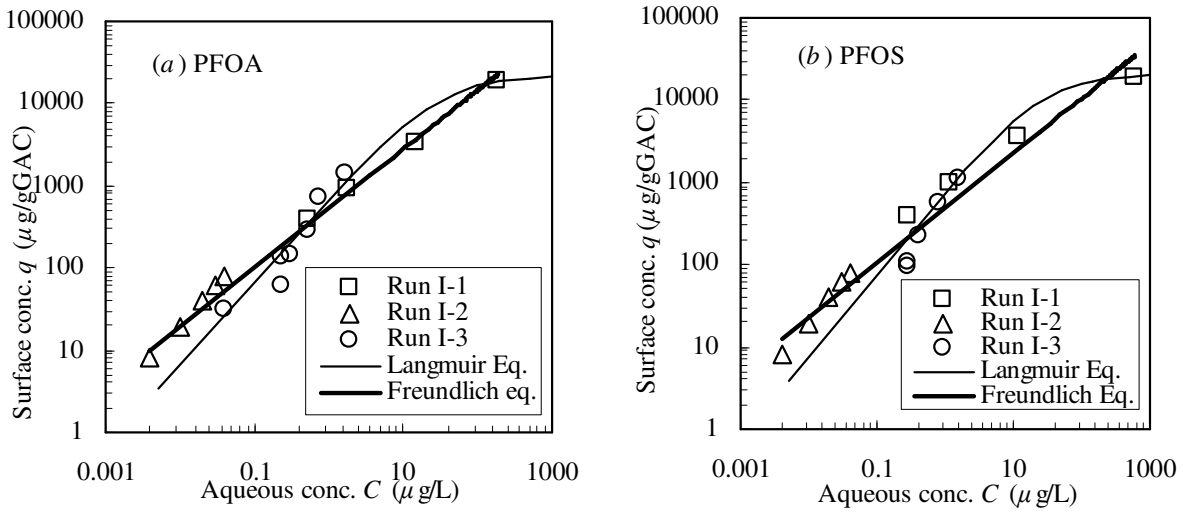

Figure 5.4 PFC isotherms interpreted by Langmuir and Freundlich equations

5.4.1.2 Simulation models for isotherms

Langmuir model and Freundlich Equation were applied to interpret isotherms acquired in equilibrium experiments. **Figure 5.4** shows equilibrium data of PFOA and PFOS in Runs I1~3. According to the figure, Freundlich equation showed good simulation to experimental data in a wide range of bulk concentrations (0.005~500 μg/L), which proved the declaration of Freundlich equation in **Table 5.1**. Langmuir equation seemed also available to interpret original data, but underestimated adsorption capacities in very low concentrations, *e.g.* when C_{eq} < 1μg/L. Therefore, Freundlich equation was better than Langmuir equation and used in this study to interpret PFCs isotherms. However, suffering from variance of LC-MS analysis and experimental operations, the isotherms were not perfect for fitting. Results of estimation might depend on range of concentrations.

5.4.1.3 Simulation models for kinetics

After equilibrium parameters were derived from isotherms in **Fig. 5.4**, s-HSDM and HSDM were applied to simulate kinetics experimental data. Simulation results for single PFOS and PFOA adsorption

by s-HSDM and HSDM are shown in **Table 5.6**, which are constrained by different objective equations such as *Z*1 and *Z*2. **Fig. 5.5** shows some examples of simulation.

Table 5.6 Kinetics estimation results by s-HSDM and HSDM

PFC	GAC	C_0	s-HSDM(Z1)	s-HSDM(Z2)	HSDM (Z1)		HSDM (Z2)	
			D_s	D_s	D_s	K_f	D_s	K_f
	g/L	μg/L	10^{-10}cm^2/s		10^{-10}cm^2/s	10^{-2}cm/s	10^{-10}cm^2/s	10^{-2}cm/s
PFOS	0.2	200	2.3	0.2	11.4	0.24	11.4	0.02
	1	500[ab]	1.0	0.2	8.7	0.12	8.7	0.10
	1	1000	1.3	0.2	5.7	0.12	11.4	0.12
	1	2000	1.4	0.3	11.4	0.12	11.4	0.21
	5	5000	0.6	0.2	11.4	0.05	11.4	0.15
PFOA	0.2	200[c]	2.9	0.7	1.2	0.23	5.7	0.23
	1	500	1.7	0.6	104.1	0.12	104.1	0.17
	1	1000	1.4	0.8	5.7	0.13	139.0	0.13
	1	2000	1.4	0.8	104.1	0.06	80.9	0.06
	5	5000[d]	0.5	0.4	69.5	0.02	69.5	0.02

Note: ***a,b,c,d*** represent sub-plotting in **Fig. 5.5**. *Z*1 and *Z*2 are objective functions.

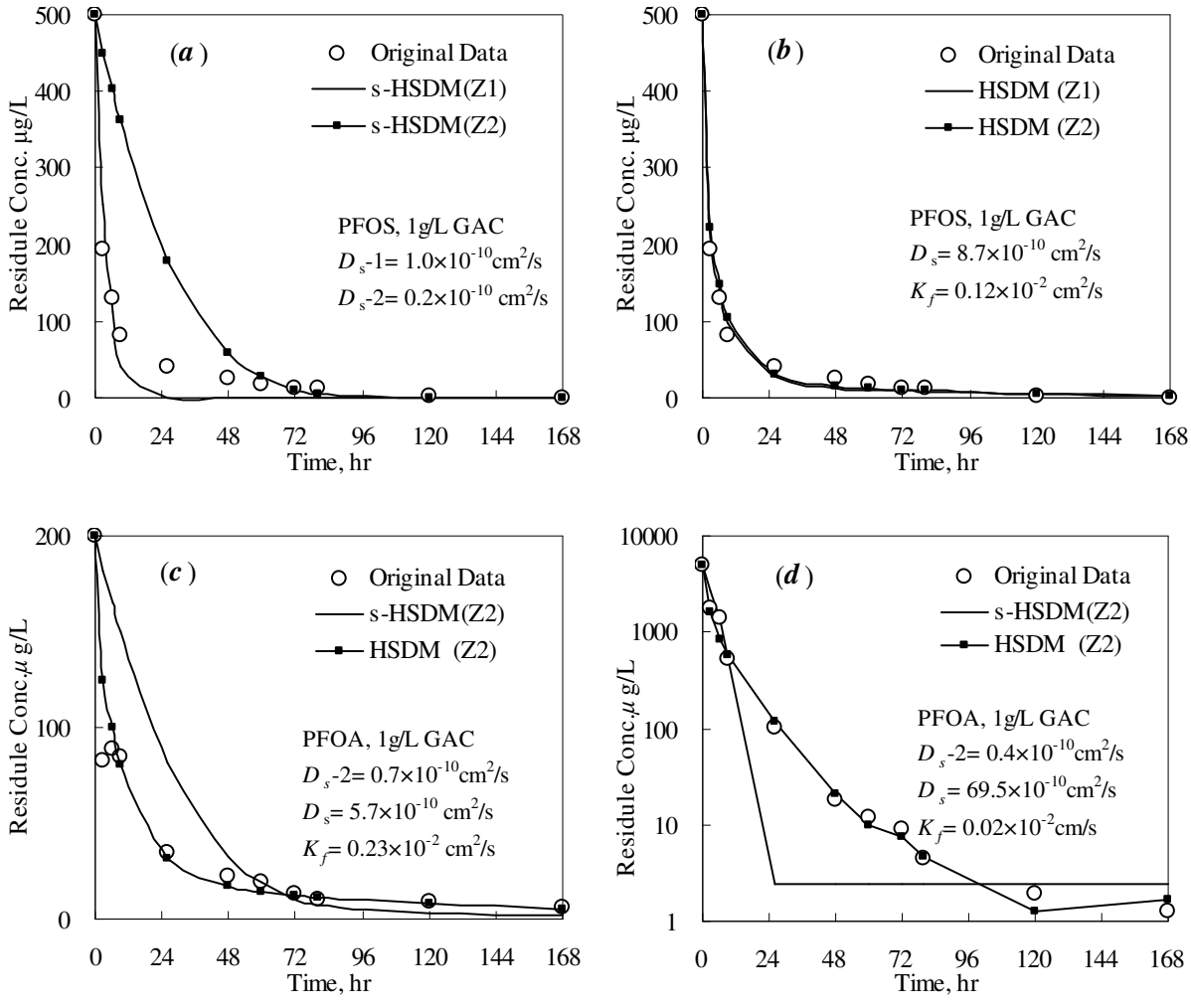

Figure 5.5 PFOS and PFOA kinetics simulated by s-HSDM and HSDM

s-HSDM can not simulate kinetics data properly, as shown in **Fig. 5.5*a***. By objective function *Z*1, model fitted data in early time very well but missed data in longer time. Opposite situation appeared for simulation by objective function *Z*2 which was sensitive to long term data. In s-HSDM, surface diffusivity was simplified to be proportional to linear driving force, as $r_p/5$ times of external mass transfer coefficient, which was not suitable for surface diffusion dominant systems. Usually the kinetics is mainly governed by external mass transfer at early time and by pore diffusion at longer time, therefore s-HSDM can not simulate the two stages simultaneously.

HSDM can fit the experimental data very well, as shown in **Fig. 5.5*b***. By considering external mass transfer and surface diffusion respectively, the model can simulate two stages simultaneously. Estimation results of D_s by the two different objective functions were same to each other, which ensure the quality of simulation. Advantages of complete HSDM to simplified form can be further identified by **Fig. 5.5*c*** and **5.5*d***. In **Fig. 5.5*d***, data was plotting in logarithm axis to demonstrate model performance on long term and low level of concentration. s-HSDM generated wrong information that adsorption goes to equilibrium at 24 hr, while HSDM can simulate to data very well.

Because objective function *Z*2 is independent of concentrations, or dimensionless, it will be applied in further study. In summary, HSDM coupled with objective function Z2 will be applied in further studies to simulate kinetics data.

5.4.2 Adsorption of PFCs in dilute solution

5.4.2.1 Isotherms of PFCs in dilute solution

Table 5.7 shows results of PFC isotherms from Run I3, including Freundlich equation coefficients *K* and *n*, linearity coefficients r^2 and range of equilibrium concentrations.

Table 5.7 Isotherms estimation of PFCs adsorption in different matrices

Adsorbent	Pure water				BAC effluent[b]				ASP effluent[c]				Preloaded GAC[d]			
	K	*n*	r^2	Range[a]	*K*	*n*	r^2	Range	*K*	*n*	r^2	Range	*K*	*n*	r^2	Range
PFBA (4)	130	0.56	0.91	(0.2~43)	30	0.58	0.95	(3~2162)	30	0.59	0.94	(3~1682)	60	0.48	0.98	(1~1426)
PFPeA (5)	290	0.85	0.97	(0.09~4)	14	0.89	0.98	(2~776)	7	1.10	0.92	(2~622)	40	0.60	0.95	(2~2048)
PFHA (6)	490	0.81	0.82	(0.05~3)	100	0.86	0.92	(0.4~140)	60	1.23	0.88	(0.7~59)	75	0.79	0.89	(1~338)
PFHpA (7)	300	0.93	0.93	(0.05~2)	170	0.76	0.95	(0.08~37)	150	0.82	0.99	(0.1~38)	120	0.92	0.93	(0.3~70)
PFOA (8)	680	1.10	0.90	(0.04~2)	150	1.44	0.88	(0.34~14)	230	1.27	0.98	(0.3~18)	130	1.26	0.91	(0.4~26)
PFNA (9)	1550	0.97	0.91	(0.05~2)	1120	0.82	0.82	(0.03~2)	1070	0.95	1.00	(0.04~5)	620	0.98	0.97	(0.1~16)
PFDA (10)	1940	0.92	0.96	(0.07~1)	1650	0.91	0.91	(0.04~1)	1240	0.91	0.99	(0.07~8)	340	0.89	0.99	(0.2~59)
PFHDA(16)	2640	1.81	1.00	(0.06~0.6)	350	1.15	0.72	(0.03~6)	280	1.28	0.94	(0.05~3)	13	0.27	0.97	(1~1242)
PFBuS (4)	240	0.55	0.89	(0.06~16)	140	0.65	0.98	(0.2~378)	100	0.80	0.96	(1~248)	70	0.75	0.95	(1~469)
PFHxS (6)	2970	0.94	0.78	(0.03~1)	1270	0.85	0.95	(0.04~20)	970	1.16	0.98	(0.1~7)	620	0.94	0.97	(0.1~32)
PFOS (8)	660	1.41	0.98	(0.27~2)	430	2.28	0.55	(0.34~2)	380	1.46	0.95	(0.2~3)	90	2.04	0.72	(0.5~3)

Note: ***a*** = range of equilibrium concentrations for estimation, μg/L; ***b*** = BAC filter effluent in K-WWTP, 2.3mgDOC/L; ***c*** = secondary clarifier effluent in K-WWTP, 4.5mgDOC/L; ***d*** = GAC preloaded in 30mgDOC/L of Wako Humic Acid (WHA) solution for 5 days.

In order to compare different behavior of PFCs with carbon chain length, values of *K* and *n* for PFC isotherms in pure water were plotted by length of PFC carbon chains as shown in **Fig 5.6**. Value of *K* in Freundlich Equation implies maximum adsorption capacities or position of isotherms, and value of *n*

determines variance of equilibrium state by bulk concentrations or the shape of isotherms. Isotherms with n>1 are convex curves, which are favorite for adsorption process design and application.

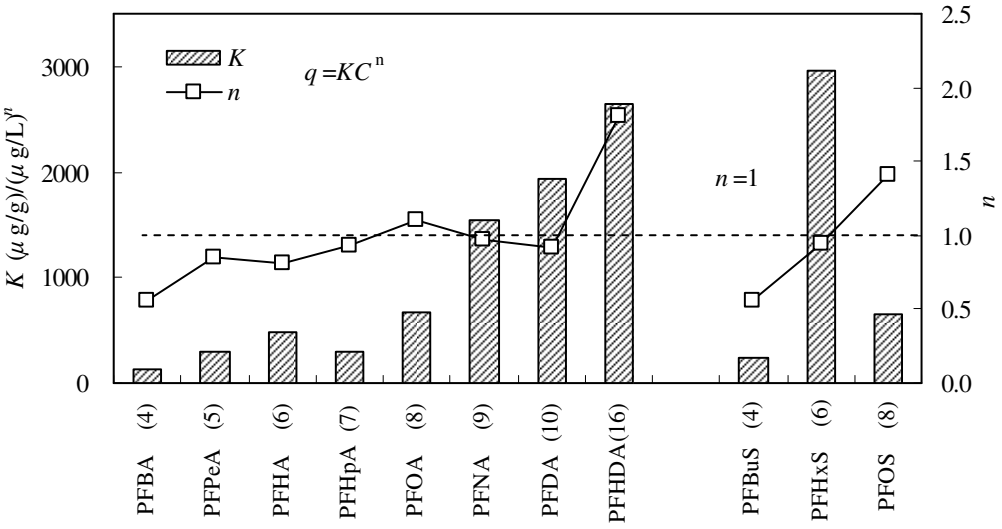

Figure 5.6 Characteristics of PFCs isotherms in pure water by GAC-F400

As shown in the figure, both K and n increased by ascendant carbon chain length for PFCA(4~10), which implied that longer chained PFCs were easier to be adsorbed by GAC-F400. This tendency could be explained by the increasing hydrophobic properties of longer chained PFCs. Usually hydrophobic interactions are the dominant mechanism for removal of most organic compounds in activated carbon adsorption (Crittenden, *et al.*, 1999; Snyder, *et al.*, 2003). With increase of carbon chain length, PFCAs had similar polarity but intensively increased hydrophobicity, therefore stronger adsorption occurred for longer chained PFCs. Exception of PFHxS(6) from this criteria was not understood clearly yet.

5.4.2.2 Kinetics in PFCs dilute solution

Table 5.8 summarizes estimated kinetic parameters for Run D-1. For most of PFCs, diffusion coefficient D_s was roughly increased by ascendant diameters of GAC. This result was accordant to reported DCBR results for pesticides adsorption (Wilmanski and van Breemen, 1990; Badruzzaman, *et al.*, 2004). Because mass transfer process in smaller size GAC was in shorter distance than bigger size GAC, resistance of diffusivity was smaller and diffusion coefficient is decreased in smaller size GAC. Although external mass transfer coefficient K_f was determined by hydraulic conditions and GAC diameters (Baup, *et al.*, 2000), there were not significant differences between GACs in different diameters except PFCA(4~5).

Despite of influence by diameter, surface diffusion seemed also affected by carbon chain length or molecular hydrophobicity. With increase of molecular weight, PFCs had smaller D_s values, which meant long chained PFCs had less diffusion potentials. This result can be explained by the strong interactions between long-chained PFCs and surface, which might resist desorption of PFC molecules from surface and further transport along pore surface. In brief words, diffusivity of PFC was decreased along with descendant diameters or ascendant carbon chain length, implies that surface diffusion are less important and dominant in both cases.

Figure 5.7 shows the results of PFOS and PFOA as examples. HSDM can fit the kinetics data in DCBR mode as well as in BP mode shown in **Fig. 5.5**. GAC in smaller size showed faster removal rate of PFOS and PFOA than GAC in larger size.

Table 5.8 Estimation of PFC adsorption kinetics by F400 in different diameters

	d (mm)	*Range* (mm)	PFBA(4)	PFPeA(5)	PFHxA(6)	PFHpA(7)	PFOA(8)	PFNA(9)	PFDA(10)	PFBuS(4)	PFHxS(6)	PFOS(8)
K			137	210	267	184	335	939	1520	217	1046	604
n			0.37	0.39	0.40	0.52	0.60	0.77	0.77	0.46	0.51	1.19
D_s 10^{-10}cm^2/s	0.1	0.075~0.106	3	3	1	2	3	1	1	12	2	12
	0.2	0.106~0.25	23	23	12	12	12	13	1	6	6	9
	0.4	0.25~0.5	6	69	35	23	14	23	6	6	23	23
	0.6	0.5~0.7	17	6	12	35	9	10	6	2	12	12
	0.8	0.7~0.84	58	69	58	69	46	69	23	58	58	69
	0.9	0.84~1.0	58	46	5	17	12	14	23	46	35	9
	1.1	1.0~1.14	69	58	7	69	35	12	12	69	58	6
K_f 10^{-3}cm/s	0.1		0.8	0.01	0.1	0.05	0.2	0.6	0.1	0.01	0.6	1.3
	0.2		0.1	0.1	0.1	0.1	0.6	0.6	0.6	0.1	1.4	3.5
	0.4		0.5	0.3	0.6	0.1	0.8	0.9	1.2	0.3	0.9	4.1
	0.6		1.7	5.8	0.2	0.2	0.8	1.5	0.9	1.2	2.1	4.1
	0.8		2.3	4.1	4.6	0.5	0.9	1.9	3.5	1.2	2.3	1.7
	0.9		4.4	0.6	1.2	0.5	0.7	2.3	1.6	0.3	1.3	2.7
	1.1		5.8	0.5	0.1	0.2	0.7	1.6	1.7	0.6	0.9	1.9

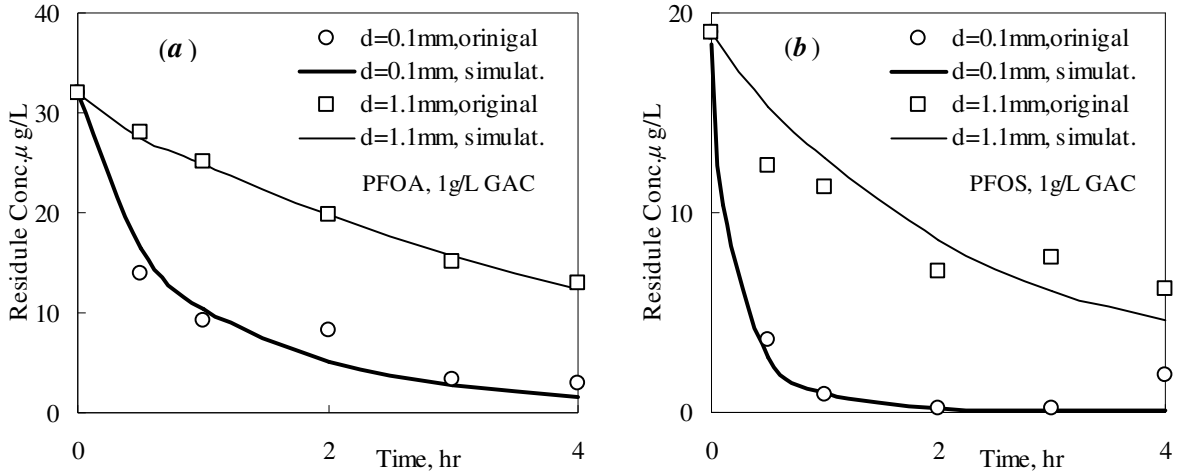

Figure 5.7 HSDM simulations for kinetics data from DCBR experiments

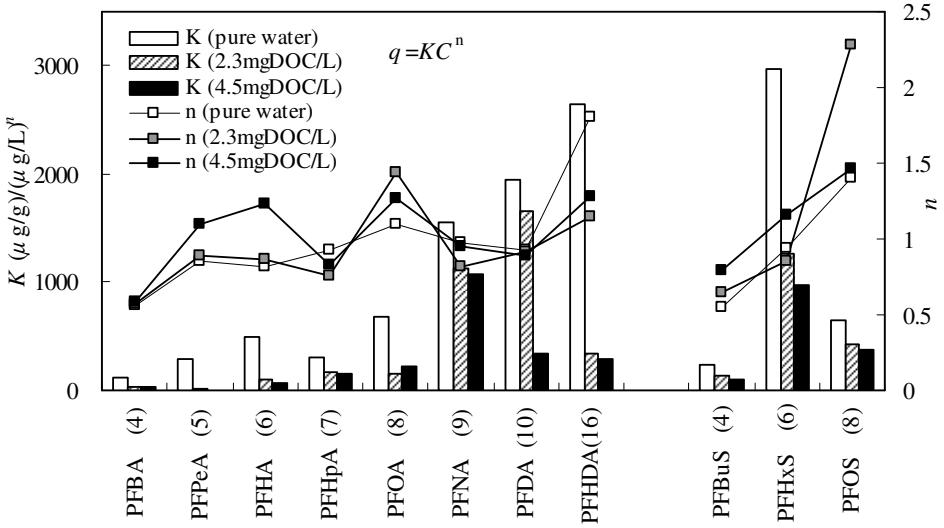

Figure 5.8 Influence of PFCs isotherms by NOM competition

5.4.3 Influence by NOM

5.4.3.1 Effects of organics competition in wastewater

Coexisted background organics have 10^3~10^6 times higher concentration than trace level of PFCs, and usually adversely affect adsorption efficiency. **Figure 5.8** shows results of isothermal estimation by FE for PFC adsorptions on fresh GAC, which occurred in two matrices such as wastewater of ASP effluent with 4.5mgDOC/L and BAC effluent with 2.3mgDOC/L from K-WWTP. Because PFCs and background organics were adsorbed simultaneously on fresh GAC, competition effects were expected dominant in matrix effects by organics.

The figure clearly showed decrease of K values for all PFC adsorptions by increasing DOC concentrations in matrix. Values of n had no obvious difference among matrix and follow similar tendency to slightly increase along carbon chain length. Two isotherm groups for PFCA(8~9) were plotted in **Fig. 5.9*ab*** for better understanding of competition effect. Similar values of n resulted in parallel isotherms, and different values of K showed distance between these isotherms.

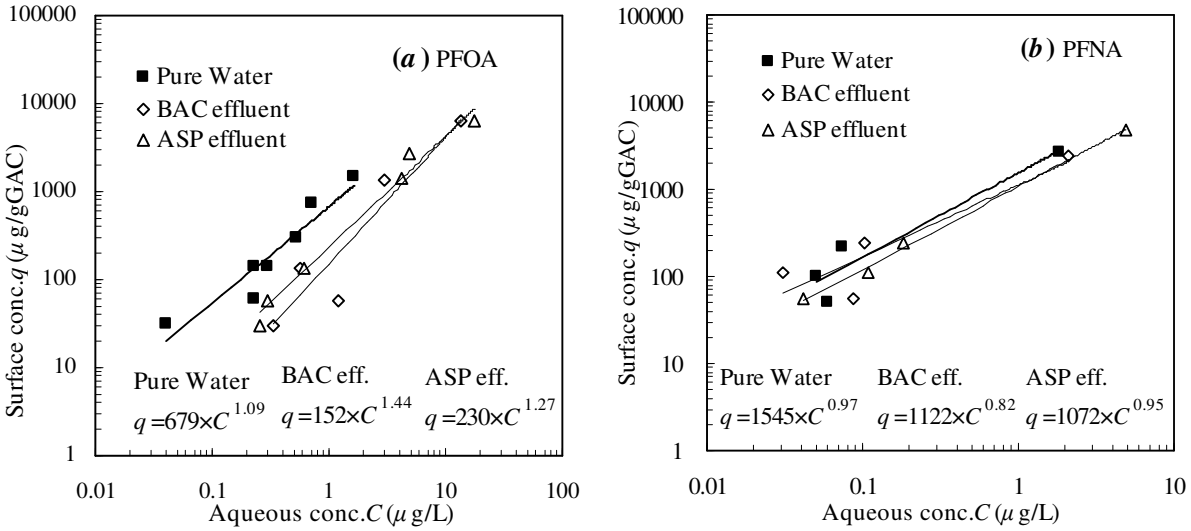

Figure 5.9 PFOA(*a*) and PFNA(*b*) isotherms by fresh GAC in wastewater matrices

The competition effects on short-chained PFCAs were stronger than medium-chained PFCAs, according to more intensive decrease of K for PFCA(4~6) than PFCA(7~10). Interactions between short-chained PFCs and GAC surface were relatively weaker than other PFCs, which might be more intensively influenced by matrix. However, increasing hydrophobicity by carbon chain can not benefit adsorption without limit. Long-chained PFCAs may also suffer from background organics, such as PFHxDA(16) in the figure. This phenomenon might be caused by different mechanism which was related with PFC molecular size and GAC pore distribution. Length of PFHxDA(16) molecule was larger than 2 nm (approx. calculated by C-C bond length), which implied that accumulated organic molecules around entrance of micropores might strongly resist the access of large size PFC molecules to micropores.

5.4.3.2 Effects of carbon fouling by humic acid

Results of isotherms for PFCs adsorption by preloaded GAC were shown in **Fig 5.10**, together with isotherms in pure water. After GAC-F400 was preloaded by high strength Wako humic acid (WHA), value of K in Freundlich equation for each PFC isotherm was decreased greatly, which implied carbon fouling adversely affect PFCs adsorption. Value of n in Freundlich for short- and medium-chained PFC

had not significant differences between fresh and preloaded GAC, which meant shapes of isotherms are parallel to each other. However, long-chained PFC as PFHxDA(16) seemed not adsorb onto preloaded GAC, because both *K* and *n* values were quite smaller than fresh GAC. Although long-chained PFCs had higher hydrophobicity and much less water solubility, they might be more intensively influenced by pore blockage because of their larger molecular sizes.

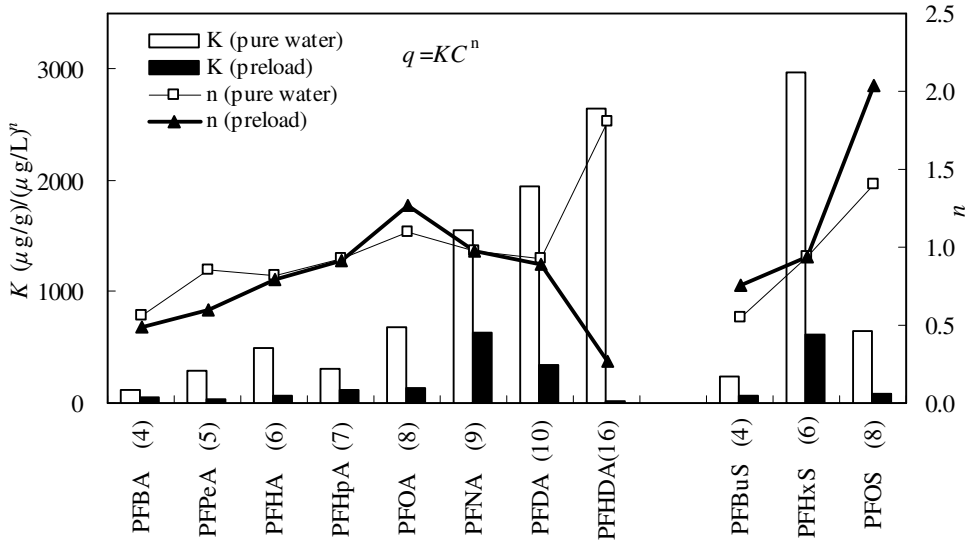

Figure 5.10 Influence on PFCs isotherms by preloaded GAC (carbon fouling)

As example of PFCs isotherms under carbon fouling, PFDA(10) and PFHxDA(16) were shown in **Fig 5.11** Isotherms of competition effects from wastewater were also shown in the figure to estimate their differences. In **Fig. 5.11*a***, isotherms of pure water and wastewater matrices were very close to each other, which demonstrated very small effects of competition by wastewater on PFDA(10) adsorption capacity by GAC-400. Isotherm of preloaded GAC was parallel to free matrix isotherm, which was similar to other organics like atrazine adsorption to activated carbon (Li, *et al.*, 2003). The adsorption capacity of PFDA(10) on preloaded GAC was less than 20% of fresh GAC, which is calculated by difference of *K* values based on similar *n* values. Most of short- and medium-chained PFCs showed similar behavior with PFDA(10). These results indicate that access of micropores is important for PFCs adsorption.

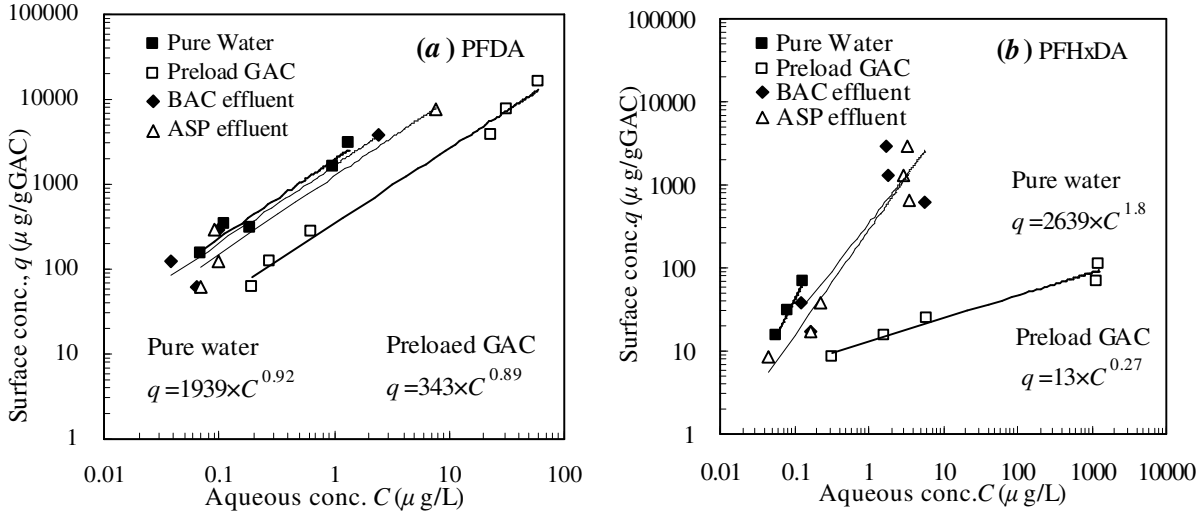

Figure 5.11 Carbon fouling effects on (*a*) PFDA and (*b*) PFHxDA isotherms

In case of long-chained PFC as PFHxDA(16), as shown in **Fig. 5.11*b***, carbon fouling reduced adsorption capacity of fresh GAC much more significantly than organic competitions. Pore blockage reduced adsorption capacities proportionally by denying access to some micropores, and therefore isotherms were parallel to fresh GAC and have similar *n* value, as shown in **Fig 5.11*a***. However, isotherm of fouling carbon for PFHxDA(16) changed its shape or *n* value greatly from fresh carbon, which implied that pore blockage was not the only mechanism, and effects of carbon surface modification might be important in this process.

Preloaded experiments showed that PFC adsorptions were strongly affected by carbon fouling, which was more significant than organic competition. Carbon fouling decreased adsorption capacities proportionally by blocking pores in short- and medium-chained PFCs. Long-chained PFCs, as PFHxDA(16), was not only affected by pore blockage, which resulted in change of isotherm shape. Fouling carbon can not remove PFHxDA(16) effectively. All results implied that PFC molecules had less potential to effectively replace NOM molecules which covered GAC surface after preloading process, and therefore adsorption capacities were strongly reduced from fresh carbons.

5.4.3.3 Influence on kinetics by background organics

Results of kinetics estimation for coexisted NOM were shown in **Table 5.9**. ASP and BAC effluent were applied as background organics. Because competition will not change isotherms greatly, *K* and *n* in pure water were used for estimation, which was shown in the table. Existence of NOM had not obvious influence on diffusivity except PFDA(10) in which D_s increased 10 times in ASP effluent than in pure water and BAC effluent, indicating organics affected long-chained PFCs more intensively. For short-chained PFCs, *e.g.* PFCA(4~5) and PFAS(4), coexisted organics resulted in decrease of diffusivity. This was related with more intensive reduction of adsorption capacities in short-chained PFCs.

Table 5.9 Influence of pH and NOM on PFC adsorption kinetics

	pH	PFBA(4)	PFPeA(5)	PFHxA(6)	PFHpA(7)	PFOA(8)	PFNA(9)	PFDA(10)	PFBuS(4)	PFHxS(6)	PFOS(8)
D_s 10^{-10}cm^2/s	3	12	6	5	2	8	12	12	6	35	12
	6.4[a]	23	23	24	12	12	13	1	6	6	9
	11	23	6	5	6	6	23	35	12	23	23
K_f 10^{-3}cm/s	3	0.9	1.0	0.1	0.6	0.8	5.8	9.3	0.2	1.4	5.8
	6.4[a]	0.1	0.1	0.1	0.1	0.6	0.6	0.6	0.1	1.4	3.5
	11	0.1	0.3	0.1	0.2	0.5	1.0	0.3	0.2	1.2	0.9
	NOM, mgDOC/L										
D_s 10^{-10}cm^2/s	0[a]	23	23	24	12	12	13	1	6	6	9
	2.3[b]	6	7	12	9	23	2	1	2	6	6
	4.5[c]	6	6	6	12	6	23	12	3	6	23
K_f 10^{-3}cm/s	0[a]	0.1	0.1	0.1	0.1	0.6	0.6	0.6	0.1	1.4	3.5
	2.3[b]	0.6	0.2	0.1	0.01	0.6	0.6	0.1	0.3	1.4	1.7
	4.5[c]	0.6	0.1	0.01	0.01	0.1	0.2	0.1	0.03	0.9	0.6

Note: ***a***=experiment in pure water, ***b***= ASP effluent in K-WWTP, ***c***=BAC effluent.

5.4.4 Influence by pH

5.4.4.1 Influence by pH of bulk solution

Figure 5.12 shows influence of pH on PFCs adsorption capacities. For each PFC, adsorbate loading rates in pH=3.6 were higher than in pH=7.2 and 11.7, which implied that adsorption was enhanced in acid

solution. Surface properties of GAC can be modified by positive or negative charge from H^+ and OH^- in bulk solution (Moreno-Castilla, *et al.*, 1995; Chen, *et al.*, 2003). In acid solution, the surface of GAC was almost positively charged and obtained stronger affiliation ability with anion PFC molecules. However, difference of adsorbate loading rate was not significant as shown in the figure, which implied that influence of pH on adsorption capacity was very small compared with carbon fouling.

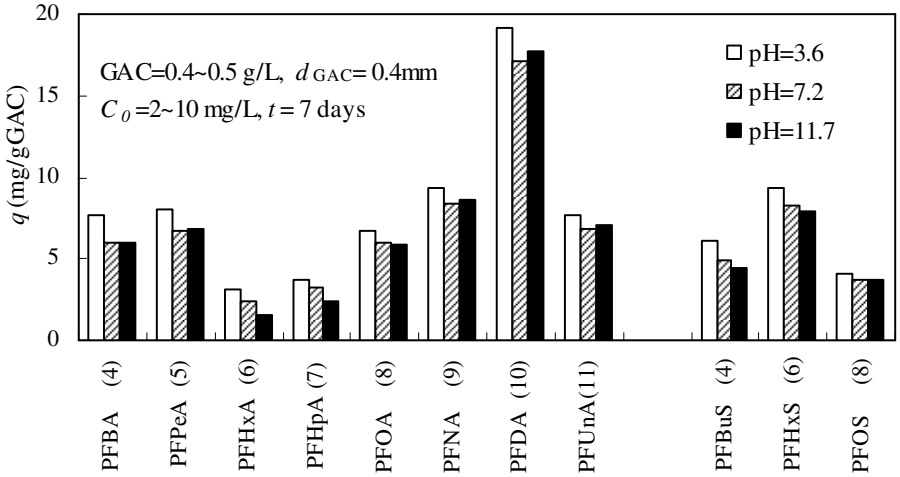

Figure 5.12 Influence of pH on PFCs adsorption capacity by GAC-F400

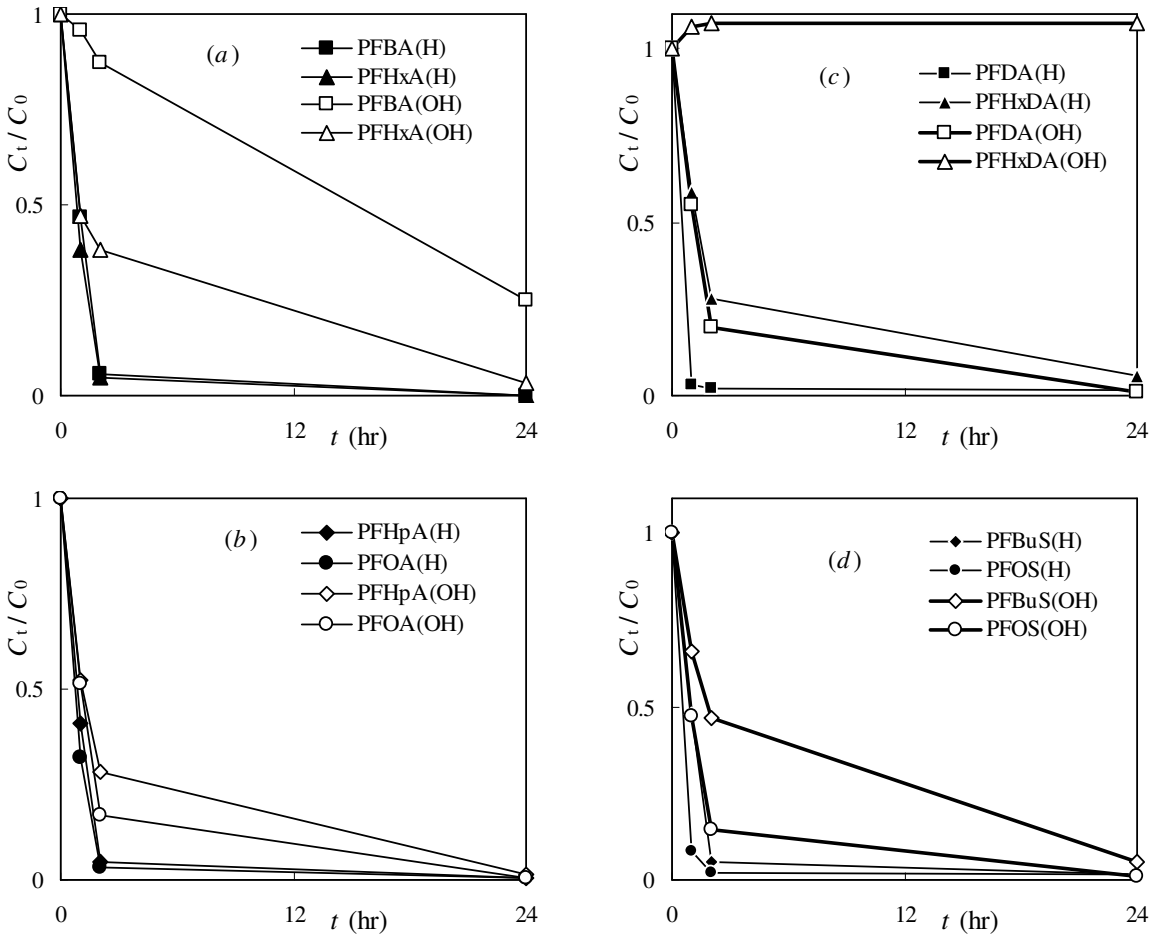

Figure 5.13 PFCs adsorption kinetics of surface modified GAC-F400

Because isotherms of PFCs seem not affected by bulk pH, their kinetics was estimated by equilibrium

data from pure water as shown in **Table 5.8**. Results of pH influence were also shown in that table together with coexisted organics. There were not significant differences of diffusivities by bulk pH. Diffusion coefficients at neutral pH for short- and medium-PFCAs were higher than acidic and basic pH, and those for PFCA(10) and PFAS(6,8) were smaller. Generally, bulk pH did not affect PFC adsorption except some long-chained PFCs.

5.4.4.2 Influence by pre-washed GAC

Modification of surface properties of GAC by pH can also affect adsorption kinetics, as shown in **Fig. 5.13**. Each PFC in the figure showed faster adsorption by acid-washed GAC than base-washed GAC. Furthermore, the intensity of influence seemed related with carbon chain length. Surface of GAC after base-washing was negative charged and changed to be hydrophilic so that repulse attachment of anion PFC molecules. The shorter is carbon chain, which means higher p*Ka* and hydrophilicity, the stronger is reduction in adsorption velocity by base-washed GAC, as shown in **Fig. 5.13*abd***. However, longer-chained PFCs as PFCA(12~18) were exceptional because they were not adsorbed by base-washed GAC at all, as PFHxDA(OH) shown in **Fig. 5.13*c***. The reason for this abnormal behavior was still unknown. In brief words, basic pre-washed process charged surface charge of GAC and resisted PFC molecules, and the resistance becomes stronger by the increase of carbon chain length.

5.4.5 Influence by GAC materials

Isotherms of PFCs on four kind GACs were estimated by Freundlich equation (FE) and shown in **Table 5.10**. As same as former results for F400 adsorption as shown in **Table 5.7** and **5.8**, values of K and n were roughly increased by carbon chain length, or by hydropobicity. The ranges of equilibrium bulk concentrations were larger than former values, therefore results for F400 were smaller than former ones due to analysis deviations by dilution operation and etc.. According to the results, Norit PK1-3 can not adsorb short-chained PFCs including PFCA(4~6) and PFBuS(4), but showed better performance to adsorb long-chain PFCAs such as PFCA(8~10,16). This result implied that GAC PK had stronger selectivity on hydrophobic molecules, which might be derived from carbon natures by materials and activation procedure.

Table 5.10 Estimation results of PFC isotherms by four kind GACs

Adsorbent	F400				PK				DW				Wako			
	K	n	r^2	Range[a]	K	n	r^2	Range	K	n	r^2	Range	K	n	r^2	Range
PFBA (4)	3	0.88	0.81	(625~1554)	0	4.39	7.00	(~)	70	0.59	0.98	(215~1447)	60	0.57	0.98	(336~1751)
PFPeA (5)	180	0.36	1.00	(105~1265)	0	3.79	0.88	(~)	250	0.51	0.95	(52~702)	270	0.43	0.99	(76~1168)
PFHA (6)	230	0.38	0.87	(22~1078)	11	0.82	0.51	(264~1394)	260	0.54	0.92	(27~845)	150	0.60	0.99	(36~854)
PFHpA (7)	200	0.45	0.99	(9~558)	140	0.45	0.88	(49~934)	170	0.76	0.91	(11~75)	190	0.68	0.99	(10~229)
PFOA (8)	170	0.75	0.99	(17~169)	300	0.54	0.96	(21~677)	6	1.91	0.92	(2~37)	30	1.33	0.84	(18~90)
PFNA (9)	1550	0.97	0.91	(3~48)	2050	0.46	0.97	(2~180)	1650	0.67	0.92	(26~59)	1230	0.79	0.67	(3~30)
PFDA (10)	1450	0.75	0.99	(2~42)	3850	0.49	0.92	(1~78)	1910	0.52	0.98	(4~83)	1710	0.86	1.00	(3~32)
PFHDA(16)	1000	0.93	0.79	(1~7)	1400	0.56	0.96	(1~45)	700	0.96	0.60	(3~19)	940	1.28	0.99	(1~8)
PFBuS (4)	160	0.48	0.90	(31~1005)	10	0.83	0.94	(322~1246)	250	0.54	0.93	(38~1064)	120	0.63	0.99	(55~1061)
PFHxS (6)	1060	0.45	1.00	(2~285)	620	0.50	0.98	(15~878)	700	0.82	0.95	(6~73)	1640	0.54	0.97	(2~108)
PFOS (8)	820	0.89	0.78	(1~7)	1000	0.55	1.00	(1~57)	2320	0.17	0.02	(1~8)	1530	1.12	0.79	(1~6)

Note: unit of q is μg/g, C is μg/L.

Results were also shown in **Fig. 5.14** by comparing only two kind GACs in one figure for better

understanding. **Figure 5.14*a*** showed that DW had better performances than F400 in most cases, for both *K* and *n* values were larger than F400. Similar results appeared in comparison of Wako GAC with F400. The two better performed GAC, as DW and Wako, were shown together in **Fig. 5.14*c***, in which both had similar isotherms for most PFCs, except decrease of *n* values in DW. This result implied that DW had disadvantage for long-chained PFCs, which might be related with its more proportion of micropores than other GACs because of original materials as nutshell. The smaller is pore size, the easier for PFC molecules to be resisted. Pore distribution of F400 and Wako GAC seemed more *average* than DW, therefore *n* values for them were not decreased for long-chained PFCs. **Figure 5.14*d*** shows advantages of PK to adsorb PFCA(9,10) over Wako GAC. However, for other PFCs, PK performed rather poor, which limited its application for PFC removal. As general summary, Wako GAC showed the best performance to adsorb PFCs, coconut based DW had larger capacity than coal based F400 but less effective for long-chained or more hydrophobic PFCs, Norit PK can not adsorb most short-chained PFCs and thus is unsuitable for water treatment process.

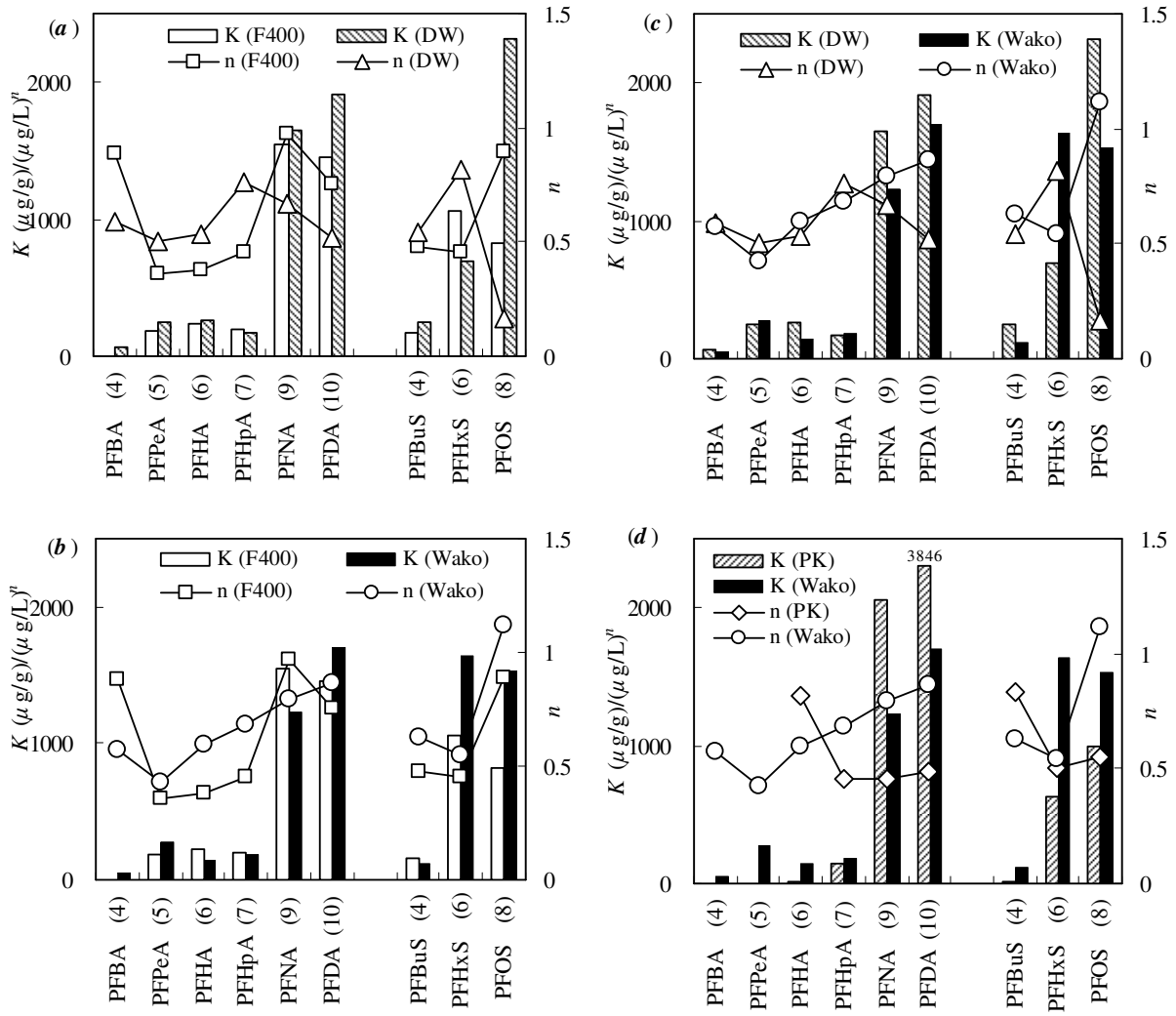

Figure 5.14 Influence of GAC materials (*a*~*d*) on PFC isotherm properties

5.4.6 Results of continuous experiments

5.4.6.1 Results of RSSCT

Results of PFCs by SBA filtration were shown in **Fig. 5.15**. Organics breaks through GAC filter very

earlier, and can be washed out by pure water easily as shown in **Fig. 5.15*a***. The reverse of matrix in short term can simulate backwash process in WWTP. **Figure 5.15*b~k*** shows behavior of each PFC in pure water and wastewater matrix, and **Fig. 5.15*l*** shows ∑PFC removal by RSSCT filter. Short-chained PFCs including PFCA(5,7) and PFAS(4) were obviously affected by wastewater matrix, and effect on other PFCs was not clear. Intensively concerned PFCs in K-WWTP, which included PFCA(8,9) and PFOS(8), seemed effectively removed by RSSCT filter, as shown in **Fig. 5.15*e f k***. ∑PFC in pure water broke 5% criteria at 2000 time of Bed Volume and kept below 10% till 6000 times of Bed Volume.

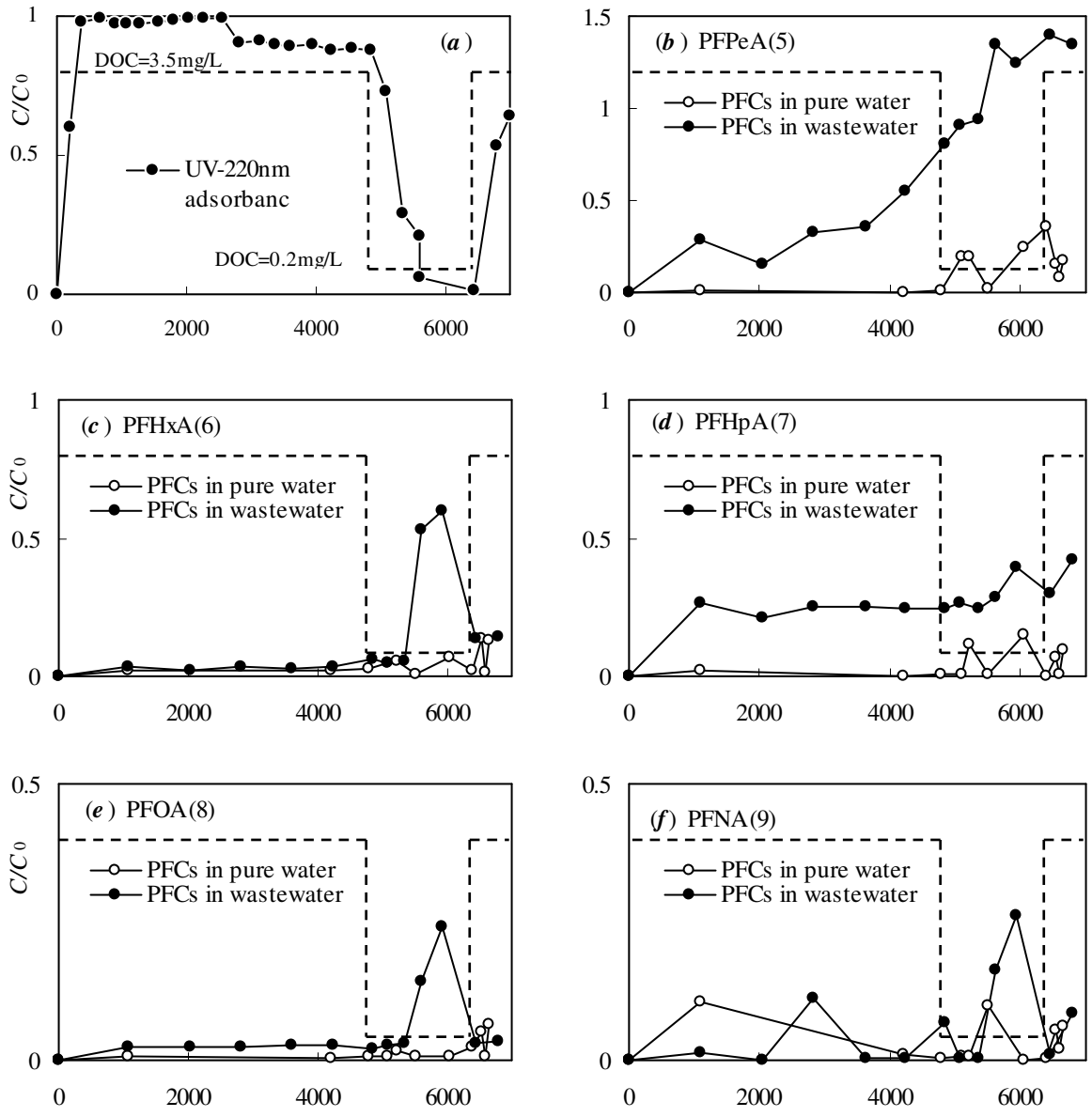

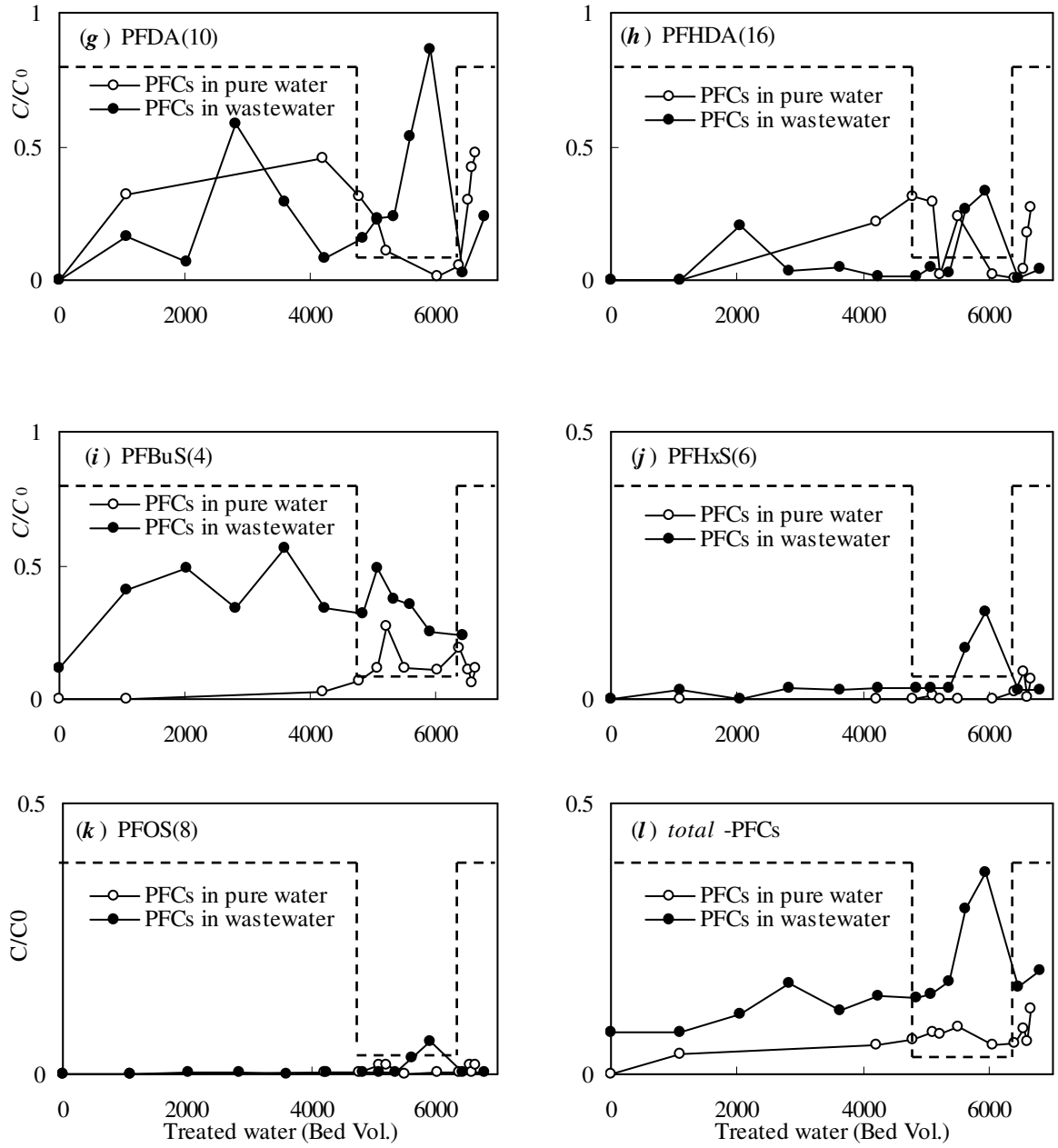

Figure 5.15 Break through curves in RSSCT experiments

One interesting finding is the opposite response of PFCs to organics by the *backwashing* step. All PFCs except shortest-chained PFC(4,5) showed increasing concentration after pure water was introduced instead of wastewater, indicating that PFC molecules might be washed out from GAC together with organics.

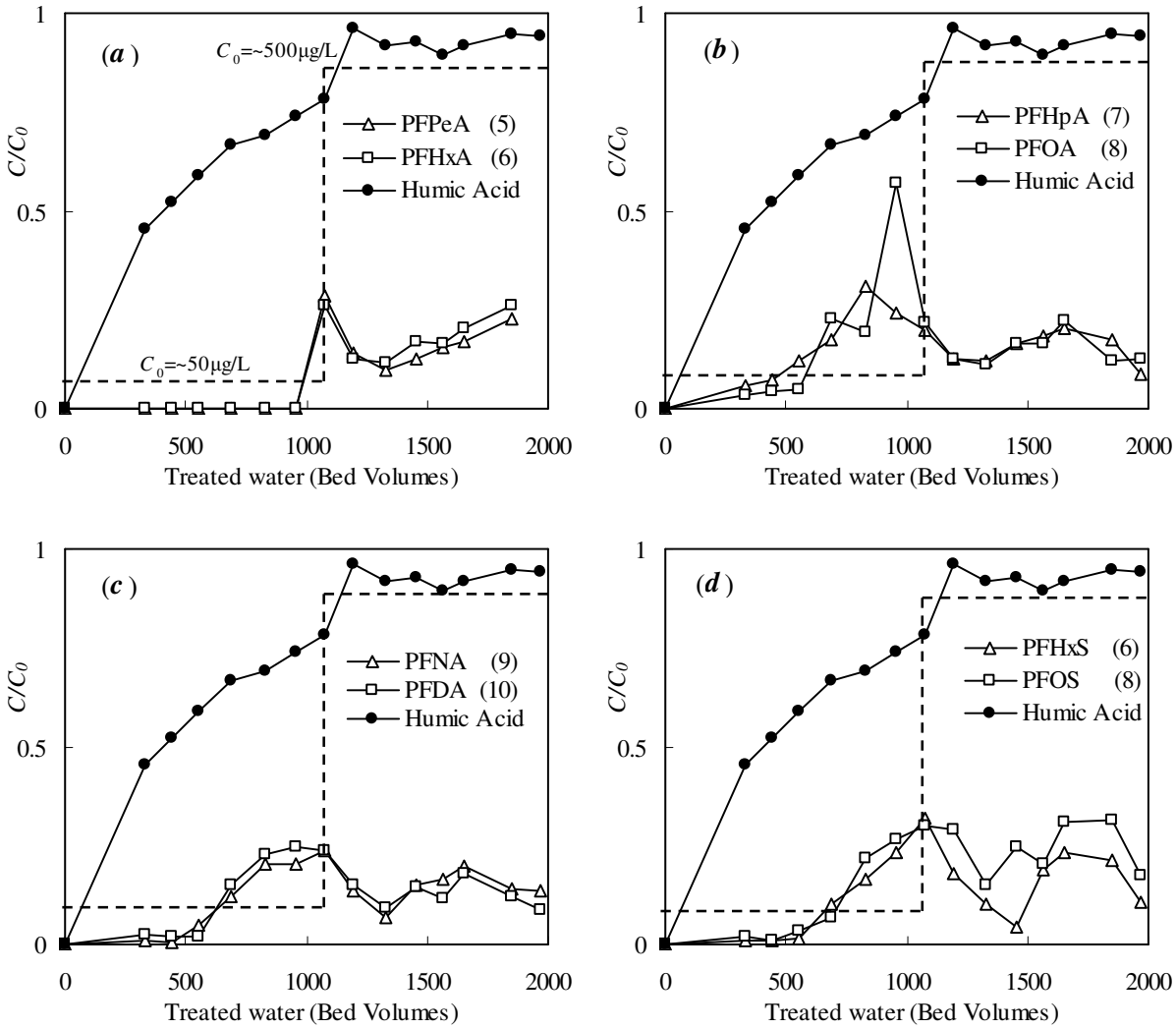

Figure 5.16 Break through curves in short bed adsorber (SBA)

5.4.6.2 Results of SBA

Results of PFCs by SBA filtration were shown in **Fig. 5.16**. PFC initial concentrations were increased about ten times in the middle of experiment. According to the figure, humic acid break through SBA much faster than other PFCs, which was usually observed in pesticide adsorption process (Wolborska and Pustelnik, 1996; Hand, *et al.*, 1997; Jarvie, *et al.*, 2005). PFCs showed similar behavior or shapes of breakthrough curves except shorter-chained PFCA(5,6). All PFCs showed similar responses to variance of influent concentrations, by which C/C_0 decreased in short time and then increased continuously.

5.5 Summary

In this chapter, adsorption properties of PFCs by GAC were studied to understand their special characteristics. Isotherms were interpreted by Freundlich equation, and influences were identified from NOM competition, carbon fouling, bulk pH and GAC materials. HSDM was successfully applied to estimated PFCs adsorption kinetics. GAC diameters influenced adsorption kinetics very much, while NOM competition and bulk pH had only slight effects on kinetics. Break through curves of PFCs in GAC fixed bed was preliminarily studied by RSSCT and SBA. Summaries are listed in detail as follows.

(1) Freundlich equation can interpret PFOA and PFOS isotherms in wide range of concentrations.

Simplified HSDM (s-HSDM) can not successfully simulate kinetics of PFCs adsorption, and complete HSDM can fit experimental data very well.

(2) In pure water, GAC-F400 adsorption showed increasing capacities for PFCs in ascendant carbon chain lengths. Kinetics study showed that diffusivity was decreased with descendant diameters of GAC and ascendant carbon chains, which implied that adsorption velocity was faster for long-chained PFCs and smaller size GAC.

(3) Coexisted NOM reduced GAC adsorption by competition and carbon fouling. Competition showed slight effect on short- and medium-chained PFCs, but obviously affected long-chained PFCs. Carbon fouling reduced adsorption capacities for all PFCs in much stronger extents than competition, especially for long-chained PFCAs. Bulk pH did not affect on adsorption capacities greatly, but influence adsorption velocity strongly. Basic washed GAC showed strong resistance to PFCs, especially for long-chained PFCAs.

(4) Four kinds of GAC were compared by their adsorption capacities to remove PFCs. Coal based GAC F400 showed moderate and average performance to remove all PFCs, which was considered the best among commercial GACs.

(5) RSSCT showed PFCA(8,9) and PFOS(8) can be effectively removed from pure water and wastewater matrix. SBA result showed that humic acid broke through GAC column much earlier than PFCs.

CHAPTER VI DEGRADATION OF PERFLUOROCHEMICALS BY PHOTOLYSIS PROCESS

6.1 Introduction

Although PFCs can be effectively removed from water by adsorption on activated carbon or resistance by membrane filtration (Tang, *et al.*, 2006; Tang, *et al.*, 2007), the concentrated PFCs were not degraded to harmless or less harmful chemicals. Therefore development of reliable process to degrade PFCs or stabilized PFCs is in urgent demand and of importance to control and alleviate PFCs contaminants.

Advanced oxidation processes (AOPs) are the first candidates. Being involved with generation of hydroxyl radicals to enhance water treatment, this kind of process shows excellent performance to control micro pollutants in water and waste water. Most common processes of AOPs include O_3/H_2O_2, O_3/UV and UV/H_2O_2. UV/TiO_2 process and Fenton's reagent also showed efficiency on specific wastewater(Gottschalk, *et al.*, 2000). However, previous researches showed that AOPs including O_3, O_3/UV, O_3/H_2O_2 and Fenton process can not degrade PFOS, but degrade PFOS precursors and partly fluorinated polymers effectively (Schröder and Meesters, 2005). Unsatisfied performance of ozonation in K-WWTP also supported this resistance. Although other PFCs can be reasonably assumed to be persisted under AOPs, there is no experimental information covered wide range of PFCs. Therefore, ozone-related process is minor part of this chapter although disappointed results may come out.

Direct photolysis by UV (220~260 nm) was reported to decompose PFOA effectively. Although reaction time was as long as three days, more than 90% of 560 mg/L PFOA can be completely degraded into CO_2 and HF under 0.48MPa oxygen. After some synthetic catalysts was applied, the degradation of PFOA was accelerated greatly (Hori, *et al.*, 2003; 2004b). Shorter wavelength UV had stronger energy per photon, therefore 185 nm mercury vapor lamp and 172 nm xenon quasi molecule laser light was applied successfully to decompose some PFCs completely(Zhang, *et al.*, 2005b). The degradation mechanisms by directly photolysis were hypothesized as stepwise break down of PFOA into shorter chain PFCAs and finally to CO_2 and HF. **Figure 6.1** shows proposal pathway of PFCA(x+1) degradation to PFCA(x)(Hori, *et al.*, 2004b). Because UV apparatus was relatively cheaper and easy for operation and maintenance, it could be applied in WWTP for PFCs removal as well as disinfection. Therefore, direct UV photolysis is major part of this chapter for development of effective degradation process for PFCs.

$$C_X F_{2X+1} COOH \xrightarrow{hr,-COOH} C_X F_{2X+1} \bullet$$
$$\xrightarrow{H_2O} C_{X-1} F_{2X-1} CF_2 OH \xrightarrow{-HF} C_{X-1} F_{2X-1} CFO$$
$$\xrightarrow{H_2O,-HF} C_{X-1} F_{2X-1} COOH \xrightarrow{hr} \cdots$$
$$\xrightarrow{H_2O,-2HF} CF_3 COOH \rightarrow \cdots \rightarrow CF_3 + CO_2$$

Figure 6.1 Stepwise degradation mechanisms for PFCAs

There are some other promising methods which performed well to degrade high strength PFCs polluted water, such as sulfate radicals generated by UV irradiation from persulfate ions(Hori, *et al.*, 2005a), sonochemical process as ultrasonic irradiation(Moriwaki, *et al.*, 2005), and strong oxidant as subcritical water catalyzed by zerovalent metals (Hori, *et al.*, 2006). Although most of these processes achieved complete removal or degradation of PFCs, they involved with sophisticated operations and critic

conditions, which limited their application in municipal WWTP.

6.2 Aims

Major aim of this study is to establish a possible degradation method for PFCAs and PFASs. Direct photolysis experiments in batch mode were conducted to study mechanism and kinetics of PFCAs degradations. Ozone related advanced oxidation process was also performed to check possibility of OH radical degradation. Objectives of this chapter are list as below.

(1) To analyze mass spectra of different PFCAs and PFASs to identify products of UV irradiation, as well as the hypothesized pathway of degradation. Study different behavior between PFCAs and PFASs in photolysis.

(2) To develop kinetics model and estimated results of kinetics experiments in batch mode to understand behavior of PFCAs during photolysis. Understand influence from matrix or natural organic matters on removal of PFCs by UV irradiation.

(3) To apply UV photolysis to treat highly polluted river water.

(4) To conduct batch experiments to determine possibility of ozone-related process to degrade PFCs. Apply semi-batch experiments to understand kinetics to remove PFCs.

6.3 Experimental Descriptions

6.3.1 UV photolysis experiments

6.3.1.1 Experimental apparatus

All of the photolysis experiments by UV are classified into two groups by using different lamps. Properties of the two kinds of UV lamps are listed in **Table 6.1**.

Table 6.1 UV lamps used in photolysis experiments

Position	Model	Power *W*	Potential *V*	Wave length *nm*	Size *cm*	Company
Upside	GL-10	10	110	254	40×*Φ* 3	Hitachi
Submerged	KL-150	7.2	390	254	15×*Φ* 1	Okayama
	ZKL-150	7.2	390	254 + 185 (10%)	15×*Φ* 1	Okayama

In upside irradiation, sample was stored in the 25mL stainless steel bottles and placed under the lamp GL-10 which was produced for indoor disinfection (Hitachi Com., Tokyo, Japan). UV irradiation was introduced to the sample from upside orientation. The lamp and sample were covered by Aluminum foil in roof shape to reflect UV light and seal the irradiation, as shown in **Fig. 6.2*a***.

In submerge irradiation, sample was prepared in the 40mL PP chromatography column and the UV lamp KL-10 or ZKL-10 (Okayama Com., Osaka, Japan) was submerged into the sample. The irradiation was introduced from the lamp inside the sample and reflected by Aluminum foil which was wrapped around the column to seal UV light, as shown in **Fig. 6.2*b***. The PP column with Aluminum foil was placed into water bath to cool the system.

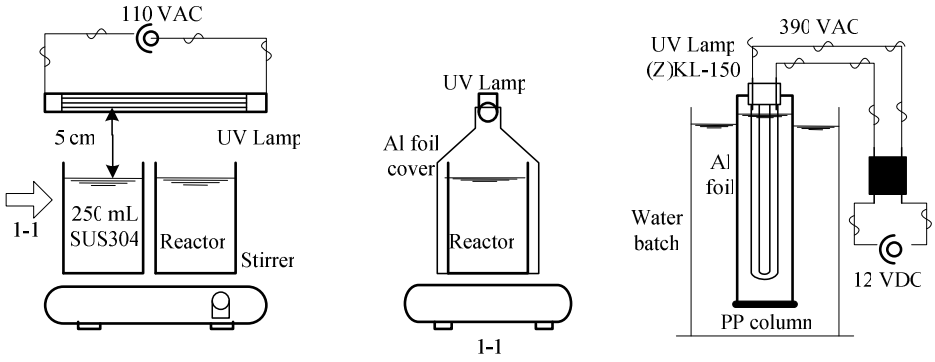

(*a*) UV lamp over the sample (*b*) UV lamp submerged inside

Figure 6.2 Scheme of UV irradiation experiments (*a*)upside and (*b*)submerge

6.3.1.2 Experimental description

Series of experiments were designed and conducted to elucidate mechanism and kinetics of UV photolysis on PFCs. Experimental conditions of UV photolysis were summarized in **Table 6.2**. Runs UM referred to mass spectra analysis, Runs UK refer to kinetics study and Runs UA involve with Ai River water treatment by UV photolysis.

Table 6.2 Experimental conditions of UV photolysis experiments

Runs			Lamp	Solutions	Initial C_0 ($\mu g/L$)	DOC (mg/L)	Volume (mL)	Time (hr)
UM	Mass spectra analysis	1	ZKL-150	PFHxDA(16)	10,000	-	30	14
		2	ZKL-150	PFDA(10)	10,000	-	30	7
		3	ZKL-150	PFOA(8)	10,000	-	30	5
		4	ZKL-150	PFOS(8)	10,000	-	30	60
		5	ZKL-150	PFHxS(6)	10,000	-	30	36
UK	Kinetics study	1	ZKL-150	PFOA(8)	82	-	30	4
		2	ZKL-150	PFNA(9)	82	-	30	4
		3	ZKL-150	PFDA(10)	133	-	30	4
		4	GL-10	PFOA(8)	75	-	25	6
		5	GL-10	PFOA(8)	18	1.7	25	12
		6	GL-10	PFOA(8)	24	4.5	25	12
		7/8	ZKL-150	PFOA(8)+PFOS(8)	47	3.3	30	3.5
UA	Treat river water	1	ZKL-151	PFOA in river water	40		30	4
		2	KL-150	PFOA in river water	40		30	6
		3	ZKL-150	PFOA in river water	40		500	6

Runs UM1~5 were designed to confirm the photolysis degradation of PFCs by mass spectra analysis. Furthermore, products of degradation can be identified by analyzing mass spectra of samples at different experimental time. Three of PFCAs, including PFHxDA(16), PFDA(10) and PFOA(8), and two of PFASs including PFOS(8) and PFHxS(6) were for mass spectra experiments. Sample was prepared by diluting stock solution at 10g/L into 10mg/L in water. Then the sample was moved to 30mL PP column and processed by submerged ZKL-150 irradiation at $UV_{254+185}$. At sampling time, 0.1mL of the liquid was taken out of the PP column and moved to PP tubes by pipette. After diluted for 10 times in pure methanol, the sample was introduced to MS system directly by syringe pump to obtain mass spectrum. There might be some lost of PFCs during dilution into water because of their relatively lower water

solubility, especially of longer-chained PFHxDA(16). Only qualified analysis was conducted on mass spectra so that small amount of lost have no influence on the analysis conclusions.

Runs UK1~3 were designed to estimate *consecutive* kinetics of PFCAs photolysis. Three PFCA(8~10) were selected for this purpose, which were medium-chained PFCs and highly concerned in K-WWTP. Another reason referred to their better water solubility, which was helpful to reduce lost of chemicals during dilution operations. Around 100 μg/L of single target PFCA solution was prepared from 10mg/L standard solution in LC mobile phase by dilution into water. After that, PFCA solution was moved into 30mL PP column and processed submerged ZKL-150 irradiation. At sampling time, 0.1mL of sample was moved from PP column to 2mL PP vials, which can introduce to LC-MS to analyze possible photolysis products.

Runs UK4~6 were designed to study the influence from background organics on the performance of UV photolysis. Effluent water from BAC filter and second clarifier (ASP) from K-WWTP was selected as matrix to study their effects. PFOA(8) solutions were prepared by spiking certain volume of 10mg/L standard solution into matrix. After that, 25mL of PFOA(8) was moved into stainless steel plate and placed under GL-10 UV disinfection lamp. During photolysis, 0.1mL of sample was taken out of the plate at sampling time, and introduced to LC-MS to analyze PFOA(8) only. UV spectra of matrix were also obtained by UV spectrometer to assist analysis for experimental results.

Runs UK7~8 were duplicate experiments to confirm variance between different lamps of ZKL-150 model. Effluent from sand filtration in K-WWTP was applied as matrix. Both PFOS(8) and PFOA(8) were spiked into matrix to prepare solution with concentration of 50μg/L. After that, submerged ZKL-150 irradiation was applied for duplicate samples by lamp A and lamp B. At sampling time, 0.1mL liquid was taken out and introduced to LC-MS to analyze PFOS(8) and PFOA(8) concentrations.

Runs UA1~3 were designed to apply UV photolysis to treat highly polluted river water. Some point source was located along Ai River and resulted in very high concentration of PFOA in the river water, which was reported by previous work (Lien, *et al.*). Ai River water was sampled in 2L of PET bottles and transported to laboratory for experiment. After filtration by glass fiber filter paper, the filtrate was directly exposed to submerged ZKL-150 for photolysis. At sampling time, 0.1mL sample was taken out and spiked by internal standard as 9H-PFNA, then introduced to LC-MS for quantification.

6.3.1.3 Model for kinetics study

Photolysis for PFCAs was assumed to obey first order kinetics according to observed data, as shown in following equation,

$$\frac{dC}{dt} = -kC \tag{6.1}$$

where C is PFCAs concentration, k is coefficient which represented velocity of degradation. Products of PFCA photolysis, which is one-carbon shorter-chained PFCAs, would be further degraded by UV irradiation, and follow similar mechanisms. Therefore, stepwise degradation of PFCAs could be described by following *consecutive* kinetics, or forward reactions

$$C_1 \xrightarrow{k_1} C_2 \xrightarrow{k_2} \cdots C_i \xrightarrow{k_i} C_{i+1} \xrightarrow{k_{i+1}} CO_2 + HF$$

in which each step was assumed to be charged by first order differential equations. Thus a set of differential equations was available to describe this *consecutive* kinetics as follows,

$$\begin{cases} \dfrac{dC_1}{dt} = -k_1 C_1 \\ \dfrac{dC_1}{dt} = \dfrac{dC_2}{dt}\bigg|_{Pdt} + \dfrac{dC_2}{dt}\bigg|_{Deg} = -\dfrac{M_2}{M_1}\dfrac{dC_1}{dt}\bigg|_{Deg} + \dfrac{dC_2}{dt}\bigg|_{Deg} = \dfrac{M_2}{M_1}k_1 C_1 - k_2 C_2 \\ \cdots \\ \dfrac{dC_i}{dt} = \dfrac{M_i}{M_{i-1}}k_{i-1} C_{i-1} - k_i C_i \end{cases} \tag{6.2}$$

where C_1 is concentration of target PFCA, C_2 to C_i are concentrations of product PFCAs in sequence, M_1 to M_i are molecular weights of PFCAs, k_1 to k_i are kinetic parameters which are independent to initial concentrations, subscript *Pdt* and *Deg* meant product and degradation respectively.

Two steps *consecutive* kinetics has analytical solutions as shown in **Eq. (6.3)**. However, with the increasing of consecutive steps, the differential equations became more and more complicated and impossible to get analytical solutions. In order to simplify the simulation, raw PFC and its first photolysis product were calculated by **Eq. (6.3)**, and the further consecutive products were calculated by numerical methods such as Runge-Kutta method.

$$\begin{cases} C_1^t = C_1^{t0} \cdot e^{-k_1 t} \\ C_2^t = \dfrac{M_2 k_1 C_1^{t0}}{M_1 k_2 - M_2 k_1}\left(e^{-\frac{M_2}{M_1}k_1 t} - e^{-k_2 t} \right) \end{cases} \tag{6.3}$$

Once value of k was identified, concentrations of product PFCAs could be calculated step by step from the target PFCA. Then an objective function $Z(k)$ was proposed to estimated kinetic parameter k at $Z_{\min}$ by least square fitting method.

$$Z(k) = \sqrt{\frac{\sum [C_{sim}(k) - C_{\exp}]^2}{n}} \tag{6.4}$$

where C_{sim} is concentration calculated by specific value of k, $C_{\exp}$ is observed concentration in experiment, n is number of samples.

As assumption, k was influenced by background absorbance and irradiation intensity, and an expression of k was proposed as follows.

$$k = \frac{K}{V}(SUVA_M - SUVA_B) = \frac{K \cdot (I_M - I_B)}{V \cdot DOC} \tag{6.5}$$

where, K is constant determined by lamp and orientation, V is sample volume, I is absorbance at 254nm, and *SUVA* is specific UV absorbance, equal to UV_{254} absorbance divided by DOC concentration. Subscript of *M* and *B* meant maximum value and background absorbance for specific matrix.

6.3.2 Ozone related processes

6.3.2.1 Analytical method

Concentration of ozone in gas flow was determined by KI titration methods. Around 80mL of 5% KI solution was prepared and stored in 100mL volumetric cylinder. While sampling, the direction of three way cock was changed to introduce ozone gas into the KI solution for 1 minute. Then the yellow liquid was titrated by 0.01 N $Na_2S_2O_3$ solution in a titrimeter (KTF-150). Before titration, 10mL of 10% citric

acid was spiked into the liquid to reduce possibly generated periodic acid. Three drops of starch solution was added after the color changed to pale yellow as index for titration termination. These two steps were described by following equations, from which the mole ratio of O_3 to $Na_2S_2O_3$ was calculated as 1:2.

$$\begin{aligned} O_3 + 2I^- + 2H^+ &\rightarrow O_2 + I_2 + H_2O \\ I_2 + 2S_2O_3^{2-} &\rightarrow 2I^- + S_4O_6^{2-} \end{aligned} \tag{6.6}$$

At last, the ozone concentration in the gas phase was calculated by **Eq. (6.7)**,

$$C_{OG} = \frac{V_{tr} \cdot 24}{C_{tr} \cdot (Q_{OG} t)} = 0.24 \frac{V_{tr}}{Q_{OG}} \tag{6.7}$$

where C_{OG} is ozone concentration in gas flow as mg/L, Q_{OG} is ozone gas flow rate in the experiments as L/min, t is the sampling time in unit of min, C_{tr} is concentration of $Na_2S_2O_3$ solution as mol/L, and V_{tr} is the volume of $Na_2S_2O_3$ solution. In this study, C_{tr} is constant as 0.01N and t is fixed as 1 min.

Determination of aqueous ozone concentration was based on the Indigo Colorimetric Method (Bader and Hoigne, 1981). At first, Indigo stock solution was prepared by dissolving 0.770 g indigo trisulfonate and 1mL phosphorous acid into ultra pure water and diluted into 1L. Then 20mL Indigo stock solution was diluted in 1L by ultra pure water with 10g NaH_2PO_4 and 7mL phosphorous acid to get Indigo (I) reagent. At sampling time, 1mL of Indigo (I) reagent was stocked into 15mL PP centrifuge tube firstly, and then 9mL of sample was taken into the PP tube. The tube was capped for seal immediately and shaken intensively by hand for half a minute. After that, the mixed liquor was introduced to UV-VIS recording spectrophotometer (UV-2500PC, Shimadzu Corp., Kyoto, Japan) to measure absorbance at 600nm. Blank sample was also prepared to confirm that the blank absorbance of Indigo (I) standard solution is higher than 0.42. The absorbance at 600 nm of the sample was recorded to determine residual ozone in the sample by **Eq. (6.8)**,

$$C_{OL} = \frac{100 \cdot \Delta I}{f \cdot b \cdot V} = \frac{I_0 - I}{0.42} \tag{6.8}$$

where C_{OL} means aqueous ozone concentration in mg/L, I is absorbance at 600 nm of samples reacted with Indigo reagent, I_0 is blank value of pure water, f is constant as 0.42, b is the cell length for absorbance spectrometer, equal to 10 mm, V is total volume of mixture equal to 10mL. The analytical limits of Indigo (I) reagent is 0.01~0.1 mgO_3/L.

6.3.2.2 Experimental description

Batch experiments were designed to identify the possibility of PFCs degradation by O_3/H_2O_2 process. Ozone saturated pure water was used in batch experiments to eliminate possible contaminations from pipeline, connectors and cocks. The experimental scheme was shown in **Fig. 6.3** and the detailed conditions were described by Runs OM and OB in **Table 6.3.**

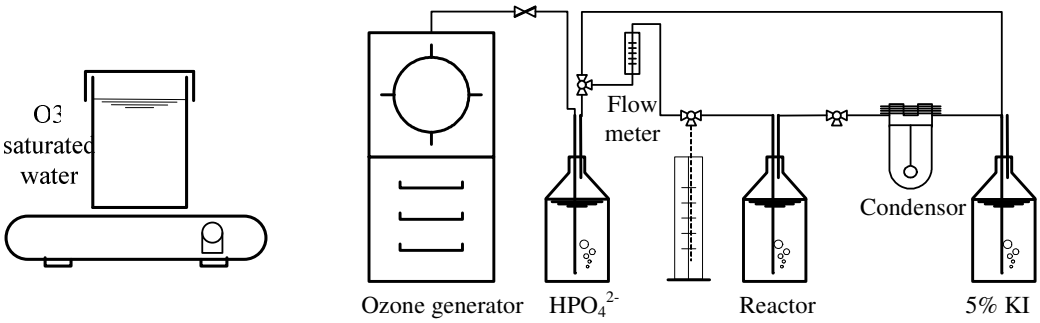

Figure 6.3 Batch and semi-batch experimental apparatus for ozone related processes

Runs OM 1~9 were designed to obtain mass spectrum for each PFCs after O_3/H_2O_2 treatment by ozone saturated water. Runs OB 1~3 were conducted to check performance of O_3/H_2O_2 process on trace level PFCs in mixture by ozone saturated water. In case of semi-batch experiments as Runs OS 1~4, ozone gas from generator was passed through a reactor to contact with multi-PFCs solutions continuously.

Ozone saturated water in Runs OM and OB was produced by passing high purity ozone gas (10, 25 and 50 mg/L) through ultra pure water in room temperature (33℃) for half an hour. Saturated concentration of ozone was calculated as 2.5, 6.3 and 12.5mg/L. In Runs OM and OB, 0.5mL of single or mixed PFCs standard solutions in 1 mg/L were firstly added into a stainless steel bottle, and then 0.3mL of 1N NaOH was added to control pH above 11. After saturated water was prepared, about 250mL was taken out immediately and pored inside the stainless steel bottle. Then, 1mL of hydrogen peroxide (~34%) was added and the cap was tightened and sealed. Thirty minutes later, 250mL sample in the reactor was extracted by SPE process and rebuilt into 1mL LC mobile phase solvent. For Runs OM 1~9, the rebuilt samples were diluted for 10 times in methanol and injected into MS by syringe to obtain mass spectra. For Runs OB 1~3, the rebuilt samples were diluted in LC mobile phase and injected into LC-MS to analyze their PFC concentrations.

Table 6.3 Experimental conditions of ozone-related process

Runs	Description	PFCs	Conc.	Volume	O_3(gas)	O_3	H_2O_2	NaOH	Time
			μg/L	mL	mg/L	L/min	mL	mL(1N)	hr
OM 1~9	Mass spectra of single PFC by O_3 saturated water	PFCA(6~12), PFAS(6,8)	~20	250	50		1	0.3	0.5
OB 1~3	Influence by O3 conc. on multi-PFCs	PFCA(6~14)+ PFAS(6,8)	~2	250	10, 25, 50		1	0.3	0.5
OS 1~4	Behavior of multi-PFCs in semi-batch experiments	PFCA(4~11)+ PFAS(4,6,8)	50~100	700	~0.5	2, 3.5; 0.5, 5			5~8

The scheme of semi-batch experiments is also shown in **Fig. 6.3** as Runs OS 1~4. Ozone gas was produced from air by an ozone generator (TYPE-1 500, *Environmental Chemical Company, Tokyo, Japan*) with capacity of $0.5gO_3$/hr. Prior to be introduced into reactor, ozone gas flow was firstly washed by phosphate buffer (5N Na_2HPO_4) to remove NO_X, which is by-product of ozone generation from air. After that, ozone gas passed through a flow meter and diffused into the reactor. Three-way cocks were placed before and after the reactor to measure ozone gas concentrations by KI method. Ozone concentration in liquid was measured by Indigo (I) method. Exhausted ozone gas was absorbed by 5% KI solution at the end of flow. A glassware condenser soaked into 0℃ ice-water bath was placed after the reactor to trap

PFCs which were possibly escaped from liquid phase into aerosol phase. Diffuser in Runs OS 1~4 was made in polyethylene, and reactor was made by polycarbonate, both were designed to avoid adsorption from PFCs. PFA tubes, Teflon 3-way cocks and PP jointers were also used in the flow line, which will not influence PFCs in reactor significantly.

At sampling time, about 1mL of sample was taken out of reactor by stopping ozone generator and open PC bottle sealed caps. The samples were stored in 2mL PP sample vials and exposed to air for one hour to ensure self decomposition of ozone. After that, the vials were sealed and introduced to LC-MS analysis within same day. Another 9mL of sample was also taken out for purpose of measuring aqueous ozone concentration by Indigo (I) method described in next section. At the end of experiment, trapped liquid in condenser was firstly moved to PP centrifuge tube. Then the condenser was washed by pure methanol for three times in total volume as 10mL. This step was designed to elute possibly adsorbed PFCs on the glassware surface. After mixing the washed methanol and trapped liquid together, the mixture was diluted by pure water into linear range of concentrations for LC-MS analysis and determined by LC-MS.

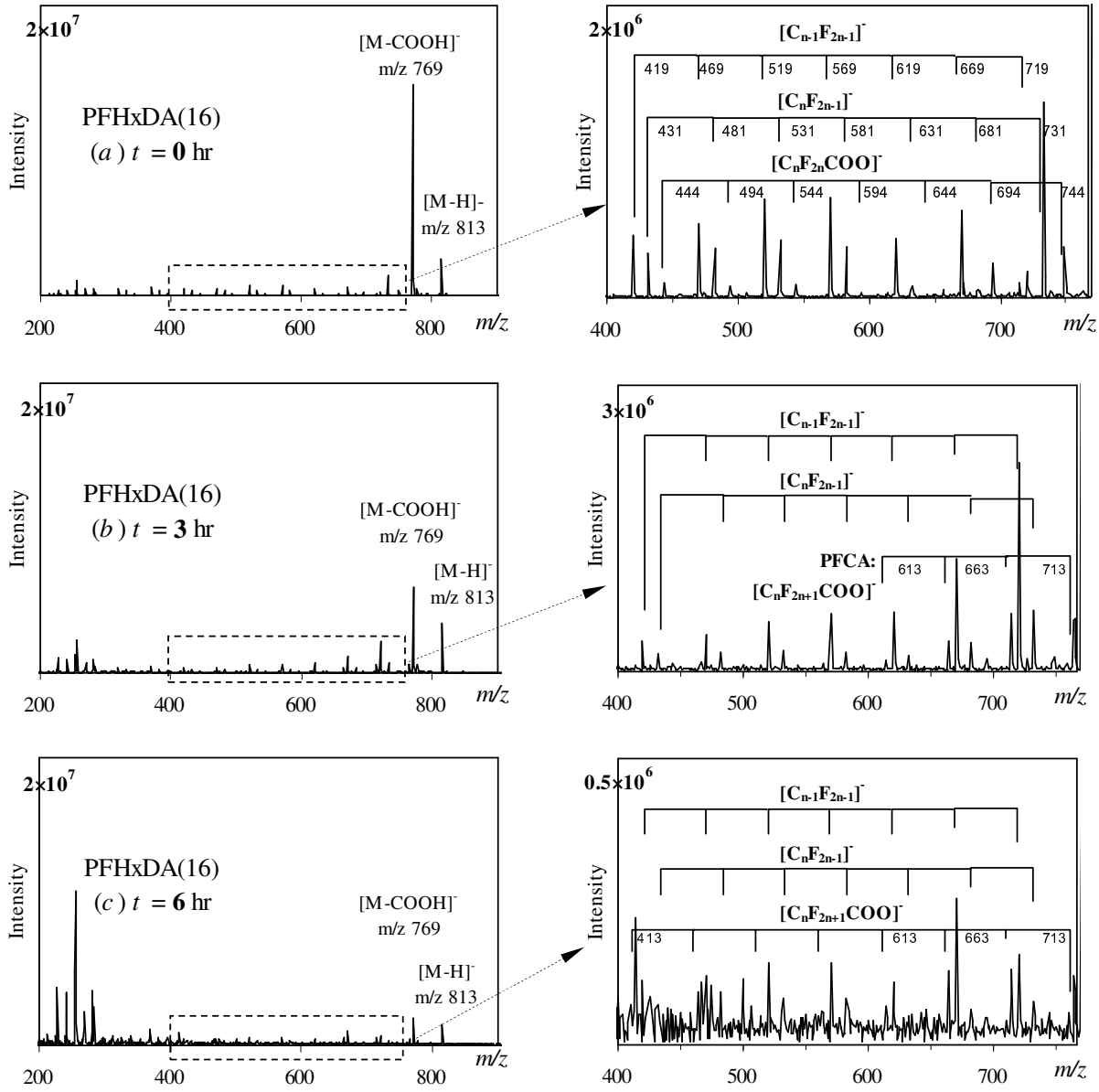

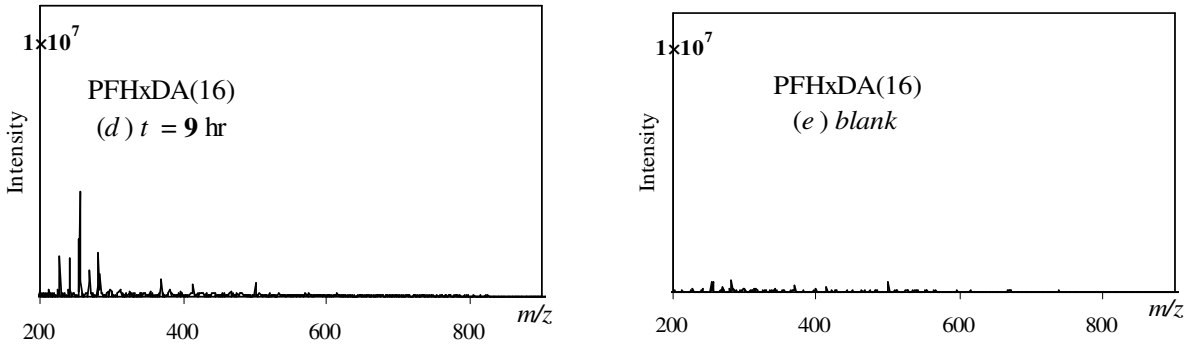

Figure 6.4 Mass spectra (*a*=0, *b*=1h, *c*=6h, *d*=9h) for PFHxDA(16) under $UV_{254+185}$

6.4 Results and Discussion

6.4.1 Mass spectra analysis for PFCs

6.4.1.1 Photolysis of PFHxDA

Results of Run UM1~9 are shown in **Fig. 6.4**, including blank and mass spectra of PFHxDA(16) and expected photolysis products. Mass spectra in range of 400~700*m/z* are zoomed into right side by dash arrows. In **Fig. 6.4*a***, peak at *m/z* 813 is represented to parent ion which released only on proton from molecule. Predominant daughter fraction is *m/z* 769 which released the carboxylic group as [COOH]. Some peaks occurred at the beginning time, which should be allocated to fractions of parent anion of molecule.

The molecular fractions of PFHxDA(16) could be classified into three catalogue, which is $[C_nF_{2n}COO]^-$, $[C_nF_{2n+1}]^-$ and $[C_nF_{2n-1}]^-$, by the collapse method shown in **Table 6.4** Each type of molecular fraction is formed by two steps. Firstly, some special parts are broken from the molecule, such as $[CF_3]$ in Type **I**, [COO] in Type **II**, [COO] and $[F_2]$ in Type **III**, which are numbered as 1~3. After that, further fraction was generated by sequentially release $[CF_2]$ group, which was labeled as 4, resulted in offset peaks in mass spectra by interval of *m/z* 50, equal to the mass of $[CF_2]$.

From **Fig. 6.4*a*** in zoomed scale, peaks of Type **II** held highest intensity among three types, and Type **I** was the lowest. Carbon bond in $[-CF_2-COO]$ was expected less strong than $[-CF_2-CF_3]$ because of the sheath effect by F atoms in latter one, therefore fraction in Type **I** were more easily occurred. As the daughter fraction of Type **II**, peaks of Type **III** were weaker than its parent ion.

Table 6.4 Three fraction types of PHxDA(16) parent ion

I	**II**	**III**
$[M-H]^-$, $-[CF_3]$, $-x[CF_2]$	$[M-H]^-$, -[COO], $-x[CF_2]$	$[M-H]^-$, -[COO], $-[F_2]$, $-x[CF_2]$
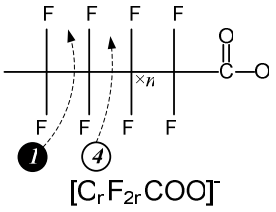	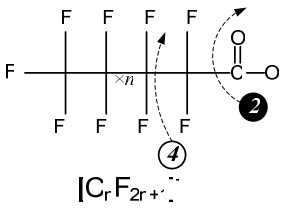	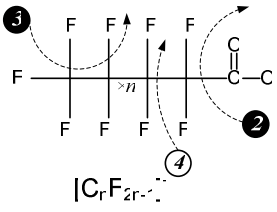
$[C_rF_{2r}COO]^-$	$[C_rF_{2r+1}]^-$	$[C_rF_{2r-1}]^-$

Note: ①= $-[CF_3]$; ②= -[COO]; ③= $-[F_2]$; ④= $-[CF_2]$.

Figure 6.4*b* showed mass spectrum at 3 hours. Compared with **Fig. 6.4*a***, intensity of *m/z* was

significantly reduced from the beginning, which implied removal or degradation of parent molecule. Except of molecular fractions in Type **I** and **II**, new molecules appeared at the *m/z* for PFCA parent anions, which were considered as products from PFHxDA(16). **Figure 6.4c** showed mass spectrum at 6 hours. The dominant peak of PFHxDA(16) was extremely weaker than at the beginning time. Peaks at *m/z* of PFCA products were also decreased significantly because of the proposed stepwise degradation. After 9 hours as shown in **Fig. 6.4*d***, PFHxDA(16) and other PFCAs almost disappeared, which proved that PFHxDA(16) was removed from water completely.

In order to understand the degradation process of PFHxDA(16) in detail, peak heights of PFCA *m/z* are shown along with experimental time in **Fig. 6.5**. Both $[M\text{-}COOH]^-$ than $[M\text{-}H]^-$ fraction could be used to present amount of PFHxDA(16), where M represented neutral molecule, and peak at *m/z* 769 as $[M\text{-}COOH]^-$ is preferable because of its predominance in mass spectra as shown in **Fig. 6.5*a***. For degradation products, $[M\text{-}H]^-$ was selected because $[M\text{-}COOH]^-$ was overlapped with Type **II** fractions of PFHxDA(16).

Target PFCA was reduced rapidly after start time, and completely removed after 9 hours of UV irradiation, as shown in **Fig.6.5*a***. All the expected degradation products, as PFCA(4~15), were detected during experiment time and showed in groups by carbon-chain length in **Fig. 6.5*b~d***. Peak intensities of PFCA(10~15) were firstly increased and arrived maximum between 3~6 hours, then decreased to small value and arrived minimum at 9 hours. Shorter-chained PFCAs as PFCA(4~9) in **Fig. 6.5*cd*** were increased from the beginning time without obvious maximums before 9 hours.

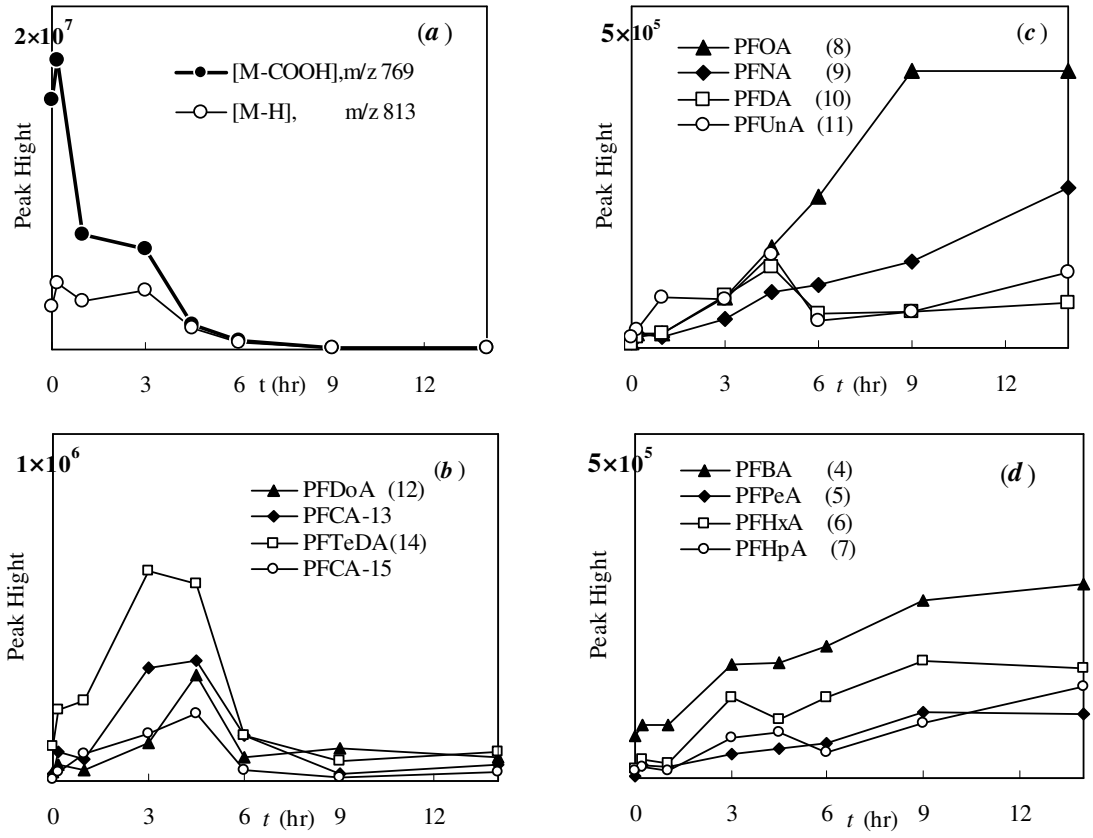

Figure 6.5 MS intensity for PFHxDA(16, *a*) and photolysis products(*b*, *c*, *d*)

Their behavior could be explained by the dynamic balance between generations from one-carbon longer PFCA and degradation of themselves to one-carbon shorter PFCA. Assumed that both generation

and degradation were charged by first order kinetics, primary products as longer-chained PFCA(10~15) were accumulated in beginning period because their generation was faster than degradation. The time of maximum value represented equal velocity of generation and degradation. After that, degradation was dominant until the end of experiment. For shorter-chained PFCAs(4~9), their generation was always faster than degradation until end of experiments, which resulted in continuous accumulation.

6.4.1.2 Photolysis of PFDA and PFOA

Mass spectra of medium-chained PFDA(10) under photolysis are shown in **Fig. 6.6**. In **Fig. 6.6*a***, primary peak of PFDA(10) appeared at *m/z* 469 as fraction of $[M\text{-}COOH]^-$. After 1 hour, PFDA(10) was reduced and peaks of PHNA(9) and PFOA(8) appeared at *m/z* for $[M\text{-}COOH]^-$ and $[M\text{-}H]^-$ fractions, as shown in **Fig. 6.6*b***. Response intensities of PFDA(10) and photolysis products, as height of relative peak, are shown along the time in **Fig. 6.6*c*** and ***d***. Considering possible overlap between primary fraction of PFCA(5~9) and Type **II** fractions of PFDA(10), proton released peak $[M\text{-}H]^-$ was selected to identify and quantify product PFCA. By similar pattern, primary product PFNA(9) were firstly increased and then decreased with maximum value at 1 hour as shown in **Fig. 6.6*c***. PFOA(8) and PFHpA(7), which were sequentially generated from PFDNA(9), reached maximum value between 2~4 and 4~6 hours. Shorter-chained PFHxA(6) and PFPA(5) kept on increasing during experimental time.

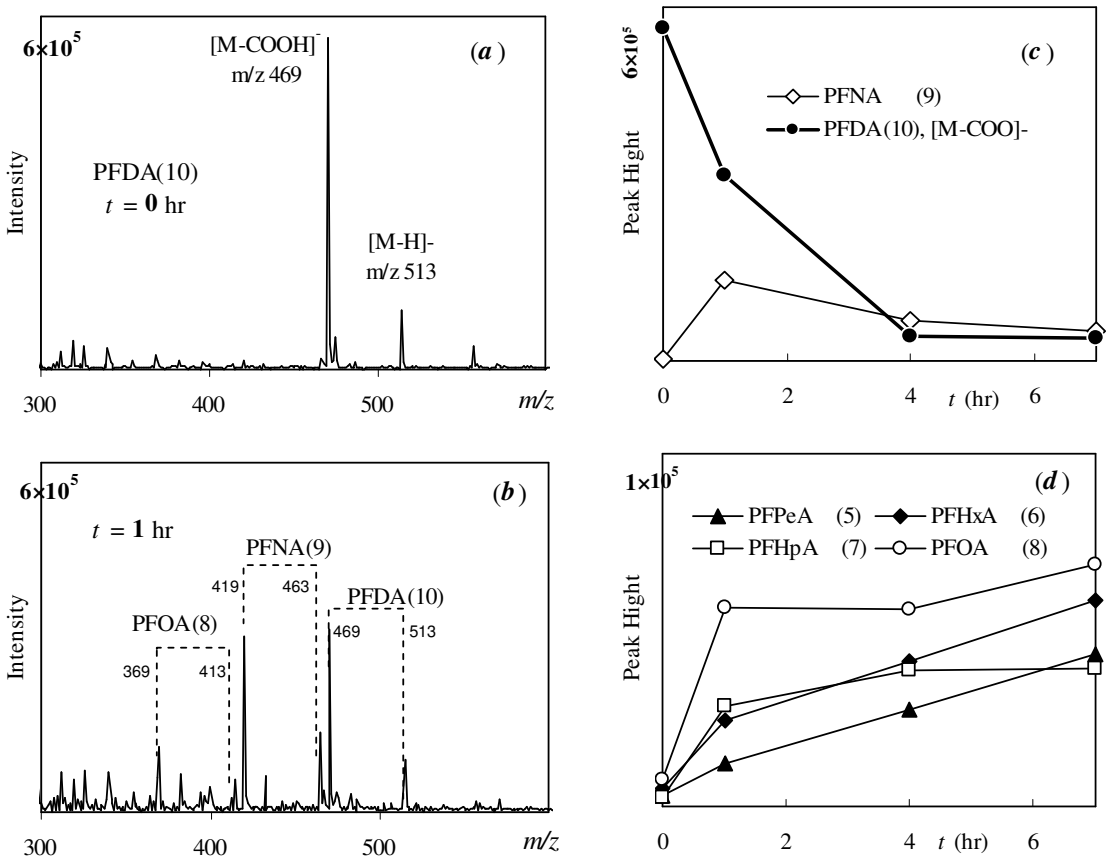

Figure 6.6 Mass spectra and intensity for PFDA(10) and photolysis products

Mass spectra of degradation products of PFOA(8) are shown in **Fig. 6.7**. Primary fraction of PFOA(8) in its mass spectrum was carboxylic releasing $[M\text{-}COOH]^-$,as shown in **Fig. 6.7*a***. PFOA(8) was also very rapidly decreased from beginning time as shown in **Fig. 6.7*c***, and product of PFCA(4~7) were identified in mass spectra and shown in **Fig. 6.7*c*** and ***d***. Maximum response to primary product as PFHpA(7)

appeared before 0.5 hour, while secondary product as PFHxA(6) appeared a little bit later, and PFBA(4) was further later, which is accordant with their generation sequences.

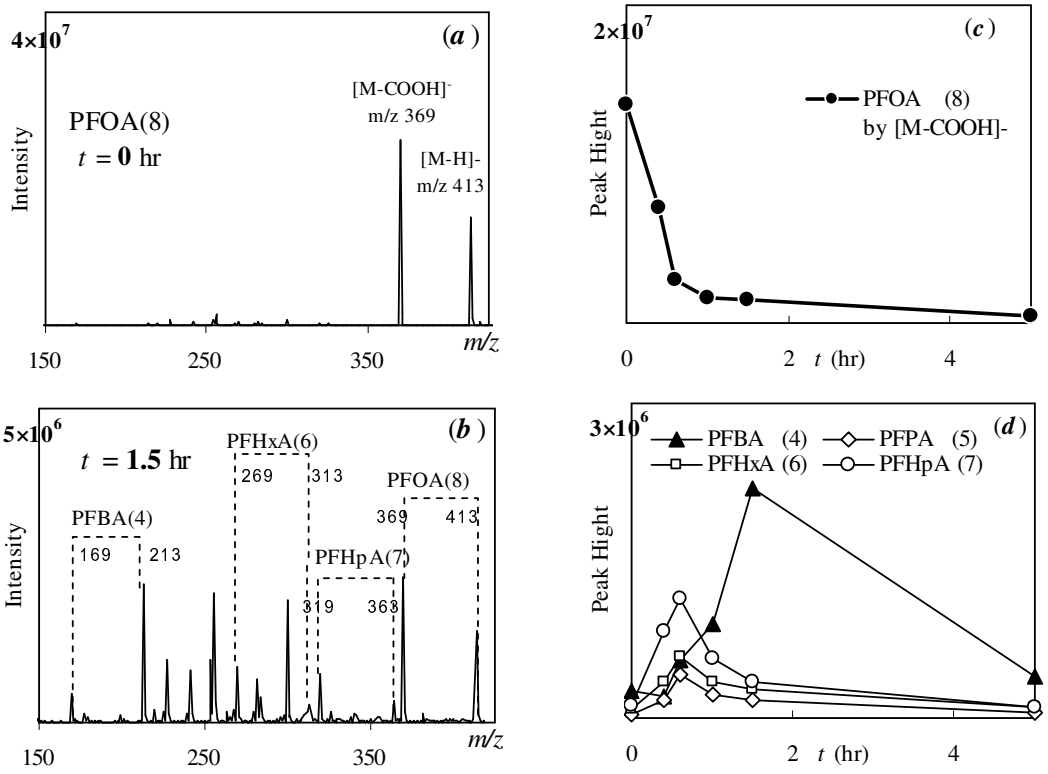

Figure 6.7 Mass spectra and intensity for PFOA(8) and photolysis products

Further analysis on their difference referred to carbon-chain length and initial concentration. With increase of carbon-chain length, PFCA were more difficult to be degradation, because excessive UV photon would be consumed by further degradation of products. This judgment was support by the half-life times of PFCA(8, 10, 16), which was increasing as 0.5, 1.5 and 2.5 hours respectively. Inflection time in the curve for PFCA product was independent on their precursor's initial concentration, and determined by kinetic parameters of generation and degradation. However the convex shape of PFCA curves was affected by initial concentration strongly, because of the linear relationship between derivations and concentration. Curves of PFCA product from PFDA(10) was not obviously convex, and far from products of PFCA(8,16), which could be explained by the lower initial concentration of PFDA(10) as 1 mg/L than latter cases of 100mg/L.

6.4.1.3 Photolysis of PFOS

Results of PFOS photolysis are shown in **Fig. 6.8** and results for PFHxS are shown in **Fig. 6.10**. Resistance of PFOS to UV irradiation was reported and inefficiency of photolysis on PFOS were concluded by other researcher (Hori, *et al.*, 2006). However, mass spectra in this study showed opposite results. Although PFOS in Runs UM4~5 was unchanged for a long time and only removed by very small amount in 12 hours as shown in **Fig. 6.8*ab***, new fractions at *m/z* 481, 463, 445 etc. appeared sequentially as shown in **Fig. 6.8*c***. Further reaction lasted to 60 hours, and PFOS seemed be completely removed at 48 hours, as shown in **Fig. 6.8*d***. The new fractions showed similar behavior with photolysis products for PFCAs. These findings implied that PFOS(8) could also be able to degrade by UV photolysis in some stepwise road other than PFCAs, and the process was much slower than photolysis of PFOA(8).

In order to identify products of PFOS(8) photolysis, MS/MS spectra of *m/z* 481 and 463 was acquired at 24 hours and analyzed because their relatively higher intensities. The collision energy was optimized as 40V to show close peak height in wide range. Because *m/z* of photolysis products offset in interval of 18, therefore this unknown process was named it as [M-*n*X], where *n* was the position from parent peak M at *m/z* 499. **Figure 6.9** showed MS/MS spectra of products at *m/z* 481 and 463, which were named by [M-X] and [M-2X]. A fraction with *m/z* 20 appeared by interval releasing from parent ion [M-*n*X], which was named by [M-*n*X-*m*Y].

Existence of *m/z* 80 and 99 proved that photolysis products contain $[SO_3]^-$, similar to PFOS whose primary daughter ions were $[SO_3]^-$ and $[FSO_3]^-$. Therefore, degradation occurred on the perfluorinated carbon chain, totally different with PFCAs which were degraded by breaking carboxylic group [COOH] from α carbon atom. There was one criteria for parent ion [M-*n*X] to release fraction Y, which is $n \leq m$ for [M-*n*X-*m*Y], or final to [M-*n*X-*n*Y]. For example, there was no further releasing after *m/z* 481→461, and *m/z* 463→443→423. This judgment implied that degradation process as [M-X] directly resulted in releasing fraction Y, or on the other words, X with *m/z* 18 should be strongly related with Y with *m/z* 20.

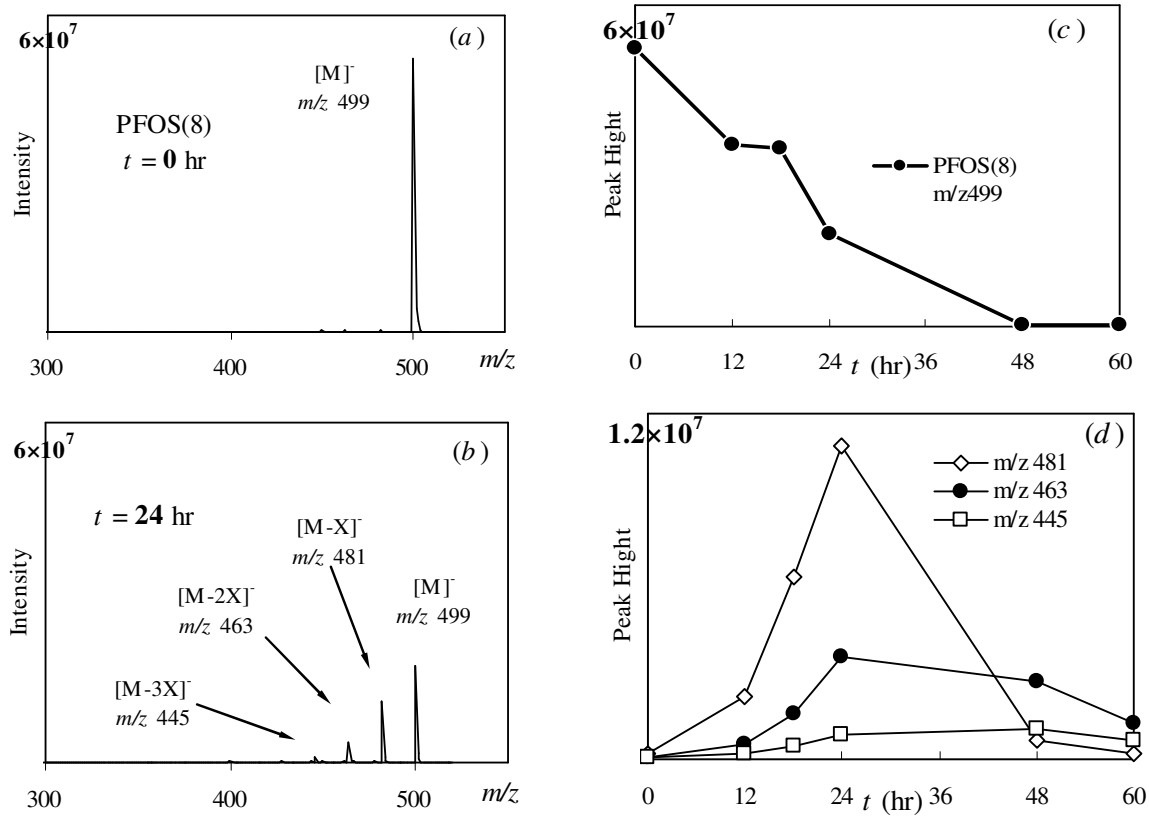

Figure 6.8 Mass spectra (*a~d*) and intensity (*e~f*) along with time in PFOS photolysis

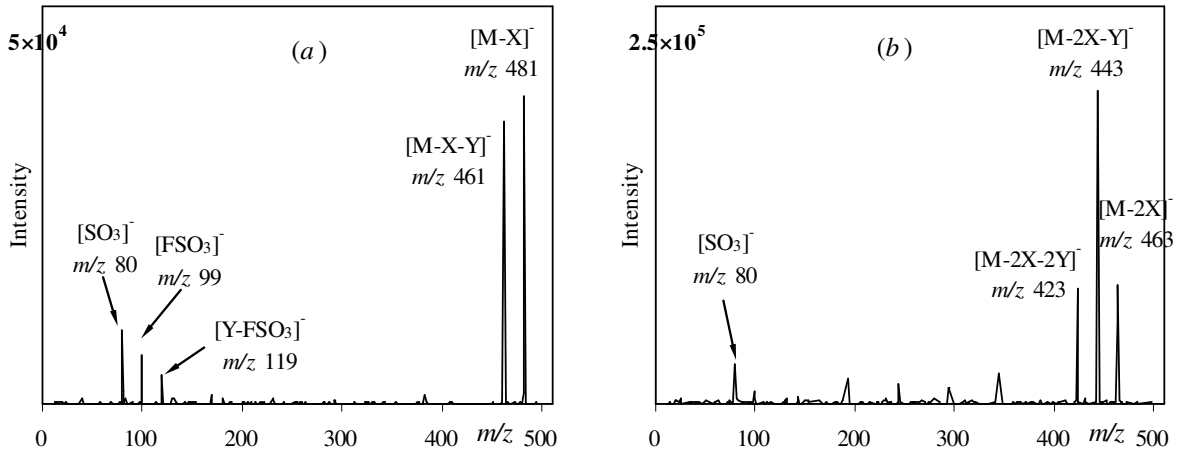

Figure 6.9 MS/MS spectra for PFOS photolysis product at *m/z* 481 and 463

One possible description was supposed that X represented substitution of F atom by H atom, and Y was faction [HF]. Considering product process of PFASs by substitution of C-H to C-F under current, and the stronger bond energy of C-F over C-H (3M Company, 1999), reverse substitution of C-F to C-H should be rather difficult and strict. The pathway still remained unknown because current system can not detect possible intermediates in the degradation.

6.4.1.4 Photolysis of PFHxS

Results of PFHxS(6) photolysis experiment are acquired and shown in **Fig. 6.10**, which are similar to PFOS. Peak at expected *m/z* 381 as product of PFHxS came out later than PFOS(8), also in weaker intensity shown in **Fig. 6.10*a***. MS/MS spectrum shown in **Fig. 6.10*b*** demonstrated similar behavior of product [M-X] which released fraction Y as [M-X-Y] and [SO_3] group. Further photolysis products were not detected.

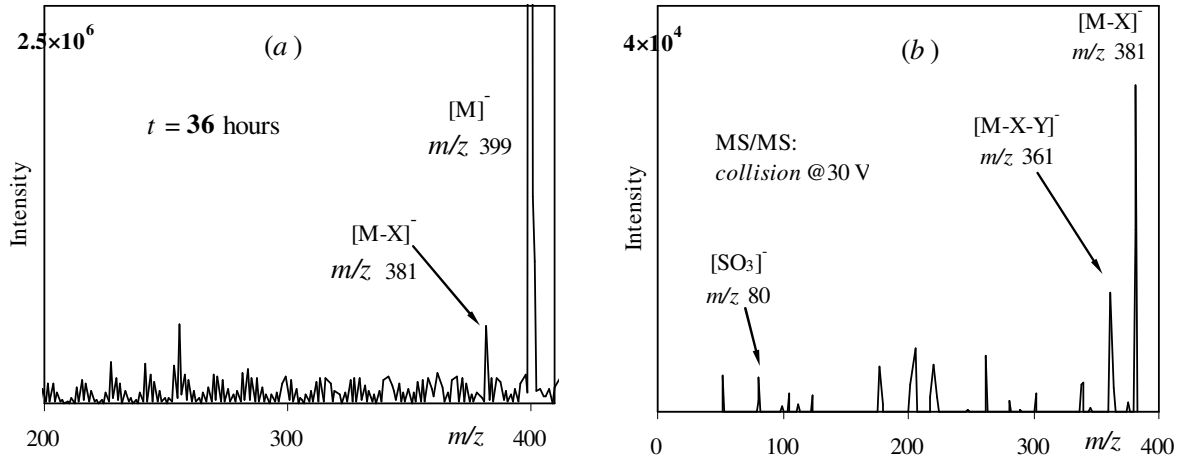

Figure 6.10 MS for PFHxS photolysis and MS/MS for product at *m/z* 381

Photolysis of both PFOS(8) and PFHxS(6) were very slow and ineffective, and their final products were still unknown because of limitation by detection method and experimental design. Furthermore, PFASs showed much stronger resistance than PFCAs in photolysis and much lower efficiency in same experimental conditions, which limited possible application of photolysis to decompose PFASs in wastewater treatment, although degradation was possible. Therefore, only PFCAs will be primarily

discussed in following kinetics study.

6.4.2 Photolysis kinetics for PFCAs

6.4.2.1 Kinetics of PFCAs photolysis in pure water

Figure 6.11 shows results of $UV_{254+185}$nm photolysis for PFOA(8), including original data and simulation. Concentrations of PFOA(8) were well fitted by first order kinetics as shown by **Eq. (6.1)**, and its coefficient k_{PFOA} could be easily determined to be 2.5 hr^{-1}. Half life time of PFOA degradation was calculated by $ln2/k$ to be 0.3 hr, which proved that PFOA degradation by photolysis was a fast process.

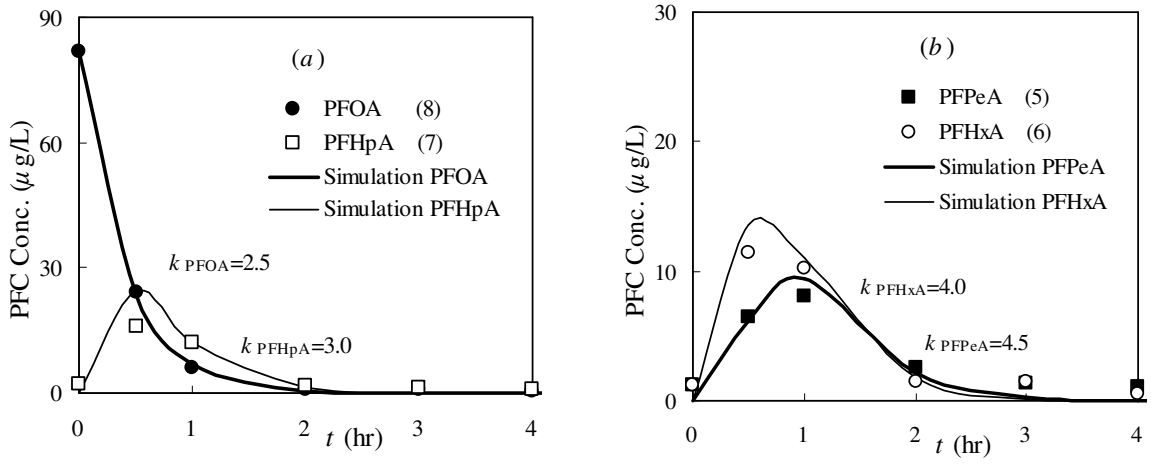

Figure 6.11 Kinetics of $UV_{254+185}$ photolysis for PFOA

Photolysis product was also simulated by **Eq. (6.2~6.4)**, as shown in **Fig. 6.11*a*** for PFHpA(7) and **Fig. 6.11*b*** for PFHxA(6) and PFPeA(5). Kinetics coefficients of these products are estimated as 3, 4 and 4.5 respectively, which were increased by decrease of carbon chain length of PFCA.

Results of photolysis on $UV_{254+185}$ for PFNA(9) and PFOA(10) are shown in **Fig. 6.12*a*** and **6.12*b*** respectively. Estimation of products was not reliable except the first reaction, because their concentrations were about 5 μg/L, lower than LOQ of LC-MS analysis. Therefore, only parent ion and product of first step degradation were shown in the figure, as well as estimated kinetic parameters.

Value of k for shorter-chained PFCA, or for product, was higher than longer-chained PFCA, or parent ion, which behaved the same with photolysis of PFOA(8) as shown in **Fig. 6.11**. However, kinetics parameter value of k was variant for same PFCAs in different experiments, for example, k_{PFOA} was 2.5 hr^{-1} as parent in **Fig 6.11*a*** but 3.5 hr^{-1} as product of PFNA(9) degradation in **Fig 6.12*a***. Variance of k value might be caused by lamps with power difference varied about ±10%, by LC-MS analysis with RSD about ±8% and by accumulation of error during estimation.

Considering the photolysis results of PFCA(8~10), which were predominant contaminants of PFCs in K-WWTP, direct $UV_{254+185}$ irradiation could be applied to degrade medium-chained PFCAs in short time with satisfaction. Photolysis followed first order kinetics and was successfully estimated by hypothesis of chain-reaction. Values of k for PFCAs were 2~6 hr^{-1} for PFCA(8~10) in pure water. Shorter-chained PFCAs showed faster removal than longer-chained PFCAs.

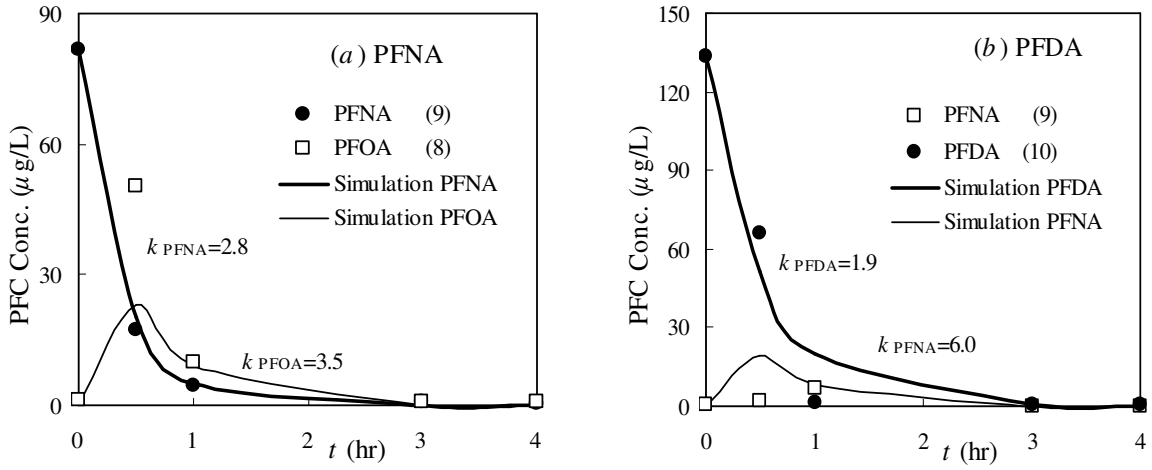

Figure 6.12 Kinetics of $UV_{254+185}$ photolysis for PFNA(*a*) and PFDA(*b*)

6.4.2.2 Influence by organic matrix

Impact of background organics on the removal of PFCs was studied by applying wastewater as matrix of photolysis experiments. UV spectra of wastewater matrix are shown in **Fig. 6.13*b***, by which absorbance of UV_{254} were quantified for experimental matrix as ASP effluent and BAC effluent in K-WWTP. SUVA values for ASP and BAC were 0.024 and 0.016 respectively. Higher UV_{254} absorbance of ASP effluent indicated that it contained more unsaturated organics like aromatics and double bonded alkenes than BAC effluent, because ozonation is introduced to process after ASP and before BAC filtration to be able to reduce DOC, UV_{254} as well as SUVA.

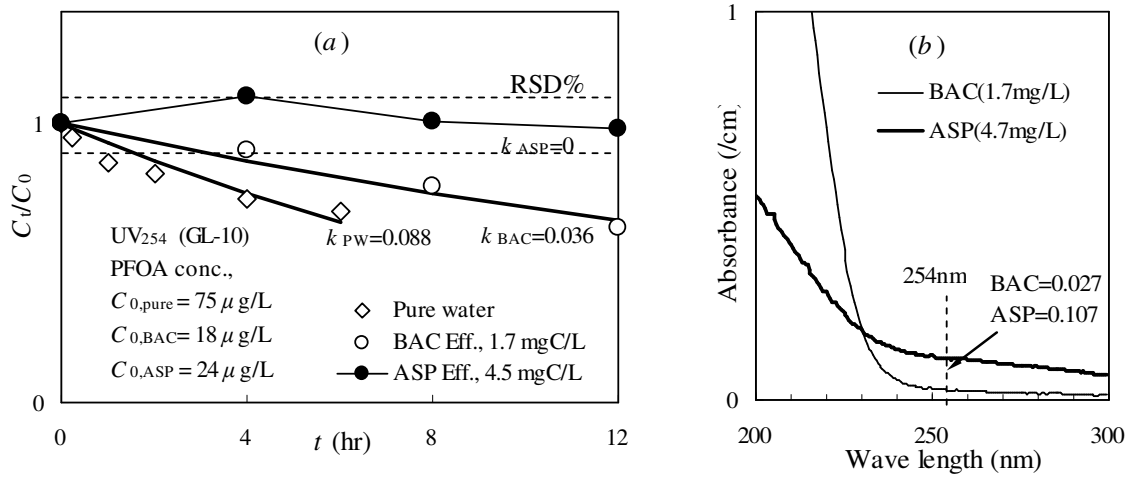

Figure 6.13 Effect of matrix on PFOA photolysis (*a*) and UV absorbance of matrix (*b*)

Figure 6.13*a* showed influence of matrix on the performance of UV photolysis to degrade PFOA. RSD was also shown in the figure to confirm the removal. Despite of results for matrix, degradation of PFOA in pure water without matrix was also plotted as the blank.

In matrix free sample, 32% of PFOA were removed in 6 hours, with initial concentration equal to 75μg/L. When coexisted with 1.7 mg/L organics in BAC effluent, time for this removal rate is delayed to 12 hours. In stronger matrix as ASP effluent with 4.5mg/L of DOC, there was no degradation detected for PFOA. In terms of kinetics, *k* was reduced from 0.088 to 0.036 by BAC effluent matrix and to zero by ASP effluent, which was roughly proportioned to the difference of SUVA as 0.024, 0.008 and zero L/mg/m

respectively. This influence could be explained by the weaker competitive ability of trace level PFOA with unsaturated background organics to absorb UV photons.

Therefore, photolysis of PFOA by UV irradiation was adversely affected by the increase of UV_{254} absorbance for background organic, or increase on proportion of unsaturated organics in matrix. If background absorbance was intensive enough, no degradation occurred because of the less competitive capability of trace level PFOA than unsaturated organics to absorb UV photons. The persistence of PFOA in environment could also be explained by this fact. UV irradiation from sunlight was relatively low and background absorbance in surface water is relative high, both of them caused no occurrence of photolysis of PFOA in natural environment.

6.4.2.3 Different behavior between PFOA and PFOS

Mass spectra analysis for PFOS(8) photolysis demonstrated slower speed and much lower efficiency than PFCAs. Results of Run UK-7/8 quantified these difference by expose PFOS(8) and PFOA(8) under $UV_{254+185}$ source with sand filtration effluent in K-WWTP as matrix, which are shown in **Fig. 6.14.** RSD is also shown in the figure to confirm the degradation.

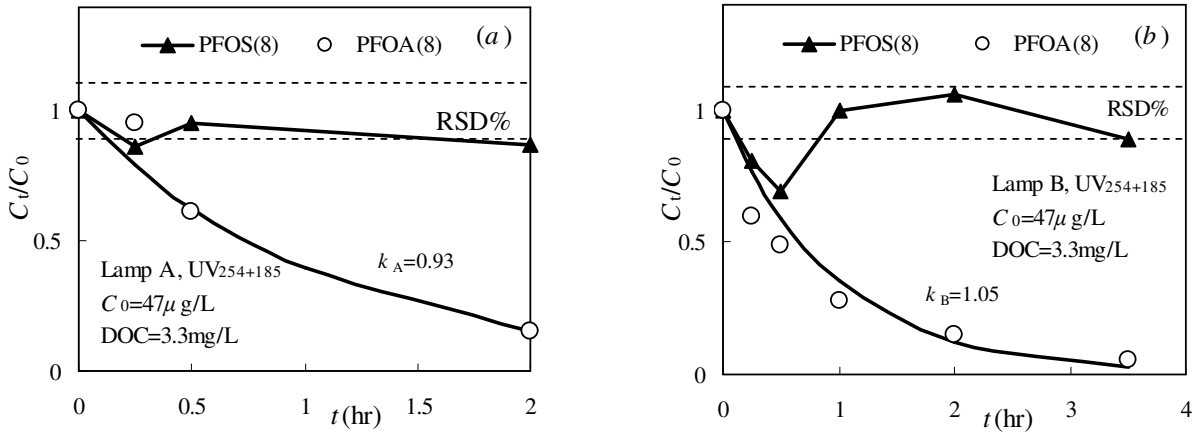

Figure 6.14 Photolysis of PFOS and PFOA under $UV_{254+185}$ in wastewater

Results of duplicated experiments by different lamp showed that PFOS(8) was not removed in wastewater matrix by $UV_{254+185}$ irradiation in sort time, because most data were located between limits of RSD, which meant variance should be attributed to analysis uncertainty firstly. This stability in short term was concordant to their mass spectra, in which degradation occurred obviously only after 12 hours by irradiation at $UV_{254+185}$.

Under same experimental conditions, photolysis showed satisfied removal efficiency on PFOA(8) in short time. By 2 hours of irradiation from both lamps, about 85% of PFOA(8) disappeared from system with initial concentration of 47μg/L. In terms of kinetics parameters, k_A was 0.93 lamp A and k_B was 1.05 for lamp B respectively. Variance between performances by different lamps A and B in same wavelength $UV_{254+185}$ was about 10%. Values of k in Run UK4~6 were much less than in UK7~8 although in similar matrix. The difference could be contributed to the less power of irradiation by GL-10 in UV_{254} than by ZKL-150 in $UV_{254+185}$, and less effective orientation to be upside than to be submerged. All these adverse influences resulted in unfavorable performance by upside irradiation from GL-10.

6.4.2.4 Photolysis of PFOA polluted river water

Photolysis by UV irradiation was applied to treat Ai river water, which was highly polluted by PFOA

from industrial discharge. **Figure 6.15*a*** shows residual rates of PFOA(8) under three different conditions, and kinetics simulation.

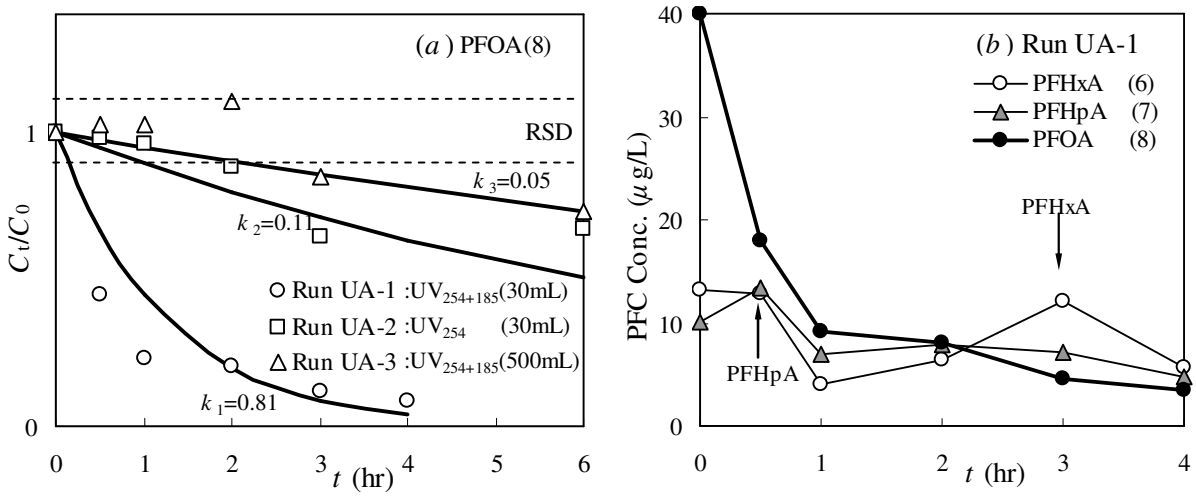

Figure 6.15 Degradation of PFOA in river water by UV photolysis

Performance of photolysis in Ai river water was strongly affected by UV source. Runs UA-1 and UA-2 were conducted in same conditions except UV irradiation type. Excessive irradiation at 185nm seemed important for degradation of PFOA in Ai river water, because value of kinetics parameter k for $UV_{254+185}$ was 0.81 and much higher than value for UV_{254}, which was only 0.11. This phenomenon can be explained by the more powerful irradiation at 185nm, which could generate ozone from dissolved oxygen in water and decompose most of natural organics to reduce background absorbance. Removal efficiency of PFOA was also decided by irradiation intensity. Value of k in Run UA-3 was only 0.05 and much less than Run UA-1, which should be caused by its large volume sample. Furthermore, Run UA-1 and UA-3 agreed with reverse proportions between k and sample volumes, which supported assumption in **Eq. (6.9)**. Briefly, photolysis at $UV_{254+185}$ was effectively to treat PFOA polluted river water, but UV_{254} was unsatisfied because of strong background absorbance.

Figure 6.15*b* showed behavior of photolysis products as PFHpA(7) and PFHxA(6). PFHpA(7) was accumulated at beginning time as results of rapid generation from PFOA(8), then decreased slowly by photolysis. PFHxA(6) was changed in opposite way of decreasing firstly by photolysis then increased by production from PFHpA(7). However, their variances were not clear and obvious because of their lower concentrations and possible interferences from precursors or intermediates in river water.

6.4.3 Ozone-related processes

6.4.3.1 Mass spectra analysis

Runs OM 1~9 were designed to check the mass spectrum of each PFC. **Figure 6.16** showed mass spectra of system blank and some single PFC after O_3/H_2O_2 treatment. System blank mass spectrum in **Fig. 6.16*f*** was obtained by inject 90% methanol/water solution into MS system. Three main peaks appeared at *m/z* 58, 255 and 285 as noise, which should be excluded in mass spectra of PFCs.

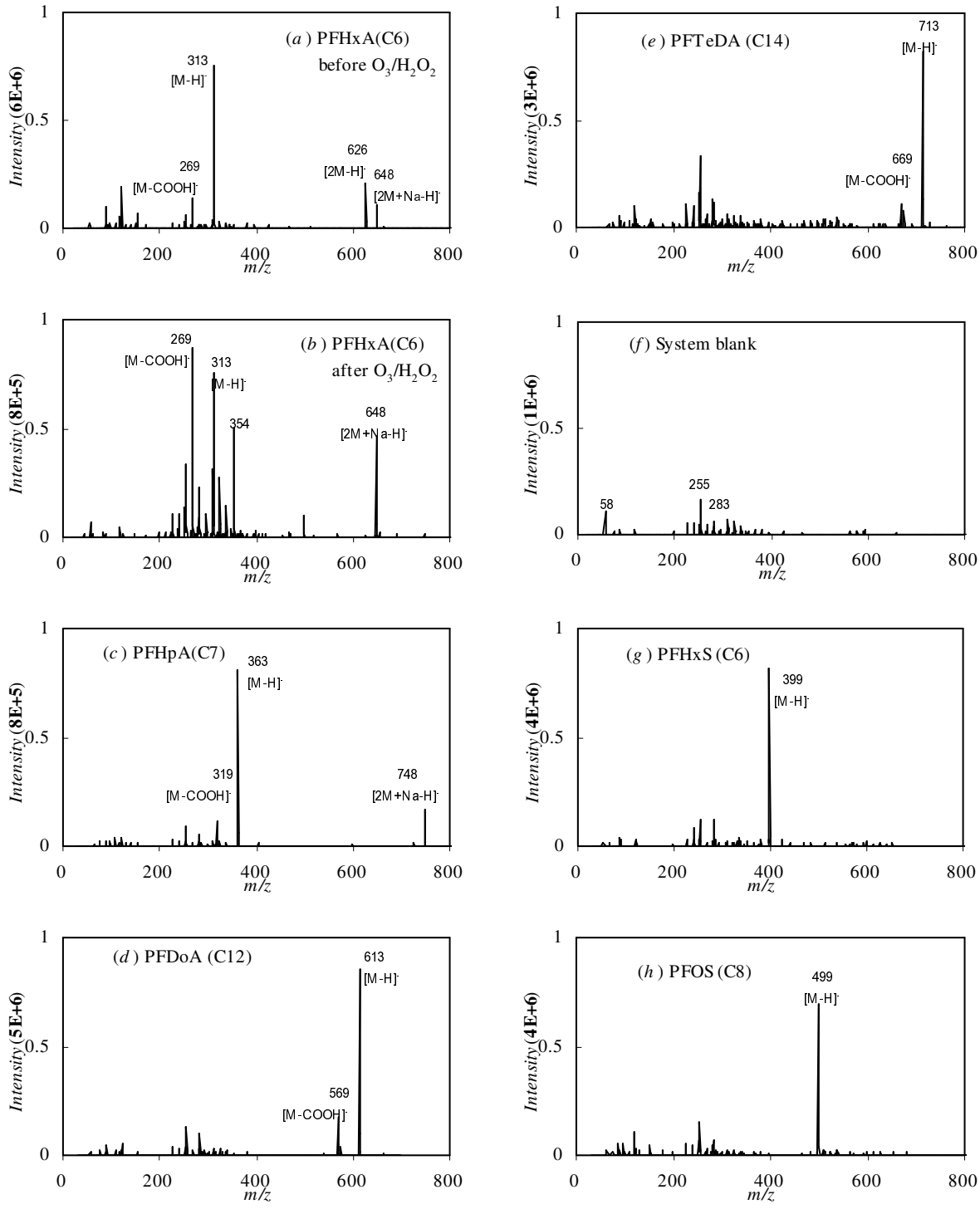

Figure 6.16 Mass spectra of single PFCs under O_3/H_2O_2 in Run OM1~9

Removal of PFHxA by O_3/H_2O_2 can be identified in **Fig. 6.16*a*** and ***b***, where the mass spectra before and after the treatment are shown together. For PFHxA, peaks at *m/z* 313 and 269 represent $[M-H]^-$ and $[M-COOH]^-$, and peaks at *m/z* 626 and 648 are $[2M-H]^-$ and $[2M+Na-H]^-$ respectively. Here $[M-H]^-$ means original molecule released one proton. Although smaller molecules are difficult to be qualified in **Fig. 6.16*a***, the intensity range is about 10 times less than **Fig. 6.16*b***, which might be caused by degradation. Mass spectra of other PFCs did not show possibility of degradations after O_3/H_2O_2 treatment, including PFCAs and PFASs, as shown in **Fig. 6.16*c~e*** and ***g~h***. Peaks around *m/z* 255 and 283 are

considered belonging to system blank. According to the analysis of mass spectra, there were no obvious peaks of degradation products, which implied that O_3/H_2O_2 is ineffective to degrade PFCs.

6.4.3.2 Batch experiments by O_3/H_2O_2

Runs OB 1~3 were designed to examine the performance of O_3/H_2O_2 on trace level of PFCs (about 2 μg/L) in mixture. **Figure 6.17** shows the influence of ozone concentration on the removals of PFCs. Ozone concentration in the figure was expressed in liquid phase which was calculated by concentration in gas flow shown by O_3 detector.

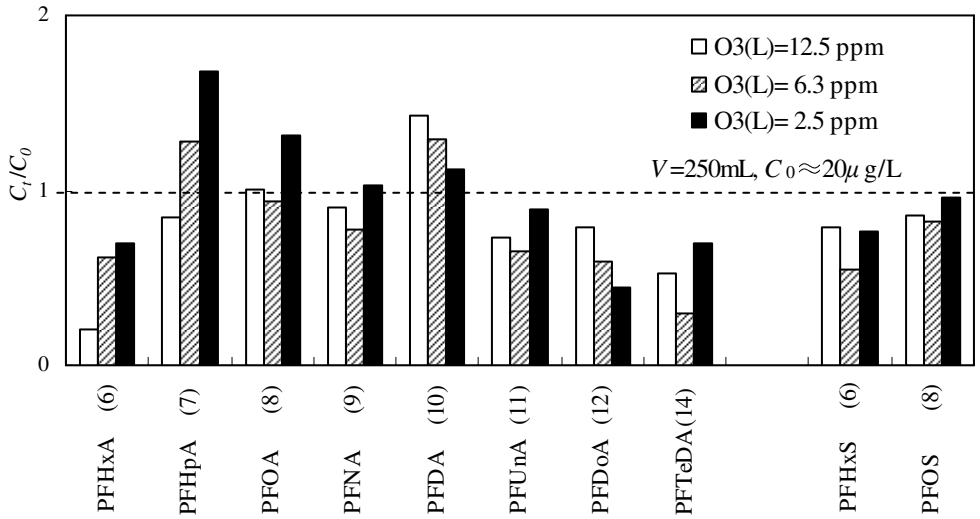

Figure 6.17 Influence of ozone concentrations on variance of PFCs by O_3/H_2O_2

PFHxA(6) and PFHpA(7) were the only PFCs obviously decreased in concentration by increasing of ozone amount. Other PFCs including PFCAs and PFASs did not shown reliable relationships with O_3 concentrations. Possible removal of shorter-chained PFCAs was supported by the mass spectra of PFHxA(6), which decreased greatly after treatment by O_3/H_2O_2 for half an hour, as shown in **Fig. 6.16*a*** and ***b***. Further evidence referred to the behavior of shorter-chained PFCs in K-WWTP, which was positively removed by ozonation unit as shown in **Table 4.6**. Therefore, O_3/H_2O_2 seemed ineffective to decompose PFCs, which confirmed the results in Runs OM.

6.4.3.3 Semi-batch experiments by O_3

Although PFCs were supposed stable on ozonation process, semi-batch experiments showed that most of PFCs were removed obviously, as two of them shown in **Fig. 6.18**. Typically as PFDA(10) and PFOS(8) in the figure, PFCs concentrations were decreased along with time, and roughly followed first order kinetics r. The data was firstly fitted by first order kinetics to obtain parameter k, and the concentration at the end of experiments was calculated by k, which would be adopted to calculate removal efficiency and average distribution.

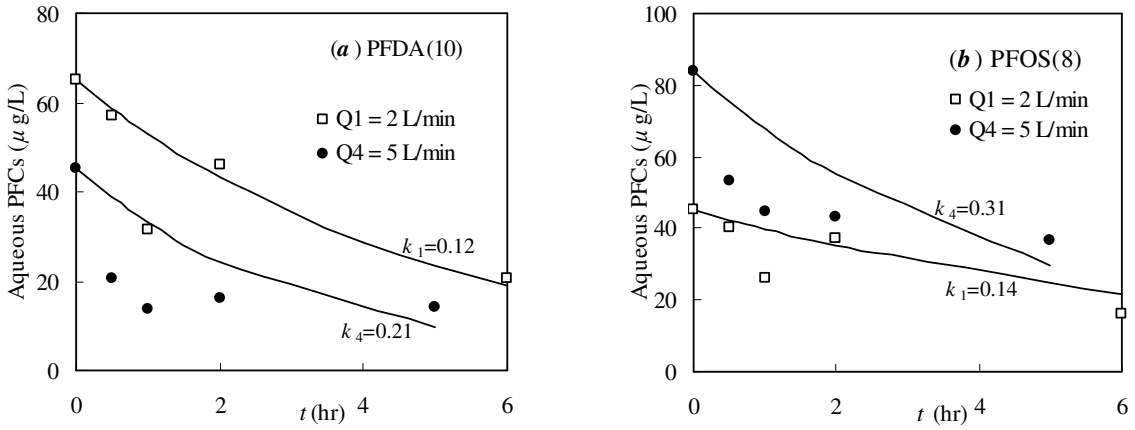

Figure 6.18 Examples of PFC concentrations in semi-batch ozone experiments

Kinetic parameter k for each PFC, which was independent on initial concentration of PFC and dependant on flow rate of ozone, was estimated and shown in **Figure 6.19**. Value of k followed the increase of carbon-chain length or water insolubility. This result implied that more hydrophobic PFCs are easier and faster to be blown out by flow of ozone gas.

Distribution of PFCs between aerosol and aqueous phase was also calculated for each Run by dividing lost of PFC from aqueous phase in reactor on residual PFC in reactor at the end of experiment. The average value for each PFC was shown in **Fig 6.19**. Distribution of PFC is independent on both of initial PFC concentration and ozone flow rates. Similar to the distribution of PFCs between particulate to aqueous phase in sludge sample as shown in **Fig. 3.9**, distribution value between aerosol and aqueous phase was also increased along with carbon-chain length for both PFCAs and PFASs.

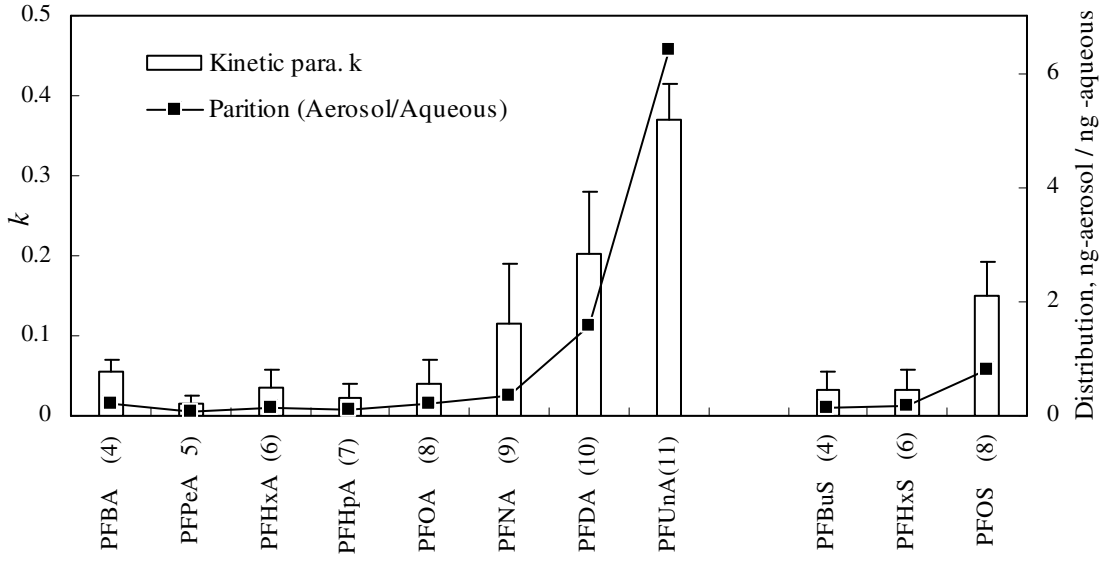

Figure 6.19 Estimation of kinetic parameter k and distribution for PFCs in ozone semi-batch experiments (n=4).

As strong surfactants, PFCs tended to accumulate at water/gas interface of small bubbles from aeration with high potentials. PFCs might be removed by attachments on aerosol particles and sequentially flow out of reactor with ozone gas. When the bubbles were broken on the water surface, PFCs on the interface could be sprayed into aerosol and flow together with droplets. This hypothesis was supported by blank

aeration experiment, in which 2L/min of air flow removed of 30% PFOS and 50% PFOA in initial concentrations of 32 and 20μg/L.

The trapped PFCs in 0℃ ice-water condenser were analyzed and used to calculate recovery rate from removed PFCs in reactor. Under ozone flow rate of 2~5 L/min, about 5~7% of ∑PFC were recovered in Run OS1, 2 and 4. However, 35% of removed ∑PFC from reactor were recovered by trap under flow rate of 0.5 L/min. The better efficiency could be attributed to the less escape of PFCs from condenser by slower gas flow.

Although PFCs were not degraded by ozone process, they can be removed by aeration according to their physical properties as surfactant. This mechanism was revealed in removal of PFOA by adsorptive bubbling separation method (Zhang, *et al.*, 2005a) and commercial available air-sparged hydrocyclone (ASH) (Schultz, *et al.*, 2003).

6.5 Summary

In this chapter, direct UV photolysis was developed to degrade PFCAs in wastewater and polluted river water. Stepwise degradation mechanism of PFCAs was confirmed by mass spectra analysis. *Consecutive* kinetics was proposed to explain UV photolysis experimental data. Background organics and sample volume affected kinetics very much. Ozone-related processes were also studied to identify the possibility to remove PFCs. Conclusions are summarized as following.

(1) Mass spectra analysis on UV photolysis of PFCA(8,10,16) confirmed stepwise degradation mechanism of PFCAs. UV photolysis can also degrade PFAS(6,8), however, the velocity was very low and final products can not be identified yet..

(2) Results of UV photolysis for PFCA(8,9,10) were successfully estimated by *consecutive* kinetics. Kinetic parameter for $UV_{254+185}$ irradiation on PFCA(8~10) was estimated as 2~6 hr^{-1} in pure water. Background absorbance can significantly reduce degradation of PFOA in wastewater, by which k was decreased from 2.5~3.5 hr^{-1} in pure water to 0.9~1 hr^{-1} in sand filtration effluent.

(3) PFOA(8) polluted river water can be cleaned by UV photolysis process. $UV_{254+185}$ showed satisfied performance to degrade more than 90% of 40 μg/L PFOA in 4 hours, with k value of 0.81 hr^{-1}. UV_{254} was ineffective to degrade PFOA because of strong background absorbance. UV wave length and sample volume showed significant influences on degradation kinetics.

(4) For ozone-related processes, mass spectra and batch experiments proved inefficiency of O_3/H_2O_2 to degrade PFCs. Semi-batch experiments showed obvious removal of PFCs in first order kinetics, which was attributed to air-floating effect by aeration.

CHAPTER VII CONCLUSIONS

7.1 Conclusions from This Study

Perfluorochemicals are persistent, bioaccumulated and toxic chemicals, and ubiquitously distributed in waster, air, human body and biota, including Japan. Current water and wastewater treatment processes seemed ineffective to remove PFCs in trace levels. This study tried to develop some proper technologies to treat trace level of PFCs in wastewater. The conclusions are drawn by chapters as follows.

In Chapter II, available literature was summarized on PFCs basic information, analytical methods, environmental behavior and engineering solutions. Basic information of PFCs was introduced in physiochemical properties, PBT properties, productions and applications, regulations and *etc*.. Analytical method for PFCs, especially LC-ESI-MS/MS, was reviewed including pretreatment processes in diverse matrices. Available control strategies were discussed in detail about alternatives, industrial recycling processes, and newly developed treatment processes.

Chapter III developed a complete procedure for PFCs analysis in wastewater. LC-MS/MS was applied to analyze PFCs. Pretreatment for aqueous sample was optimized between C_{18} and WAX SPE process, and pretreatment for particulate sample was optimized among IPE, AD-WAX and ASE-WAX processes. 9H-PFNA was applied as internal standard to estimate matrix effect. A complete and optimized procedure for PFCs analysis in wastewater was proposed and validated in this chapter. The achievement was concluded as follows.

(1) Quality of LC-MS/MS analysis was represented by RSD as 13%, LOD and LOQ as 3 and 16μg/L, which were about two times higher than LC-MS analysis. Process recoveries in wastewater varied in a wide range but averaged in recovery of 0.6~0.7 based on all available data.

(2) For aqueous samples, both C_{18} and WAX cartridge can be used for pretreatment with average recovery of 0.6. WAX-SPE performed well for short-chained PFCs, and C_{18}-SPE was better for long-chained PFCs. WAX-SPE process can control matrix effect, and was recommended to apply for strong matrix samples. Ionization suppression was increased with DOC concentration and saturated at 60%.

(3) For pretreatment of particulate samples, ASE-WAX process was recommended for its time saving and automatic operations. Condensed sludge in wet state seemed more suitable for extraction than in oven-dried state by ASE.

(4) For wastewater samples, a complete procedure was integrated from aqueous and particulate phases. PFCs distribution between two phases in sludge sample were calculated and applied as criteria to evaluate the quality of analytical data.

Chapter IV summarized periodical surveys in K-WWTP. Behavior of PFCs in WWTP process was classified into "*Medium*", "*Long*" and "*Short*" patterns according to their carbon chain lengths. PFCs showed similar behavior in same pattern, and different properties to other patterns. "*Medium*" PFC were considered primary contaminants in K-WWTP. Individual facilities and combined processes were estimated by their remove performances of PFCs. Conclusions of this chapter were shown as follows.

(1) K-WWTP influent contained 36 mgDOC/L and 160 mgSS/L in average, which were mainly

removed in primary clarifier and aeration tank.

(2) All PFCs were detected at each sampling site. About 50% of ∑PFC in aqueous phase was removed by overall processes. PFCA(8,9,14) had highest aqueous concentrations in influent as 95, 125 and 92 ng/L respectively. PFCA(8,9) and PFOS(8) occupied 50% of discharged ∑PFC, which should be seriously concerned.

(3) Behavior of PFCs in K-WWTP was classified into "*Medium*", "*Long*" and "*Short*" patterns according to their carbon chain lengths. "*Medium*" pattern consisted of PFCA(8~9) and PFOS(8). "*Long*" pattern included longer-chained PFCs as PFCA(10~12,14,16,18). "*Short*" pattern contained PFCA(4~7) and PFAS(4,6).

(4) "*Medium*" PFCs were poorly removed by current process. The average removal rate in aqueous phase was only 2% by overall processes. "*Long*" PFCs attached on particles strongly and were effectively removed by clarification. They occupied 49% in influent and but contributed only 13% to effluent. "*Short*" PFCs were less toxic and effectively removed by current processes.

(5) Clarifier was very important for removal of all PFCs in K-WWTP. Activated sludge process showed removal of "*Long*" PFCs but increased concentrations of "*Medium*" PFCs. Sand filtration, ozonation, BAC filter seemed unable to remove "*Medium*" and "*Long*" PFCs effectively.

(6) All of PFCs were accumulated in activated sludge for different extents and circulated with return sludge. Activated sludge process couple with clarifier can remove 40~70% of "*Medium*" PFCs, 95% of "*Long*" PFCs and 80% of "*Short*" PFCs.

Chapter V studied PFC behavior in GAC adsorption. Isotherms and kinetics were interpreted by Freundlich equation and HSDM respectively. Influences from coexisted NOMs, bulk pH and GAC properties were studied for isotherms and kinetics. Break through curves of PFCs in GAC fixed bed were preliminarily studied by RSSCT and SBA. Summaries are listed in detail as follows.

(1) Freundlich equation can interpret PFOA and PFOS isotherms in wide range of concentrations and complete HSDM can fit experimental data very well.

(2) In pure water, GAC-F400 adsorption showed increasing capacities for PFCs in ascendant carbon chain lengths. Kinetics study showed that diffusivity was decreased with descendant diameters of GAC and ascendant carbon chains, which implied that adsorption velocity was faster for long-chained PFCs and smaller size GAC.

(3) Coexisted NOM reduced GAC adsorption capacities by competition and carbon fouling. Competition showed slight effects on short and medium-chained PFCs, but obviously affected long-chained PFCs. Carbon fouling reduced adsorption capacities for all PFCs in much stronger extents than competition. Bulk pH did not affect on adsorption capacities greatly, but obviously influenced adsorption velocities.

(4) Four kinds of GAC were compared by their adsorption capacities to remove PFCs. Coal based GAC F400 showed moderate and average performance to remove all PFCs, which was considered the best among commercial GACs.

(5) RSSCT showed that PFCA(8,9) and PFOS(8) can be effectively removed from pure water and wastewater by fresh GAC filtration. SBA result showed that humic acid broke through the GAC column much earlier than PFCs.

Chapter VI developed direct photolysis process to decompose PFCAs completely. Stepwise degradation mechanism of PFCAs was confirmed by mass spectra analysis. *Consecutive* kinetics was proposed to explain UV photolysis experimental data. Background organics and sample volume affected kinetics very much. Ozone-related processes were also studied to identify the possibility to remove PFCs. Conclusions are summarized as following.

(1) Mass spectra analysis on UV photolysis of PFCA(8,10,16) confirmed stepwise degradation mechanism of PFCAs. UV photolysis can also degrade PFAS(6,8), however, the velocity was very low and final products can not be identified yet..

(2) Results of UV photolysis for PFCA(8,9,10) were successfully estimated by *consecutive* kinetics. Kinetic parameter for $UV_{254+185}$ irradiation on PFCA(8~10) was estimated as 2~6 hr^{-1} in pure water. Background absorbance can significantly reduce degradation of PFOA in wastewater, by which k was decreased from 2.5~3.5 hr^{-1} in pure water to 0.9~1 hr^{-1} in sand filtration effluent.

(3) PFOA(8) polluted river water can be cleaned by UV photolysis process. $UV_{254+185}$ showed satisfied performance to degrade more than 90% of 40 μg/L PFOA in 4 hours, with k value of 0.81 hr^{-1}. UV_{254} was ineffective to degrade PFOA because of strong background absorbance. UV wave length and sample volume showed significant influences on degradation kinetics.

(1) For ozone-related processes, mass spectra and batch experiments proved inefficiency of O_3/H_2O_2 to degrade PFCs. Semi-batch experiments showed obvious removal of PFCs in first order kinetics, which was attributed to air-floating effect by aeration.

7.2 Recommendations for Further Researches

For analytical methods, isotopically labeled internal standards were strongly recommended to improve analytical qualities and control data uncertainties. In WWTP surveys, PFC-related precursors should be identified and quantified. For GAC adsorption process, more lab column and pilot scale experiments were necessary to obtain practical parameters. For UV photolysis process, future of industrial application was not clear and thus more industry oriented studies were necessary.

REFERENCES

3M Chemolite (2005), Perfluorochemical release at the 3M-Cottage Grove facility -City of Cottage grove, Washington county, Minnesota, 89 pp, US Department of Health and Human Services, Atlanta, Georgia, US.

3M Company (1999), The science of organic fluorochemistry, 12 pp, USEPA docket: EPA-HQ-OPPT-2002-0043-0006.

Alzaga, R. and J. M. Bayona (2004). Determination of perfluorocarboxylic acids in aqueous matrices by ion-pair solid-phase microextraction-in-port derivatization-gas chromatography-negative ion chemical ionization mass spectrometry, *J. Chromatogr. A*, **1042** (1-2), 155-162.

Andersen, M. P. S., M. D. Hurley, T. J. Wallington, J. C. Ball, J. W. Martin, D. A. Ellis and S. A. Mabury (2003). Atmospheric chemistry of C2F5CHO: mechanism of the C2F5C(O)O-2+HO2 reaction, *Chemical Physics Letters*, **381** (1-2), 14-21.

Andersen, M. P. S., O. J. Nielsen, M. D. Hurley, J. C. Ball, T. J. Wallington, D. A. Ellis, J. W. Martin and S. A. Mabury (2005). Atmospheric chemistry of 4 : 2 fluorotelomer alcohol (n-C4F9CH2CH2OH): Products and mechanism of Cl atom initiated oxidation in the presence of NOx, *Journal of Physical Chemistry A*, **109** (9), 1849-1856.

Andersen, M. P. S., C. Stenby, O. J. Nielsen, M. D. Hurley, J. C. Ball, T. J. Wallington, J. W. Martin, D. A. Ellis and S. A. Mabury (2004). Atmospheric chemistry of n-CxF2x+1CHo (x=1,3,4): Mechanism of the CxF2x+1C(O)O-2+HO2 reaction, *Journal of Physical Chemistry A*, **108** (30), 6325-6330.

Armitage, J., I. T. Cousins, R. C. Buck, K. Prevedouros, M. H. Russell, M. MacLeod and S. H. Korzeniowski (2006). Modeling global-scale fate and transport of perfluorooctanoate emitted from direct sources, *Environ. Sci. Technol.*, **40** (22), 6969-6975.

Bader, H. and J. Hoigne (1981). Determination of ozone in waster by the Indigo method, *Water Research*, **15**, 499-456.

Badruzzaman, M., P. Westerhoff and D. R. U. Knappe (2004). Intraparticle diffusion and adsorption of arsenate onto granular ferric hydroxide (GFH), *Water Research*, **38** (18), 4002-4012.

Barkauskas, J. and F. S. Cannon (2003), Potentiometric titrations: Characterize functional groups and adsorbed species on activated carbon, paper presented at Carbon'2003 - An International Conference on Carbon, Oviedo, Spain, July 6 - 10.

Baup, S., C. Jaffre, D. Wolbert and A. Laplanche (2000). Adsorption of pesticides onto granular activated carbon: determination of surface diffusivities using simple batch experiments, *Adsorption*, **6**, 219-228.

Bec, R. L. (2006), Process for the recovery of fluorosurfactants by active charcoal, U. S. Patent: No.6991732, Assign to: Arkema, Application No.10/875146.

Berends, A. G., J. C. Boutonnet, C. G. d. Rooij and R. S. Thompson (1999). Toxicity of trifluoroacetate to aquatic organisms, *Environ. Toxicol. Chem.*, **18** (5), 1053-1059.

Berger, U. and M. Haukas (2005). Validation of a screening method based on liquid chromatography coupled to high-resolution mass spectrometry for analysis of perfluoroalkylated substances in biota, *J. Chromatogr. A*, **1081** (2), 210-217.

Berger, U., I. Langlois, M. Oehme and R. Kallenborn (2004). Comparison of three types of mass spectrometer for high-performance liquid chromatography/mass spectrometry analysis of perfluoroalkylated substances and fluorotelomer alcohols, *European Journal of Mass Spectrometry*, **10** (5), 579-588.

Bjelopavlic, M., G. Newcombe and R. Hayes (1999). Adsorption of NOM onto Activated Carbon: Effect of Surface Charge, Ionic Strength, and Pore Volume Distribution, *Journal of Colloid and Interface Science*, **210** (2), 271-280.

Boehm, H. P. (2002). Surface oxides on carbon and their analysis: a critical assessment, *Carbon*, **40** (2), 145-149.

Bossi, R., F. F. Riget and R. Dietz (2005). Temporal and Spatial Trends of Perfluorinated Compounds in Ringed Seal (*Phoca hispida*) from Greenland, *Environ. Sci. Technol.*, **39** (19), 7416-7422.

Boudreau, T. M., C. J. Wilson, W. J. Cheong, P. K. Sibley, S. A. Mabury, D. C. G. Muir and K. R. Solomon (2003). Response of the zooplankton community and environmental fate of perfluorooctane sulfonic acid in aquatic microcosms, *Environ. Toxicol. Chem.*, **22** (11), 2739-2745.

Boulanger, B., J. Vargo, J. L. Schnoor and K. C. Hornbuckle (2004). Detection of perfluorooctane surfactants in Great Lakes water, *Environ. Sci. Technol.*, **38** (15), 4064-4070.

Boulanger, B., J. D. Vargo, J. L. Schnoor and K. C. Hornbuckle (2005). Evaluation of perfluorooctane surfactants in a wastewater treatment system and in a commercial surface protection product, *Environ. Sci. Technol.*, **39** (15), 5524-5530.

Brooke, D., A. Footitt and T. A. Nwaogu (2004), Environmental risk evaluation report: perfluorooctanesulphonate (PFOS), 1-104 pp, Environment Agency, UK, Wallingford, UK.

Budarin, V. L., J. H. Clark, S. J. Tavener and K. Wilson (2004). Chemical reactions of double bonds in activated carbon: microwave and bromination methods, *Chem. Commun.*, **23**, 2736-2737.

Burkard, G., K. Hintzer and G. Lohr (2004), Method for recovering fluorinated emulsifiers from aqueous phases, U. S. Patent: No.6706193, Assign to: 3M Innovative Properties Company, Application No.10/009757.

Burke, G. M., D. E. Wurster, M. J. Berg, P. Veng-Pedersen and D. D. Schottelius (1992). Surface characterization of activated charcoal by x-ray photoelectron spectroscopy (XPS): correlation with phenobarbital adsorption data, *Pharm. Res*, **9**, 126.

Butt, C. M., D. C. G. Muir, I. Stirling, M. Kwan and S. A. Mabury (2007). Rapid response of Arctic Ringed Seals to changes in perfluoroalkyl production, *Environ. Sci. Technol.*, **41** (1), 42-49.

Cahill, T. M., C. M. Thomas, S. E. Schwarzbach and J. N. Seiber (2001). Accumulation of Trifluoroacetate in Seasonal Wetlands in California, *Environ. Sci. Technol.*, **35** (5), 820-825.

Calafat, A. M., Z. Kuklenyik, S. P. Caudill, J. A. Reidy and L. L. Needham (2006). Perfluorochemicals in Pooled Serum Samples from United States Residents in 2001 and 2002, *Environ. Sci. Technol.*, **40** (7), 2128-2134.

Canada, H. (2004), Perfluorooctane sulfonate, its salts and its precursors that contain the C8F17SO2 or C8F17SO3 moiety, 28 pp.

Carta, G. and R. K. Lewus (2000). Film model approximation for multicomponent adsorption, *Adsorption*, **6**, 5-13.

Chen, J., P. Zhang and L. Zhang (2006). Photocatalytic decomposition of environmentally persistent perfluorooctanoic acid, *Chemistry Letters*, **35** (2), 230-231.

Chen, J. P., S. Wu and K.-H. Chong (2003). Surface modification of a granular activated carbon by citric acid for enhancement of copper adsorption, *Carbon*, **41** (10), 1979-1986.

Claude R. Mallet, Z. L. J. R. M. (2004). A study of ion suppression effects in electrospray ionization from mobile phase additives and solid-phase extracts, *Rapid Commun. Mass Spectrom.*, **18** (1), 49-58.

Cooney, D. O. (1998), *Adsorption design for wastewater treatment*, CRC Press LLC, Boca Raton, Florida.

Corporate Remediation Group of DuPont and URS Diamond (2003), DuPont telomer manufacturing sites: environmental assessment of PFOA levels in air and water, 70 pp, USEPA docket: EPA-HQ-OPPT-2003-0012-0217.

Crittenden, J. C., S. Sanongraj, J. L. Bulloch, D. W. Hand, T. N. Rogers, T. F. Speth and M. Ulmer (1999). Correlation of aqueous-phase adsorption isotherms, *Environ. Sci. Technol.*, **33**, 2926-2933.

Dai, J., M. Li, Y. Jin, N. Saito, M. Xu and F. Wei (2006). Perfluorooctanesulfonate and perfluorooctanoate in Red Panda and Giant Panda from China, *Environ. Sci. Technol.*, **40** (18), 5647-5652.

de Silva, A. O. and S. A. Mabury (2004). Isolating isomers of perfluorocarboxylates in polar bears (Ursus maritimus) from two geographical locations, *Environ. Sci. Technol.*, **38** (24), 6538-6545.

de Silva, A. O. and S. A. Mabury (2006). Isomer distribution of perfluorocarboxylates in human blood:

Potential correlation to source, *Environ. Sci. Technol.*, **40** (9), 2903-2909.

de Voogt, P. and W. Saez (2006). Analytical chemistry of perfluoroalkylated substances, *Trac-Trends in Analytical Chemistry*, **25** (4), 326-342.

Dillert, R., D. Bahnemann and H. Hidaka (2007). Light-induced degradation of perfluorocarboxylic acids in the presence of titanium dioxide, *Chemosphere*, **67** (4), 785-792.

Dimitrov, S., V. Kamenska, J. D. Walker, W. Windle, R. Purdy, M. Lewis and O. Mekenyan (2004). Predicting the biodegradation products of perfluorinated chemicals using CATABOL, *SAR QSAR Environ. Res.*, **15** (1), 69-82.

Dinglasan, M. J. A., Y. Ye, E. A. Edwards and S. A. Mabury (2004). Fluorotelomer alcohol biodegradation yields poly- and perfluorinated acids, *Environ. Sci. Technol.*, **38** (10), 2857-2864.

Dionex (2004), Accelerated Solvent Extraction (ASE) of Hydrocarbon Contaminants (BTEX, Diesel, and TPH) in Soils, 324 pp.

Dutta, M., N. N. Dutta and K. G. Bhattacharya (1999). Aqueous phase adsorption of certain beta-lactam antibiotics onto polymeric resins and activated carbon, *Separation and Purification Technology*, **16** (3), 213-224.

Ellis, D. A., K. A. Denkenberger, T. E. Burrow and S. A. Mabury (2004a). The use of F-19 NMR to interpret the structural properties of perfluorocarboxylate acids: A possible correlation with their environmental disposition, *Journal of Physical Chemistry A*, **108** (46), 10099-10106.

Ellis, D. A., S. A. Mabury, J. W. Martin and D. C. G. Muir (2001). Thermolysis of fluoropolymers as a potential source of halogenated organic acids in the environment *Nature*, **412**, 321-324.

Ellis, D. A., J. W. Martin, A. O. De Silva, S. A. Mabury, M. D. Hurley, M. P. S. Andersen and T. J. Wallington (2004b). Degradation of fluorotelomer alcohols: A likely atmospheric source of perfluorinated carboxylic acids, *Environ. Sci. Technol.*, **38** (12), 3316-3321.

Ellis, D. A., J. W. Martin, S. A. Mabury, M. D. Hurley, M. P. S. Andersen and T. J. Wallington (2003). Atmospheric lifetime of fluorotelomer alcohols, *Environ. Sci. Technol.*, **37** (17), 3816-3820.

EPA, U. (2000), *Denifition and procedure for the determination of the method detection limit (revision 1.11)*, US EPA.

Felix, B., T. Zipplies, S. Fuhrer, T. Kaiser and A. Budesheim (2003), Process for the recovery of fluorinated alkandic acids from wastewater, U. S. Patent: No.6518442, Assign to: Dyneon GmbH and Axiva GmbH, Application No.09/700639.

Ferrero, S. and E. Deregibus (2006), Elimination process of fluorinated anionic surfactants, U. S. Patent: No.7011696, Assign to: Solvay Solexis SpA, Application No.10/620418.

Field, J. A., S. Simonich and D. Barofsky (2005). Comment on "Detection of perfluorooctane surfactants in Great Lakes water" and "Mass budget of perfluorooctane surfactants in Lake Ontario", *Environ. Sci. Technol.*, **39** (10), 3883-3884.

Fluoride Action Network Pesticide Project (2005), TIMELINE for PFOS and PFOS perfluorinated chemicals, http://www.fluorideaction.org/pesticides/effect.pfos.class.timeline.htm.

Footitt, A., T. A. Nwaogu and D. Brooke (2004), Perfluorooctane sulphonate: risk reduction strategy and analysis of advantages and drawbacks, 266 pp, RPA in association with BRE Environment, Norfolk, UK.

Fritsche, U. and S. H. Hüttenhain (1994). A method for analysis of fluorotensides, *Chemosphere*, **29** (9-11), 1797-1802.

Fuda, K., T. Matsunaga, T. Kamiya and K. Omori (2004), Method of treating fluorine compound, U. S. Patent: No.6743957, Assign to: JEMCO, Inc, Application No.10/070756.

Furdui, V. I., N. L. Stock, D. A. Ellis, C. M. Butt, D. M. Whittle, P. W. Crozier, E. J. Reiner, D. C. G. Muir and S. A. Mabury (2007). Spatial distribution of perfluoroalkyl contaminants in lake trout from the Great Lakes, *Environ. Sci. Technol.*, **41** (5), 1554.

Gaspard, S., S. Altenor, N. Passe-Coutrin, A. Ouensanga and F. Brouers (2006). Parameters from a new kinetic equation to evaluate activated carbons efficiency for water treatment, *Water Research*, **40** (18),

3467-3477.

Gauden, P. A., A. P. Terzyk, M. S. Cwiertnia, G. Rychlicki, G. Newcombe and P. Kowalczyk (2007). Benzene adsorption on carbonaceous materials: The influence of pore structure on the state of the adsorbate, *Applied Surface Science*, **In Press, Corrected Proof**.

Giesy, J. P. and K. Kannan (2001). Global Distribution of Perfluorooctane Sulfonate in Wildlife, *Environ. Sci. Technol.*, **35** (7), 1339-1342.

Gottschalk, C., J. A. Libra and A. Saupe (2000), *Ozonation of Water and Waste Water - A practical guide to understanding ozone and its application*, Wiley-VCH, Weinheim, Germany

Gulkowska, A., Q. Jiang, M. K. So, S. Taniyasu, P. K. S. Lam and N. Yamashita (2006). Persistent perfluorinated acids in seafood collected from two cities of China, *Environ. Sci. Technol.*, **40** (12), 3736-3741.

Han, X., T. A. Snow, R. A. Kemper and G. W. Jepson (2003). Binding of perfluorooctanoic acid to ratandhumanplasma proteins, *Chem. Res. Toxicol.*, **16**, 775-781.

Hand, D. W., J. C. Crittenden, D. R. Hokanson and J. L. Bulloch (1997). Predicting the performance of fixed-bed granular activated carbon adsorbers, *Water Science and Technology*, **35** (7), 235-241.

Hansen, K. J., L. A. Clemen, M. E. Ellefson and H. O. Johnson (2001). Compound-Specific, Quantitative Characterization of Organic Fluorochemicals in Biological Matrices, *Environ. Sci. Technol.*, **35** (4), 766-770.

Hansen, K. J., H. O. Johnson, J. S. Eldridge, J. L. Butenhoff and L. A. Dick (2002). Quantitative characterization of trace levels of PFOS and PFOA in the Tennessee River, *Environ. Sci. Technol.*, **36** (8), 1681-1685.

Hanson, M. L., P. K. Sibley, R. A. Brain, S. A. Mabury and K. R. Solomon (2005a). Microcosm evaluation of the toxicity and risk to aquatic macrophytes from perfluorooctane sulfonic acid, *Arch. Environ. Contam. Toxicol.*, **48** (3), 329-337.

Hanson, M. L., J. Small, P. K. Sibley, T. M. Boudreau, R. A. Brain, S. A. Mabury and K. R. Solomon (2005b). Microcosm evaluation of the fate, toxicity, and risk to aquatic macrophytes from perfluorooctanoic acid (PFOA), *Arch. Environ. Contam. Toxicol.*, **49** (3), 307-316.

Harada, K., K. Inoue, A. Morikawa, T. Yoshinaga, N. Saito and A. Koizumi (2005). Renal clearance of perfluorooctane sulfonate and perfluorooctanoate in humans and their species-specific excretion, *Environ. Res.*, **99** (2), 253-261.

Harada, K., N. Saito, K. Inoue, T. Yoshinaga, T. Watanabe, S. Sasaki, S. Kamiyama and A. Koizumi (2004). The influence of time, sex and geographic factors on levels of perfluorooctane sulfonate and perfluorooctanoate in human serum over the last 25 years, *J. Occup. Health*, **46** (2), 141-147.

Hatfield, T. L. (2001a), Hydrolysis reactions of perfluorooctanoic acid (PFOA), 3M Environmental Laboratory, USEPA docket: EPA-HQ-OPPT-2002-0051-0013.

Hatfield, T. L. (2001b), Screening studies on the aqueous photolytic degradation of perfluorooctanoic acid (PFOA), 3M Environmental Laboratory, USEPA docket: EPA-HQ-OPPT-2002-0051-0023.

Hebert, G. N., M. A. Odom, S. C. Bowman and S. H. Strauss (2004). Attenuated total reflectance ftir detection and quantification of low concentrations of aqueous polyatomic anions, *Anal. Chem.*, **76** (3), 781-787.

Hekster, F., J. Pijnenburg, R. W. P. M. Laane and P. d. Voogt (2002), Perfluoroalkylated substances: Aquatic environmental assessment, ministry of transport, public works and water management, 99 pp, Report RIKZ 2002.043, Hague, Netherlands.

Higgins, C. P., J. A. Field, C. S. Criddle and R. G. Luthy (2005). Quantitative Determination of Perfluorochemicals in Sediments and Domestic Sludge, *Environ. Sci. Technol.*, **39** (11), 3946-3956.

Hintzer, K., E. Obermaier and W. Schwertfeger (2006), Removal of fluorinated surfactants from waste water, U. S. Patent: No.7018541, Assign to: 3M Innovative Properties Company, Application No.11/034188.

Ho, L. S. W. (2004), The removal of cyanobacterial metabolites from drinking water using ozone and

granular activated carbon, 266 pp, University of South Australia.

Hoff, P. T., K. Van Campenhout, K. de Vijver, A. Covaci, L. Bervoets, L. Moens, G. Huyskens, G. Goemans, C. Belpaire, R. Blust and W. De Coen (2005). Perfluorooctane sulfonic acid and organohalogen pollutants in liver of three freshwater fish species in Flanders (Belgium): relationships with biochemical and organismal effects, *Environ. Pollut.*, **137** (2), 324-333.

Holm, A., S. R. Wilson, P. Molander, E. Lundanes and T. Greibrokk (2004). Determination of perfluorooctane sulfonate and perfluorooctanoic acid in human plasma by large volume injection capillary column switching liquid chromatography coupled to electrospray ionization mass spectrometry, *J. Sep. Sci.*, **27** (13), 1071-1079.

Holmström, K. E., U. Järnberg and A. Bignert (2005). Temporal Trends of PFOS and PFOA in Guillemot Eggs from the Baltic Sea, 1968-2003, *Environ. Sci. Technol.*, **39** (1), 80-84.

Hori, H., E. Hayakawa, H. Einaga, S. Kutsuna, K. Koike, T. Ibusuki, H. Kiatagawa and R. Arakawa (2004a). Decomposition of environmentally persistent perfluorooctanoic acid in water by photochemical approaches, *Environ. Sci. Technol.*, **38** (22), 6118-6124.

Hori, H., E. Hayakawa, K. Koike, H. Einaga and T. Ibusuki (2004b). Decomposition of nonafluoropentanoic acid by heteropolyacid photocatalyst H3PW12O40 in aqueous solution, *Journal of Molecular Catalysis a-Chemical*, **211** (1-2), 35-41.

Hori, H., E. Hayakawa, N. Yamashita, S. Taniyasu, F. Nakata and Y. Kobayashi (2004c). High-performance liquid chromatography with conductimetric detection of perfluorocarboxylic acids and perfluorosulfonates, *Chemosphere*, **57** (4), 273-282.

Hori, H., Y. Nagaoka, A. Yamamoto, T. Sano, N. Yamashita, S. Taniyasu, S. Kutsuna, I. Osaka and R. Arakawa (2006). Efficient decomposition of environmentally persistent perfluorooctanesulfonate and related fluorochemicals using zerovalent iron in subcritical water, *Environ. Sci. Technol.*, **40** (3), 1049-1054.

Hori, H., Y. Takano, K. Koike, S. Kutsuna, H. Einaga and T. Ibusuki (2003). Photochemical decomposition of pentafluoropropionic acid to fluoride ions with a water-soluble heteropolyacid photocatalyst, *Applied Catalysis B-Environmental*, **46** (2), 333-340.

Hori, H., A. Yamamoto, E. Hayakawa, S. Taniyasu, N. Yamashita and S. Kutsuna (2005a). Efficient decomposition of environmentally persistent perfluorocarboxylic acids by use of persulfate as a photochemical oxidant, *Environ. Sci. Technol.*, **39** (7), 2383-2388.

Hori, H., A. Yamamoto and S. Kutsuna (2005b). Efficient photochemical decomposition of long-chain perfluorocarboxylic acids by means of an aqueous/liquid CO2 biphasic system, *Environ. Sci. Technol.*, **39** (19), 7692-7697.

Houde, M., T. A. D. Bujas, J. Small, R. S. Wells, P. A. Fair, G. D. Bossart, K. R. Solomon and D. C. G. Muir (2006a). Biomagnification of perfluoroalkyl compounds in the Bottlenose Dolphin (*Tursiops truncatus*) food web, *Environ. Sci. Technol.*, **40** (13), 4138-4144.

Houde, M., J. W. Martin, R. J. Letcher, K. R. Solomon and D. C. G. Muir (2006b). Biological Monitoring of Polyfluoroalkyl Substances: A Review, *Environ. Sci. Technol.*, **40** (11), 3463-3473.

Houde, M., R. S. Wells, P. A. Fair, G. D. Bossart, A. A. Hohn, T. K. Rowles, J. C. Sweeney, K. R. Solomon and D. C. G. Muir (2005). Polyfluoroalkyl compounds in free-ranging bottlenose dolphins (Tursiops truncatus) from the Gulf of Mexico and the Atlantic Ocean, *Environ. Sci. Technol.*, **39** (17), 6591-6598.

Hui, C. W., B. Chen and G. McKay (2003). Pore-surface diffusion model for batch adsorption processes, *Langmuir*, **19** (10), 4188-4196.

Hurley, M. D., M. P. S. Andersen, T. J. Wallington, D. A. Ellis, J. W. Martin and S. A. Mabury (2004a). Atmospheric chemistry of perfluorinated carboxylic acids: Reaction with OH radicals and atmospheric lifetimes, *Journal of Physical Chemistry A*, **108** (4), 615-620.

Hurley, M. D., J. C. Ball, T. J. Wallington, M. P. S. Andersen, D. A. Ellis, J. W. Martin and S. A. Mabury (2004b). Atmospheric chemistry of 4 : 2 fluorotelomer alcohol (CF3(CF2)(3)CH2CH2OH): Products and mechanism of Cl atom initiated oxidation, *Journal of Physical Chemistry A*, **108** (26), 5635-5642.

Hurley, M. D., T. J. Wallington, M. P. S. Andersen, D. A. Ellis, J. W. Martin and S. A. Mabury (2004c).

Atmospheric chemistry of fluorinated alcohols: Reaction with Cl atoms and OH radicals and atmospheric lifetimes, *Journal of Physical Chemistry A*, **108** (11), 1973-1979.

Ingrid Langlois, M. O. (2006). Structural identification of isomers present in technical perfluorooctane sulfonate by tandem mass spectrometry, *Rapid Commun. Mass Spectrom.*, **20** (5), 844-850.

Inoue, K., F. Okada, R. Ito, S. Kato, S. Sasaki, S. Nakajima, A. Uno, Y. Saijo, F. Sata, Y. Yoshimura, R. Kishi and H. Nakazawa (2004a). Perfluorooctane sulfonate (PFOS) and related perfluorinated compounds in human maternal and cord blood samples: Assessment of PFOS exposure in a susceptible population during pregnancy, *Environ. Health Perspect.*, **112** (11), 1204-1207.

Inoue, K., F. Okada, R. Ito, M. Kawaguchi, N. Okanouchi and H. Nakazawa (2004b). Determination of perfluorooctane sulfonate, perfluorooctanoate and perfluorooctane sulfonylamide in human plasma by column-switching liquid chromatography-electrospray mass spectrometry coupled with solid-phase extraction, *J. Chromatogr. B*, **810** (1), 49-56.

IUPAC (1972). Manual of symbols and terminology, Appendix 2, part 1: colloid and surface chemistry, *Pure Applied Chemistry* **31**, 578

JACM, J. A. o. C. M. (1984), *Foundation and application of activated carbon*.

Jahnke, A., L. Ahrens, R. Ebinghaus and C. Temme (2006). Urban versus Remote Air Concentrations of Fluorotelomer Alcohols and Other Polyfluorinated Alkyl Substances in Germany, *Environ. Sci. Technol.*

Jarvie, M. E., D. W. Hand, S. Bhuvendralingam, J. C. Crittenden and D. R. Hokanson (2005). Simulating the performance of fixed-bed granular activated carbon adsorbers: Removal of synthetic organic chemicals in the presence of background organic matter, *Water Research*, **39** (11), 2407-2421.

Jones, C. W. and T.-W. Fu (2004), Fluorinated carboxylic acid recovery and reuse, U. S. Patent: No.6720437, Assign to: E. I. du Pont de Nemours and Company, Application No.10/060995.

Jones, P. D., W. Hu, W. de Coen, J. L. Newsted and J. P. Giesy (2003). Binding of perfluorinated fatty acids to serum proteins, *Environ. Toxicol. Chem.*, **22**, 2639-2649.

Kannan, K., S. Corsolini, J. Falandysz, G. Fillmann, K. S. Kumar, B. G. Loganathan, M. A. Mohd, J. Olivero, N. Van Wouwe, J. H. Yang and K. M. Aldous (2004). Perfluorooctanesulfonate and related fluorochemicals in human blood from several countries, *Environ. Sci. Technol.*, **38** (17), 4489-4495.

Kannan, K., S. Corsolini, J. Falandysz, G. Oehme, S. Focardi and J. P. Giesy (2002). Perfluorooctanesulfonate and related fluorinated hydrocarbons in marine mammals, fishes, and birds from coasts of the Baltic and the Mediterranean Seas, *Environ. Sci. Technol.*, **36** (15), 3210-3216.

Kannan, K., L. Tao, E. Sinclair, S. D. Pastva, D. J. Jude and J. P. Giesy (2005). Perfluorinated compounds in aquatic organisms at various trophic levels in a Great Lakes food chain, *Arch. Environ. Contam. Toxicol.*, **48** (4), 559-566.

Kärrman, A., B. v. Bavel, L. Hardell, G. Lindström and U. Järnberg (2004), Perfluoroalkylated compounds in whole blood and plasma from the Swedish population, 16 pp, Department of Natural Sciences, MTM Research Centre, Örebro, Sweden.

Kärrman, A., J. F. Mueller, B. vanBavel, F. Harden, L. M. L. Toms and G. Lindstrom (2006). Levels of 12 Perfluorinated Chemicals in Pooled Australian Serum, Collected 2002-2003, in Relation to Age, Gender, and Region, *Environ. Sci. Technol.*, **40** (12), 3742-3748.

Kärrman, A., B. van Bavel, U. Jarnberg, L. Hardell and G. Lindstrom (2005). Development of a solid-phase extraction-HPLC/single quadrupole MS method for quantification of perfluorochemicals in whole blood, *Analytical Chemistry*, **77** (3), 864-870.

Kimura, K. (2007), Adsorption characteristics of perfluorooctane sulfonate and perfluorooctane acid onto activated carbons, Undergraduate Thesis thesis, 43 pp, Kyoto University, Kyoto, Japan.

Komiyama, H. and J. M. Smith (1974). Surface diffusion in liquid-filled pores, *AIChE Journal*, **20** (6), 1110-1117.

Krusic, P. J., A. A. Marchione and D. C. Roe (2005). Gas-phase NMR studies of the thermolysis of perfluorooctanoic acid, *J. Fluor. Chem.*, **126** (11-12), 1510-1516.

Kudo, N. and Y. Kawashima (2003). Toxicity and toxicokinetics of perfluorooctanoic acid in humans and animals, *Journal of Toxicological Sciences*, **2**, 49-57.

Kuehl, D. W. and B. Rozynov (2003). Chromatographic and mass spectral studies of perfluorooctanesulfonate and three perfluorooctanesulfonamides, *Rapid Commun. Mass Spectrom.*, **17** (20), 2364-2369.

Kuhls, J. (1981), Recovery of fluorinated emulsifying acids from basic anion exchangers, U. S. Patent: No.4282162, Assign to: Hoechst Aktiengesellschaft, Application No.06/115803.

Kuklenyik, Z., J. A. Reich, J. S. Tully, L. L. Needham and A. M. Calafat (2004). Automated solid-phase extraction and measurement of perfluorinated organic acids and amides in human serum and milk, *Environ. Sci. Technol.*, **38** (13), 3698-3704.

Kumar, K. V., K. Subanandam, V. Ramamurthi and S. Sivanesan (2004), Solid liquid adsorpton for wastewater treatment: principle design and operation, Department of Chemical Engineering, Anna University, India, online published, http://www.eco-web.com/editorial/040201.html.

Lampert, D. J., M. A. Frisch and G. E. Speitel (2007). Removal of perfluorooctanoic acid and perfluorooctane sulfonate from wastewater by ion exchange, *Practice periodical of hazardous, toxic, and radioactive waste management*, **60**, 60-68.

Lange, F. T., C. Schmidt and H. J. Brauch (2006), Perfluoroalkylcarboxylates and -sulfonates: emerging contaminants for drinking water supplies?, 31 pp, Association of River Waterworks (RIWA), Netherlands.

László, K., E. Tombácz and k. Josepovits (2003). Surface characterization of a polyacrylonitrile based activated carbon and the effect of pH on its adsorption from aqueous phenol and 2,3,4-trichlorophenol solution, *Periodica Polytechnica Ser. Chem. Eng.*, **47** (2), 105-116.

Lau, C., J. L. Butenhoff and J. M. Rogers (2004). The developmental toxicity of perfluoroalkyl acids and their derivatives, *Toxicol. Appl. Pharmacol.*, **198** (2), 231-241.

Lau, C., J. R. Thibodeaux, R. G. Hanson, J. M. Rogers, B. E. Grey, M. E. Stanton, J. L. Butenhoff and L. A. Stevenson (2003). Exposure to perfluorooctane sulfonate during pregnancy in rat and mouse. II: Postnatal evaluation, *Toxicol. Sci.*, **74** (2), 382-392.

Levine, A. D., E. L. Libelo, G. Bugna, T. Shelley, H. Mayfield and T. B. Stauffer (1997). Biogeochemical assessment of natural attenuation of JP-4-contaminated ground water in the presence of fluorinated surfactants, *Sci. Total Environ.*, **208** (3), 179-195.

Li, Q., V. L. Snoeyink, B. J. Mariaas and C. Campos (2003). Elucidating competitive adsorption mechanisms of atrazine and NOM using model compounds, *Water Research*, **37** (4), 773-784.

Lien, N. P. H., S. Fujii, S. Tanaka, M. Nozoe, W. Wirojanagud, A. Anton and G. Lindström (2006). Perfluorinated substances in tap water of Japan and several countries and their relationship to surface water contamination, *Environmental Engineering Research*, **43**, 611-618.

Loewen, M., T. Halldorson, F. Wang and G. Tomy (2005). Fluorotelomer Carboxylic Acids and PFOS in Rainwater from an Urban Center in Canada, *Environ. Sci. Technol.*, **39** (9), 2944-2951.

Maestri, L., S. Negri, M. Ferrari, S. Ghittori, F. Fabris, P. Danesino and M. Imbriani (2006). Determination of perfluorooctanoic acid and perfluorooctanesulfonate in human tissues by liquid chromatography/single quadrupole mass spectrometry, *Rapid Commun. Mass Spectrom.*, **20** (18), 2728-2734.

Marta, V., A. Maria López de and B. Damià (2006). Environmental analysis of fluorinated alkyl substances by liquid chromatography–(tandem) mass spectrometry: a review, *Analytical and Bioanalytical Chemistry*, **386** (4), 953-972.

Martin, J. W., D. A. Ellis, S. A. Mabury, M. D. Hurley and T. J. Wallington (2006). Atmospheric chemistry of perfluoroalkanesulfonamides: Kinetic and product studies of the OH radical and Cl atom initiated oxidation of N-ethyl perfluorobutanesulfonamide, *Environ. Sci. Technol.*, **40** (3), 864-872.

Martin, J. W., J. Franklin, M. L. Hanson, K. R. Solomon, S. A. Mabury, D. A. Ellis, B. F. Scott and D. C. G. Muir (2000). Detection of chlorodifluoroacetic acid in precipitation: A possible product of fluorocarbon degradation, *Environ. Sci. Technol.*, **34** (2), 274-281.

Martin, J. W., S. A. Mabury, K. Kannan, U. Berger, P. D. Voogt, J. Field, J. Franklin, J. P. Giesy, T. Harner, D. C. G. Muir, B. Scott, M. Kaiser, U. Jarnberg, K. C. Jones, H. Schroeder, M. Simcik, C. Sottani, B. V. Bavel, A. Karrman, G. Lindström and S. V. Leeuwen (2004a). Analytical challenges hamper perfluoroalkyl research, *Environ. Sci. Technol. A-Pages*, **38** (13), 248-255.

Martin, J. W., S. A. Mabury, K. R. Solomon and D. C. G. Muir (2003a). Bioconcentration and tissue distribution of perfluorinated acids in rainbow trout (*oncorhynchus mykiss*), *Environ. Toxicol. Chem.*, **22** (1), 196-204.

Martin, J. W., S. A. Mabury, K. R. Solomon and D. C. G. Muir (2003b). Dietary accumulation of perfluorinated acids in juvenile rainbow trout (*oncorhynchus mykiss*), *Environ. Toxicol. Chem.*, **22** (1), 189-195.

Martin, J. W., D. C. G. Muir, C. A. Moody, D. A. Ellis, W. C. Kwan, K. R. Solomon and S. A. Mabury (2002). Collection of airborne fluorinated organics and analysis by gas chromatography/chemical ionization mass spectrometry, *Anal. Chem.*, **74** (3), 584-590.

Martin, J. W., M. M. Smithwick, B. M. Braune, P. F. Hoekstra, D. C. G. Muir and S. A. Mabury (2004b). Identification of Long-Chain Perfluorinated Acids in Biota from the Canadian Arctic, *Environ. Sci. Technol.*, **38** (2), 373-380.

Matuszewski, B. K., M. L. Constanzer and C. M. Chavez-Eng (1998). Matrix Effect in Quantitative LC/MS/MS Analyses of Biological Fluids: A Method for Determination of Finasteride in Human Plasma at Picogram Per Milliliter Concentrations, *Anal. Chem.*, **70** (5), 882-889.

Matuszewski, B. K., M. L. Constanzer and C. M. Chavez-Eng (2003). Strategies for the Assessment of Matrix Effect in Quantitative Bioanalytical Methods Based on HPLC-MS/MS, *Anal. Chem.*, **75** (13), 3019-3030.

Menendez, J. A., M. J. Illan-Gomez, C. A. L. Leon and L. R. Radovic (1995). On the difference between the isoelectric point and the point of zero charge of carbons, *Carbon*, **33** (11), 1655-1657.

Minnesota Department of Health (2007), Environmental Health Information - Perfluorochemicals and Health, Minnesota, US.

Mohan, D., K. P. Singh, S. Sinha and D. Gosh (2004). Removal of pyridine from aqueous solution using low cost activated carbons derived from agricultural waste materials, *Carbon*, **42** (12-13), 2409-2421.

Mohanty, K., D. Das and M. Biswas (2006). Preparation and characterization of activated carbons from Sterculiaalata nutshell by chemical activation with zinc chloride to remove phenol from wastewater, *Adsorption*, **12** (2), 119-132.

Moody, C. A. and J. A. Field (2000). Perfluorinated surfactants and the environmental implications of their use in fire-fighting foams, *Environ. Sci. Technol.*, **34** (18), 3864-3870.

Moody, C. A., W. C. Kwan, J. W. Martin, D. C. Muir and S. A. Mabury (2001). Determination of perfluorinated surfactants in surface water samples by two independent analytical techniques: liquid chromatography/tandem mass spectrometry and ^{19}F NMR, *Anal. Chem.* , **73** (2200).

Moody, C. A., J. W. Martin, W. C. Kwan, D. C. G. Muir and S. A. Mabury (2002). Monitoring perfluorinated surfactants in biota and surface water samples following an accidental release of fire-fighting foam into etobicoke creek, *Environ. Sci. Technol.*, **36** (4), 545-551.

Moreno-Castilla, C., M. A. Ferro-Garcia, J. P. Joly, I. Bautista-Toledo, F. Carrasco-Marin and J. Rivera-Utrilla (1995). Activated carbon surface modifications by nitric acid, hydrogen peroxide, and ammonium peroxydisulfate treatments, *Langmuir*, **11** (11), 4386-4392.

Morikawa, A., N. Kamei, K. Harada, K. Inoue, T. Yoshinaga, N. Saito and A. Koizumi (2006). The bioconcentration factor of perfluorooctane sulfonate is significantly larger than that of perfluorooctanoate in wild turtles (Trachemys scripta elegans and Chinemys reevesii): An Ai river ecological study in Japan, *Ecotox. Environ. Safe.*, **65** (1), 14-21.

Moriwaki, H., Y. Takagi, M. Tanaka, K. Tsuruho, K. Okitsu and Y. Maeda (2005). Sonochemical Decomposition of Perfluorooctane Sulfonate and Perfluorooctanoic Acid, *Environ. Sci. Technol.*, **39** (9), 3388-3392.

Moriwaki, H., Y. Takata and R. Arakawa (2003). Concentrations of perfluorooctane sulfonate (PFOS) and

perfluorooctanoic acid (PFOA) in vacuum cleaner dust collected in Japanese homes, *J. Environ. Monit.*, **5** (5), 753-757.

Newcombe, G., M. Drikas and R. Hayes (1997). Influence of characterised natural organic material on activated carbon adsorption: II. Effect on pore volume distribution and adsorption of 2-methylisoborneol, *Water Research*, **31** (5), 1065-1073.

Newcombe, G., R. Hayes and M. Drikas (1993). Granular activated carbon: Importance of surface properties in the adsorption of naturally occurring organics, *Colloids and Surfaces A: Physicochemical and Engineering Aspects*, **78**, 65-71.

Nicholas, P. C. and N. C. Paul (1993), *Carbon adsorption for pollution control*, PTR Prentice Hall, Englewood Cliffs, NJ

North California Division of Water Quality (2006), Recommended interim maximum allowable concentration for perfluorooctanoic acid, North California, US.

Nozoe, M. (2006), Study on analysis methods of PFOS and PFOA in sewage water and their behavior in a wastewater treatment plant, 47 pp, Kyoto University, Kyoto, Japan.

Nozoe, M., S. Fujii, S. Tanaka, H. Tanaka and N. Yamashita (2006). Investigation of PFOS and PFOA in a wastewater treatment plant, *Environmental Engineering Research*, **43**, 105-111.

Obermeier, R. and G. Stefaniak (1995), Process for the recovery of fluorinated carboxylic acids, U. S. Patent: No.5442097, Assign to: Hoechst Aktiengesellschaft, Application No.08/251752.

OECD (2002), Co-operation on existing chemicals hazard assessment of perfluorooctane sulfonate (PFOS) and its salts, 362 pp, ENV/JM/RD(2002)17/FINAL.

OECD (2005), Results of survey on production and use of PFOS, PFAS and PFOA, related substances and products/ mixtures containing these substances, 59 pp, ENV/JM/MONO(2005)1, Paris, France.

Ohya, T., N. Kudo, E. Suzuki and Y. Kawashima (1998). Determination of perfluorinated carboxylic acids in biological samples by high-performance liquid chromatography, *J. Chromatogr. B*, **720** (1-2), 1-7.

Oliaei, F., D. Kriens and K. Kessler (2006), Inverstigation of perlfuorochemical(PFC) contaminant in Minnesota: Phase one, Report to Senate Environment Committee, 79 pp, Minnesota Pollution Control Agency (MPCA), Minnesota, USA.

Olsen, G. W., T. R. Church, J. P. Miller, J. M. Burris, K. J. Hansen, J. K. Lundberg, J. B. Armitage, R. M. Herron, Z. Medhdizadehkashi, J. B. Nobiletti, E. M. O'Neill, J. H. Mandel and L. R. Zobel (2003). Perfluorooctanesulfonate and other fluorochemicals in the serum of American Red Cross adult blood donors, *Environ. Health Perspect.*, **111** (16), 1892-1901.

Poulsen, P. B., A. A. Jensen and E. Wallström (2005), More environmentally friendly alternatives to PFOS-compounds and PFOA, 162 pp, Danish Environmental Protection Agency, Denmark.

Powley, C. R., S. W. George, T. W. Ryan and R. C. Buck (2005a). Matrix effect-free analytical methods for determination of perfluorinated carboxylic acids in environmental matrixes, *Analytical Chemistry*, **77** (19), 6353-6358.

Powley, C. R., M. J. Michalczyk, M. A. Kaiser and L. W. Buxton (2005b). Determination of perfluorooctanoic acid (PFOA) extractable from the surface of commercial cookware under simulated cooking conditions by LC/MS/MS, *Analyst*, **130** (9), 1299-1302.

Prevedouros, K., I. T. Cousins, R. C. Buck and S. H. Korzeniowski (2006). Sources, Fate and Transport of Perfluorocarboxylates, *Environ. Sci. Technol.*, **40** (1), 32-44.

Renner, R. (2001). Growing concern over perfluorinated chemicals, *Environ. Sci. Technol. A-Pages*, **35** (7), 154-160.

Renner, R. (2006a). 3-D modeling substantiates perfluorinated theory, *Environ. Sci. Technol. A-Pages*, **40** (3), 632-633.

Renner, R. (2006b). It's in the microwave popcorn, not the Teflon pan, *Environ. Sci. Technol. A-Pages*, **40** (1), 4.

Renner, R. (2006c). The long and the short of perfluorinated replacements, *Environ. Sci. Technol. A-Pages*, **40** (1), 12-13.

Risha, K., J. Flaherty, R. Wille, W. Buck, F. Morandi and T. Isemura (2005). Method for trace level analysis of C8, C9, C10, C11, and C13 perfluorocarbon carboxylic acids in water, *Analytical Chemistry*, **77** (5), 1503-1508.

Roy, D., G.-t. Wang and D. D. Adrian (1993). A simplified solution technique for carbon adsorption model, *Water Research*, **27** (6), 1033-1040.

Rudolph, W. and J. Massonne (1977), Process for the purification and separation of perhaloalkanoic acids from mixtures thereof with perhaloalkanes, U. S. Patent: No.4005137, Assign to: Kali-Chemie Aktiengesellschaft, Application No.05/548818.

Saito, N., K. Harada, K. Inoue, K. Sasaki, T. Yoshinaga and A. Koizumi (2004). Perfluorooctanoate and perfluorooctane sulfonate concentrations in surface water in Japan, *J. Occup. Health*, **46** (1), 49-59.

Saito, N., K. Sasaki, K. Nakatome, K. Harada, T. Yoshinaga and A. Koizumi (2003). Perfluorooctane sulfonate concentrations in surface water in Japan, *Arch. Environ. Contam. Toxicol.*, **45** (2), 149-158.

Sanderson, H., T. M. Boudreau, S. A. Mabury and K. R. Solomon (2003). Impact of perfluorooctanoic acid on the structure of the zooplankton community in indoor microcosms, *Aquat. Toxicol.*, **62** (3), 227-234.

Sanderson, H., T. M. Boudreau, S. A. Mabury and K. R. Solomon (2004). Effects of perfluorooctane sulfonate and perfluorooctanoic acid on the zooplanktonic community, *Ecotox. Environ. Safe.*, **58** (1), 68-76.

Sasaki, K., K. Harada, N. Saito, T. Tsutsui, S. Nakanishi, H. Tsuzuki and A. Koizumi (2003). Impact of Airborne Perfluorooctane Sulfonate on the Human Body Burden and the Ecological System, *Bulletin of Environmental Contamination and Toxicology*, **71** (2), 0408-0413.

Schaefer, A. (2006), Perfluorinated surfactants contaminate German waters, *Environ. Sci. Technol. Online News*, November 1.

Schröder, H. F. (2003). Determination of fluorinated surfactants and their metabolites in sewage sludge samples by liquid chromatography with mass spectrometry and tandem mass spectrometry after pressurised liquid extraction and separation on fluorine-modified reversed-phase sorbents, *J. Chromatogr. A*, **1020** (1), 131-151.

Schröder, H. F. and R. J. W. Meesters (2005). Stability of fluorinated surfactants in advanced oxidation processes - A follow up of degradation products using flow injection-mass spectrometry, liquid chromatography-mass spectrometry and liquid chromatography-multiple stage mass spectrometry, *J. Chromatogr. A*, **1082** (1), 110-119.

Schultz, J. A. (2001), Fluorinated alkanoic acid purification process, U. S. Patent: No.6281374, Assign to: EI duPont de Nemours and Company, Application No.09/644165.

Schultz, M. M., D. F. Barofsky and J. A. Field (2003). Fluorinated alkyl surfactants, *Environ. Eng. Sci.*, **20** (5), 487-501.

Schultz, M. M., D. F. Barofsky and J. A. Field (2004). Quantitative determination of fluorotelomer sulfonates in groundwater by LC MS/MS, *Environ. Sci. Technol.*, **38** (6), 1828-1835.

Schultz, M. M., D. F. Barofsky and J. A. Field (2006a). Quantitative determination of fluorinated alkyl substances by large-volume-injection liquid chromatography tandem mass spectrometry - Characterization of municipal wastewaters, *Environ. Sci. Technol.*, **40** (1), 289-295.

Schultz, M. M., C. P. Higgins, C. A. Huset, R. G. Luthy, D. F. Barofsky and J. A. Field (2006b). Fluorochemical Mass Flows in a Municipal Wastewater Treatment Facility, *Environ. Sci. Technol.*, **40** (23), 7350-7357.

Schultz, M. M., C. P. Higgins, C. A. Huset, R. G. Luthy and j. A. Field (2006c). Fluorochemical mass flows in a municipal wastewater treatment facility, *Environ. Sci. Technol.*, **40**, 7350-7357.

Seki, S. and K. Sato (1975), Method for recovering fluorinated carboxylic acid, U. S. Patent: No.3882153, Assign to: Kureha Kagaku Kogyo Kabushiki Kaisha, Application No.05/347665.

Shoeib, M., T. Harner and P. Vlahos (2006). Perfluorinated Chemicals in the Arctic Atmosphere, *Environ. Sci. Technol.*, **40** (24), 7577-7583.

Shtarov, A. B., S. J. Getty and A. H.-J. Herzog (2006), Purification of fluorinated alcohols, U. S. Patent:

No.7138551, Assign to: E. I. du Pont de Nemours and Company, Application No.10/983201.

Sinclair, E. and K. Kannan (2006). Mass loading and fate of perfluoroalkyl surfactants in wastewater treatment plants, *Environ. Sci. Technol.*, **40** (5), 1408-1414.

Sinclair, E., D. T. Mayack, K. Roblee, N. Yamashita and K. Kannan (2006). Occurrence of perfluoroalkyl surfactants in water, fish, and birds from New York State, *Arch. Environ. Contam. Toxicol.*, **50** (3), 398-410.

Skutlarek, D., M. Exner and H. Färber (2006). Perfluorinated surfactants in surface and drinking waters, *Environ Sci Pollut Res Int*, **13** (5), 299-307.

Smithwick, M., S. A. Mabury, K. R. Solomon, C. Sonne, J. W. Martin, E. W. Born, R. Dietz, A. E. Derocher, R. J. Letcher, T. J. Evans, G. W. Gabrielsen, J. Nagy, I. Stirling, M. K. Taylor and D. C. G. Muir (2005). Circumpolar study of perfluoroalkyl contaminants in polar bears (Ursus maritimus), *Environ. Sci. Technol.*, **39** (15), 5517-5523.

Snyder, S. A., P. Westerhoff, Y. Yoon and D. L. Sedlak (2003). Pharmaceuticals, personal care products and endocrine disrupters in water: Implications for water treatment, *Environ. Eng. Sci.*, **20**, 449-469.

So, M. K., S. Taniyasu, P. K. S. Lam, G. J. Zheng, J. P. Giesy and N. Yamashita (2006a). Alkaline digestion and solid phase extraction method for perfluorinated compounds in mussels and oysters from south China and Japan, *Arch. Environ. Contam. Toxicol.*, **50** (2), 240-248.

So, M. K., S. Taniyasu, N. Yamashita, J. P. Giesy, J. Zheng, Z. Fang, S. H. Im and P. K. S. Lam (2004). Perfluorinated compounds in coastal waters of Hong Kong, South China, and Korea, *Environ. Sci. Technol.*, **38** (15), 4056-4063.

So, M. K., N. Yamashita, S. Taniyasu, Q. T. Jiang, J. P. Giesy, K. Chen and P. K. S. Lam (2006b). Health risks in infants associated with exposure to perfluorinated compounds in human breast milk from Zhoushan, China, *Environ. Sci. Technol.*, **40** (9), 2924-2929.

Strauss, S. H., M. A. Odom, G. N. Hebert and B. J. Clapsaddle (2002). ATR-FTIR detection of <= 25 mu g/L aqueous cyanide, perchlorate, and PFOS, *J. Am. Water Work Assoc.*, **94** (2), 109-115.

Sulzbach, R. A., W. Kowatsch and D. Steidl (1999), Recovery of highly fluorinated carboxylic acids from the gas phase, U. S. Patent: No.5990330, Assign to: Dyneon GmbH, Application No.08/612388.

Swedish Chemicals Inspectorate (KemI) and Swedish EPA (2004), Perfluorooctane sulfonate (PFOS) - Dossier prepared in support for a nomination of PFOS to the UN-ECE LRTAP Protocol and the Stockholm Convention, 1-46 pp, Sweden.

Takino, M., S. Daishima and T. Nakahara (2003). Determination of perfluorooctane sulfonate in river water by liquid chromatography/atmospheric pressure photoionization mass spectrometry by automated on-line extraction using turbulent flow chromatography, *Rapid Commun. Mass Spectrom.*, **17** (5), 383-390.

Tang, C. Y., Q. S. Fu, C. S. Criddle and J. O. Leckie (2007). Effect of Flux (Transmembrane Pressure) and Membrane Properties on Fouling and Rejection of Reverse Osmosis and Nanofiltration Membranes Treating Perfluorooctane Sulfonate Containing Wastewater, *Environ. Sci. Technol.*, **41** (6), 2008-2014.

Tang, C. Y., Q. S. Fu, A. P. Robertson, C. S. Criddle and J. O. Leckie (2006). Use of reverse osmosis membranes to remove perfluorooctane sulfonate (PFOS) from semiconductor wastewater, *Environ. Sci. Technol.*, **40** (23), 7343-7349.

Taniyasu, S., K. Kannan, Y. Horii and N. Yamashita (2002), The first environmetal survey of perfluorooctane sulfonate (PFOS) and related compounds in Japan, paper presented at Dioxin 2002, Barcelona, Spain, August 11-16, 2002.

Taniyasu, S., K. Kannan, M. K. So, A. Gulkowska, E. Sinclair, T. Okazawa and N. Yamashita (2005). Analysis of fluorotelomer alcohols, fluorotelorner acids, and short- and long-chain perfluorinated acids in water and biota, *J. Chromatogr. A*, **1093** (1-2), 89-97.

Tao, L., K. Kannan, N. Kajiwara, M. M. Costa, G. Fillmann, S. Takahashi and S. Tanabe (2006). Perfluorooctanesulfonate and Related Fluorochemicals in Albatrosses, Elephant Seals, Penguins, and Polar Skuas from the Southern Ocean, *Environ. Sci. Technol.*, **40** (24), 7642-7648.

Thibodeaux, J. R., R. G. Hanson, J. M. Rogers, B. E. Grey, B. D. Barbee, J. H. Richards, J. L. Butenhoff, L. A. Stevenson and C. Lau (2003). Exposure to perfluorooctane sulfonate during pregnancy in rat and mouse. I: Maternal and prenatal evaluations, *Toxicol. Sci.*, **74** (2), 369-381.

Tseng, C. L., L. L. Liu, C. M. Chen and W. H. Ding (2006). Analysis of perfluorooctanesulfonate and related fluorochemicals in water and biological tissue samples by liquid chromatography-ion trap mass spectrometry, *J. Chromatogr. A*, **1105** (1-2), 119-126.

UNEP (2006), Perfluorooctane sulfonate - Risk profile, Persistent organic pollutants review committe.

US EPA (2002), Hazard assessment of perfluorooctanoic acid and its salts, 107 pp, Office of Pollution Prevention and Toxics - Risk Assessment Division, US.

US EPA (2003), Preliminary risk assessment of the developmental toxicity associated with exposure to perfluorooctanoic acid and its salts, 64 pp, Office of Pollution Prevention and Toxics - Risk Assessment Division, US.

Valdes, H., M. Sanchez-Polo, J. Rivera-Utrilla and C. A. Zaror (2002). Effect of Ozone Treatment on Surface Properties of Activated Carbon, *Langmuir*, **18** (6), 2111-2116.

Valdes, H., M. Sanchez-Polo and C. A. Zaror (2003). Effect of ozonation on the activated carbon surface chemical properties and on 2-mercaptobenzothiazole adsorption, *Latin American Applied Research*, **33**, 219-223.

Van de Vijver, K. I., P. T. Hoff, K. Das, W. Van Dongen, E. L. Esmans, T. Jauniaux, J. M. Bouquegneau, R. Blust and W. De Coen (2003). Perfluorinated chemicals infiltrate ocean waters: Link between exposure levels and stable isotope ratios in marine mammals, *Environ. Sci. Technol.*, **37** (24), 5545-5550.

van Leeuwen, S. P. J. and J. de Boer (2007). Extraction and clean-up strategies for the analysis of poly- and perfluoroalkyl substances in environmental and human matrices, *J. Chromatogr. A*, **In Press, Corrected Proof**, 53.

van Leeuwen, S. P. J., A. Karrman, B. vanBavel, J. deBoer and G. Lindstrom (2006). Struggle for Quality in Determination of Perfluorinated Contaminants in Environmental and Human Samples, *Environ. Sci. Technol.*, **40** (24), 7854-7860.

Verreault, J., M. Houde, G. W. Gabrielsen, U. Berger, M. Haukas, R. J. Letcher and D. C. G. Muir (2005). Perfluorinated alkyl substances in plasma, liver, brain, and eggs of glaucous gulls (Larus hyperboreus) from the Norwegian Arctic, *Environ. Sci. Technol.*, **39** (19), 7439-7445.

Vidic, R. D., C. H. Tessmer and L. J. Uranowski (1997). Impact of surface properties of activated carbons on oxidative coupling of phenolic compounds, *Carbon*, **35** (9), 1349-1359.

Wallington, T. J., M. D. Hurley, J. Xia, D. J. Wuebbles, S. Sillman, A. Ito, J. E. Penner, D. A. Ellis, J. Martin, S. A. Mabury, O. J. Nielsen and M. P. S. Andersen (2006). Formation of C7F15COOH (PFOA) and other perfluorocarboxylic acids during the atmospheric oxidation of 8 : 2 fluorotelomer alcohol, *Environ. Sci. Technol.*, **40** (3), 924-930.

Wang, E. H. (1977), Bioassay of air force FC-206 fire-fighting foam, University of New Mexico, USEPA docket: EPA-HQ-OPPT-2003-0012-0152.

Wang, N., B. Szostek, R. C. Buck, P. W. Folsom, L. M. Sulecki, V. Capka, W. R. Berti and J. T. Gannon (2005a). Fluorotelomer alcohol biodegradation - Direct evidence that perfluorinated carbon chains breakdown, *Environ. Sci. Technol.*, **39** (19), 7516-7528.

Wang, N., B. Szostek, P. W. Folsom, L. M. Sulecki, V. Capka, R. C. Buck, W. R. Berti and J. T. Gannon (2005b). Aerobic biotransformation of C-14-labeled 8-2 telomer B alcohol by activated sludge from a domestic sewage treatment plant, *Environ. Sci. Technol.*, **39** (2), 531-538.

Waters (2006), Topics in solid-phase extraction: part 1. ion suppression in LCMS.

Weber, W. J. and J. M. Smith (1987). Simulation and Design Models for Adsorption Processes, *Environ. Sci. Technol.*, **21** (11), 1040-1050.

Welcker, K. (2006). Quantification, removal, and recovery of APFO from contaminated drinking water with a concomitant endocrinological and epidemiological assessment, *doi:10.2175/ SJWP(2006)*, **1**, 111-126.

Weremiuk, A. M., S. Gerstmann and H. Frank (2006). Quantitative determination of perfluorinated surfactants in water by LC-ESI-MS/MS, *J. Sep. Sci.*, **29** (14), 2251-2255.

West Virginia Department of Environmental Protection (2002). Final ammonium perfluorooctanoate (C8) Assessment of Toxicity Team (CATT) report.

Wilmanski, K. and A. N. van Breemen (1990). Competitive adsorption of trichloroethylene and humic substances from groundwater on activated carbon, *Water Research*, **24** (6), 773-779.

Wolborska, A. and P. Pustelnik (1996). A simplified method for determination of the break-through time of an adsorbent layer, *Water Research*, **30** (11), 2643-2650.

Yamada, T., P. H. Taylor, R. C. Buck, M. A. Kaiser and R. J. Giraud (2005). Thermal degradation of fluorotelomer treated articles and related materials, *Chemosphere*, **61** (7), 974-984.

Yamashita, N., K. Kannan, S. Taniyasu, Y. Horii, T. Okazawa, G. Petrick and T. Gamo (2004). Analysis of perfluorinated acids at parts-per-quadrillion levels in seawater using liquid chromatography-tandem mass spectrometry, *Environ. Sci. Technol.*, **38** (21), 5522-5528.

Yamashita, N., K. Kannan, S. Taniyasu, Y. Horii, G. Petrick and T. Gamo (2005). A global survey of perfluorinated acids in oceans, *Mar. Pollut. Bull.*, **51** (8-12), 658-668.

Yang, B., S. Nan, X. Yu and M. Dou (2006). Treatment of wastewater with low concentration organofluorine, *Water Treatment Technology (in Chinese)*, **4**.

Young, C. J., V. I. Furdui, J. Franklin, R. M. Koerner, D. C. G. Muir and S. A. Mabury (2007). Perfluorinated acids in Arctic snow: New evidence for atmospheric formation, *Environ. Sci. Technol.*, **In Press**.

Young, M. S. and K. V. Tran (2006), Oasis WAX sorbent for UPLC/MS determination of PFOS and related compounds in water and tissue, Waters Corporation, Milford, MA, USA.

Zhang, H., S. Nan and M. Dou (2005a). Research on recovery of ammoniun perfluorooctanoate from waste water by adsorptive bubble separation method, *Chemical Engineer (in Chinese)*, **12**.

Zhang, P., J. Chen, L. Zhang, G. Yu and X. Chang (2005b), Method for defluorinating and degrading complete fluorine substituted compounds: No.CN1680219-A, Assign to: Univ Qinghua (Uyqi), Application No.CN1680219-A CN10011126 07 Jan 2005.

Zhao, X., J. Li, Y. Shi, Y. Cai, S. Mou and G. Jiang (2007). Determination of perfluorinated compounds in wastewater and river water samples by mixed hemimicelle-based solid-phase extraction before liquid chromatography-electrospray tandem mass spectrometry detection, *J. Chromatogr. A*, **In Press, Corrected Proof**.

APPENDIX A

Mass flow of each PFC along treatment process in K-WWTP, in average of data from six regular field surveys from Aug. 17th , 2006 to Dec. 7th, 2006.

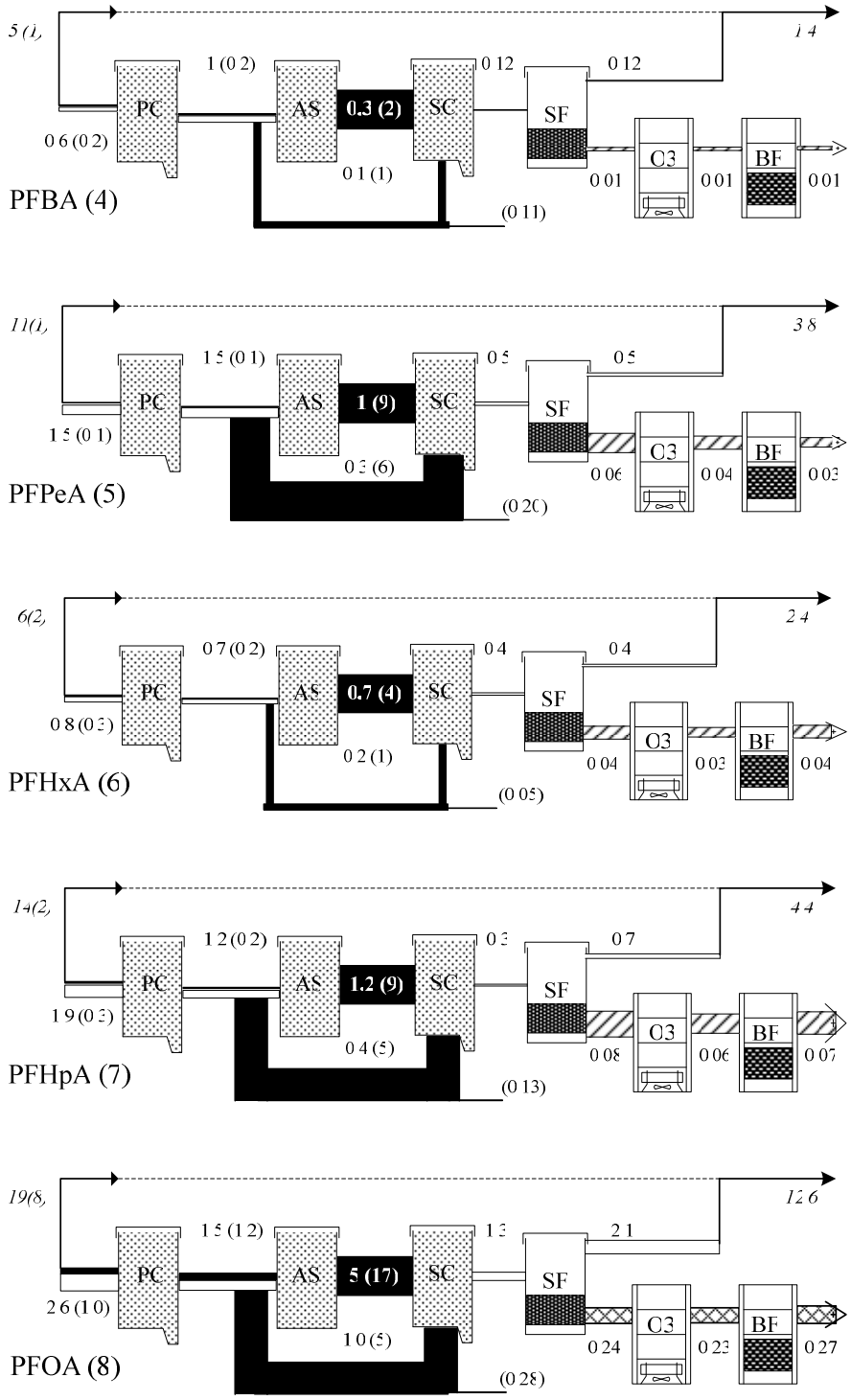

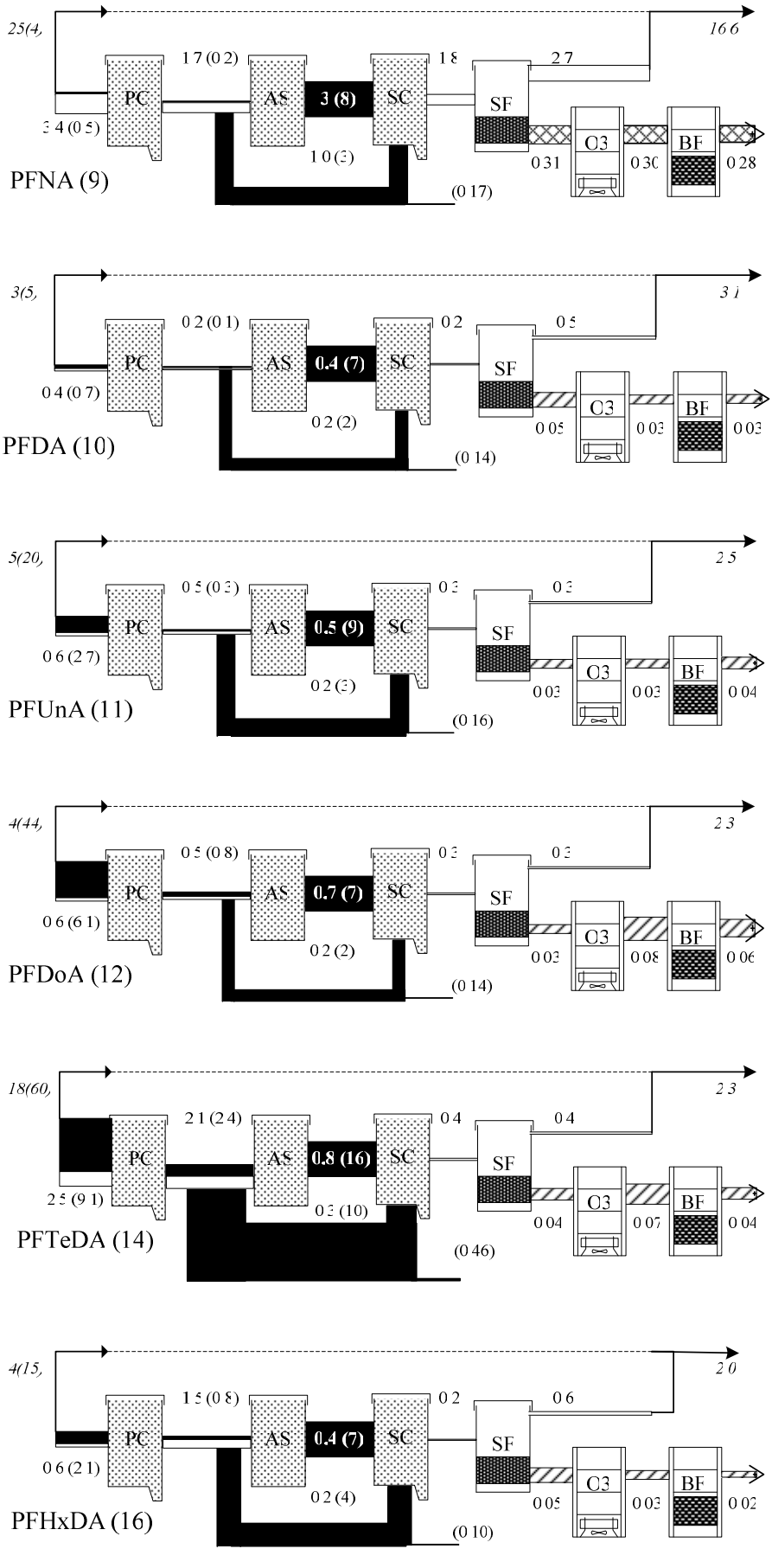
PFNA (9)
PC
AS
3 (8)
SC
SF
O3
BF
PFDA (10)
0.4 (7)
PFUnA (11)
0.5 (9)
PFDoA (12)
0.7 (7)
PFTeDA (14)
0.8 (16)
PFHxDA (16)
0.4 (7)

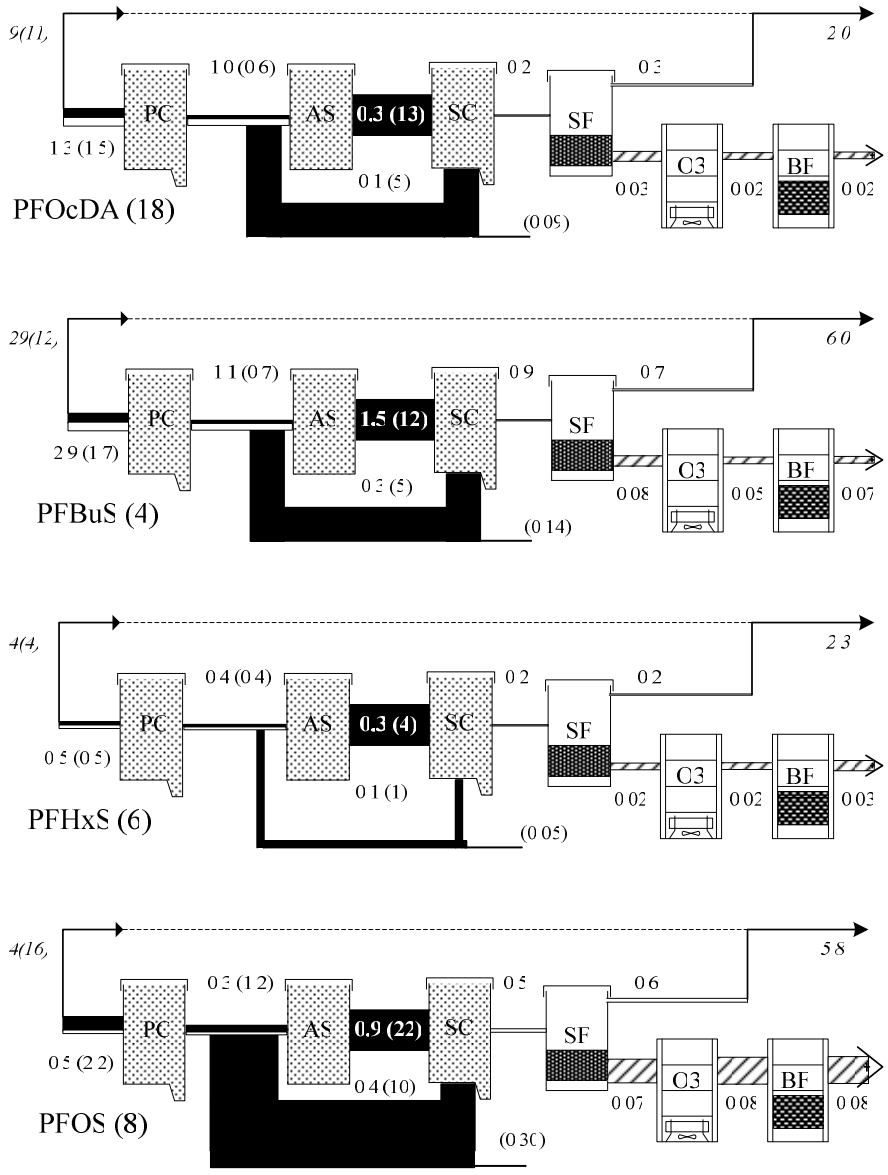
9(11)
20
10 (0 6)
0 2
0 3
PC
AS
0.3 (13)
SC
SF
1 3 (1 5)
0 1 (5)
C3
BF
0 0 3
0 0 2
0 0 2
PFOcDA (18)
(0 0 5)
29(12)
60
1 1 (0 7)
0 9
0 7
PC
AS
1.5 (12)
SC
SF
2 9 (1 7)
0 3 (5)
C3
BF
0 0 8
0 0 5
0 0 7
PFBuS (4)
(0 1 4)
4(4)
23
0 4 (0 4)
0 2
0 2
PC
AS
0.3 (4)
SC
SF
0 5 (0 5)
0 1 (1)
C3
BF
0 0 2
0 0 2
0 0 3
PFHxS (6)
(0 0 5)
4(16)
58
0 3 (1 2)
0 5
0 6
PC
AS
0.9 (22)
SC
SF
0 5 (2 2)
0 4 (10)
C3
BF
0 0 7
0 0 8
0 0 8
PFOS (8)
(0 3 0)
4(16) : aqueous (particulate) for WWTP
0.9(22) : aqueous (particulate) for series 4
: particulate phase, 1 g/day
aqueous phase, 0.01 g/day
aqueous phase, 0.1 g/day
aqueous phase, 1 g/day

APPENDIX B

Description of Homogeneous Surface Diffusion Model (HSDM)

Assumptions for models

The main hypothesis of HSDM is that porous diffusion is negligible and internal mass transfer process is only due to surface diffusion. This model contains following assumptions.

(1)The particle is spherical and homogenous.

(2)Concentrations in solid and liquid phase at interface are in equilibrium.

(3)External mass transfer is governed by linear driving force.

(4)Internal mass transfer is only governed by surface diffusion.

(5)At interface external transfer flux is same to surface diffusion.

(6)Mass is balanced in contactor.

By these assumptions coupled with boundary conditions, seven equations are derived as shown in **Fig. B.1**. The procedure to derive these equations is shown in successive sections.

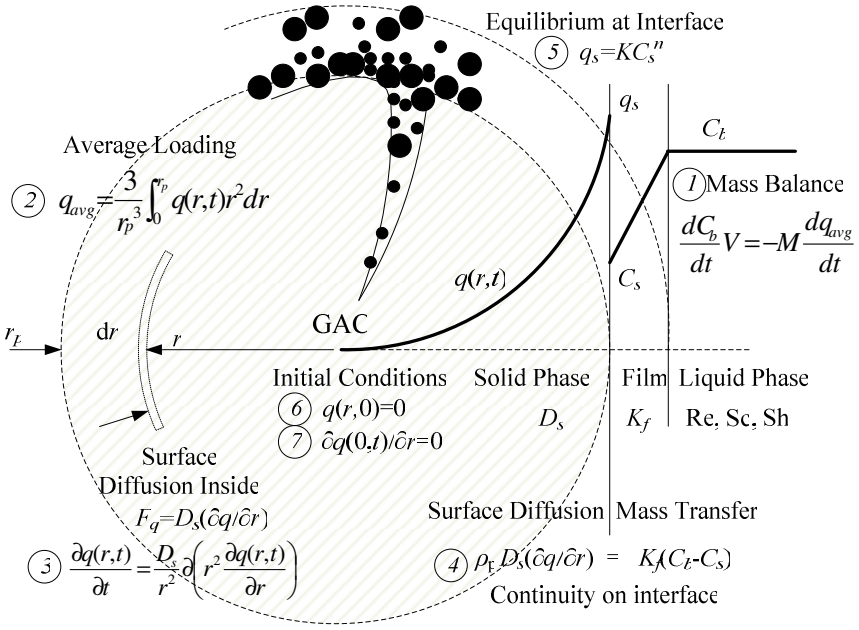

Figure B.1 Concept of HSDM for GAC adsorption

Mass balance

Average loading rate q_{avg}, which represents average occupation of adsorbate inside of GAC, could be calculated in two ways, one of which is to calculate from bulk adsorbate concentration C_b by following mass balance, and the other is to integrate $q(r, t)$ along radius r and divided by total volume V_s of GAC sphere

$$\frac{dC_b}{dt}V = -M\frac{dq_{avg}}{dt}$$

$$q_{avg} = \frac{\int_0^{r_p} q(r,t)dV_s}{V_s} = \frac{\int_0^{r_p} q(r,t)4\pi r^2 dr}{4/3\pi r_p^3} = \frac{3}{r_p^3}\int_0^{r_p} q(r,t)r^2 dr$$

where V is bulk volume, V_s is GAC apparent volume, M is mass of GAC, r_p is sphere radius. By introduction of q_{avg}, temporal and spatial distributed loading rate $q(r, t)$ is related to bulk adsorbate concentrations C_b, which could be observed by experiments directly.

Surface diffusion process

By assuming homogenous surface diffusion inside GAC, transfer process of adsorbate obeys Fick's Law, in which diffusion coefficient D_s was applied to show potential and intensity of diffusion. Therefore, variance of loading per unit of time equals to amount of adsorbate diffused into per unit of volume.

$$\frac{\partial q(r,t)}{\partial t} = \frac{\partial(F_q A_s)}{\partial V_s} = \frac{\partial(D_s \partial q/\partial r \cdot 4\pi r^2)}{4\pi r^2 \partial r} = \frac{D_s}{r^2}\partial\left(r^2 \frac{\partial q(r,t)}{\partial r}\right)$$

where F_q is transfer flux in terms of loading rate $q(r, t)$, A_s is surface area at radius r, V_s is differential GAC volume at radius r, D_s is surface diffusion coefficient inside GAC, r is sphere radius. By applying D_s, distribution of loading rate $q(r, t)$ at specific time t could be calculated by current state of distribution, which is helpful to predict adsorption performance.

Liquid-solid interface constrains

At interface of liquid-solid phase, there are two constrains for adsorption. One refers to equilibrium state at surface of GAC, which follows Langmiur isotherm or Freundlich equation. In this study, Freundlich equation is more suitable and adapted. Another is related with continuity of mass transfer at liquid-solid interface, where mass transfer flux to GAC surface should be equal to surface diffusion from GAC surface to inside pores. Therefore surface diffusion process by D_s was connected with mass transfer process charged by K_f.

$$\frac{dC}{dr} = K_f(C_b - C_s)$$

$$F_q = \frac{V_s}{M}\frac{dC}{dr} = \frac{K_f}{\rho_p}(C_b - C_s) = D_s\frac{\partial q}{\partial r}$$

$$\rho_p D_s \frac{\partial q}{\partial r} = K_f(C_b - C_s)$$

where F_q is transfer flux in terms of loading rate $q(r, t)$, M is mass of GAC, V_s is GAC volume, ρ_p is apparent density of GAC equal to M/V_s, D_s is surface diffusion coefficient inside GAC, K_f is mass transfer coefficient in film zone between liquid and solid phase.

Initial and boundary conditions

As temporal initial condition, loading rate $q(r, 0)$ is equal to zero for everywhere inside GAC.

$$q(r,0) = 0, \frac{\partial q(0,t)}{\partial t} = 0$$

Boundary conditions

For spatial boundary conditions, loading rate $q(0, t)$ in center position of GAC is equal to zero for anytime along experiments.

$$q(r,0)=0, \frac{\partial q(0,t)}{\partial t}=0$$

Normalization of HSDM equations

In order to solve HSDM in general methods, equations are firstly uniformed by dimensionless variants. Usually, HSDM equations are normalized to be dimensionless which is helpful for general solutions. Necessary expressions are shown below.

$$C_b^*=\frac{C}{C_0}, q^*=\frac{q}{q_0}, T=\frac{4D_s t}{d_p^2}, D_g=\frac{M}{V}\frac{q_0}{C_0}, Bi=\frac{K_f r_p C_0}{\rho_p D_s q_0}, R=\frac{2r}{d_p}$$

where C is bulk concentration, q is adsorbate loading on GAC, M is mass of GAC, V is volume of bulk solution, C_0 is initial concentration in bulk solution, $q_0=KC_0^n$. Biot number Bi could be used to determine which of mass transfer and surface diffusion dominants the adsorption process, K_f and D_s are mass transfer and surface diffusion coefficients, d_p is diameter of GAC particles, ρ_p is apparent density of GAC. By these variants, HSDM is rewritten in dimensionless equations, as shown in **Table B.1**.

Table B.1 Normalized HSDM equations

Description	Model equations	Dimensionless forms
Mass Balance	$\frac{dC}{dt}V=-M\frac{d\overline{q}}{dt}$	$C_b^*+D_g q^*=1$
Average Loading	$\overline{q}=\frac{3}{r_p^3}\int_0^{r_p} q(r,t)r^2 dr$	$q^*=3\int_0^1 q^*(R)R^2 dR$
Surface Diffusion	$\frac{\partial q}{\partial t}=\frac{D_s}{r_p^2}\partial\left(r^2\frac{\partial q}{\partial r}\right)$	$\frac{\partial q^*}{\partial T}=\frac{1}{R^2}\frac{d}{dR}\left(R^2\frac{dq^*}{dR}\right)$
Continuity	$\rho_p D_s\frac{\partial q}{\partial r}=K_f(C_b-C_s)$	$\frac{\partial q(1,T)}{\partial R}=Bi\left(C_b^*-C_s^*\right)$
Equilibrium	$q_s=KC_s^n$	$q^*=C_s^{*n}$
Boundary Condition	$\frac{\partial q(0,t)}{\partial r}=0$	$\frac{\partial q^*(0,T)}{\partial R}=0$
Initial Condition	$q(r,0)=0$	$q^*(R,0)=0$

Solution of HSDM

By complicated calculation including Laplace transform and inverse Lapalce transform, partial differential equations in HSDM can be approximately solved by orthogonal collocation method (Roy, *et al.*, 1993). Solution for three points collocation is shown as below, which is a continuous function of time t and further numeric calculation is acquired. The positions of collocation points are [0.4058, 0.7415, 0.9491, 1]r from center to boundary along radius.

$$\begin{bmatrix} q_1^* \\ q_2^* \\ q_3^* \\ q_4^* \end{bmatrix} = \begin{bmatrix} 0.999 & -0.10727 & 0.702755 & -1.59 \\ 0.9999 & 0.239778 & -0.44308 & -0.797097 \\ 1.00 & -0.554656 & -0.22628 & -0.219297 \\ 1 & 0 & 0 & 0 \end{bmatrix} \cdot \begin{bmatrix} 1 \\ \exp\left(-142.634\cdot t\left(D_s/r_p^2\right)\right) \\ \exp\left(-39.996\cdot t\left(D_s/r_p^2\right)\right) \\ \exp\left(-9.8686\cdot t\left(D_s/r_p^2\right)\right) \end{bmatrix} C_s^{*n}$$

where D_s is surface diffusion coefficient, r_p is radius of GAC, q_1^* to q_4^* are dimensionless loading rates at i collocation point, C_s^* is surface adsorbate concentration equal to C_s/C_0, and $q_0=KC_0^n$.

Boundary conditions are also rewritten as follows, in which two bulk concentration C_b^* can be calculated. By trying different values of C_s^*, these two values can be equal and q_i^* is obtained as well as bulk concentration C_b^*.

$$\begin{bmatrix} (1-C_b^*)/3D_g \\ (C_b^*-C_s^*)Bi \end{bmatrix} = \begin{bmatrix} 0.0457 & 0.1259 & 0.1340 & 0.0278 \\ -1.0727 & 5.3256 & -20.753 & 16.5 \end{bmatrix} \cdot \begin{bmatrix} q_1^* \\ q_2^* \\ q_3^* \\ q_4^* \end{bmatrix}$$

Detailed simulation result of one experiment in Run K-1 is shown in **Table B.2**, including distribution profile inside GAC at [0.4058, 0.7415, 0.9491, 1]r_p. The variances of q_i along time demonstrate distribution of PFOS molecules, which is not ceased until end of experiment. Equilibrium state is arrived at around 20 days, because all q_i show similar values and C_b equal to C_s, which implies that PFOS has been homogenously distributed inside of GAC.

Table B.2 Example of HSDM simulation for PFOS

Time	q_1	q_2	q_3	q_4	C_s	C_b	Expmt.
hr	μg/g	μg/g	μg/g	μg/g	μg/L	μg/L	μg/L
0						1000	1000
3	26	26	819	2965	9.8	429	344
6	16	43	1210	2703	8.7	269	294
9	6	141	1388	2491	7.8	180	208
26	73	572	1416	1818	5.1	52	55
48	290	784	1274	1477	3.8	28	37
60	401	839	1222	1376	3.5	22	32
72	497	874	1181	1302	3.2	18	24
80	553	892	1159	1264	3.1	16	13
120	748	942	1084	1139	2.7	10	5
168	869	969	1042	1069	2.5	6	1
240	949	988	1016	1026	1.9	3	
480	995	998	999	1000	1.8	2	